Self-interaction and charge transfer in organic semiconductors

Genehmigte Abhandlung

zur Erlangung des akademischen Grades eines
Doktors der Naturwissenschaften (Dr. rer. nat.)
im Fach Physik der Fakultät für Mathematik, Physik und Informatik
der Universität Bayreuth

**UNIVERSITÄT
BAYREUTH**

von

Thomas Körzdörfer

geboren in Bayreuth

1. Gutachter: Prof. Dr. Stephan Kümmel
2. Gutachter: Prof. Dr. Matthias Schmidt
3. Gutachter: Prof. Dr. Manfred Lein

Tag der Einreichung : 2. Oktober 2009
Tag des Kolloquiums: 18. Dezember 2009

Nothing shocks me. I'm a scientist.

Dr. Henry Jones, Jr. alias Indiana Jones

Abstract

The fascinating properties of organic molecular semiconductors paved the way for a new class of electronic devices such as organic light-emitting diodes, transistors, or solar cells. Despite an inferior efficiency as compared to commonly used silicon-based technologies, organic semiconductors promise the advent of fully flexible devices for large-area displays and solar cells, printed transistors as low-cost radio frequency identification (RFID) tags, displays for electronic books, and disposable measuring instruments for medical diagnosis. Hence, the investigation of organic molecular semiconductors has emerged as a vibrant field of development both in industry and in academia, spanning a wide range of subjects from physics, chemistry, and materials science to engineering and technology. Theoretical physicists can contribute to this progress by developing methods that allow to determine the electronic properties of organic semiconductors from first principles and thus deepen our knowledge of the underlying electronic processes in organic electronic devices.

The calculation of the electronic properties of molecular semiconductors issues a serious challenge to theoretical physicists and chemists. Typically, organic semiconductor molecules employ several hundreds of electrons. For systems of that size, approaches that work with model Hamiltonians are typically not accurate enough in predicting many important electronic properties. However, solving the many-particle Schrödinger-equation by employing highly accurate perturbation theory approaches is often numerically too expensive to be considered as a convenient alternative. Hence, density functional theory (DFT) naturally arises as the method of choice. However, although in theory DFT yields an exact formulation of quantum mechanics, the quality of the results obtained from DFT calculations in practice strongly depends on the used approximations to the so-called exchange-correlation functional. This work concentrates on the problem of self-interaction, which is one of the most serious problems of commonly used approximative density functionals.

As a major result of this work, it is demonstrated that self-interaction plays a decisive role for the performance of different approximative functionals in predicting accurate electronic properties of organic molecular semiconductors. This is particularly true for the calculation of ionization potentials, photoelectron spectra, dissociation, and charge-transfer processes. In search for a solution to the self-interaction problem, a new concept for correcting commonly used density functionals for self-interaction is introduced and applied to a variety of systems, spanning small molecules, extended molecular chains, and organic molecular semiconductors. It is further shown that the performance of functionals that are not free from self-interaction can vary strongly for different systems and observables of interest, thus entailing the danger of misinterpretation of the results obtained from those functionals. The underlying reasons for the varying performance of commonly used density functionals are discussed thoroughly in this work. Finally, this thesis provides strategies that allow to analyze the reliability of commonly used approximations to the exchange-correlation functional for particular systems of interest.

This cumulative dissertation is divided into three parts. Part I gives a short introduction into DFT and its time-dependent extension (TDDFT). Part II provides further insights into the self-interaction problem, presents a newly developed concept for the correction of self-interaction, gives an introduction into the publications, and discusses their basic results. Finally, the four publications on self-interaction and charge-transfer in extended molecular systems and organic molecular semiconductors are collected in Part III.

Kurzfassung

Die faszinierenden Eigenschaften organischer molekularer Halbleiter bilden die Grundlage für eine neue Klasse an elektronischen Bauteilen wie etwa organischen Leuchtdioden, Transistoren und Solarzellen. Trotz ihrer deutlich schlechteren Effizienz gegenüber herkömmlichen Silizium-Technologien verspricht der Einsatz von organischen Materialien die Entwicklung von voll flexiblen, großflächigen Displays und Solarzellen, gedruckten Transistoren als Radio Frequency Identification (RFID)-Etiketten in der Warenlogistik, Displays für elektronische Bücher und gedruckten Einweg-Messgeräten für die medizinische Diagnostik. Die Untersuchung organischer molekularer Halbleiter bietet damit ein interessantes Feld sowohl für die industrielle Anwendung als auch für die Grundlagenforschung in Physik, Chemie, Material- und Ingenieurwissenschaften. Die Theoretische Physik kann zu dieser Entwicklung beitragen indem sie Methoden bereitstellt, welche die Berechnung der elektronischen Eigenschaften von organischen Halbleitermaterialien ermöglicht und damit erlaubt das Verständnis der zugrundeliegenden Prozesse zu vertiefen.

Aus Sicht der theoretischen Physik stellt die Berechnung der elektronischen Eigenschaften von Molekülen mit einigen hundert Elektronen eine spezielle Herausforderung dar. Für Systeme dieser Größe ist der Zugang über Modell-Hamiltonians für gewöhnlich nicht ausreichend exakt. Die Lösung der Vielteilchen-Schrödingergleichung mithilfe quantenmechanischer Störungstheorie hingegen ist oftmals numerisch zu teuer. Diese Konstellation führt auf die Dichtefunktionaltheorie (DFT) als Methode der Wahl. Obwohl die DFT im Prinzip eine exakte quantenmechanische Formulierung darstellt, ist in der Praxis die Qualität der mithilfe der DFT erzielten Ergebnisse stark von der Näherung für das sog. Austausch-Korrelations-Funktional abhängig. Die vorliegende Arbeit beschäftigt sich in erster Linie mit dem Problem der Selbstwechselwirkung in gewöhnlich verwendeten Dichtefunktionalen.

Bei der Berechnung der elektronischen Eigenschaften von organischen Halbleitern mithilfe der DFT spielt die Freiheit der verwendeten Funktionale von Selbstwechselwirkung eine zentrale Rolle, insbesondere für die Berechnung von Ionisationspotentialen, Photoelektronenspektren, Dissoziations- und Ladungstransferprozessen. Die Gründe für das Versagen von nicht selbstwechselwirkungsfreien Näherungen an das Austausch-Korrelations-Funktional sind dabei vielfältig und werden in dieser Arbeit im Einzelnen diskutiert. Zur Lösung der Selbstwechselwirkungsproblematik wird ein neues Konzept zur Selbstwechselwirkungskorrektur gewöhnlich verwendeter Dichtefunktionale vorgestellt und auf eine Reihe an Systemen angewendet. Darüber hinaus werden Strategien vorgeschlagen, welche es erlauben, die Zuverlässigkeit von Dichtefunktionalen für bestimmte Systeme und Observablen zu testen. Die dabei erarbeiteten Erkenntnisse werden schließlich genutzt um die zugrundeliegenden elektronischen Prozesse in einem jüngst experimentell untersuchten System aus zwei fluoreszierenden und elektronisch gekoppelten organischen Halbleitermolekülen aufzuklären.

Diese kumulative Dissertationsschrift ist in drei Teile gegliedert. Teil I gibt eine kurze Einführung in die Grundlagen der DFT und ihrer zeitabhängigen Erweiterung (TDDFT). Weitergehende Einblicke in das Problem der Selbstwechselwirkung und dessen Korrektur, eine Zusammenfassung der wichtigsten mathematischen und numerischen Hintergründe der vorgestellten Methodik und eine Einführung in die Publikationen sind in Teil II dargestellt. Den Abschluss bilden die vier Publikationen zum Thema Selbstwechselwirkungskorrektur und Ladungstransfer in organischen Halbleitermolekülen in Teil III.

Contents

III. Publications

P1. Electrical Response of Molecular Systems:
    The Power of Self-Interaction Corrected Kohn-Sham Theory

P2. Self-interaction correction and the optimized effective potential

P3. When to trust photoelectron spectra from Kohn-Sham eigenvalues:
    The case of organic semiconductors

P4. Fluorescence quenching in an organic donor-acceptor dyad:
    A first principles study

Part I.

Introduction and Background

Chapter 1.

Density functional theory

1.1. Introduction

There is an oral tradition that, shortly after Schrödingers fundamental equation of quantum mechanics had been spectacularly validated for the Helium atom, P. A. M. Dirac declared solemnly that chemistry had come to end - its content was entirely contained in that equation. Too bad, he is said to have added, that in almost all cases this equation was far too complex to allow for solution.

More than eight decades later, researchers have learned that Dirac was just partly right: Of course, even with the most modern computers and with the most effective algorithms we are not able to find the exact solution of Schrödinger's equation, even for rather small molecules, and we most probably will never be. This has a very simple and pragmatic reason: storing the many-electron wavefunction of a system with only 1000 electrons would require a computer's memory to keep track of more information bits than the estimated number of particles in the universe. In order to classify this number one should relate it to the size of a typical biomolecule: the largest human chromosome is approximately 220 million base pairs long, each of which contains several hundreds of electrons.

However, today we know that Schrödinger's equation is not the end of the story. In particular, we have learned that the many-electron wavefunction is not a very effective way of describing the properties of atoms, molecules or solids. This is very impressively demonstrated in the seminal work of Hohenberg and Kohn [46], which in the early 1960s set the stage for the nowadays most widely used method for electronic structure calculations in quantum chemistry and condensed matter physics: density functional theory (DFT).

One of the main achievements of Hohenberg and Kohn was to demonstrate that, at least in principle, it is possible to gain any information about a system from its ground-state density $n(\mathbf{r})$. This makes it possible to work with the electron density as a basic variable. The drastic advantage of this approach is obvious: While the density only depends on 3 spatial coordinates, a many-particle wavefunction scales with the number of particles N in the system as 3^N.

Formally, the work of Hohenberg and Kohn can be summarized in two central theorems. The *first Hohenberg-Kohn theorem* states that for a given particle-particle interaction $W(\mathbf{r}, \mathbf{r}')$ there exists a one-to-one mapping between the one-particle ground-state density $n(\mathbf{r})$ and the local multiplicative external potential $v(\mathbf{r})$ (up to a constant in the potential which has no physical consequences). As a consequence, the Hamiltonian $\hat{H} = \hat{T} + \hat{W} + \hat{V}$ of a system, where $\hat{T} = \sum_i \frac{\hat{p}_i^2}{2m}$, $\hat{V} = \sum_i v(\hat{r}_i)$, and $\hat{W} = \sum_{i \neq j} w(\hat{r}_i, \hat{r}_j)$, is sufficiently and completely determined by its ground-state density. In other words, the ground state $|\psi_0\rangle$ itself, where

$\hat{H}|\psi_0\rangle = E_0|\psi_0\rangle$, as well as every other observable is a functional of the ground-state density.

The *second Hohenberg-Kohn theorem* sets the stage for a methodology that allows to find the ground-state density for any system of interest. By reworking the Rayleigh-Ritz variational principle, Hohenberg and Kohn showed the existence of a universal functional $F[n] = \langle\psi_0|\hat{T} + \hat{W}|\psi_0\rangle$ which via straightforward minimization of the total energy

$$E[n] = F[n] + \int v(\mathbf{r})\, n(\mathbf{r})\, d\mathbf{r} \tag{1.1}$$

yields the exact ground-state energy E_0 and density $n(\mathbf{r})$ corresponding to a given local potential $v(\mathbf{r})$.

As a consequence of the Hohenberg-Kohn theorems, the Schrödinger equation is formally replaced by a simple but exact variational equation, i.e.,

$$\frac{\delta E[n]}{\delta n(\mathbf{r})} = 0\,. \tag{1.2}$$

However, the complexity of solving Schrödingers equation has turned into a new problem that is equally complex [118] to solve exactly: finding the exact functional $F[n]$ for an interacting many-particle system. In the light of Dirac's comment on the Schrödinger equation one may be tempted to say: too bad that in almost all cases this functional is probably far too complex to find.

1.2. The Kohn-Sham scheme

In order to practically exploit the Hohenberg-Kohn theorems one has to find a way to approximate the functional $F[n]$ as good as possible. The most successful scheme that allows to find such an approximation has been provided by Kohn and Sham in 1965. Hence, it is called the *Kohn-Sham scheme* [59].

The basic idea of Kohn and Sham was to introduce an auxiliary system of non-interacting particles moving in a local multiplicative potential v_σ^{KS}, i.e., the *Kohn-Sham potential*. In this system, the many-electron problem is reduced to a system of one-electron Schrödinger equations, called the *Kohn-Sham equations*:

$$\left[-\frac{\hbar^2}{2m}\nabla^2 + v_\sigma^{\mathrm{KS}}(\mathbf{r})\right]\varphi_{i\sigma}(\mathbf{r}) = \epsilon_{i\sigma}\,\varphi_{i\sigma}(\mathbf{r})\,, \tag{1.3}$$

$$n(\mathbf{r}) = \sum_{\sigma=\uparrow,\downarrow} n_\sigma(\mathbf{r}) = \sum_{\sigma=\uparrow,\downarrow}\sum_{i=1}^{N_\sigma} n_{i\sigma}(\mathbf{r}) = \sum_{\sigma=\uparrow,\downarrow}\sum_{i=1}^{N_\sigma} f_{i\sigma}\,|\varphi_{i\sigma}(\mathbf{r})|^2\,, \tag{1.4}$$

$$\sum_{\sigma=\uparrow,\downarrow}\sum_{i=1}^{N_\sigma} f_{i\sigma} = M\,. \tag{1.5}$$

Here, $\varphi_{i\sigma}(\mathbf{r})$ are the orthonormal *Kohn-Sham orbitals* for spin σ, $f_{i\sigma}$ are their occupation numbers, $n_\sigma(\mathbf{r})$ are the total spin densities, N_σ the number of occupied orbitals with spin σ and M is the total number of electrons. In the Kohn-Sham (KS) approach, the total energy

reads

$$E^{\mathrm{KS}} = E_{\mathrm{kin}}\left[n\right] + E_{\mathrm{ext}}\left[n\right] + E_{\mathrm{Hart}}\left[n\right] + E_{\mathrm{xc}}\left[n\right] . \tag{1.6}$$

The interaction energy of the electron density with an external potential $v_{\mathrm{ext}}\left(\mathbf{r}\right)$ (which includes the potential of the atomic cores as well as external fields)

$$E_{\mathrm{ext}}\left[n\right] = \int n\left(\mathbf{r}\right) v_{\mathrm{ext}}\left(\mathbf{r}\right) d\mathbf{r} \tag{1.7}$$

and the classical mean-field Coulomb interaction, i.e., the *Hartree interaction energy*

$$E_{\mathrm{Hart}}\left[n\right] = \frac{e^2}{2} \iint \frac{n\left(\mathbf{r}\right) n(\mathbf{r}')}{\left|\mathbf{r} - \mathbf{r}'\right|} d\mathbf{r}\, d\mathbf{r}' \tag{1.8}$$

are known as explicit functionals of the ground-state density. Importantly, the non-interacting kinetic energy

$$E_{\mathrm{kin}} = \sum_{\sigma=\uparrow,\downarrow} \sum_{i=1}^{N_\sigma} f_{i\sigma} \langle \varphi_{i\sigma}| -\frac{\hbar^2}{2m}\nabla^2 |\varphi_{i\sigma}\rangle \tag{1.9}$$

is not an explicit but an implicit functional of the ground-state density: due to the first Hohenberg-Kohn theorem, the KS potential is a functional of the ground-state density. Then, by virtue of the KS equations, the KS orbitals and thus the kinetic energy are implicit density functionals.

The so-called exchange-correlation energy functional $E_{\mathrm{xc}}\left[n\right] = \sum_{\sigma=\uparrow,\downarrow} E_{\mathrm{xc},\sigma}\left[n_\uparrow, n_\downarrow\right]$, which by definition carries everything that has been neglected or approximated in $E_{\mathrm{kin}}\left[n\right]$, $E_{\mathrm{ext}}\left[n\right]$, and $E_{\mathrm{Hart}}\left[n\right]$ (such as all non-classical particle-particle interactions and the interacting part of the kinetic energy), is not known explicitly and therefore has to be approximated. The quality of the used approximation to $E_{\mathrm{xc}}\left[n\right]$ is decisive for the success of any DFT-calculation. Frequently used approximations and their properties will be discussed in section 1.4.

The KS potential $v_\sigma^{\mathrm{KS}}\left(\mathbf{r}\right)$ results from the functional derivative of Eq. (1.6) with respect to $n_\sigma\left(\mathbf{r}\right)$. One thus obtains the *Kohn-Sham Hamiltonian*

$$
\begin{aligned}
\hat{h}_\sigma^{\mathrm{KS}}\left(\mathbf{r}\right) &= -\frac{\hbar^2}{2m}\nabla^2 + v_\sigma^{\mathrm{KS}}\left(\mathbf{r}\right) \\
&= -\frac{\hbar^2}{2m}\nabla^2 + v_{\mathrm{Hart}}\left(\mathbf{r}\right) + v_{\mathrm{ext}}\left(\mathbf{r}\right) + v_{\mathrm{xc},\sigma}\left(\mathbf{r}\right) ,
\end{aligned}
\tag{1.10}
$$

which includes the Hartree-potential $v_{\mathrm{Hart}}\left(\mathbf{r}\right) = e^2 \int \frac{n(\mathbf{r}')}{\left|\mathbf{r}-\mathbf{r}'\right|} d\mathbf{r}'$ and the exchange-correlation potential $v_{\mathrm{xc},\sigma}\left(\mathbf{r}\right) = \delta E_{\mathrm{xc}}/\delta n_\sigma\left(\mathbf{r}\right)$.

By definition, the KS potential is that auxiliary external potential for which non-interacting particles yield the same total density $n\left(\mathbf{r}\right)$ as the fully interacting particles in the physical external potential $v_{\mathrm{ext}}\left(\mathbf{r}\right)$. Note that it is not clear *per se* that such a potential exists for all possible densities. However, all reasonably well-behaved densities that are of practical importance correspond to an existing external potential, i.e., they are *v-representable*. For a detailed discussion of the *v-representability problem* the reader is referred to Ref. [24] and

references therein.

Solving the KS equations (1.3), i.e., diagonalizing the KS Hamiltonian, lies at the very heart of any implementation of KS DFT. Importantly, only the exchange correlation potential is approximated in the KS equations. This clearly emphasizes the importance of the used approximation to $v_{\mathrm{xc},\sigma}$.

1.3. The self-interaction problem

One of the most basic and most often discussed problems in DFT is also one of the oldest ones. Its origin lies at the very heart of the KS scheme, and actually it is even older than DFT itself: the *self-interaction problem* [106].

From a historical point of view, the KS equations can be seen as an improvement of the equations published by Hartree only few years earlier. Whereas Hartree's equations ignored all non-classical electron-electron interactions, Kohn and Sham introduced the exchange-correlation potential which, by definition, carries everything that has been neglected in the Hartree formulation. However, many important features of Hartree's equations are shared by the formulation of Kohn and Sham, such as the treatment of the kinetic energy and the formulation of the classical Coulomb interaction as a functional of the charge density. This is why the Coulomb interaction energy of Eq. (1.8) is called the *Hartree energy*. If one evaluates Eq. (1.8) for a one-electron problem, e.g., the hydrogen atom, the non-zero Hartree energy describes the Coulomb interaction of one electron with itself. Of course, this spurious self-interaction is also present in many-electron systems, although in this case it is much less palpable.

At first sight this erroneous treatment of the classical particle-particle interaction is not disturbing, as the exchange-correlation functional E_{xc} should, by construction, correct for it. However, while the exact E_{xc} naturally corrects for Hartree self-interaction, commonly used approximations do not entirely correct for self-interaction in many-electron systems. Even worse, being approximate functionals of the density themselves, they typically introduce a second self-interaction error. As will be demonstrated in this thesis (see, e.g., section 3.3.1), one of the key features of the commonly used approximations to E_{xc} is that these two contributions to the self-interaction energy cancel to a large extent. In the following section, some of the most important approximations to E_{xc} and their performance in correcting the self-interaction error will be discussed.

Self-interaction and its correction play a central role in this thesis. A main step for correcting self-interaction, however, is the definition of self-interaction in systems with many electrons. Possible definitions and their consequences will be discussed in detail in chapter 2.

1.4. Approximate exchange correlation functionals

Although KS DFT is exact in principle, the exact exchange-correlation functional is generally unknown. Hence, it has to be approximated in practice. Numerous approximations to the exact E_{xc} can be found in the literature and an exhaustive discussion certainly goes beyond the scope of this thesis. The most commonly used approximations can be classified upon the number and kind of their ingredients. In the following, three classes of functionals and

their most important representatives will be discussed. Note that appendix A.4 provides a list of all functionals used in this thesis and their abbreviations.

1.4.1. Semilocal functionals

Functionals that employ only local quantities such as the spin-density $n_\sigma(\mathbf{r})$ and its derivatives or the kinetic energy density are called *semilocal functionals*. This class of functionals is by far the most popular and most often used one. This is due to their excellent accuracy-to-computational-cost ratio and, with some reservations, the ease of their implementation in DFT codes.

In general however, semilocal functionals are not able to correct entirely for self-interaction and, as a consequence, often suffer from notorious failures (see, e.g., Ref. [67] and publication 2 for an overview and pertinent references). In semilocal functionals, self interaction typically leads to incorrect dissociation limits, underestimation of energy barriers to chemical reactions, and a wrong asymptotic behavior of the exchange-correlation potential (with all its consequences, such as instability of many experimentally stable anions, the absence of a Rydberg series, wrong long range interactions, etc.). Semilocal functionals are usually not able to describe electron-localization effects in transition metal oxides and widely overestimate charge transfer properties such as the polarizability of molecular chains and electronic transport in molecular devices.

The oldest and most popular representative of the class of semilocal functionals is the *local density approximation* (LDA) [46]. This approximation is based on the homogeneous electron gas limit, for which the exact exchange energy density is known analytically as [22]

$$\epsilon_{\mathrm{x}}^{\mathrm{hom}}[n] = -\frac{3}{4}\left(\frac{3}{\pi}\,n\right)^{\frac{1}{3}}e^2 \tag{1.11}$$

and the numerically exact correlation energy density $\epsilon_{\mathrm{c}}^{\mathrm{hom}}$ can be evaluated on the basis of a suitable parametrization [14, 106, 105]. With $\epsilon_{\mathrm{xc}}^{\mathrm{hom}} = \epsilon_{\mathrm{x}}^{\mathrm{hom}} + \epsilon_{\mathrm{c}}^{\mathrm{hom}}$ the LDA-energy then reads

$$E_{\mathrm{xc}}^{\mathrm{LDA}}[n] = \int n(\mathbf{r})\,\epsilon_{\mathrm{xc}}^{\mathrm{hom}}[n(\mathbf{r})]\,d\mathbf{r}\,. \tag{1.12}$$

A straightforward improvement of the LDA approach can be achieved by introducing the density gradients $\nabla n_\sigma(\mathbf{r})$ weighted by fitting parameters as corrections to Eq. (1.12). These approaches are called *generalized gradient approximations* (GGAs). The parameters can either be determined via a *constrained satisfaction* technique, i.e., the functional is fitted to satisfy as many exact constraints as possible, or by *empirical fitting*, i.e., numerical fitting to selected data sets from experiment or more involved wave-function-based studies. Among the most popular GGAs are the non-empirical GGA provided by Perdew, Burke and Ernzerhof (PBE) [101] and the semiempirical BLYP which combines Becke88 exchange [7] with the correlation functional given by Lee, Yang, and Parr [72].

A special type of semilocal functionals is given by the so-called *meta-GGAs*. A functional is called a meta-GGA if it employs the kinetic energy density $\tau_\sigma(\mathbf{r}) = \frac{\hbar^2}{2m}\sum_{i=1}^{N_\sigma} f_{i\sigma}|\nabla\varphi_{i\sigma}(\mathbf{r})|^2$ or the Laplacian $\nabla^2 n_\sigma$ in $E_{\mathrm{xc},\sigma}$. Hence meta-GGAs, although employing only local quantities and their derivatives, can also fall into another category, i.e, the *orbital functionals*.

1.4.2. Orbital functionals

Functionals that employ the orbitals $\varphi_{i\sigma}$ explicitely in E_{xc} are called *orbital functionals*. Equivalent to the case of the kinetic energy density (see Eq. (1.9) and following discussion), orbital functionals are implicit density functionals by virtue of the KS equations. For a detailed review on orbital functionals the reader is referred to Ref. [67].

There are several arguments for using orbitals in the construction of improved exchange-correlation functionals, the probably strongest one being the fact that the inclusion of orbitals allows to compensate for Hartree self-interaction. The most prominent orbital-functional is given by the formulation of the Fock integral in terms of the KS orbitals, i.e, the *exact exchange functional* (EXX)

$$E_{\mathrm{x}}\left[\{\varphi_{i\tau}\}\right] = -\frac{e^2}{2} \sum_{\sigma=\uparrow,\downarrow} \sum_{j,k=1}^{N_\sigma} f_{j\sigma} f_{k\sigma} \iint \frac{\varphi_{j\sigma}^*\left(\mathbf{r}\right)\varphi_{k\sigma}^*(\mathbf{r}')\varphi_{k\sigma}\left(\mathbf{r}\right)\varphi_{j\sigma}(\mathbf{r}')}{|\mathbf{r}-\mathbf{r}'|}\, d\mathbf{r}\, d\mathbf{r}'\,. \quad (1.13)$$

In this approach, the Hartree self-interaction energy is compensated by the intra-orbital exchange, whereas the inter-orbital exchange energy is treated exactly. However, the remaining parts of E_{xc}, i.e., the interacting kinetic energy as well as the correlation energy, are neglected completely. Although being able to heal many of the above-mentioned problems of semilocal functionals (see, e.g., Ref. [67] for an overview), EXX suffers from the absence of a compatible correlation functional, the significant increase in numerical costs as compared to semilocal functionals, and the unfavorable quadratic scaling of the exchange energy with the number of electrons.

Orbital functionals allow to introduce additional flexibility in the construction of functionals. However, there is a price that one has to pay. Solution of the KS scheme requires an expression for the exchange-correlation potential $v_{\mathrm{xc},\sigma}\left(\mathbf{r}\right) = \delta E_{\mathrm{xc}}/\delta n_\sigma\left(\mathbf{r}\right)$. For the case of an orbital functional $E_{\mathrm{xc}}\left[\{\varphi_{j\tau}\}\right]$ however, taking this functional derivative is significantly more involved than for explicit density functionals. By virtue of the chain rule

$$v_{\mathrm{xc},\sigma} = \sum_{\alpha=\uparrow,\downarrow} \sum_{\beta=\uparrow,\downarrow} \sum_{i=1}^{N_\alpha} \iint \left(\frac{\delta E_{\mathrm{xc}}\left[\{\varphi_{j\tau}\}\right]}{\delta\varphi_{i\alpha}(\mathbf{r}')} \frac{\delta\varphi_{i\alpha}(\mathbf{r}')}{\delta v_\beta^{\mathrm{KS}}(\mathbf{r}'')} + \mathrm{c.c.} \right) \frac{\delta v_\beta^{\mathrm{KS}}(\mathbf{r}'')}{\delta n_\sigma\left(\mathbf{r}\right)}\, d\mathbf{r}'\, d\mathbf{r}'' \quad (1.14)$$

and by evaluating the functional derivative $\delta\varphi_{i\alpha}(\mathbf{r}')/\delta v_\beta^{\mathrm{KS}}(\mathbf{r}'')$ on the basis of the KS equations one obtains an integral equation for $v_{\mathrm{xc},\sigma}$:

$$\sum_{i=1}^{N_\sigma} f_{i\sigma} \int \varphi_{i\sigma}^*(\mathbf{r}') \left(v_{\mathrm{xc},\sigma}^{\mathrm{OEP}}(\mathbf{r}') - u_{\mathrm{xc},i\sigma}(\mathbf{r}') \right) G_{i\sigma}(\mathbf{r}',\mathbf{r})\, \varphi_{i\sigma}\left(\mathbf{r}\right) d\mathbf{r}' + \mathrm{c.c.} = 0\,, \quad (1.15)$$

where

$$u_{\mathrm{xc},i\sigma}\left(\mathbf{r}\right) \quad := \quad \frac{1}{f_{i\sigma}\,\varphi_{i\sigma}^*\left(\mathbf{r}\right)} \frac{\delta E_{\mathrm{xc}}\left[\{\varphi_{j\tau}\}\right]}{\delta\varphi_{i\sigma}\left(\mathbf{r}\right)}\,, \quad (1.16)$$

$$G_{i\sigma}(\mathbf{r},\mathbf{r}') \quad := \quad \sum_{\substack{k=1 \\ k\neq i}}^{\infty} \frac{\varphi_{k\sigma}\left(\mathbf{r}\right)\varphi_{k\sigma}^*(\mathbf{r}')}{\epsilon_{i\sigma}-\epsilon_{k\sigma}}\,. \quad (1.17)$$

Eq. (1.15) is the *optimized effective potential equation* [121, 124, 37]. Solving this equation for

$v_{\mathrm{xc},\sigma}^{\mathrm{OEP}}$ yields the *optimized effective potential* (OEP), i.e., the exchange-correlation potential which by virtue of the KS equation yields those KS orbitals that minimize the total energy corresponding to the orbital-functional $E_{\mathrm{xc}}\left[\{\varphi_{j\tau}\}\right]$. The OEP-equation plays a central role in the theory of orbital functionals. Its detailed derivation and a thorough discussion of its properties can be found, e.g., in Ref. [67].

As demonstrated in Ref. [60] and further clarified in Refs. [37] and [69], the OEP equation (1.15) can be written in an alternative form that takes a simple interpretation:

$$-\delta n\left(\mathbf{r}\right) = -\sum_{i=1}^{N_\sigma} \delta\varphi_{i\sigma}^*\left(\mathbf{r}\right)\varphi_{i\sigma}\left(\mathbf{r}\right) + c.c. = 0\,, \tag{1.18}$$

where

$$\delta\varphi_{i\sigma}^*\left(\mathbf{r}\right) = f_{i\sigma} \sum_{\substack{j=1 \\ j\neq i}}^{\infty} \frac{\int \varphi_{i\sigma}^*(\mathbf{r}') \left[u_{\mathrm{xc},i\sigma}(\mathbf{r}') - v_{\mathrm{xc},\sigma}^{\mathrm{OEP}}(\mathbf{r}')\right] \varphi_{j\sigma}(\mathbf{r}')\, d\mathbf{r}'}{\epsilon_{i\sigma} - \epsilon_{j\sigma}}\, \varphi_{j\sigma}^*\left(\mathbf{r}\right) \tag{1.19}$$

is the first-order perturbation-theory shift in $\varphi_{i\sigma}^*$ subject to the perturbation potential

$$\Delta v_{i\sigma}\left(\mathbf{r}\right) = u_{\mathrm{xc},i\sigma}\left(\mathbf{r}\right) - v_{\mathrm{xc},\sigma}^{\mathrm{OEP}}\left(\mathbf{r}\right)\,. \tag{1.20}$$

Eq. (1.18) states that the optimal (i.e., yielding the lowest total energy) exchange-correlation potential $v_{\mathrm{xc},\sigma}^{\mathrm{OEP}}\left(\mathbf{r}\right)$ to replace the orbital-specific potential $u_{\mathrm{xc},i\sigma}\left(\mathbf{r}\right)$ is the one that makes the change in the density vanish to first order in the perturbation $\Delta v_{i\sigma}\left(\mathbf{r}\right)$.

Note that Eq. (1.18) does not only yield an alternative interpretation of the OEP but also opens the way for an algorithm to numerically solve the OEP equation [69, 70] (further details on this approach will be provided in section 3.1). However, solving the OEP-equation exactly is computationally very costly. Thus, there is a need for good approximations to the exact OEP. In the literature, a number of approximations to the OEP can be found, the most popular one being the approximation given by Krieger, Lee, and Iafrate (KLI) [61, 60]. The basic idea of the KLI-approach is the approximation $\epsilon_{i\sigma} - \epsilon_{k\sigma} \approx \Delta\epsilon = \mathrm{const.}$, for which Eq. (1.15) can be solved analytically. Importantly, the resulting KLI potential

$$v_{\mathrm{xc},\sigma}^{\mathrm{KLI}}\left(\mathbf{r}\right) = \frac{1}{2n_\sigma}\sum_{i=1}^{N_\sigma}\left\{\left|\varphi_{i\sigma}\left(\mathbf{r}\right)\right|^2\left[u_{\mathrm{xc},i\sigma}\left(\mathbf{r}\right) + \left(\bar{v}_{\mathrm{xc},i\sigma}^{\mathrm{KLI}} - \bar{u}_{\mathrm{xc},i\sigma}\right)\right]\right\} + c.c.\,, \tag{1.21}$$

where

$$\bar{v}_{\mathrm{xc},i\sigma}^{\mathrm{KLI}} \quad := \quad \int \varphi_{i\sigma}^*(\mathbf{r}')\, v_{\mathrm{xc},\sigma}^{\mathrm{KLI}}(\mathbf{r}')\, \varphi_{i\sigma}(\mathbf{r}')\, d\mathbf{r}'\,, \tag{1.22}$$

$$\bar{u}_{\mathrm{xc},i\sigma} \quad := \quad \int \varphi_{i\sigma}^*(\mathbf{r}')\, u_{\mathrm{xc},i\sigma}(\mathbf{r}')\, \varphi_{i\sigma}(\mathbf{r}')\, d\mathbf{r}'\,, \tag{1.23}$$

is thus derived from an approximation in the potential and not in the energy functional. Strictly speaking, the KLI-approximation therefore defines a *potential functional*. A corresponding energy functional does not exist. This leads to a couple of fundamental and numerical problems, especially when evaluating the energy functional or its derivatives directly (see, e.g., Ref. [66]) or in the time-dependent case [92, 93]. However, the KLI-approximation can

be formally justified by the fact that, given the set of orbitals derived from a self-consistent OEP calculation, changing the potential from OEP to KLI does not (directly) affect the total energy [60, 37]. Hence, the KLI-approach yields a reasonable approximation to OEP as long as the employed approximation in the potential does not substantially affect the self-consistent iteration of the KS equations. However, in publication 1 it is demonstrated that the latter assumption does not always hold. As a consequence, the KLI-approximation can fail dramatically.

As will be shown in chapter 2, standard OEP is not a suitable approach for all orbital functionals. Hence, a generalized version of the OEP equation is derived in section 2.2.2. In this context, further details on the OEP formalism will be provided.

1.4.3. Hybrid functionals

Exact exchange as well as the Hartree-Fock (HF) approach correct for Hartree self-interaction, but they do not employ correlation. In contrast, semilocal functionals employ a consistent definition of local exchange and correlation, however, without being able to correct entirely for Hartree self-interaction. The idea of *hybrid functionals* is to take advantage of the best of both worlds by mixing a fixed fraction of HF-exchange $E_{\mathrm{x}}^{\mathrm{HF}}$ with a fixed fraction of semilocal exchange $E_{\mathrm{x}}^{\mathrm{sl}}$ and correlation $E_{\mathrm{c}}^{\mathrm{sl}}$, i.e.,

$$E_{\mathrm{xc}}^{\mathrm{hybrid}} = a_0^{\mathrm{HF}} E_{\mathrm{x}}^{\mathrm{HF}} + \left(1 - a_0^{\mathrm{HF}}\right) E_{\mathrm{x}}^{\mathrm{sl}} + E_{\mathrm{c}}^{\mathrm{sl}}. \tag{1.24}$$

The parameter a_0^{HF} depends on the used semilocal functional. Typically, it is determined empirically [8] or rationalized via the fundamental *adiabatic connection theorem* [75, 103].

Strictly speaking, a hybrid functional is just a special case of an orbital functional, and the corresponding exchange-correlation potential could be derived via the OEP equation (1.15). In practice however, one typically derives the KS potential for hybrids as the sum of a fraction of the orbital-specific Fock potential operator coming from the exact exchange part and a fraction of the exchange-correlation potential coming from the employed semilocal functional. This proceeding is computationally less costly and pragmatically justified by the fact that the usually small difference between the thus obtained potential and the corresponding OEP can largely be buried in the fitting parameter a_0^{HF}. Formally, the introduction of an integral operator in the potential can be justified on the basis of a concept known as the *generalized Kohn-Sham scheme* [119]. In this scheme, DFT is conceptually based on an interacting reference system that can still be represented by a single Slater determinant. For a more detailed discussion the reader is referred to Ref. [67] and references therein.

Another pragmatic step in the development of hybrid functionals was to include more than one fittable parameter in the functional form. Today, most of the commonly used hybrid functionals employ 3 parameters that are fitted to yield good results for a large set of systems and observables. The most popular representative of this new class of hybrids is the B3LYP-functional [122]

$$E_{\mathrm{xc}}^{\mathrm{B3LYP}} = E_{\mathrm{xc}}^{\mathrm{LDA}} + a_0^{\mathrm{HF}} \left(E_{\mathrm{x}}^{\mathrm{HF}} - E_{\mathrm{x}}^{\mathrm{LDA}}\right) + a_x \left(E_{\mathrm{x}}^{\mathrm{B88}} - E_{\mathrm{x}}^{\mathrm{LDA}}\right) + a_c \left(E_{\mathrm{c}}^{\mathrm{LYP}} - E_{\mathrm{c}}^{\mathrm{LDA}}\right), \tag{1.25}$$

which employs the Becke88 GGA for exchange $E_{\mathrm{x}}^{\mathrm{B88}}$ [7], the GGA for correlation given by Lee, Yang, and Parr $E_{\mathrm{c}}^{\mathrm{LYP}}$ [72], and $E_{\mathrm{xc}}^{\mathrm{LDA}}$ in the parametrization of Vosko, Wilk and Nusair [137]. By fitting a set of atomization energies, ionization potentials, proton affinities and

total atomic energies, the empirical parameters were determined to $a_0^{\mathrm{HF}} = 0.20$, $a_x = 0.72$, and $a_c = 0.81$. Note that by including the semi-empirical GGA expressions Becke88 and LYP, the effective number of parameters in B3LYP is 8, not 3.

Hybrid functionals only correct for a fraction of the total Hartree self-interaction energy. Hence, hybrids are generally not free from self-interaction. However, many of the above mentioned failures of semilocal functionals can be cured by including a fraction of exact exchange in the functional and by fitting the empirical parameters to ever larger training sets. As a consequence, modern hybrid functionals such as B3LYP usually yield very accurate results for a wide range of observables. Due to its slightly better performance as compared to other hybrids and despite its *ad hoc* construction, B3LYP has become the most popular among all hybrid functionals and a work horse for practical applications of KS DFT, in particular within the organic chemistry community.

1.5. Properties of the exact functional

The overview of functionals provided in the previous section shows that a large variety of different approaches to approximate the exact exchange-correlation functional exists. All functionals have certain pros and cons related to their accuracy and computational costs. However, at the end of the day it all depends on the accuracy of a functional in determining the observable of interest. Therefore, the first step of every DFT calculation is to ensure the reliability of the used functional for the investigated system. A convenient way to test the accuracy of a functional is to compare its properties to those of the exact one. This section introduces those properties of the exact functional which are of direct importance for the problems studied in this work.

I start this overview with a discussion of the behavior of the exact functional for fractional particle numbers. The latter has been shown to be decisive for a functional's ability to correctly predict charge transfer properties such as the polarizabilities of molecular chains or charge transfer excitations. Hence, this discussion yields important background for sections 1.6.3 and 4.1 as well as for publication 1.

1.5.1. Kohn-Sham DFT for fractional particle numbers

Mermin's generalization of the Hohenberg-Kohn theorem to equilibrated systems in a reservoir [84] allows to introduce the concept of fractional particle numbers to ground-state DFT. This concept provides the basis for the inclusion of fractional occupation numbers into the KS scheme, i.e., using $f_{i\sigma}$ with $0 \leq f_{i\sigma} \leq 1$ in the equations of section 1.2. In doing this, it allows to determine several decisive properties of the exact functional.

Following an argument of Janak [48], the derivative of the total energy with respect to the occupation numbers $f_{i\sigma}$ (orbitals are kept fixed) yields

$$\frac{\partial E}{\partial f_{i\sigma}} = \epsilon_{i\sigma} \,, \tag{1.26}$$

where $\epsilon_{i\sigma}$ and $f_{i\sigma}$ are KS eigenvalue and occupation number corresponding to the ith orbital of spin σ, respectively. Eq. (1.26) is known as *Janak's theorem*.

Minimizing E with respect to $f_{i\sigma}$ subject to the constraint of particle conservation (see

Eq. (1.5)) is equivalent to the minimization of $E - \mu M$ (using the Lagrange multiplier μ), which yields

$$\delta(E - \mu M) = \sum_{\sigma=\uparrow,\downarrow} \sum_{i=1}^{N_\sigma} (\epsilon_{i\sigma} - \mu)\, \delta f_{i\sigma} \geq 0 \,. \tag{1.27}$$

Note that it's the additional constraints $0 \leq f_{i\sigma} \leq 1$ that make Eq. (1.27) an inequality [106]. Eq. (1.27) states that orbitals $\varphi_{i\sigma}$ with eigenvalues $\epsilon_{i\sigma} < \mu$ are fully occupied, i.e., $\delta f_{i\sigma} \leq 0$ and thus $f_{i\sigma} = 1$ and those with $\epsilon_{i\sigma} > \mu$ have $\delta f_{i\sigma} \geq 0$ and thus $f_{i\sigma} = 0$. Degeneracy aside, fractional occupation is thus only allowed for the one orbital $\varphi_{H\sigma}$ for which $\epsilon_{H\sigma} = \mu$. Eq. (1.27) is called *aufbau principle*, μ can be identified as the *chemical potential* or the *negative electronegativity* of the system and $\varphi_{H\sigma}$ is called the *highest occupied molecular orbital* (HOMO) of spin σ. In combination with Janak's theorem, the aufbau principle thus yields

$$\frac{\partial E}{\partial f_{H\sigma}} = \frac{\partial E}{\partial M} = \mu = \epsilon_{H\sigma} \,. \tag{1.28}$$

Hence, the KS eigenvalue of the HOMO has a clear physical meaning. If calculated with the exact functional, it equals the exact ionization potential. In this sense, Janak's theorem can be interpreted as an analog of Koopman's theorem within KS DFT, the latter stating that *all* HF-eigenvalues can be interpreted as approximative electron removal energies. Note however, that in KS DFT only the KS eigenvalue corresponding to the HOMO has a clear and distinct physical meaning. Still, it is possible to interpret KS eigenvalue differences as well-defined approximations to excitation energies (see discussion in section 1.5.5).

Further insight was provided by Perdew *et al.* who, by employing the *constrained search* technique, showed that the relaxed ground-state energy of a system consisting of $N + \omega$ particles, where N is an integer and $0 \leq \omega \leq 1$, is given by [104]

$$E_{N+\omega} = (1 - \omega)\, E_N + \omega\, E_{N+1} \,. \tag{1.29}$$

Here, E_N is the exact ground-state energy of the N-particle system. Thus, the exact total energy of a finite system with non-integer particle number varies linearly with the fractional occupation as shown in Fig. 1.1. At integer occupations however, the derivative of the energy with respect to the fractional occupation jumps discontinuously. The value of this discontinuity Δ is given by the difference of the system's ionization potential $I(N)$ and electron affinity $A(N)$, which according to Eq. (1.28) can be written as (spin indices omitted)

$$I(N) = -\lim_{\omega \to 0} \mu(N - \omega) \,, \qquad A(N) = -\lim_{\omega \to 0} \mu(N + \omega) \,, \tag{1.30}$$

$$\Delta := I(N) - A(N) \,. \tag{1.31}$$

Using the *variational principle*, i.e., $\delta\left(E - \mu M\right) = \delta\left(E - \mu \int n\left(\mathbf{r}\right) d\mathbf{r}\right) = 0$, one can further derive the *Euler equation* [104]

$$\frac{\delta E\left[n\right]}{\delta n\left(\mathbf{r}\right)} = \mu \,. \tag{1.32}$$
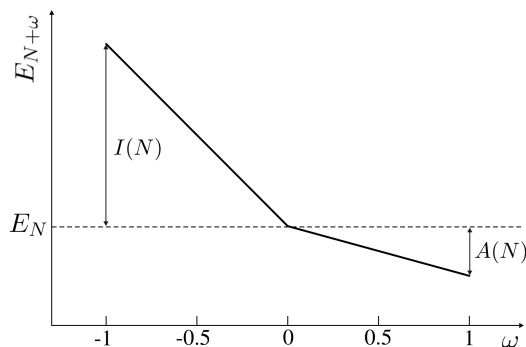
Figure 1.1:
Exact ground-state energy of a finite system with non-integer electron number $N + \omega$. $I(N)$ is the ionization potential and $A(N)$ the electron affinity of the system with integer electron number N. Note the discontinuous derivative of the energy at integer electron number.

Hence, Δ can be split into two contributions:

$$
\begin{aligned}
\Delta = I(N) - A(N) &= \lim_{\omega \to 0} \{ \mu(N + \omega) - \mu(N - \omega) \} \qquad (1.33) \\
&= \lim_{\omega \to 0} \left\{ \left. \frac{\delta E[n]}{\delta n(\mathbf{r})} \right|_{N+\omega} - \left. \frac{\delta E[n]}{\delta n(\mathbf{r})} \right|_{N-\omega} \right\} \\
&= \underbrace{\epsilon_{N+1} - \epsilon_N}_{\Delta_{KS}} + \underbrace{\lim_{\omega \to 0} \left\{ \left. v_{\mathrm{xc}}(\mathbf{r}) \right|_{N+\omega} - \left. v_{\mathrm{xc}}(\mathbf{r}) \right|_{N-\omega} \right\}}_{\Delta_{\mathrm{xc}}} \\
&= \phantom{\underbrace{\epsilon}} \Delta_{KS} + \Delta_{\mathrm{xc}} \, .
\end{aligned}
$$

As an important consequence, the exact exchange-correlation potential $v_{\mathrm{xc}}(\mathbf{r})$ jumps discontinuously by a constant Δ_{xc} when the particle number crosses an integer. Δ_{xc} is called the *derivative discontinuity of* E_{xc}. Note that, strictly speaking, the concept of the derivative discontinuity is only applicable to open systems with a non-integer number of electrons. However, as will be discussed in the following two sections, it has very important consequences also in systems with an integer number of electrons.

1.5.2. The gap-problem

Following Janak's theorem, the HOMO-eigenvalue as calculated with the exact functional equals a system's ionization potential. Inspired by this exact relation, it seems a natural approach to calculate the energy gap between a system's ground state and its lowest excited state as the difference between the eigenvalues of HOMO and HOMO+1, i.e., the *Kohn-Sham gap* $\Delta_{KS} = \epsilon_{H+1} - \epsilon_H$. However, calculations routinely find KS gaps that are significantly smaller than experimental excitation gaps. This ambiguity is a frequent source of confusion in the literature and will be referred to as the *gap-problem* in the following.

There are two fundamentally different experimental gaps that should be distinguished in a thorough discussion of the gap problem. The *optical gap* is the energy difference between a system's ground state and its first optically accessible excited state. The proper way for computing the optical gap is to use time-dependent DFT (TDDFT), which will be discussed in section 1.6. However, on the basis of *Görling-Levy perturbation theory* [76, 36] (see section 1.5.5 for a discussion), it has been argued that KS eigenvalue differences calculated from a suitable functional can be interpreted as zeroth-order approximations to optical excitation energies. Still, despite this formal argument there is no fundamental reason why KS eigenvalue differences should agree *exactly* with optical excitation energies, even if they are calculated with the exact functional.

The *fundamental gap* is the difference between a system's ionization potential and its electron

affinity. Although from a fundamental point of view the fundamental gap is an excited state property, it could in principle be derived exactly from two separate ground-state calculations on the N and the $N+1$ electron system. However, it can not be derived from a single ground-state calculation on the neutral system. The reason for this is buried in Eq. (1.33): while the KS gap Δ_{KS} can be evaluated on the basis of a single ground-state calculation, the derivative discontinuity Δ_{xc} can only be evaluated on the basis of at least two separate calculations that employ a different total number of electrons.

Hence, even for the exact functional the KS gap does not agree with any experimental gap. Therefore, any search for the "ultimate functional" that would yield highly accurate excitation gaps from a single ground-state calculation is inherently doomed. Still, there are high hopes to find functionals that are able to predict reasonable gaps based on a systematic cancellation of errors. E.g., it has been shown that in many cases B3LYP yields KS gaps that are very close to the optical gap, especially for π-systems such as organic semiconductors. Note that an example of this cancellation of errors in the B3LYP KS gap of organic semiconductors is provided in publication 4.

1.5.3. Step-like structure of the exchange-correlation potential

As discussed above, the derivative discontinuity in the exact E_{xc} only shows up if one varies the fractional number of electrons in a system across an integer. However, under certain circumstances a doppelganger of the derivative discontinuity can be found in calculations with fixed, integer occupation numbers. This doppelganger is usually referred to as the *step-like structure of the exchange-correlation potential*. A typical situation in which the step-like structure of the potential becomes apparent is also a particularly important one: charge transfer between two separated atoms or molecules.

Imagine two equal atoms A and B at large separation. If the atoms are sufficiently separated, the exact exchange-correlation potential v_{xc} of this model-system is basically a sum of the potentials of the single atoms as indicated in Fig. 1.2 a). Now assume that an infinitesimal fraction ω of an electron is transfered from B to A (note that ω represents a *negative* fractional charge). According to the discussion in section 1.5.1, the potential of A jumps by a constant Δ_{xc}^A while the potential of B basically remains unaffected by the infinitesimal charge transfer. As a consequence, a step appears in v_{xc} which counteracts the charge transfer (see Fig. 1.2 b)). As observed already early by Perdew *et al.* [104], this step in v_{xc} has important physical consequences as it suppresses charge fluctuations between neighboring atoms and molecules and thus assures the principle of *integer preference*: in a collection of separated objects, nature prefers to locate an integer number of electrons on each object.

Due to its charge-transfer counteracting behavior, the occurrence of a step-like structure in v_{xc} is of fundamental importance. In general, approximative functionals without a step-like structure will significantly overestimate charge transfer properties. However, as indicated by the above analysis, the occurrence of a step-like structure in the exchange-correlation potential requires a strong spatial non-locality in the functional. Hence, semilocal functionals fail badly in predicting charge transfer properties such as polarizabilities of molecular chains (see publication 1) or energies of charge-transfer excitations (see section 1.6.3 and publication 4). Although considerable progress has been made in including a step-like structure in semilocal functionals [4], a common approach to improve upon the performance of semilocal functionals is to go over to orbital functionals or hybrids [34, 68]. However, in several stud-
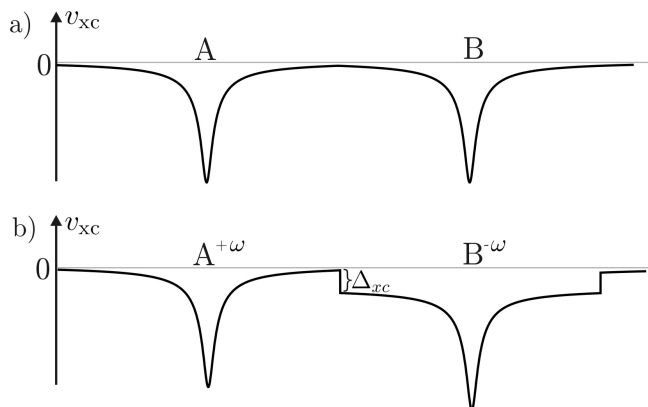
Figure 1.2:
a) Schematic description of the exact v_{xc} of a system of two equal subsystems A and B at large separation (arbitrary units).
b) Transfer of an infinitesimal fraction ω of an electron from B to A yields a discontinuous step in v_{xc} which counteracts the charge-transfer. Note that the potential is rescaled as compared to the one in a) so that it falls off to zero at infinity.

ies it has been found that a functionals treatment of the self-interaction error (SIE) plays a decisive role for its performance in charge-transfer problems (see, e.g., Refs. [99, 113] and publication 1). Therefore, the relation between the SIE and the derivative discontinuity will be the topic of the following section.

1.5.4. Self-interaction and the derivative discontinuity

The derivative discontinuity is a property of the generally unknown exact exchange-correlation functional in open systems. The step-like structure in the exact v_{xc} of a closed system is a direct consequence of the derivative discontinuity. In a number of publications, it has been shown that a step-like structure occurs in those approximations to E_{xc} that correct for the SIE. In contrast, functionals that are not at least approximately free from self-interaction typically show no step-like structure in the potential. These facts strongly indicate a close relation of self-interaction and the derivative discontinuity. This section provides an approximative but descriptive explanation of this relationship.

Imagine the following gedanken experiment: Take a system composed of two well separated and initially neutral atoms, e.g., Na and Cl, and assume an externally applied field that gradually transfers an electron from the HOMO of Na to the LUMO (*lowest unoccupied molecular orbital*) of Cl. In the following, let the total energy of the system be the observable of interest. Now consider two different situations. First, assume that this problem is treated with an approximative functional that does not suffer from self-interaction. Then, as the number of transfered electrons ω varies from 0 to 1, the atomic orbital being filled basically "sees" the potential of a neutral Cl-atom. Thus, the energy of the Cl-atom varies almost as if the extra orbital density is being filled in a constant potential, i.e., linearly with ω. The energy of the Na-atom also varies almost linearly with ω, as does the total energy. If however ω crosses an integer, the transferred electron will suddenly "see" a new potential, e.g., at $\omega = 0$ the potential on the Cl-side changes from of that of a positively charged Cl-ion to that of a neutral Cl-atom. This sudden jump of the potential yields an abrupt change in the slope of the total energy (see Fig. 1.3), i.e., a derivative discontinuity.

Then, assume that the same problem is treated with a functional that suffers from self-interaction, i.e., an approach in which the total energy accounts for the interaction of single electron densities with themselves. In this case, the potentials of Na and Cl and thus the total energy of the system vary smoothly with the number of transfered electrons. In
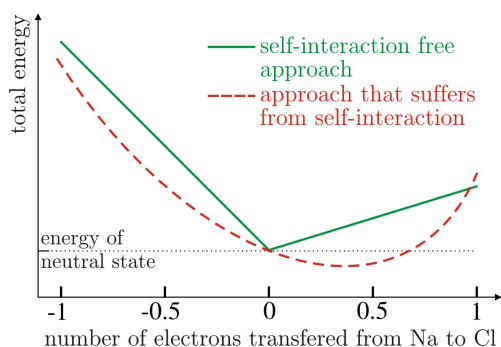
Figure 1.3:
Gedanken experiment: change in the total energy of a system composed of two well-separated atoms (Na and Cl) as a function of the number of electrons transfered from sodium to chlorine. Note that a self-interaction free approach yields a kink in the total energy at integer particle number whereas the energy varies rather smoothly in an approach that suffers from self-interaction.

particular, there is no sudden change in the potential at integer particle number. This is because the difference between the Cl-potential constructed from $17 - \omega$ electrons and the one constructed from $17 + \omega$ electrons (where $\omega \ll 1$) is negligible if the self-interaction of the transfered electron is accounted for in the construction of the potential. Further, as there is no discontinuity in the derivative of the total energy, no charge-transfer counteracting step-structure in the potential can be expected. As the chemical potential of Cl is lower in energy than the one of Na, the system can therefore gain energy by transferring a fraction of an electron from Na to Cl. Hence, a functional that suffers from self-interaction can yield a minimum of the total energy for a fractional number of transfered electrons and thereby violate the principle of integer preference.

Note that, although Fig. 1.3 can be constructed solely on the basis of the above gedanken experiment, the predicted behavior of the total energy for a system of well-separated Na- and Cl-atoms has in fact been proven by calculations that employ the LDA functional and a self-interaction corrected approach [100]. Note also that the above reasoning assumes a couple of approximations such as the neglect of relaxation effects. The influence of these approximations will be discussed in further detail in section 2.1.2.

The central statement of this section is that a functional's freeness from self-interaction is decisive for the inclusion of a step-like structure in the corresponding exchange-correlation potential and thus for an accurate prediction of charge-transfer properties. The question of how to correct semilocal functionals for self-interaction will be discussed in section 2.

1.5.5. The physical interpretation of Kohn-Sham eigenvalues

The combination of Janak's theorem and the aufbau principle as provided in Eq. (1.28) allows to assign a physical meaning to the eigenvalue of the HOMO: if calculated from the exact functional, it equals the exact ionization potential of the studied system. However, such a distinct statement does not exist for other KS eigenvalues. In particular, there is no one-to-one DFT-analog of Koopman's theorem, which states that the i-th HF-eigenvalue approximates the energy difference between the $(i + 1)$- and the i-particle system if the many-electron wave function of the system is approximated by a single Slater determinant of HF-orbitals.

Yet, *Görling-Levy perturbation theory* [76, 36] yields a methodology which allows to base the physical interpretation of KS eigenvalues on rigorous grounds. Its basic idea is to express the eigenenergies of the fully interacting system in terms of ground-state properties of the KS system by virtue of an *adiabatic connection* [42, 71, 41], which is characterized by the

Schrödinger equation

$$\left[\hat{T} + \alpha \, \hat{V}_{ee} + \hat{v}^{\alpha} \right] \psi_n^{\alpha} = E_n^{\alpha} \, \psi_n^{\alpha} \,, \tag{1.34}$$

with the kinetic energy $\hat{T}$, the electron-electron repulsion $\hat{V}_{ee}$ and the potential $\hat{v}^{\alpha}$. The square root of the *coupling constant* α can be interpreted as a factor scaling the elementary charge of the electron. Eq. (1.34) represents a continuous connection between the noninteracting KS system and the real physical system: for $\alpha = 1$ Eq. (1.34) turns into the Schrödinger equation of the fully interacting system in an external potential $\hat{v}^1 = v_{\text{ext}}$, whereas for $\alpha = 0$ the corresponding KS equations with $\hat{v}^0 = v_{\text{KS}}$ result. The requirement that the ground state ψ_0^{α} yields the density $n_0 \, (\mathbf{r})$ independently of the value of α defines the potential $v^{\alpha} \, [n_0, \mathbf{r}]$ along the coupling constant path up to an α-dependent additive constant.

In Ref. [36] Görling used the adiabatic connection methodology to show that the eigenenergies E_n^{α} of the fully interacting system can be developed in a Taylor series

$$E_n^{\alpha} = \sum_{k=0}^{\infty} \alpha^k \, {}^kE_n \,, \tag{1.35}$$

where the terms ${}^kE_n$ can be expressed in terms of KS eigenvalue differences, KS orbitals, and the external potential. In particular, the zeroth order contribution to the excitation energy between the ground state of the fully interacting system and the excited state that is adiabatically connected to the two KS states obtained by promoting an electron from orbital φ_i into orbital φ_j is given by the difference of the corresponding KS eigenvalues, i.e., $\epsilon_j - \epsilon_i$. In this sense, Görling-Levy perturbation theory assigns a well defined physical meaning to KS eigenvalues: their differences are approximations to excitation energies of *zeroth order in the electron-electron interaction*. In combination with Eq. (1.28), the KS eigenvalues themselves can be interpreted as zeroth order approximations to electron removal energies.

In order that the interpretation of KS eigenvalues is useful in practice, it is of course crucial that the approximation of zeroth order in the coupling constant is in fact a good one. However, this is not at all clear *per se* and must be tested thoroughly. In a number of publications [11, 2, 56, 62, 63, 132, 92], in particular in the work of Chong *et al.* [20], it is shown that KS eigenvalues usually compare surprisingly well to vertical ionization potentials, especially if they are calculated from high-quality KS potentials obtained from highly accurate *ab initio* densities. Clearly, these results warrant the physical reliability of the zeroth order approximation, yet at the same time they emphasize the importance of using high-quality functionals. In publication 3, it is demonstrated that it is mainly the absence of self-interaction in the used functional that plays a decisive role for the physical reliability of the occupied eigenvalue spectrum.

1.6. Time-dependent density functional theory

Following the Hohenberg-Kohn theorem, the ground-state density of a system uniquely determines its many-body Hamiltonian and thus all its properties. Hence, all ground and excited state properties are, at least in principle, encoded in the ground-state density. However, an explicit link between excited state properties and the ground-state density is not

known. Therefore, KS DFT is not a suitable approach to calculate excited state quantities. Yet, there is also a rigorous way for calculating excited state properties within a density functional framework, i.e., *time-dependent density functional theory* (TDDFT). More than twenty years after the formulation of its basic theorems, TDDFT has become one of the most prominent and most widely used approaches for the calculation of excitation energies, oscillator strengths and excited state geometries of medium to large molecular systems.

1.6.1. Background

The formal foundation of TDDFT is the *Runge-Gross theorem* [111]. This theorem can be interpreted as the time-dependent analogue of the first Hohenberg-Kohn theorem and it has been shown to be valid on rather general grounds [73]. Its central statement is that the densities $n(\mathbf{r}, t)$ and $n'(\mathbf{r}, t)$ evolving from a common initial state under the influence of two local potentials $v(\mathbf{r}, t)$ and $v'(\mathbf{r}, t)$ are always different provided that the potentials differ by more than a purely time-dependent function. In close analogy to the static case, most TDDFT calculations are based on the *time-dependent KS equations*

$$i\hbar \frac{\partial}{\partial t} \varphi_{j\sigma}(\mathbf{r}, t) = \left[-\frac{\hbar^2}{2m} \nabla^2 + v_\sigma^{\mathrm{KS}}(\mathbf{r}, t) \right] \varphi_{j\sigma}(\mathbf{r}, t) , \qquad (1.36)$$

in which the fully-interacting system is mapped to a non-interacting system evolving under the local *time dependent KS potential*

$$v_\sigma^{\mathrm{KS}}(\mathbf{r}, t) = v_{\mathrm{Hart}}(\mathbf{r}, t) + v_{\mathrm{ext}}(\mathbf{r}, t) + v_{\mathrm{xc},\sigma}(\mathbf{r}, t) . \qquad (1.37)$$

Although the time-dependent KS equations are exact in principle, the exchange-correlation part of the potential again has to be approximated in practice. As for ground-state DFT, the accuracy of TDDFT results strongly depends on the employed functional and the system and observable of interest. For many of the approximative functionals discussed in section 1.4 the extension to the time-dependent case is straightforward. Usually, one employs the *adiabatic approximation* in which the memory effects in the exact potential are neglected. As a consequence of this approximation, $v_{\mathrm{xc},\sigma}^{adiabatic}(\mathbf{r}, t)$ only depends on the density at time t and not on the density at all prior times $t' < t$. For a detailed discussion of memory effects the reader is referred to Ref. [127]. Detailed reviews on TDDFT, used functionals, and methodologies can be found, e.g., in Refs. [80, 25, 28].

The time-dependent KS equations can be solved explicitly by propagating the KS orbitals in time. This method is referred to as real-time TDDFT [142] (see also Refs. [92] and [127] for an overview). The most prominent and most often used TDDFT-approach however focuses on the analysis of the linear response regime within the Casida-formalism [13], which will be discussed in the following section.

1.6.2. Excitations from linear response and Casida's equations

According to the Runge-Gross theorem, any observable is a functional of the time-dependent density and of the initial state. Usually, one chooses the initial state to be the system's ground-state. In this case, the initial state itself is a functional of the density via the Hohenberg-Kohn theorem, and thus every observable is again a pure density functional. Then, in order to probe a system's excited state properties, an external field $v_{\mathrm{ext}}(\mathbf{r}, t)$ is

applied. The idea of *linear response TDDFT* is to analyze the first order density response to a weak excitation. By Fourier-transformation in time, one can identify the excitation energies of a system as the poles of its KS density response function in frequency space. Numerous reviews on linear response TDDFT can be found in the literature [80, 25, 28]. Therefore, only a short introduction is given in the following.

The central equations of the linear response formalism in TDDFT are *Casida's equations* [13] (spin indices and occupation numbers are omitted for clarity)

$$
\begin{bmatrix} \mathbf{A} & \mathbf{B} \\ \mathbf{B}^* & \mathbf{A}^* \end{bmatrix} \begin{bmatrix} \mathbf{X}_\omega \\ \mathbf{Y}_\omega \end{bmatrix} = \omega \begin{bmatrix} \mathbb{1} & 0 \\ 0 & -\mathbb{1} \end{bmatrix} \begin{bmatrix} \mathbf{X}_\omega \\ \mathbf{Y}_\omega \end{bmatrix} ,
\tag{1.38}
$$

where (in a general notation for hybrid functionals in the spirit of Eq. (1.24))

$$
\begin{aligned}
A_{ia,jb} &= \delta_{ij}\,\delta ab\,(\epsilon_a - \epsilon_i) + (ia|jb) - a_0^{\mathrm{HF}}(ij|ab) + (1 - a_0^{\mathrm{HF}})(ia|f_{\mathrm{xc}}|jb), \tag{1.39} \\
B_{ia,jb} &= (ia|bj) - a_0^{\mathrm{HF}}(ib|aj) + (1 - a_0^{\mathrm{HF}})(ia|f_{\mathrm{xc}}|bj) . \tag{1.40}
\end{aligned}
$$

Here, the two-electron integrals are given in *Mulliken notation*, i.e.,

$$
(ia|jb) := \iint \varphi_i^*(\mathbf{r})\varphi_a(\mathbf{r}) \frac{1}{|\mathbf{r} - \mathbf{r}'|} \varphi_j(\mathbf{r}')\varphi_b^*(\mathbf{r}') \, d\mathbf{r}\, d\mathbf{r}' ,
\tag{1.41}
$$

$$
(ia|f_{\mathrm{xc}}|jb) := \iint \varphi_i^*(\mathbf{r})\varphi_a(\mathbf{r})\, f_{\mathrm{xc}}(\mathbf{r}, \mathbf{r}')\, \varphi_j(\mathbf{r}')\varphi_b^*(\mathbf{r}') \, d\mathbf{r}\, d\mathbf{r}' ,
\tag{1.42}
$$

f_{xc} is the *exchange correlation kernel* of the semilocal functional $E_{\mathrm{xc}}^{\mathrm{sl}}$ used in Eq. (1.24)

$$
f_{\mathrm{xc}}(\mathbf{r}, \mathbf{r}') = \frac{\delta E_{\mathrm{xc}}^{\mathrm{sl}}}{\delta n(\mathbf{r})\,\delta n(\mathbf{r}')} ,
\tag{1.43}
$$

φ_i are the occupied (indices i and j) and unoccupied (indices a and b) KS orbitals of the system's ground-state, and ϵ_i are the corresponding KS eigenvalues. $\mathbf{A}$ and $\mathbf{B}$ are matrices of rank $(N_{\mathrm{occ}} \times N_{\mathrm{unocc}})^2$, where N_{occ} is the number of occupied and N_{unocc} the (finite) number of unoccupied orbitals in the employed basis. If both the KS orbitals and the kernel f_{xc} are real-valued, Eq. (1.38) can be cast into a Hermitian eigenvalue problem of dimension $N_{\mathrm{occ}} \times N_{\mathrm{unocc}}$ [13]

$$
(\mathbf{A} - \mathbf{B})^{1/2}\,(\mathbf{A} + \mathbf{B})\,(\mathbf{A} - \mathbf{B})^{1/2}\,\mathbf{Z}_\omega = \omega^2\,\mathbf{Z}_\omega ,
\tag{1.44}
$$

where

$$
\mathbf{Z}_\omega = (\mathbf{A} - \mathbf{B})^{-1/2}\,(\mathbf{X}_\omega + \mathbf{Y}_\omega) .
\tag{1.45}
$$

The eigenvalues ω^2 equal the square of the excitation frequency ω, and the eigenvectors $\mathbf{Z}_\omega$ are the corresponding *transition density matrices* in the basis of KS orbitals. One thus obtains the *transition density* $\rho_\omega(\mathbf{r})$ at energy ω

$$
\rho_\omega(\mathbf{r}) = \sum_i^{N_{\mathrm{occ}}} \sum_a^{N_{\mathrm{unocc}}} Z_{ia,\omega}\,(\epsilon_a - \epsilon_i)^{-1/2}\,\varphi_i(\mathbf{r})\,\varphi_a(\mathbf{r})
\tag{1.46}
$$

in terms of products of occupied and unoccupied KS orbitals. Oscillator strengths γ_ω for

dipole transitions can be obtained via

$$\gamma_\omega = \frac{2}{3} \sum_{\beta=1}^{3} \left| \mathbf{R}_\beta^T \, \mathbf{Q}^{1/2} \mathbf{Z}_\omega \right|^2 , \tag{1.47}$$

where

$$(\mathbf{R}_\beta)_{ia} = \int \varphi_i^* (\mathbf{r}) \, r_\beta \, \varphi_a (\mathbf{r}) \, d\mathbf{r}, \qquad (r_1, r_2, r_3) = (x, y, z) , \tag{1.48}$$

and

$$Q_{ia,jb} = \delta_{ij} \delta_{ab} \, (\epsilon_a - \epsilon_i) . \tag{1.49}$$

Note that a_0^{HF} vanishes for proper (non-hybrid) density functionals. By setting a_0^{HF} in Eqs. (1.39) and (1.40) to 1 one immediately obtains the linear response time-dependent Hartree-Fock (TDHF) equations. This shows the close analogy in the methodology of linear response TDDFT and TDHF. In general however, it is found that TDDFT excitation energies improve significantly upon those obtained from TDHF.

1.6.3. Charge-transfer excitations

Imagine two spatially separated molecules A and B where the orbitals of molecule A and the orbitals of molecule B have zero overlap. An excitation in which an electron is transfered from an occupied state on A to an unoccupied state of B is called a charge-transfer (CT) excitation. As the obtained negative and positive charges on A and B electrostatically attract each other, the energy of the CT state has a $1/R$-dependence, where R is the distance between A and B. In the limit $R \to \infty$, the CT excitation energy approaches the difference between the ionization potential of A and the electron affinity of B, i.e., $I_A - A_B$.

The behavior of linear response TDDFT for charge transfer excitations can be understood on the basis of Eqs. (1.39) and (1.40). As the overlap between orbitals i, j at molecule A and orbitals a, b at molecule B is negligible, one obtains

$$
\begin{align}
A_{ia,jb} &= \delta_{ij} \, \delta_{ab} \, (\epsilon_a - \epsilon_i) - a_0^{\mathrm{HF}} (ij|ab) + (1 - a_0^{\mathrm{HF}})(ia|f_{\mathrm{xc}}|jb), \tag{1.50} \\
B_{ia,jb} &= (1 - a_0^{\mathrm{HF}})(ia|f_{\mathrm{xc}}|bj) . \tag{1.51}
\end{align}
$$

As long as the used exchange-correlation kernel f_{xc} does not have a singularity which is able to compensate for the vanishing overlap of the orbitals, $\mathbf{B}$ and the last term in $\mathbf{A}$ vanish. As a result of Eq. (1.44), the excitation energy of a CT state as calculated from a pure density functional ($a_0^{\mathrm{HF}} = 0$) is then simply given by the difference of the KS eigenvalues of the electron-donating and the electron-accepting molecular orbitals ϵ_a and ϵ_i, thus failing to restore the correct $1/R$ behavior. In TDHF ($a_0^{\mathrm{HF}} = 1$) however, the correct $1/R$-dependence of the excitation energy is obtained due to the second term in the $\mathbf{A}$-matrix of Eq. (1.50).

The failure of commonly used functionals to correctly predict CT excitation energies is well known and frequently discussed in the literature. Quite often, this failure is understood to be a failure of TDDFT itself. However, it should be noted that, despite the above reasoning, TDDFT yields correct CT excitation energies if the exact exchange-correlation functional is employed. This is due to the step-like structure in the exact exchange-correlation potential,

which has been discussed in section 1.5.3. In case of an electron transfer from molecule A to molecule B, the exact exchange-correlation potential at B jumps by a constant. This leads to a discontinuous step in the overall exchange-correlation potential and, as a consequence, to a singularity in the derivative of v_{xc} with respect to the density, i.e., the exchange-correlation kernel f_{xc}. This singularity compensates for the vanishing orbital overlap between the orbitals of A and B in the last terms of Eqs. (1.50) and (1.51). Therefore, these terms in fact contribute to CT excitations and the correct $1/R$-dependence is obtained.

In the spirit of section 1.5.4, the failure of TDDFT for CT excitations can also be traced back to a SIE in the employed functionals. As discussed above, the $1/R$-dependence of the exact CT excitation energy is a consequence of the Coulombic interaction of the transfered electron with the hole it left behind. If the employed functional suffers from self-interaction, the transfered electron in orbital a experiences the electrostatic repulsion with itself still being in orbital i, i.e., it experiences the A-molecule as being neutral. Therefore, there is no electrostatic interaction between hole and electron and no $1/R$-dependence. Again, this demonstrates the close relation of self-interaction in the functional and step-like structure in the potential.

Note that a reliable criterion whether an excitation energy calculated from a common density functional suffers from the CT problem or not arises from Eqs. (1.50) and (1.51). If the excitation of interest is a CT excitation, then its energy is particularly sensitive to the fraction of HF-exchange in the employed hybrid functional. In this case, the excitation energy usually varies by several eV when tuning a_0^{HF} between 0 and 1, whereas the energy-variation in non-CT excitations is usually much smaller. In publication 4 this criterion is used to test the reliability of the calculated excitations.

1.6.4. Visualizing electronic excitations

The composition of electronic excitations into transitions between single-particle orbitals as done in Eq. (1.46) provides a possibility to obtain more information about the nature of electronic excitations. In particular, it is often of interest "which electron is transfered from where to where", especially in the case of CT excitations. If in the spirit of Eq. (1.46) one can identify certain leading occupied and unoccupied orbitals in the transition of interest, a plot of these orbitals can often help to distinguish quickly between CT states and valence-excited states.

A more general approach to study the nature of excitations is to plot the *natural transition orbitals* (NTOs) introduced in Ref. [81]. Analogous to the well-known *natural orbitals*, which are obtained by diagonalization of the ground-state single-electron density matrix, the NTOs of a certain excitation result from the diagonalization of the corresponding transition density matrix Z_{ia}. As shown in the previous sections, the transition density matrices and the corresponding excitation energies are obtained as eigenvectors and eigenvalues of Casida's matrix. However, as Z_{ia} is a rectangular $N_{occ} \times N_{unocc}$ matrix, it cannot simply be diagonalized. Instead one uses a singular value decomposition

$$\mathbf{Z} = \mathbf{U}\,\mathbf{S}\,\mathbf{V}^{\dagger}, \tag{1.52}$$

where $\mathbf{U}$ and $\mathbf{V}$ are $N_{occ} \times N_{occ}$ and $N_{unocc} \times N_{unocc}$ unitary matrices, respectively, and $\mathbf{S}$

is a singular matrix containing the singular values of $\mathbf{Z}$, i.e.,

$$S_{ia} = \sqrt{\lambda_i}\,\delta_{ia}\,. \tag{1.53}$$

Employing several matrix multiplications, Eq. (1.52) can be reformulated to

$$\mathbf{U}^\dagger\,\mathbf{Z}\,\mathbf{Z}^\dagger\,\mathbf{U} = \mathbf{V}^\dagger\,\mathbf{Z}^\dagger\,\mathbf{Z}\,\mathbf{V} = \mathbf{S}^2\,. \tag{1.54}$$

The unitary transformations $\mathbf{U}$ and $\mathbf{V}$ diagonalize the matrices $\mathbf{Z}\,\mathbf{Z}^\dagger$ and $\mathbf{Z}^\dagger\,\mathbf{Z}$, respectively, and thus contain their eigenvectors as columns. Although the matrices $\mathbf{Z}\,\mathbf{Z}^\dagger$ and $\mathbf{Z}^\dagger\,\mathbf{Z}$ have different dimensions, i.e., $N_{\text{occ}} \times N_{\text{occ}}$ and $N_{\text{unocc}} \times N_{\text{unocc}}$, respectively, their first N_{occ} eigenvalues λ_i are identical. The λ_i are the quadratic singular values of $\mathbf{S}$, which satisfy

$$0 \le \lambda_i \le 1\,, \qquad i = 1, 2, ..., N_{\text{occ}} \tag{1.55}$$

$$\lambda_a = 0\,, \qquad a \ge N_{\text{occ}} + 1 \tag{1.56}$$

$$\sum_{i=1}^{N_{\text{occ}}} \lambda_i = 1\,. \tag{1.57}$$

The additional zero eigenvalues λ_a arise from mapping the transition density matrix onto the larger matrix $\mathbf{Z}^\dagger\,\mathbf{Z}$.

One can now define the *occupied and virtual natural transition orbitals* Φ_j and Φ_b', respectively, as

$$\begin{aligned}
(\Phi_1, \Phi_2, ..., \Phi_{N_{\text{occ}}}) &:= (\varphi_1, \varphi_2, ..., \varphi_{N_{\text{occ}}})\,\mathbf{U}\,, \tag{1.58} \\
\left(\Phi_1', \Phi_2', ..., \Phi_{N_{\text{unocc}}}'\right) &:= \left(\varphi_1', \varphi_2', ..., \varphi_{N_{\text{unocc}}}'\right)\mathbf{V}\,, \tag{1.59}
\end{aligned}$$

where φ_i and φ_a' are occupied and unoccupied ground-state KS orbitals, respectively. Following Eq. (1.54), the matrices $\mathbf{U}$ and $\mathbf{V}$ can be obtained from diagonalizing $\mathbf{Z}\,\mathbf{Z}^\dagger$ and $\mathbf{Z}^\dagger\,\mathbf{Z}$, respectively.

Note that in Eq. (1.59) one actually obtains only N_{occ} and not N_{unocc} NTOs. The remaining unoccupied orbitals are mapped onto the null vector due to Eq. (1.56). The NTOs thus allow to associate each hole in the occupied space with one single corresponding particle in the virtual space. The importance of such a particle-hole pair for a certain electronic excitation is reflected by the corresponding eigenvalue λ_i. The main advantage of this approach is however that usually electronic transitions can be expressed by one single particle-hole pair with $\lambda_i \simeq 1$, even if the transition is of a highly mixed nature in the basis of KS orbitals. One can thus assign one hole- and one electron-NTO to each electronic transition obtained from Casida's equations. If a transition is mainly a transition between two KS orbitals, the NTO-approach will basically yield these two orbitals as hole- and electron-NTO, respectively.

It should be mentioned that there are several other approaches to visualize the transition density matrix. An overview can be found, e.g., in Refs. [130, 25]. For more details on the NTO approach the reader is referred to Ref. [81]. An example which demonstrates how NTOs can help to gain information about electronic transitions in complex molecular structures is provided in publication 4.

Part II.

Insights

Chapter 2.

Self-interaction

Self-interaction is one of the oldest, most substantial, and most often discussed problems in DFT. Therefore, the question arises why it is that hard to find a functional which is completely free from self-interaction. In the following, this question will be discussed in two steps. Section 2.1 concentrates on the problem of how to define self-interaction in a system of many electrons, while section 2.2 presents ways to approximately correct for self-interaction in many-electron systems.

2.1. The ambiguity in defining self-interaction

Although KS DFT is per construction a many-particle scheme, the one-particle system is an interesting limit revealing crucial properties of the unknown exact functional. This is due to the trivial fact that there is no electron-electron interaction in a one-electron system. As an important consequence, all electron-electron interaction parts of the total energy (see Eq. (1.6)) and of the KS Hamiltonian (see Eq. (1.10)) have to cancel exactly, i.e.,

$$E_{\mathrm{Hart}}\left[n_1\right] + E_{\mathrm{xc}}\left[n_1\right] \;\; = \;\; 0 \,, \tag{2.1}$$

$$v_{\mathrm{Hart}}\left[n_1\right]\left(\mathbf{r}\right) + v_{\mathrm{xc}}\left[n_1\right]\left(\mathbf{r}\right) \;\; = \;\; 0 \,, \tag{2.2}$$

for every v-representable density $n_1\left(\mathbf{r}\right)$ with

$$\int n_1\left(\mathbf{r}\right) \, d\mathbf{r} = 1 \,. \tag{2.3}$$

While the exact functional fulfills Eqs. (2.1) and (2.2) by definition, most of the commonly used approximations to E_{xc}, in particular all semilocal functionals, violate these conditions.

The discussion of the one-electron system thus reveals a substantial drawback of semilocal density functionals. Obviously, this problem still exists in many-electron systems. However, in this case self-interaction is much harder to pin down. This is due to one of the central statements of quantum mechanics: in a system of many interacting particles, it is not possible to distinguish between single particles. This leads to an ambiguity in the definition of self-interaction in many-electron systems, which is made a subject of discussion in the following sections.

2.1.1. One-electron self-interaction and the unitary invariance problem

As the definition of self-interaction via Eqs. (2.1) and (2.2) is straightforward for one-electron densities, the question arises whether a similar idea can be carried forward to many-electron systems. There is an approach that appears quite naturally: By identifying orbital-densities $n_{i\sigma} = f_{i\sigma} |\varphi_{i\sigma}(\mathbf{r})|^2$ with electrons, one can define an interaction energy for every single electron by

$$\delta_{i\sigma} = E_{\text{Hart}}[n_{i\sigma}] + E_{\text{xc}}^{\text{app}}[n_{i\sigma}, 0] \,. \tag{2.4}$$

Then, if

$$\sum_{\sigma=\uparrow,\downarrow} \sum_{i=1}^{N_\sigma} \delta_{i\sigma} = 0 \tag{2.5}$$

holds, declare the approximative functional $E_{\text{xc}}^{\text{app}}[n_\uparrow, n_\downarrow]$ as being free from self-interaction. For the exact functional $E_{\text{xc}}^{\text{ex}}[n_\uparrow, n_\downarrow]$ all $\delta_{i\sigma}$ vanish independently as every interacting v-representable one-electron density $n_{i\sigma}$ can be interpreted as the ground-state density of some one-electron system. Consequently, Eq. (2.5) is a necessary property of $E_{\text{xc}}^{\text{ex}}[n_\uparrow, n_\downarrow]$.

The application of Eqs. (2.4) and (2.5) to commonly used density functionals however reveals *two* drawbacks of these approximations. First, $\delta_{i\sigma}$ does not vanish in general for one-electron densities. Most functionals show this failure, i.e., they suffer from *one-electron self-interaction* [114, 88]. Second, for most of the common density functionals, $\delta_{i\sigma}$ takes different values for different one-electron densities. This failure will be referred to as the *unitary invariance problem* in the following.

As will be shown in section 2.2, the unitary invariance problem poses a severe difficulty when it comes to correcting functionals for self-interaction. Here, the central aspect is that in a many-electron system there is no unique way of defining a density for a single electron. Especially, identifying orbital densities with single electrons, as done in Eq. (2.4), raises the question which orbitals to use. Of course, from a KS DFT perspective it seems natural to use the KS orbital densities as the one-electron densities needed in Eq. (2.4). However, orbitals are quantities that are intrinsically linked to the one-electron picture. Strictly speaking, KS orbitals are just auxiliary quantities which yield, when correctly summed up, the ground-state density. Therefore, KS orbital-densities can be associated with electrons no less and no more than all other orbital-densities which add up to the correct ground-state density. Consequently, a quantification of self-interaction in a many-electron system should be invariant under unitary transformation, i.e., a transformation which changes the individual orbital densities but leaves the total density unchanged. However, for common density functionals Eq. (2.5) does not have this property. Clearly, this is a profound drawback of this definition.

Note that the EXX functional (see Eq. (1.13)) solves both the one-electron self-interaction problem and the unitary invariance problem: the diagonal elements of the Fock-integral cancel out the Hartree self-interaction while the Fock-integral itself is invariant under unitary transformation of the orbitals. However, EXX does not include correlation and therefore suffers from many other problems.

2.1.2. Many-electron self-interaction and relaxation effects

The above discussed problems arising from the definition of one-electron self-interaction via Eq. (2.5) have led to the search for a more suitable definition of self-interaction in many-electron systems. The findings of section 1.5 lay the foundation for such an alternative approach. In section 1.5.1 it was demonstrated that the exact total energy of a finite system with non-integer particle number varies linearly with the fractional occupation, thus yielding kinks at the integers. Section 1.5.4 discussed the relationship of the straight-line behavior and the self-interaction problem. It was shown in this context that functionals which suffer from self-interaction are not able to reproduce the straight-line behavior of the exact functional. This finding suggests an alternative definition of self-interaction: A functional is said to be free from *many-electron self-interaction* if its relaxed ground-state energy yields a straight line with the correct slope for noninteger particle numbers [114, 88].

It has been demonstrated that none of the known density, orbital, or hybrid functionals is able to fulfill this stringent requirement for a wide range of systems, at least not without including a system-dependent parameter [88, 139]. At first sight, this empirical finding seems to contradict the rationale of the gedanken experiment of section 1.5.4. According to Fig. 1.3, a functional which is free from one-electron self-interaction, such as EXX, should at least approximately show a straight-line behavior with kinks at integer occupations. The explanation for this discrepancy lies in the approximations used in the descriptive gedanken experiment of Fig. 1.3. In the following, these approximations as well as their consequences for the straight-line behavior will be discussed in further detail.

A concept which has been neglected in the discussion of section 1.5.4 are the *relaxation effects*. A clear definition of *relaxation* can be made on the basis of the exact functional. In this case, it is known that the ground-state energy of a finite system with non-integer particle number varies linearly with the fractional occupation. According to Eq. (1.28), the exact HOMO-eigenvalue ϵ_H (degeneracy of the HOMO and spin indices are omitted for clarity in this whole section) is therefore constant for occupation numbers $0 < f_H \le 1$. Yet, all other occupied and unoccupied eigenvalues are free to change with varying f_H. As a change in f_H implies a change in the density and thus a change in the KS potential and the KS Hamiltonian, respectively, all other eigenvalues, all orbitals and thus the total energy will be affected by the change in the HOMO-occupation. These second order effects are referred to as *relaxation effects* in the following.

A quantification of relaxation effects can be gained by comparing the relaxed energy with the unrelaxed one. In the unrelaxed case, the HOMO φ_H and the residual density $\bar{n}_H := n - n_H = n - f_H|\varphi_H|^2$ are kept fixed while varying f_H between 0 and 1. For $f_H \ll 1$ relaxation effects are very small and the unrelaxed energy equals the relaxed one. The influence of relaxation effects on the energy increases with increasing f_H. For the exact functional one therefore expects a deviation of the unrelaxed energy from the linearity of the exact energy as indicated in Fig. 2.1. Note that the gedanken experiment of Fig. 1.3 basically focuses on the unrelaxed case, i.e., filling an electron in a constant potential. Still, the exact functional does not vary linearly in this case as relaxation effects are in general nonlinear. Clearly, this emphasizes that the straight-line behavior of the relaxed energy warrants more than the freedom from one-electron self-interaction.

Further insight can be gained by discussing the scaling of the *unrelaxed* total KS energy with f_H. According to Eqs. (1.7) and (1.9), the external energy E_{ext} as well as the kinetic

energy E_{kin} scale linearly with f_{H}. The Hartree energy can be split into three contributions with different scaling, i.e.,

$$
\begin{aligned}
E_{\text{Hart}}\left[n\right] \;=\;& \frac{e^2}{2}\iint \frac{n\left(\mathbf{r}\right)n(\mathbf{r}')}{|\mathbf{r}-\mathbf{r}'|}\,d\mathbf{r}\,d\mathbf{r}' = \frac{e^2}{2}\sum_{i,j=1}^{H-1} f_i f_j \iint \frac{|\varphi_i\left(\mathbf{r}\right)|^2|\varphi_j(\mathbf{r}')|^2}{|\mathbf{r}-\mathbf{r}'|}\,d\mathbf{r}\,d\mathbf{r}' \qquad (2.6)\\
+\;& e^2\sum_{i=1}^{H-1} f_i f_{\text{H}} \iint \frac{|\varphi_i\left(\mathbf{r}\right)|^2|\varphi_{\text{H}}(\mathbf{r}')|^2}{|\mathbf{r}-\mathbf{r}'|}\,d\mathbf{r}\,d\mathbf{r}' + \frac{e^2}{2}f_{\text{H}}^2 \iint \frac{|\varphi_{\text{H}}\left(\mathbf{r}\right)|^2|\varphi_{\text{H}}(\mathbf{r}')|^2}{|\mathbf{r}-\mathbf{r}'|}\,d\mathbf{r}\,d\mathbf{r}'\\
=\;& E_{\text{Hart}}\left[\bar{n}_{\text{H}}\right] + E_{\text{Hart}}^{\text{L}}\left[\bar{n}_{\text{H}},n_{\text{H}}\right] + E_{\text{Hart}}\left[n_{\text{H}}\right]\,,
\end{aligned}
$$

where

$$
E_{\text{Hart}}^{\text{L}}\left[\bar{n}_{\text{H}},n_{\text{H}}\right] := e^2 \iint \frac{\bar{n}_{\text{H}}\left(\mathbf{r}\right)n_{\text{H}}(\mathbf{r}')}{|\mathbf{r}-\mathbf{r}'|}\,d\mathbf{r}\,d\mathbf{r}' \qquad (2.7)
$$

is the Coulomb-interaction energy of the HOMO-density n_{H} with the residual density $\bar{n}_{\text{H}}$. In the unrelaxed case, $E_{\text{Hart}}\left[\bar{n}_{\text{H}}\right]$ is constant, $E_{\text{Hart}}^{\text{L}}\left[\bar{n}_{\text{H}},n_{\text{H}}\right]$ scales linearly and the spurious Hartree self-interaction of the HOMO $E_{\text{Hart}}\left[n_{\text{H}}\right]$ quadratically in f_{H}. Although its general form is unknown, the same type of splitting can formally be done for the exchange-correlation functional E_{xc} by defining

$$
E_{\text{xc}}^{\text{R}}\left[\bar{n}_{\text{H}},n_{\text{H}}\right] := E_{\text{xc}}\left[n\right] - E_{\text{xc}}\left[\bar{n}_{\text{H}}\right] - E_{\text{xc}}\left[n_{\text{H}}\right]\,. \qquad (2.8)
$$

For different functionals, E_{xc}^{R} is a different function of f_{H}. The scaling of E_{xc}^{R} for the exact functional is in general unknown.

Eqs. (2.6)-(2.8) together with Eq. (2.4) yield

$$
E_{\text{Hart}}\left[n\right] + E_{\text{xc}}\left[n\right] = E_{\text{Hart}}\left[\bar{n}_{\text{H}}\right] + E_{\text{xc}}\left[\bar{n}_{\text{H}}\right] + E_{\text{Hart}}^{\text{L}}\left[\bar{n}_{\text{H}},n_{\text{H}}\right] + E_{\text{xc}}^{\text{R}}\left[\bar{n}_{\text{H}},n_{\text{H}}\right] + \delta_{\text{H}}\,. \qquad (2.9)
$$

The scaling of different functionals for fractional particle numbers in the unrelaxed case can now be evaluated on the basis of Eq. (2.9). As stated above, the first two terms of Eq. (2.9) are constant and the third term scales linearly in f_{H}. Hence, the scaling of $E_{\text{xc}}^{\text{R}}\left[\bar{n}_{\text{H}},n_{\text{H}}\right]$ and the one-electron self-interaction energy of the HOMO $\delta_{\text{H}} \sim f_{\text{H}}^2$ are decisive for the overall scaling of the unrelaxed energy corresponding to a given functional.

For semilocal functionals, δ_{H} does not vanish in general. Therefore, their overall scaling behavior is usually dominated by the quadratic scaling of δ_{H}, which is overlayed with the functional-specific scaling of E_{xc}^{R}. This leads to the parabola-like behavior shown in Fig. 2.1. Additional non-linear relaxation effects lower the energy, but the typical parabola-like form remains. Another interesting example is the EXX-functional. Here, it is straightforward to show that the Fock integral from Eq. (2.6) can be split up into three parts just as the Hartree energy. One thus finds a part which is constant for the unrelaxed system, a part that is linear in f_{H} and a third part which corresponds to the diagonal element of the Fock-integral corresponding to the HOMO. The third part exactly cancels out the Hartree self-interaction of the HOMO, i.e., $\delta_{\text{H}}^{\text{EXX}} = 0$. As $E_{\text{x}}^{\text{R}}\left[\bar{n}_{\text{H}},n_{\text{H}}\right]$ is linear in f_{H}, the unrelaxed total energy for the EXX-functional yields straight lines for non-integer particle numbers. As the correlation part of the derivative discontinuity Δ_{xc} is missing, kinks at the integers are underestimated. Nonlinear relaxation effects then lead to a nonlinear relaxed energy. Both the relaxed and unrelaxed energies are sketched in Fig. 2.1.
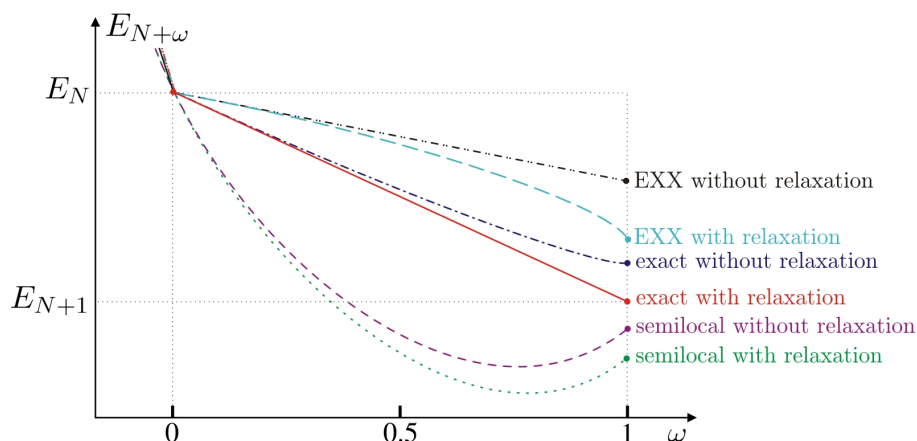
Figure 2.1: Sketch of the relaxed and unrelaxed ground-state energies of a finite system with non-integer particle number $N + \omega$ for different functionals. The energies are shifted to match at $\omega = 0$. Note that the exact functional has a linear relaxed and and a nonlinear unrelaxed energy while the exact exchange functional (EXX) has a linear unrelaxed and a nonlinear relaxed energy. Note that freedom from one-electron self-interaction does imply a derivative discontinuity at integers but not a straight-line behavior for noninteger particle numbers.

Again, the exact functional is of particular interest. Here, the one-electron self-interaction vanishes, i.e., $\delta_H = 0$, and the derivative discontinuity at integers is correct due to vanishing relaxation effects for $f_H \ll 1$. Although the scaling of $E_{xc}^R [\bar{n}_H, n_H]$ is in general unknown, it is clear from these findings that $E_{xc}^R [\bar{n}_H, n_H]$ has to compensate for all relaxation effects. Hence, the energy $E_{xc}^R [\bar{n}_H, n_H]$ as defined in Eq. (2.8) can be interpreted as the negative relaxation energy. However, this is only true for the exact functional. For approximative functionals relaxation effects and $E_{xc}^R [\bar{n}_H, n_H]$ do not cancel in general. As a result, the freedom from one-electron self-interaction does not necessarily lead to a straight-line behavior of the relaxed ground-state energy.

In the light of the above findings, it becomes clear that the requirement of absence of many-electron self-interaction as defined above is a very stringent one. A functional that strictly yields straight lines with the correct slope between all integer occupations for a large variety of systems (without having to adjust any parameters when going from one system to another) fulfills that many exact constraints that it is likely to be the exact functional. Therefore, it is at least debatable whether it makes sense to distinguish between *being free from many-electron self-interaction* and *being exact*. One may further argue that the definition of many-electron self-interaction is not a very feasible one. This is especially true when it comes to correcting functionals for self-interaction, as the definition via the straight-line behavior does not trigger an obvious correction scheme. In contrast, the definition of one-electron self-interaction suggests an obvious and manageable correction scheme, which will be discussed in the following section.

2.2. Self-interaction corrections (SICs)

2.2.1. The concept of Perdew and Zunger

As early as 1981, Perdew and Zunger [106] proposed a self-interaction correction (SIC) scheme which today is by far the most commonly used SIC. Its basic idea is to subtract the one-electron self-interaction energy as defined in Eqs. (2.4) and (2.5) directly from the usually semilocal functional $E_{\mathrm{xc}}^{\mathrm{sl}}[n_\uparrow, n_\downarrow]$. The obtained SIC-functional

$$
\begin{aligned}
E_{\mathrm{xc}}^{\mathrm{SIC}}[n_\uparrow, n_\downarrow] &= E_{\mathrm{xc}}^{\mathrm{sl}}[n_\uparrow, n_\downarrow] - \sum_{\sigma=\uparrow,\downarrow} \sum_{i=1}^{N_\sigma} \delta_{i\sigma} \\
&= E_{\mathrm{xc}}^{\mathrm{sl}}[n_\uparrow, n_\downarrow] - \sum_{\sigma=\uparrow,\downarrow} \sum_{i=1}^{N_\sigma} \left[E_{\mathrm{Hart}}[n_{i\sigma}] + E_{\mathrm{xc}}^{\mathrm{sl}}[n_{i\sigma}, 0] \right]
\end{aligned}
\tag{2.10}
$$

is free from one-electron self-interaction by construction. Yet at the same time, it carries along the unpleasant features of Eq. (2.4). The functional depends on the orbitals explicitly, i.e., it is no longer an explicit density functional. In addition $E_{\mathrm{xc}}^{\mathrm{SIC}}[n_\uparrow, n_\downarrow]$ is not invariant under unitary transformation of the orbitals. This means that one can define various different and a priori equally valid $E_{\mathrm{xc}}^{\mathrm{SIC}}$ that correspond to a given charge density. Therefore, the usual way of minimizing the total energy with respect to the density in order to find a system's ground state

$$
\frac{\delta E}{\delta n_\sigma} = 0
\tag{2.11}
$$

can not be applied in a straightforward manner. As a further consequence, there is no unique way of finding an exchange-correlation potential corresponding to Eq. (2.10). Thereby, the unitary invariance problem in defining self-interaction in a many-electron system strikes one through the backdoor in the Perdew-Zunger-SIC approach.

Due to its explicit dependence on the orbitals and its variance under unitary transformation among these, the self-consistent minimization of the SIC-functional of Eq. (2.10) is more involved than the one for standard density functionals. In their original work [106], Perdew and Zunger directly minimized the functional with respect to the orbitals. This procedure, which is justified as discussed in Ref. [74], leads to single-particle equations

$$
\left[-\frac{\hbar^2}{2m}\Delta + v_{\mathrm{eff},i\sigma}\left(\mathbf{r}\right) \right] \psi_{i\sigma}^{\mathrm{PZ}}\left(\mathbf{r}\right) = \epsilon_{i\sigma} \psi_{i\sigma}^{\mathrm{PZ}}\left(\mathbf{r}\right)
\tag{2.12}
$$

with the effective, orbital specific potentials

$$
v_{\mathrm{eff},i\sigma} = v_{\mathrm{ext}}\left(\mathbf{r}\right) + v_{\mathrm{Hart}}\left[n\right]\left(\mathbf{r}\right) + v_{\mathrm{xc},\sigma}^{\mathrm{sl}}\left[n_\uparrow, n_\downarrow\right]\left(\mathbf{r}\right) - v_{\mathrm{Hart}}\left[n_{i\sigma}\right]\left(\mathbf{r}\right) - v_{\mathrm{xc},\sigma}^{\mathrm{sl}}\left[n_{i\sigma}, 0\right]\left(\mathbf{r}\right). \tag{2.13}
$$

By introducing orbital specific potentials, this approach (PZ-SIC) is outside the foundations of KS theory while not leaving the realm of the Hohenberg-Kohn theorem.

The PZ-SIC-orbitals $\psi_{i\sigma}^{\mathrm{PZ}}$ are generally speaking non-orthogonal. By imposing an orthogonality constraint in the minimization of the energy functional, i.e., by making use of the

Lagrange multipliers

$$\lambda_{ij}^\sigma = \langle \tilde{\psi}_{j\sigma} | \tilde{H}_{i\sigma} \tilde{\psi}_{i\sigma} \rangle \tag{2.14}$$

with the effective one-electron Hamiltonian

$$\tilde{H}_{i\sigma} = H_{0\sigma} + \tilde{v}_{i\sigma}^{\text{SIC}} \tag{2.15}$$

where (using $\tilde{n}_{i\sigma} = \tilde{f}_{i\sigma} \big| \tilde{\psi}_{i\sigma}(\mathbf{r}) \big|^2$)

$$
\begin{aligned}
H_{0\sigma} &= -\frac{\hbar^2}{2m}\Delta + v_{\text{ext}}(\mathbf{r}) + v_{\text{Hart}}[n](\mathbf{r}) + v_{\text{xc},\sigma}^{\text{sl}}[n_\uparrow, n_\downarrow](\mathbf{r}) \,, \tag{2.16} \\
\tilde{v}_{i\sigma}^{\text{SIC}} &= -v_{\text{Hart}}[\tilde{n}_{i\sigma}](\mathbf{r}) - v_{\text{xc},\sigma}^{\text{sl}}[\tilde{n}_{i\sigma}, 0](\mathbf{r}) \,, \tag{2.17}
\end{aligned}
$$

one derives [43] the system of self-consistent equations

$$\tilde{H}_{i\sigma} \tilde{\psi}_{i\sigma} = \left(H_{0\sigma} + \tilde{v}_{i\sigma}^{\text{SIC}} \right) \tilde{\psi}_{i\sigma} = \sum_{j=1}^{N_\sigma} \lambda_{ij}^\sigma \tilde{\psi}_{j\sigma} \,. \tag{2.18}$$

Again, the one-electron Hamiltonian $\tilde{H}_{i\sigma}$ and thus the matrix of Lagrange multipliers is not invariant under unitary transformation of the orbitals. At the minimum of the PZ-SIC energy, the matrix of Lagrange multipliers becomes hermitian and thus unitarily diagonalizable [96, 97, 98, 35]. This has led to the definition of two different types of orbitals: The orthogonal orbitals that minimize the PZ-SIC energy are often referred to as localized orbitals $\tilde{\psi}_{i\sigma}$, as localization of the orbitals naturally increases $E_{\text{Hart}}[n_{i\sigma}]$ and thus minimizes $E_{\text{xc}}^{\text{SIC}}[n_\uparrow, n_\downarrow]$ in many systems. These orbitals are similar to the PZ-SIC orbitals but incorporate the additional orthogonality constraint. In contrast, the so called canonical orbitals $\psi_{i\sigma}$ are delocalized orbitals that diagonalize the matrix of Lagrange multipliers. They are related to the localized orbitals by the unitary transformation U_{ij}^σ,

$$\tilde{\psi}_{i\sigma} = \sum_{j=1}^{N_\sigma} U_{ij}^\sigma \, \psi_{j\sigma}. \tag{2.19}$$

As the canonical orbitals diagonalize the Lagrange multipliers matrix in the minimum of the SIC energy, they can be interpreted as KS-type eigenorbitals of the transformed one-electron Hamiltonians $H_{j\sigma}$. The eigenvalues of λ_{ij} are often used as equivalents to KS orbital energies [96, 97, 98], although recent work suggests a different interpretation [139].

The existence of two different kinds of orbitals in this approach is a direct consequence of the unitary invariance problem. The orbitals $\tilde{\psi}_{i\sigma}$ that minimize the PZ-SIC energy under the constraint of orthonormality are different from the canonical eigenorbitals $\psi_{i\sigma}$ of the PZ-SIC-Hamiltonians. However, as the localized orbitals are related to the canonical orbitals by unitary transformation, they both yield the same density.

The treatment of the SIC functional with orbital-specific potentials instead of a global KS potential for all orbitals has many serious drawbacks. The existence of a global potential is one of the features that makes KS DFT attractive, as it considerably simplifies the numerical efforts and facilitates the interpretation of results. For instance, the KS eigenvalues can directly be used for evaluating Janak's theorem, they can be interpreted on the basis

of Görling-Levy perturbation theory, or used as input to time dependent linear response methods in the spirit of Eq. (1.38). In contrast, for the PZ-SIC approach it is much more unclear how to interpret orbital-energies (see, e.g., Ref. [139] for a discussion) and many exact relations of KS DFT such as Janak's theorem do not hold. Therefore, it is highly desirable to bring the SIC functional back under the umbrella of KS DFT. The following sections deal with the question of how to achieve that consistently.

2.2.2. A generalized optimized effective potential scheme (GOEP)

As discussed in section 1.4.2, a correct treatment of orbital functionals within the KS scheme requires to solve the OEP equation (1.15). The idea of the OEP scheme is to find the exchange-correlation potential which, by virtue of the KS equation, yields those KS orbitals that, employed in the orbital functional of interest, minimize the total energy. In the derivation of the OEP equation, one thus makes explicit use of the fact that the orbitals employed in the functional are eigenstates of the KS Hamiltonian, i.e., KS orbitals. However, having in mind the unitary invariance problem this seems to be a rather crude constraint. Although from a fundamental point of view all orbital representations of a given charge density should be equivalent, it is well established in the literature that, e.g., *natural orbitals* [21] or the spatially localized *Foster-Boys orbitals* [12, 31] yield a more intuitive picture of chemical bonds and lone-pairs than the KS orbitals. In this sense, it may be possible that approximative orbital functionals constructed from natural or localized orbitals improve upon those constructed from KS orbitals, e.g., when it comes to capture the correct physics of chemical bonds or self-interaction.

However, for quite a long time this inherent constraint of the OEP scheme has not been brought into focus in the literature. The reason for this is simple: so far, most implementations used the OEP methodology in the context of the EXX functional (see Eq. (1.13)), which is invariant under unitary transformation of the orbitals. Hence, the orbital representation of EXX can always be chosen such that it conforms with the constraint of OEP, i.e., the orbitals in Eq. (1.13) are chosen to be the KS orbitals.

The SIC-functional of Eq. (2.10) however constitutes a more complicated case. The unitary invariance problem allows for the definition of different functionals with different properties yielding different OEP-potentials and overall different results in practical applications, depending on which orbital-densities are used in the correction terms. Yet, all of these functionals correspond to the same orbital-dependent energy expression. This is a typical situation in which it may be useful to use other orbitals than the KS orbitals in the orbital functional, e.g., in order to capture the correct physics of self-interaction in many-particle systems. However, as explained above this is impossible within the standard OEP scheme. Hence, the main goal of this section is to generalize the OEP methodology so that it allows to treat functionals that are variant under unitary transformation of the orbitals.

As a start, assume an orbital-functional $E_{xc}^{G}\left[\{\tilde{\varphi}_{i\sigma}\}\right]$ which depends on orbitals $\tilde{\varphi}_{i\sigma}$ that are linked to the KS orbitals $\varphi_{j\sigma}$ by a unitary transformation U_{ij}^{σ} via

$$\tilde{\varphi}_{i\sigma}\left(\mathbf{r}\right) = \sum_{j=1}^{N_{\sigma}} U_{ij}^{\sigma}\, \varphi_{j\sigma}\left(\mathbf{r}\right) . \tag{2.20}$$

In this section all occupation numbers $f_{j\sigma}$ and $\tilde{f}_{i\sigma}$ of $\varphi_{j\sigma}$ and $\tilde{\varphi}_{i\sigma}$, respectively, are assumed

to be 1 for $i, j \leq N_\sigma$ and 0 for $i, j > N_\sigma$, i.e., there is no fractional occupation. Note that fractional occupation numbers lead to a number of problems in the definition of Eq. (2.20), which will be referred to in detail in section 3.2. With this in mind, the chain rule of Eq. (1.14) becomes

$$
\begin{aligned}
v_{\mathrm{xc},\sigma}\left(\mathbf{r}\right) \;=\; & \sum_{\alpha=\uparrow,\downarrow} \sum_{\beta=\uparrow,\downarrow} \sum_{\gamma=\uparrow,\downarrow} \sum_{i=1}^{N_\alpha} \sum_{j=1}^{N_\beta} \\
& \iiint \left(\frac{\delta E_{\mathrm{xc}}^{\mathrm{G}}\left[\{\tilde{\varphi}_{k\tau}\}\right]}{\delta\tilde{\varphi}_{i\alpha}(\mathbf{r}')} \frac{\delta\tilde{\varphi}_{i\alpha}(\mathbf{r}')}{\delta\varphi_{j\beta}(\mathbf{r}'')} \frac{\delta\varphi_{j\beta}(\mathbf{r}'')}{\delta v_\gamma^{\mathrm{KS}}(\mathbf{r}''')} + \text{c.c.} \right) \frac{\delta v_\gamma^{\mathrm{KS}}(\mathbf{r}''')}{\delta n_\sigma(\mathbf{r})}\, d\mathbf{r}' d\mathbf{r}'' d\mathbf{r}''' \,.
\end{aligned}
\tag{2.21}
$$

By evaluating Eq. (2.21) on the basis of Eqs. (1.3) and (2.20) and after some algebra (see publication 2 for details) one obtains the central result of this section, the *generalized optimized effective potential* (GOEP) equation for unitarily variant orbital functionals:

$$
\sum_{j=1}^{N_\sigma} \int \varphi_{j\sigma}^*(\mathbf{r}') \left(v_{\mathrm{xc},\sigma}(\mathbf{r}') - u_{\mathrm{xc},j\sigma}^{\mathrm{G}}(\mathbf{r}') \right) G_{j\sigma}(\mathbf{r}',\mathbf{r})\, \varphi_{j\sigma}\left(\mathbf{r}\right) d\mathbf{r}' + \text{c.c.} = 0 \,,
\tag{2.22}
$$

where

$$
u_{\mathrm{xc},j\sigma}^{\mathrm{G}}(\mathbf{r}) \;:=\; \frac{1}{\varphi_{j\sigma}^*(\mathbf{r})} \sum_{i=1}^{N_\sigma} \left(U_{ij}^\sigma + \frac{\delta U_{ij}^\sigma}{\delta\varphi_{j\sigma}(\mathbf{r})}\, \varphi_{j\sigma}(\mathbf{r}) \right) \frac{\delta E_{\mathrm{xc}}^{\mathrm{G}}\left[\{\tilde{\varphi}_{n\tau}\}\right]}{\delta\tilde{\varphi}_{i\sigma}(\mathbf{r})} \,,
\tag{2.23}
$$

$$
G_{j\sigma}(\mathbf{r},\mathbf{r}') \;:=\; \sum_{\substack{k=1 \\ k\neq j}}^{\infty} \frac{\varphi_{k\sigma}(\mathbf{r})\, \varphi_{k\sigma}^*(\mathbf{r}')}{\epsilon_{j\sigma} - \epsilon_{k\sigma}} \,.
\tag{2.24}
$$

The interpretation of this equation is: Solving Eq. (2.22) yields the unique local potential $v_{\mathrm{xc},\sigma}^{\mathrm{GOEP}}(\mathbf{r})$ that by virtue of the KS equations leads to KS orbitals which, when transformed according to Eq. (2.20), yield the lowest total energy that can possibly be obtained with two sets of orbitals linked by the unitary transformation U_{ij}^σ. Eq. (2.22) represents a generalized version of the OEP equation for arbitrary orbital functionals. It includes the standard OEP equation (1.15) as a limiting case for unitarily invariant orbital functionals such as EXX or if the unitary transformation is chosen to be the identity matrix.

A detailed derivation of the GOEP equation as well as a thorough discussion of its properties and its relationship to non-KS DFT approaches using orbital-specific potentials in the spirit of Eq. (2.18) are presented in publication 2. Moreover, strategies to solve the GOEP equation numerically can be found in section 3.1. Note however that an important property of Eq. (2.22) is that it reflects the basic structure of the standard OEP equation, while the consequences of the additional unitary transformation can formally be incorporated into the orbital-specific potentials $u_{\mathrm{xc},j\sigma}^{\mathrm{G}}$. Hence, most of the algorithms known for solving the standard OEP equation can still be applied for GOEP. Moreover, this formal equivalence allows to define an approximation to the GOEP in the spirit of the approximation to the OEP provided by Krieger, Lee, and Iafrate [61, 60]. The KLI approximation to GOEP (GKLI) yields

$$
v_{\mathrm{xc},\sigma}^{\mathrm{GKLI}}\left(\mathbf{r}\right) = \frac{1}{2n_\sigma} \sum_{i=1}^{N_\sigma} \left\{ |\varphi_{i\sigma}\left(\mathbf{r}\right)|^2 \left[u_{\mathrm{xc},i\sigma}^{\mathrm{G}}\left(\mathbf{r}\right) + \left(\bar{v}_{\mathrm{xc},i\sigma}^{\mathrm{GKLI}} - \bar{u}_{\mathrm{xc},i\sigma}^{\mathrm{G}} \right) \right] \right\} + \text{c.c.} \,,
\tag{2.25}
$$

where $\bar{v}_{\mathrm{xc},i\sigma}^{\mathrm{GKLI}}$ and $\bar{u}_{\mathrm{xc},i\sigma}^{\mathrm{G}}$ are defined analogous to Eqs. (1.22) and (1.23).

Although the GOEP scheme generally allows to treat any orbital functional of interest, the main motivation for its derivation was the variance of the SIC-functional under unitary transformation of the orbitals. In contrast to standard OEP, the GOEP scheme allows to treat the SIC consistently within the KS scheme although orbitals different from the KS orbitals are employed in Eq. (2.10). Indeed, there is a hint that using orbitals different from the KS orbitals may be a useful approach for the SIC: strictly speaking, by employing KS orbital densities in Eq. (2.10) one does not fulfill the variational principle. The orbitals that minimize the SIC-energy for a given charge density are those orbitals which maximize the one-electron self-interaction energy $\sum_{\sigma,i}\delta_{i\sigma}$. As will be demonstrated in section 3.3.1, these orbitals are usually spatially localized, i.e., the Hartree self-interaction is maximized. This is in agreement with the empirical finding that the direct variation of the SIC-energy with respect to the orbitals, as done in the PZ-SIC approach, typically also yields spatially localized orbitals. Therefore, the orbitals that minimize the SIC energy for a given charge density will be referred to as *localized orbitals* in the following. Strategies to find localized orbitals will be discussed in section 3.3. The concept of using localized orbitals in the SIC energy expression and to use the GOEP equation in order to derive the corresponding exchange-correlation potential will be referred to as *localized SIC-GOEP (LOC-OEP)* in the following.

Although many reasons plead for employing localized orbitals in the SIC energy expression, the most transparent way of calculating an OEP potential corresponding to Eq. (2.10) is to use the KS orbitals. With the trivial ansatz, $U_{ij}^{\sigma} = \delta_{ij}$ the difference between the two sets of orbitals vanishes, i.e., $\tilde{\varphi}_{i\sigma} = \varphi_{i\sigma}$ and Eq. (2.22) reduces to the standard OEP equation. The concept of finding the corresponding OEP will be referred to as *Kohn-Sham SIC-GOEP (KS-OEP)*. The problems and prospects of both the LOC-OEP and the KS-OEP approach will be discussed in the following sections.

2.2.3. Kohn-Sham SIC-GOEP

By identifying each KS orbital density $n_{i\sigma}(\mathbf{r}) = f_{i\sigma}|\varphi_{i\sigma}(\mathbf{r})|^2$ of a many-electron system with an electron, one can define a SIC of the LDA [105] by virtue of Eq. (2.10), i.e.,

$$E_{\mathrm{xc}}^{\mathrm{KSOEP}}[\{\varphi_{j\tau}\}] = E_{\mathrm{xc}}^{\mathrm{LDA}}[n_\uparrow, n_\downarrow] - \sum_{\sigma=\uparrow,\downarrow}\sum_{i=1}^{N_\sigma}\left[E_{\mathrm{Hart}}[n_{i\sigma}] + E_{\mathrm{xc}}^{\mathrm{LDA}}[n_{i\sigma}, 0]\right]. \qquad (2.26)$$

The GOEP-methodology discussed in the previous section then allows to find the corresponding exchange-correlation potential. As the orbitals used in Eq. (2.26) are the KS orbitals, $U_{ij}^{\sigma} = \delta_{ij}$ and $\tilde{\varphi}_{i\sigma} = \varphi_{i\sigma}$ hold, the GOEP equation reduces to the standard OEP equation and the orbital-specific potentials $u_{\mathrm{xc},i\sigma}^{\mathrm{KS}}$ can be derived following Eq. (1.16), i.e.,

$$
\begin{aligned}
u_{\mathrm{xc},i\sigma}^{\mathrm{KS}}(\mathbf{r}) &= \frac{1}{f_{i\sigma}\,\varphi_{i\sigma}^*(\mathbf{r})}\frac{\delta E_{\mathrm{xc}}^{\mathrm{KSOEP}}[\{\varphi_{j\tau}\}]}{\delta\varphi_{i\sigma}(\mathbf{r})} \\
&= v_{\mathrm{xc},\sigma}^{\mathrm{LDA}}[n_\uparrow, n_\downarrow](\mathbf{r}) - v_{\mathrm{Hart}}[n_{i\sigma}](\mathbf{r}) - v_{\mathrm{xc},\sigma}^{\mathrm{LDA}}[n_{i\sigma}, 0](\mathbf{r}).
\end{aligned}
\qquad (2.27)
$$

In publication 1, the KS-OEP approach is used to calculate the electrical response of molecular chains (note that a detailed introduction into publication 1 and a discussion of its basic

results is presented in section 4.1). In this context, it is demonstrated that the KS-OEP approach yields excellent results for the polarizabilities of model hydrogen chains, whereas the KLI-approximation breaks down dramatically. Importantly, the failure of KS-KLI is general for extended molecular systems and has been known in the literature for several years [33, 95]. However, being the first application of full KS-OEP calculations on extended molecular systems, publication 1 is able to show that this failure is due to the breakdown of the KLI approximation and not, as previously expected, due to a general failure of the SIC-OEP approach. Note that the reasons for the breakdown of KS-KLI are discussed in publication 2. In addition, appendix A.2 offers an alternative perspective on the breakdown of KS-KLI for extended molecular systems based on more recent findings.

Considering the fact that solving the OEP equation exactly is numerically very expensive, the breakdown of KS-KLI makes the KS-OEP approach as a whole unfeasable for a large number of systems. Although KS-KLI has been shown to yield good results for atoms [19] and small clusters [134], an alternative SIC-approach is clearly needed for extended molecular systems such as polymers or organic semiconductors.

2.2.4. Localized SIC-GOEP

Localized orbitals $\tilde{\varphi}_{j\sigma}$ minimize the SIC energy for a given spin density $n_\sigma = \sum_{i=1}^{N_\sigma} |\varphi_{i\sigma}(\mathbf{r})|^2 = \sum_{j=1}^{N_\sigma} |\tilde{\varphi}_{j\sigma}(\mathbf{r})|^2$ (again, occupation numbers are set to 0 or 1, respectively, throughout this section). Employing localized orbital densities $\tilde{n}_{j\sigma}(\mathbf{r}) = |\tilde{\varphi}_{j\sigma}(\mathbf{r})|^2$ in Eq. (2.10) thus yields the absolute minimum of the total energy corresponding to the SIC that can be obtained within KS theory. The SIC of the LDA [105] then reads

$$E_{\text{xc}}^{\text{LOCOEP}}\left[\{\tilde{\varphi}_{i\tau}\}\right] = E_{\text{xc}}^{\text{LDA}}[n_\uparrow, n_\downarrow] - \sum_{\sigma=\uparrow,\downarrow} \sum_{j=1}^{N_\sigma} \left[E_{\text{Hart}}[\tilde{n}_{j\sigma}] + E_{\text{xc}}^{\text{LDA}}[\tilde{n}_{j\sigma}, 0]\right] . \qquad (2.28)$$

As the orbitals used in Eq. (2.28) are not eigenorbitals of the KS Hamiltonian, the full GOEP equation has to be solved in order to find the corresponding exchange-correlation potential. By neglecting the second-order term $\delta U_{ij}^\sigma / \delta \varphi_{j\sigma}$ in Eq. (2.23) (see publication 2 for an interpretation of this approximation), the orbital specific potentials $u_{\text{xc},j\sigma}^{\text{LOC}}$ read

$$u_{\text{xc},j\sigma}^{\text{LOC}}(\mathbf{r}) = \sum_{i=1}^{N_\sigma} U_{ij}^\sigma \frac{\tilde{\varphi}_{i\sigma}^*(\mathbf{r})}{\varphi_{j\sigma}^*(\mathbf{r})} \left(v_{\text{xc},\sigma}^{\text{LDA}}[n_\uparrow, n_\downarrow](\mathbf{r}) - v_{\text{Hart}}[\tilde{n}_{i\sigma}](\mathbf{r}) - v_{\text{xc},\sigma}^{\text{LDA}}[\tilde{n}_{i\sigma}, 0](\mathbf{r})\right). \quad (2.29)$$

Publication 2 deals with the derivation, implementation, and interpretation of LOC-OEP. In addition, its performance is tested and compared to other SIC approaches for a set of systems. Publication 2 shows that LOC-OEP yields good results for ionization potentials and excellent dissociation curves. In particular, it is demonstrated that LOC-KLI yields a very good approximation to LOC-OEP even for extended molecular systems. This is a clear advantage over KS-OEP and makes Eq. (2.28) a suitable approach for a large number of systems in which SIEs degrade the results obtained from semilocal functionals. E.g., in publication 3 the LOC-KLI approach is used to calculate accurate eigenvalue spectra of organic semiconductors for which semilocal functionals fail. Note that an introduction into publication 3 as well as a summary of its basic results is provided in section 4.3.

As noted above, the failure of KS-KLI for molecules has been known for quite a few years in

the literature. In the light of the findings of the orbital-specific SIC methods in the spirit of Eq. (2.18), this failure has been suspected to be related to missing orbital localization effects in KS-KLI. As a consequence, several early approaches to use localized orbitals in the SIC energy of Eq. (2.10) can be found in the literature. However, it is important to point out the differences of these methods to the LOC-OEP approach.

Garza *et al.* [33] and others [95, 99] directly replaced the KS orbitals in the KS-KLI potential by Foster-Boys- [12, 31] or Pipek-Mezey- [108] orbitals, respectively. As discussed in detail in publication 2, the resulting potential is not equal to the GKLI-potential of the corresponding unitary transformation. Hence, there is no straightforward way of improving this approximative approach to a full OEP level. Moreover, the localizing transformations used in these approaches do not yield energy-minimizing orbitals but only approximations to those (see also section 3.3 for a discussion of orbital localization and energy minimization).

In contrast, the authors of Ref. [85] used energy minimizing orbitals in their SIC-OEP approach. However, these calculations are based on the most crude approximation to the GOEP, i.e., the *generalized Slater-approximation*, an approximation in the potential which results from setting $\bar{v}_{\mathrm{xc},i\sigma}^{\mathrm{GKLI}} - \bar{u}_{\mathrm{xc},i\sigma}^{\mathrm{G}} = 0$ in Eq. (2.25). The part of the GOEP-potential that is neglected in the Slater-approximation is usually called the *response part* of $v_{\mathrm{xc},i\sigma}^{\mathrm{GOEP}}$. The reason for this is that this part of the potential is responsible for the step-like structure in the SIC-OEP potential and thus for the good performance of the SIC-OEP approaches in calculating the electric response of extended molecular systems (see publication 1 and Ref. [99]) and other charge transfer properties. As a result, the generalized Slater approximation [85] misses some of the most important advantages of LOC-OEP without being able to yield a significant improvement in computational efficiency as compared to LOC-KLI.

2.2.5. Prospects of Localized SIC-GOEP

The main purpose of LOC-OEP is to consistently correct LDA from self-interaction without introducing any empirical parameters. In contrast to most GGAs and hybrid functionals, LOC-OEP is completely derived from first principles. As a consequence of its construction, LOC-OEP is not expected to yield results as close to experiment as many hybrid functionals do. This is particularly true for those systems and observables that are typically included in the training sets for empirical functionals. However, it is important to make clear that the prospect of SIC-approaches such as LOC-OEP is not to improve upon the accuracy of hybrid functionals for standard test systems and observables. Its main aim is rather to exploit those fields of application where GGAs and hybrid functionals fail and thereby improve our understanding of self-interaction effects in DFT. In addition to the applications discussed in this thesis, LOC-OEP and in particular the less expensive LOC-KLI offer a wide range of possibilities for future implementations in DFT and TDDFT. The prospects and problems of some of these possible realizations will be discussed in the following.

A problem that is of high interest in the solid state community is how to describe the electron localization effects that occur in the Mott transition, e.g., in transition-metal oxides, correctly within KS DFT. An overview of the performance of DFT for transition-metal oxides, a thorough comparison of several functionals for the Mott transition of MnO, and an overview of the pertinent literature in this field can be found, e.g., in Ref. [54]. As orbital densities coming from semilocal functionals usually tend to be delocalized due to the self-interaction problem, LDA and GGAs are not able to describe electron localization effects

correctly. The Mott transition of transition-metal oxides however is characterized by the fact that some electrons (e.g., the 3d-band electrons in MnO) localize at certain regions of space whereas the other electrons stay itinerant. It has been shown that a SIC methodology using orbital-specific potentials is able to distinguish naturally between localized and delocalized electron-densities and thus yields a significantly improved description of the Mott transition as compared to semilocal functionals [126, 125]. However, this scheme leaves the framework of KS DFT and thus suffers from the same problems as the PZ-SIC approach discussed in section 2.2.1. The LOC-OEP approach allows to bring the SIC approach back into KS DFT. The unitary transformation introduces an additional variational freedom which allows to distinguish naturally between localized (Wannier states) and delocalized orbitals (Bloch states). Yet, the KS orbitals and the KS Hamiltonian can have the full symmetry of the system. This is an important difference to KS-OEP. In an infinite periodic system, the KS Hamiltonian has the full symmetry of the system and the KS orbitals are Bloch states, for which the one-electron self-interaction energy vanishes [106]. As a consequence, KS-OEP reduces to standard LDA for periodic boundary conditions. The main problem in using LOC-OEP and LOC-KLI with periodic boundary conditions is to find the energy minimizing unitary transformation. The currently implemented algorithms (see section 3.3 and appendix A.3) only work for finite systems, and the transformation of Bloch orbitals to Wannier orbitals [140, 82, 128] does not strictly guarantee the minimization of the total energy. Although this obviously presents a challenge to future implementations, one can be optimistic that in the near future LOC-KLI will yield an interesting alternative for the description of electron localization effects in transition-metal oxides.

Another promising field of application for LOC-KLI is real-time TDDFT for charge-transfer problems. Clearly, the correction of self-interaction improves the description of charge-transfer, while the superior scaling behavior of the SIC (linear in particle number M) as compared to EXX methods ($\sim M^2$) contains the computational effort. In addition, the energy-minimizing unitary transformation might offer a possibility to artificially restore the *zero force theorem*, which is violated in the KLI-approximation [93, 92]. For an introduction into the real-time TDDFT LOC-KLI approach see Ref. [45].

The discussion of many-electron self-interaction in section 2.1.2 provides for a third interesting field of application for LOC-KLI. It is based on the close analogy between the unitary invariance problem and the many-electron SIE. For a one-electron system, the definition of self-interaction is clear: it is equal to the definition of one-electron self-interaction. For a many-electron system however, the definition of self-interaction becomes ambiguous, i.e., the unitary invariance problem emerges. At the same time, the many-electron SIE occurs. In this light, the unitary invariance problem may be interpreted as the manifestation of the missing link between one- and many-electron self-interaction. Note that the close relation between the localization of orbitals and the many-electron SIE is also discussed in detail in Ref. [89]. The authors of this letter argue that the many-electron SIE of HF and semilocal functionals can be traced back to a *localization* and *delocalization error* of the corresponding orbitals, respectively.

In summary, these findings trigger the idea to relate the one-electron SIE and the many-electron SIE by a certain unitary transformation. The goal of such an approach would be to correct a functional from many-electron SIE by virtue of the SIC-GOEP approach. The procedure would thus be as follows: for integer particle numbers choose the usual energy-minimizing unitary transformation and derive the corresponding GOEP; for non-integer particle numbers however choose the unitary transformation such that the total

energy varies linearly with the fractional occupation. The resulting functional would be free from one-electron SIE and almost free from many-electron SIE (of course, the slopes of the straight lines may not be completely accurate). However, it is not clear *per se* that a unitary transformation which fulfills this additional constraint does exist in general. Moreover, if such a scheme even exists, it requires an algorithm to find this unitary transformation as well as a GOEP scheme for fractional occupation numbers. While the latter will be introduced in section 3.2, the former certainly requires significant additional efforts and ideas.

2.2.6. The orbital self-interaction error

Eq. (2.10) measures how one-electron self-interaction influences the exchange-correlation energy of a system of interest. In many cases however (see, e.g., section 4.3 and publication 3), the influence of self-interaction on the KS eigenvalues themselves is of particular interest. A straightforward way to test this influence is to run two independent self-consistent calculations, e.g., one employing a semilocal functional and one using a self-interaction correction within the GOEP methodology in the spirit of sections 2.2.1 - 2.2.4 and compare the resulting eigenvalues, i.e., calculate the difference

$$\Delta\epsilon_{i\sigma} = \epsilon_{i\sigma}^{\mathrm{sl}} - \epsilon_{i\sigma}^{\mathrm{GOEP}} = \left\langle \varphi_{i\sigma}^{\mathrm{sl}} \left| \hat{h}_{\sigma}^{\mathrm{sl}} \right| \varphi_{i\sigma}^{\mathrm{sl}} \right\rangle - \left\langle \varphi_{i\sigma}^{\mathrm{GOEP}} \left| \hat{h}_{\sigma}^{\mathrm{GOEP}} \right| \varphi_{i\sigma}^{\mathrm{GOEP}} \right\rangle . \qquad (2.30)$$

$\Delta\epsilon_{i\sigma}$ is the change in the i*th* eigenvalue of spin σ when going from a semilocal functional (KS Hamiltonian $\hat{h}_{\sigma}^{\mathrm{sl}}$) to a self-interaction corrected one using the GOEP methodology (KS Hamiltonian $\hat{h}_{\sigma}^{\mathrm{GOEP}}$). It therefore measures the influence of self-interaction on the KS eigenvalue spectrum. However, as SIC-GOEP calculations are usually rather expensive, this proceeding is often inconvenient, especially as the size of the studied systems increases. Having done a calculation employing a standard semilocal functional one would like to have an easy criterion which estimates the influence of self-interaction effects on the obtained eigenvalue spectrum without having to go through a full SIC-GOEP calculation. As will be shown in the following, such a criterion can be based on Eq. (2.30) if one introduces a number of approximations. Note that the justification of these approximations will be discussed in detail in the appendix A.1.

The first approximation is that, although the order of orbitals may change due to a shift of the corresponding eigenvalues, the self-consistency effects of the SIC on the orbitals themselves are sufficiently small, i.e., for every orbital $\varphi_{i\sigma}^{\mathrm{sl}}$ there exists an orbital $\varphi_{j\sigma}^{\mathrm{GOEP}}$ with

$$\varphi_{i\sigma}^{\mathrm{sl}} \approx \varphi_{j\sigma}^{\mathrm{GOEP}} =: \varphi_{i\sigma} \qquad (2.31)$$

and therefore

$$n^{\mathrm{sl}} = \sum_{\sigma=\uparrow,\downarrow} \sum_{i=1}^{N_{\sigma}} \left| \varphi_{i\sigma}^{\mathrm{sl}} \right|^2 \approx \sum_{\sigma=\uparrow,\downarrow} \sum_{j=1}^{N_{\sigma}} \left| \varphi_{j\sigma}^{\mathrm{GOEP}} \right|^2 = n^{\mathrm{GOEP}} =: n \, . \qquad (2.32)$$

Using Eqs. (2.31) and (2.32), one obtains

$$\Delta\epsilon_{i\sigma} \stackrel{(2.31)}{\approx} \left\langle \varphi_{i\sigma} \left| \hat{h}_{\sigma}^{\mathrm{sl}} - \hat{h}_{\sigma}^{\mathrm{GOEP}} \right| \varphi_{i\sigma} \right\rangle \stackrel{(2.31)+(2.32)}{\approx} \left\langle \varphi_{i\sigma} \left| v_{\mathrm{xc},\sigma}^{\mathrm{sl}}[n] - v_{\mathrm{xc},\sigma}^{\mathrm{GOEP}}[n] \right| \varphi_{i\sigma} \right\rangle . \quad (2.33)$$

Note that in the second step of Eq. (2.33), the Hartree-parts of the KS Hamiltonians cancel due to Eq. (2.32) whereas the kinetic parts cancel as a consequence of Eq. (2.31), respectively.

The second approximation is to replace the GOEP by the orbital-specific potentials $u_{\mathrm{xc},i\sigma}^{\mathrm{G}}$. This approximation can be formally justified on the basis of a first-order perturbation-theory argument in the spirit of Eq. (1.18): the change in the density subject to the replacement of the GOEP by $u_{\mathrm{xc},i\sigma}^{\mathrm{G}}$ vanishes to first order. An alternative interpretation of this approximation can be gained by adding a zero to Eq. (2.33), i.e.,

$$\Delta\epsilon_{i\sigma} \overset{(2.33)}{\approx} \left\langle \varphi_{i\sigma} \,\big|\, v_{\mathrm{xc},\sigma}^{\mathrm{sl}}\,[n] - u_{\mathrm{xc},i\sigma}^{\mathrm{G}} \,\big|\, \varphi_{i\sigma} \right\rangle + \left\langle \varphi_{i\sigma} \,\big|\, u_{\mathrm{xc},i\sigma}^{\mathrm{G}} - v_{\mathrm{xc},\sigma}^{\mathrm{GOEP}}\,[n] \,\big|\, \varphi_{i\sigma} \right\rangle \quad (2.34)$$
$$= \left\langle \varphi_{i\sigma} \,\big|\, v_{\mathrm{xc},\sigma}^{\mathrm{sl}}\,[n] - u_{\mathrm{xc},i\sigma}^{\mathrm{G}} \,\big|\, \varphi_{i\sigma} \right\rangle - \left(\bar{v}_{\mathrm{xc},i\sigma}^{\mathrm{GOEP}} - \bar{u}_{\mathrm{xc},i\sigma}^{\mathrm{G}} \right),$$

where $\bar{v}_{\mathrm{xc},i\sigma}^{\mathrm{GOEP}}$ and $\bar{u}_{\mathrm{xc},i\sigma}^{\mathrm{G}}$ are defined analogous to Eqs. (1.22) and (1.23), respectively. Thus, replacing the GOEP in Eq. (2.33) by the orbital-specific potentials is formally equivalent to setting

$$\bar{v}_{\mathrm{xc},i\sigma}^{\mathrm{GOEP}} - \bar{u}_{\mathrm{xc},i\sigma}^{\mathrm{G}} = 0. \quad (2.35)$$

Using Eqs. (2.31)-(2.35), one can thus define the *orbital self-interaction error* (OSIE) as

$$e_{i\sigma} := \left\langle \varphi_{i\sigma} \,\big|\, v_{\mathrm{xc},\sigma}^{\mathrm{sl}}\,[n] - u_{\mathrm{xc},i\sigma}^{\mathrm{G}} \,\big|\, \varphi_{i\sigma} \right\rangle \approx \epsilon_{i\sigma}^{\mathrm{sl}} - \epsilon_{i\sigma}^{\mathrm{GOEP}}. \quad (2.36)$$

$e_{i\sigma}$ is the approximative shift of the *i*th eigenvalue of spin σ when changing the potential functional from $v_{\mathrm{xc},\sigma}^{\mathrm{sl}}$ to $v_{\mathrm{xc},\sigma}^{\mathrm{GOEP}}$. The obvious advantage of Eq. (2.36) as compared to Eq. (2.30) is that it can be evaluated solely on the basis of one calculation employing a semilocal functional.

As discussed in the previous sections, the SIC-GOEP can be defined in various ways due to the unitary invariance problem of the SIC energy expression. A detailed discussion of the orbital self-interaction error in KS-OEP and LOC-OEP is presented in the appendix A.1.

The combination of Eq. (2.36) with Eq. (2.27) plays a central role in publication 3. There, it is shown that the OSIE can serve as a warning against the possible misinterpretation of KS eigenvalue spectra obtained from semilocal functionals. A detailed introduction into the problems discussed in publication 3 is given in section 4.3.

Chapter 3.

GOEP Methodology

3.1. Solving the GOEP equation

The GOEP equation (2.22) can be formally written in a way that allows to split up its solution into two separate steps. Both steps need to be taken once in every cycle of the self-consistent iteration of the KS equations (1.3). Step one is to find the energy minimizing unitary transformation U_{ij}^σ of the given KS orbitals and to incorporate it into the orbital-specific potentials $u_{\text{xc},j\sigma}^{\text{G}}$ of Eq. (2.23). This procedure will be discussed in detail in section 3.3. Step two is to solve equation (2.22) for the GOEP. For this, one can formally use the methodologies known from solving the standard OEP equation.

Following Refs. [69] and [70], the OEP equation can be solved iteratively on the basis of Eq. (1.18). With the help of the *orbital shifts* $\delta\varphi_{i\sigma}^*(\mathbf{r})$ derived in Eq. (1.19) one defines

$$S_\sigma(\mathbf{r}) = \sum_{i=1}^{N_\sigma} \delta\varphi_{i\sigma}^*(\mathbf{r})\ \varphi_{i\sigma}(\mathbf{r}) + c.c.\ . \tag{3.1}$$

Given a certain $v_{\text{xc},\sigma}(\mathbf{r})$, the corresponding $S_\sigma(\mathbf{r})$ can be calculated by evaluating the orbital shifts following Eq. (1.19). For the exact OEP, $S_\sigma(\mathbf{r})$ vanishes according to Eq. (1.18). For any other $v_{\text{xc},\sigma}(\mathbf{r})$ however, $S_\sigma(\mathbf{r})$ is in general non-zero. Since $S_\sigma(\mathbf{r})$ is an indicator for the error inherent in a given approximation to the OEP, one can improve this approximation by adding the corresponding $S_\sigma(\mathbf{r})$ to it:

$$v_{\text{xc},\sigma}^{\text{new}}(\mathbf{r}) = v_{\text{xc},\sigma}^{\text{old}}(\mathbf{r}) + c\,S_\sigma(\mathbf{r})\ . \tag{3.2}$$

Here, c is an empirical parameter that is introduced because $S_\sigma(\mathbf{r})$ is not an exact representation of the error in $v_{\text{xc},\sigma}^{\text{old}}(\mathbf{r})$ but just an estimate. Although c influences the convergence of the so-called *S-iteration*, i.e., the self-consistent iteration of Eqs. (3.2), (1.19), and (1.3), it does not influence the final result. Usually, the KLI-approximation as derived from Eq. (1.21) yields a convenient initial guess for the *S*-iteration. A more detailed discussion of the *S*-iteration can be found in Ref. [69].

For the KS-OEP and LOC-OEP calculations presented in this thesis, the GOEP methodology including both the KLI-approximation and the *S*-iteration was implemented in a customized version of the *PARSEC program package* [64]. PARSEC is an open-source code for electronic structure calculations employing finite differences on a uniform Cartesian real-space grid. The true atomic potentials are replaced with effective norm conserving pseudopotentials [131]. For further computational details see Ref. [64].

3.2. Fractional occupation numbers in GOEP

In section 2.2.2, the GOEP methodology has been introduced only for integer occupation numbers $f_{j\sigma}$ of the KS orbitals $\varphi_{j\sigma}$. However, according to the aufbau principle fractional occupation numbers can occur if the HOMO is degenerate. Moreover, as discussed in section 1.5.1, one can formally introduce the concept of fractional particle numbers (and thus a fractional occupation of the HOMO) in ground-state DFT by coupling the KS system to a particle-reservoir. In particular, fractional occupation numbers become important when discussing the problem of many-electron self-interaction. However, it turns out that the introduction of fractional particle numbers to the GOEP scheme is an intricate topic. The reasons for this will be discussed in this section.

As a start, assume N occupied KS orbitals $\varphi_j(\mathbf{r})$ with fractional occupation numbers $0 < f_j \leq 1 \, \forall \, j = 1, N$. Note that spin-indices are omitted for clarity. According to the aufbau principle, fractional occupations are only allowed for those orbitals with eigenvalues $\epsilon_j = \epsilon_{\mathrm{H}}$. The number of electrons in the system is $M = \sum_{j=1}^{N} f_j$ and the density is derived via $n(\mathbf{r}) = \sum_{j=1}^{N} f_j \, |\varphi_j(\mathbf{r})|^2$. Further, assume a second set of orbitals $\tilde{\varphi}_i(\mathbf{r})$ with occupation numbers $0 < \tilde{f}_i \leq 1 \, \forall \, i = 1, N$. Note that there is no aufbau principle for the $\tilde{\varphi}_i(\mathbf{r})$. Hence, fractional occupation is allowed for all $i = 1, N$.

In the following, we claim both sets of orbitals to represent the same total number of electrons, i.e., $\tilde{M} = \sum_{i=1}^{N} \tilde{f}_i = \sum_{j=1}^{N} f_j = M$ and the same density, i.e., $\tilde{n}(\mathbf{r}) = n(\mathbf{r})$. Employing the unitary transformation U_{ij} between the two sets of orbitals as done in Eq. (2.20), i.e.,

$$\tilde{\varphi}_i(\mathbf{r}) = \sum_{k=1}^{N} U_{ik} \, \varphi_k(\mathbf{r}) \,, \tag{3.3}$$

yields the density

$$\tilde{n}(\mathbf{r}) = \sum_{i=1}^{N} \tilde{f}_i \, |\tilde{\varphi}_i(\mathbf{r})|^2 \overset{(3.3)}{=} \sum_{j,k=1}^{N} \sum_{i=1}^{N} \tilde{f}_i \, U_{ij}^* \, U_{ik} \, \varphi_j^*(\mathbf{r}) \, \varphi_k(\mathbf{r}) \overset{!}{=} \sum_{j=1}^{N} f_j \, |\varphi_j(\mathbf{r})|^2 = n(\mathbf{r}) \,. \tag{3.4}$$

It is straightforward to show that Eq. (3.4) holds if and only if

$$\sum_{i=1}^{N} \tilde{f}_i \, U_{ij}^* \, U_{ik} = f_j \, \delta_{jk} \, \forall \, j, k = 1, N \,. \tag{3.5}$$

However, this is only true if $\tilde{f}_i = f_j \, \forall \, i, j = 1, N$ holds, i.e., for the trivial cases $\tilde{f}_i = f_j = 0$ or $\tilde{f}_i = f_j = 1 \, \forall \, i, j = 1, N$. Hence, the unitary transformation as defined in Eq. (2.20) does not allow for fractional occupation of the orbitals.

Yet, there is a way to define a unitary transformation for fractional occupation numbers that preserves the density. Employing the unitary transformation K_{ij} in

$$\sqrt{\tilde{f}_i} \, \tilde{\varphi}_i(\mathbf{r}) = \sum_{k=1}^{N} K_{ik} \, \sqrt{f_k} \, \varphi_k(\mathbf{r}) \,, \tag{3.6}$$

yields the density

$$\tilde{n}\left(\mathbf{r}\right) = \sum_{i=1}^{N} \tilde{f}_i \left|\tilde{\varphi}_i\left(\mathbf{r}\right)\right|^2 \stackrel{(3.6)}{=} \sum_{j,k=1}^{N} \underbrace{\sum_{i=1}^{N} K_{ij}^* K_{ik}}_{=\delta_{jk}} \sqrt{f_j f_k}\, \varphi_j^*\left(\mathbf{r}\right) \varphi_k\left(\mathbf{r}\right) = \sum_{j=1}^{N} f_j \left|\varphi_j\left(\mathbf{r}\right)\right|^2 = n\left(\mathbf{r}\right). \quad (3.7)$$

Of course, the $\tilde{\varphi}_i\left(\mathbf{r}\right)$ of Eq. (3.6) are chosen to be normalized, i.e., $\langle\tilde{\varphi}_i\left(\mathbf{r}\right)|\tilde{\varphi}_i\left(\mathbf{r}\right)\rangle = 1$, thus determining the occupation $\tilde{f}_i$ as

$$\tilde{f}_i = \tilde{f}_i \left\langle\tilde{\varphi}_i\left(\mathbf{r}\right)|\tilde{\varphi}_i\left(\mathbf{r}\right)\right\rangle = \sum_{j,k=1}^{N} K_{ij}^* \, K_{ik} \, \sqrt{f_j\, f_k}\, \underbrace{\left\langle\varphi_j\left(\mathbf{r}\right)|\varphi_k\left(\mathbf{r}\right)\right\rangle}_{=\delta_{jk}} = \sum_{k=1}^{N} K_{ik}^* \, K_{ik}\, f_k\,. \quad (3.8)$$

With this also the number of particles is conserved, i.e.,

$$\tilde{M} = \sum_{i=1}^{N} \tilde{f}_i \stackrel{(3.8)}{=} \sum_{k=1}^{N} \underbrace{\sum_{i=1}^{N} K_{ik}^* \, K_{ik}}_{=\delta_{kk}=1}\, f_k = \sum_{k=1}^{N} f_k = M\,. \quad (3.9)$$

However, the definition of Eq. (3.6) suffers from a different inherent problem: in contrast to the KS orbitals, the transformed orbitals $\tilde{\varphi}_i\left(\mathbf{r}\right)$ are no longer orthogonal. This can be demonstrated by calculating the integral

$$\left\langle\tilde{\varphi}_i\left(\mathbf{r}\right)|\tilde{\varphi}_j\left(\mathbf{r}\right)\right\rangle = \sum_{k,l=1}^{N} K_{ik}^* \, K_{jl}\, \frac{\sqrt{f_k\, f_l}}{\sqrt{\tilde{f}_i\, \tilde{f}_j}}\, \underbrace{\left\langle\varphi_k\left(\mathbf{r}\right)|\varphi_l\left(\mathbf{r}\right)\right\rangle}_{=\delta_{kl}} = \frac{1}{\sqrt{\tilde{f}_i\, \tilde{f}_j}}\, \sum_{k} K_{ik}^* \, K_{jk}\, f_k \neq \delta_{ij} \quad (3.10)$$

for fractional occupation numbers f_k. For integer occupation numbers however, the localized orbitals are orthogonal.

From a pragmatic point of view, the non-orthogonality of the transformed orbitals $\tilde{\varphi}_i\left(\mathbf{r}\right)$ can be accepted as a curious by-product of the unitary invariance problem and the theory of fractional particle numbers. As the localized orbitals are just auxiliary quantities in the GOEP methodology, there are no fundamental reasons that oppose the non-orthogonality. Therefore, Eq. (3.6) allows to introduce fractional occupation numbers in the GOEP scheme. Rederivation of the GOEP equation for fractional particle numbers straightforwardly yields (now with spin-indices σ)

$$\sum_{j=1}^{N_\sigma} f_{j\sigma} \int \varphi_{j\sigma}^*(\mathbf{r}') \left(v_{\mathrm{xc},\sigma}(\mathbf{r}') - u_{\mathrm{xc},j\sigma}^{\mathrm{G}}(\mathbf{r}')\right) G_{j\sigma}(\mathbf{r}',\mathbf{r})\, \varphi_{j\sigma}\left(\mathbf{r}\right) d\mathbf{r}' + \mathrm{c.c.} = 0\,, \quad (3.11)$$

where

$$u_{\mathrm{xc},j\sigma}^{\mathrm{G}}(\mathbf{r}) \quad := \quad \frac{1}{f_{j\sigma}\, \varphi_{j\sigma}^*(\mathbf{r})} \sum_{i=1}^{N_\sigma} \sqrt{\frac{f_{j\sigma}}{\tilde{f}_{i\sigma}}} \left(K_{ij}^\sigma + \frac{\delta K_{ij}^\sigma}{\delta\varphi_{j\sigma}(\mathbf{r})}\, \varphi_{j\sigma}(\mathbf{r})\right) \frac{\delta E_{\mathrm{xc}}^{\mathrm{G}}\left[\{\tilde{\varphi}_{n\tau}\}\right]}{\delta\tilde{\varphi}_{i\sigma}(\mathbf{r})}\,. \quad (3.12)$$

A case of particular interest is LOC-OEP. Here, Eq. (3.12) yields (compare also to Eq. (2.29))

$$u_{\mathrm{xc},j\sigma}^{\mathrm{LOC}}(\mathbf{r}) = \sum_{i=1}^{N_\sigma} K_{ij}^\sigma \frac{\sqrt{\tilde{f}_{i\sigma}}\,\tilde{\varphi}_{i\sigma}^*(\mathbf{r})}{\sqrt{f_{j\sigma}}\,\varphi_{j\sigma}^*(\mathbf{r})} \left(v_{\mathrm{xc},\sigma}^{\mathrm{LDA}}\left[n_\uparrow, n_\downarrow\right](\mathbf{r}) - v_{\mathrm{Hart}}\left[\tilde{n}_{i\sigma}\right](\mathbf{r}) - v_{\mathrm{xc},\sigma}^{\mathrm{LDA}}\left[\tilde{n}_{i\sigma}, 0\right](\mathbf{r}) \right), \; (3.13)$$

where

$$\tilde{n}_{i\sigma} := \tilde{f}_{i\sigma}\left|\tilde{\varphi}_{i\sigma}\right|^2 . \tag{3.14}$$

Of course, it remains an open question how to choose the unitary transformation K_{ij} in the case of fractional occupation numbers. As discussed in section 2.2.5, K_{ij} could in principle be chosen such that the many-electron SIE is reduced. This is of course an interesting idea, however, it requires the introduction of completely new concepts for the determination of the unitary transformation. A second possibility is to choose the energy-minimizing unitary transformation as usually done for integer occupation numbers. A methodology that allows to find this energy-minimizing transformation will be discussed in section 3.3.3.

3.3. Localizing transformations

The orbitals that minimize the SIC energy are usually called *localized orbitals*. This is due to the empirical finding that the PZ-orbitals found from solving the orbital-specific PZ-SIC equations (2.12) are typically rather localized in space. Commonly, this finding is rationalized by the argument that the Hartree self-interaction energy, which is supposed to be the leading term in the SIC of Eq. (2.10), increases with growing localization of the orbital densities. However, there are two inaccuracies in this argument. First, not only $E_{\mathrm{Hart}}\left[n\right]$ increases with the localization of n but also the absolute value of $E_{\mathrm{xc}}\left[n\right]$. While $E_{\mathrm{Hart}}\left[n\right]$ represents an anti-binding interaction, $E_{\mathrm{xc}}\left[n\right]$ acts binding, i.e., it has a negative sign. Hence, there are two different contributions with different signs to the SIC that in general scale differently with the localization of n (note that this different scaling is a manifestation of the unitary invariance problem). The energy-minimizing n thus represents the best tradeoff between both contributions. The second inaccuracy in the above argument refers to the term *localization*. As will be demonstrated in section 3.3.2, there are several equally valid but substantially different definitions for the localization of orbitals. As a consequence, orbitals that are maximally localized, e.g., in the sense of the *Foster-Boys* orbitals [12, 31], do not necessarily yield a minimal SIC energy.

The relationship of localization and self-interaction is an intricate problem. This is reflected in the large number of SIC-approaches employing different kinds of localization schemes for orbitals [96, 35, 33, 95, 99, 85]. The purpose of this section is thus to discuss the relationship of localization and self-interaction in detail. This is particularly important for the correct usage of the LOC-OEP methodology, as the energy-minimizing unitary transformation enters the LOC-OEP-equations as a decisive factor.

3.3.1. Localization and self-interaction

One way to look at the relationship between localization and self-interaction without having to deal with different definitions of localization is to consider a simple test case for which an
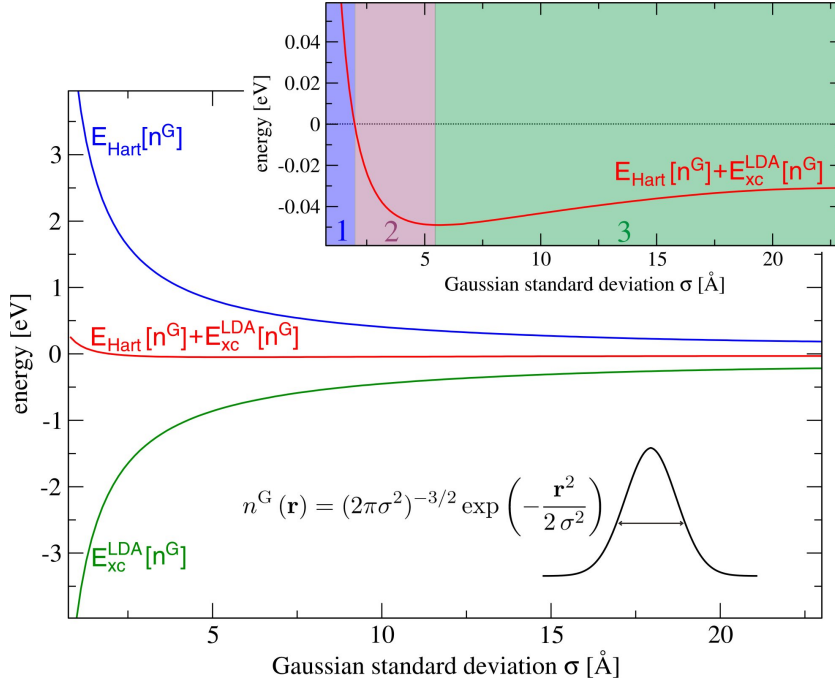
Figure 3.1: Simple model for understanding the relationship of one-electron self-interaction and localization: Hartree energy $E_{\text{Hart}}\left[n^{\text{G}}\right]$, LDA energy $E_{\text{xc}}^{\text{LDA}}\left[n^{\text{G}}\right]$, and sum of both for a Gaussian density distribution $n^{\text{G}}\left(\mathbf{r}\right)$ are plotted as a function of the Gaussian standard deviation σ. The total self-interaction energy is plotted again on a magnified energy scale in the upper part of the figure. It is positive for strongly localized densities and negative for delocalized ones. Note, that in region 2 (purple area in upper plot) the self-interaction energy is negative, i.e., the LDA self-interaction is larger than the Hartree self-interaction, yet the system can still gain energy by delocalizing the one-electron density.

obvious and straightforward definition of localization exists, e.g., the 3-dimensional Gaussian distribution of a one-particle density

$$n^{\text{G}}\left(\mathbf{r}\right) = (2\pi\sigma^2)^{-3/2}\exp\left(-\frac{\mathbf{r}^2}{2\,\sigma^2}\right)\,. \tag{3.15}$$

The advantage of this density distribution is that its localization can be varied smoothly just by varying the Gaussian standard deviation σ. For this purpose, the density of Eq. (3.15) has been sampled on the real-space grid of PARSEC [64] and its Hartree energy $E_{\text{Hart}}\left[n^{\text{G}}\right]$, LDA energy $E_{\text{xc}}^{\text{LDA}}\left[n^{\text{G}}\right]$, and sum of both have been calculated for a set of Gaussian standard deviations σ. The result is plotted in Fig. 3.1.

The first observation that can be drawn from Fig. 3.1 is that $E_{\text{Hart}}\left[n^{\text{G}}\right]$ and $E_{\text{xc}}^{\text{LDA}}\left[n^{\text{G}}\right]$ largely cancel out so that the remaining self-interaction energy is more than an order of magnitude smaller than its individual contributions. The second observation is that, at least on the energy scale of the lower part of Fig. 3.1, the remaining self-interaction energy looks more or less constant for a large range of σ. Note, that these two findings reflect important features of the LDA. In fact, the large cancellation of the Hartree self-interaction by the LDA self-interaction is one of the main reasons for the surprisingly good performance of LDA for

a wide range of systems. The third interesting observation in Fig. 3.1 is that $E_{\text{Hart}}\left[n^{\text{G}}\right]$ exceeds $E_{\text{xc}}^{\text{LDA}}\left[n^{\text{G}}\right]$ only for very localized Gaussians (region 1: blue area in upper plot) whereas for more delocalized densities (regions 2 and 3: purple and green area in upper plot) $E_{\text{xc}}^{\text{LDA}}\left[n^{\text{G}}\right]$ exceeds $E_{\text{Hart}}\left[n^{\text{G}}\right]$. Of course, one may argue that the Gaussian distribution is a special case and that for real orbital-densities things look different. However, for systems with rather delocalized KS orbitals, e.g., π-systems such as organic semiconductors (see, e.g., publications 3 and 4), it is consistently found that the LDA self-interaction exceeds the Hartree self-interaction for most orbital densities.

Fig. 3.1 shows why the orbitals that minimize the SIC energy are typically localized in space: the maximum of the self-interaction energy can be found for very localized Gaussians. However, a curiosity can be found in the region of mid-level localization, i.e., region 2 in the upper plot of Fig. 3.1. Here, the absolute value of $E_{\text{xc}}^{\text{LDA}}\left[n^{\text{G}}\right]$ exceeds the Hartree energy $E_{\text{Hart}}\left[n^{\text{G}}\right]$, yet at the same time the system can still gain energy by delocalizing the one-electron density. In other words: although the self-interaction energy $E_{\text{Hart}}\left[n^{\text{G}}\right] + E_{\text{xc}}^{\text{LDA}}\left[n^{\text{G}}\right]$ is negative, self-interaction can still yield a spurious delocalization of n^{G}. For one-electron densities in region 3 however, self-interaction yields spurious localization.

3.3.2. Common localization schemes

As demonstrated in the previous section, there exists a clear relationship between localization and the self-interaction energy of a simple Gaussian one-electron density distribution. In practice however, one has to deal with significantly more complex orbital densities, for which the total energy needs to be minimized by a unitary transformation. Further, the maximum possible degree of localization is significantly restricted by the constraint of reproducing the density given by the KS orbitals. Still, it is an empirical finding that also in this more complicated case, the energy-minimizing orbitals are typically localized in space. This observation has led to a number of approximative approaches for finding the energy-minimizing orbitals by applying localizing unitary transformations which were originally introduced to find orbitals that mimic the chemist's intuition of chemical bonds. Among the most popular localized orbitals are those introduced by Forster and Boys [12, 31], Edminston and Ruedenberg [27], and Pipek and Mezey [108].

The difference between these methods is to be found in the definition of localization (see, e.g., Ref. [108] for an overview). The Foster-Boys orbitals for example can be obtained by minimizing the functional [12, 31]

$$L_{\text{FB}}^{\sigma} = \sum_{i=1}^{N_{\sigma}} \iint \left|\varphi_{i\sigma}\left(\mathbf{r}\right)\right|^{2} \left(\mathbf{r} - \mathbf{r}'\right)^{2} \left|\varphi_{i\sigma}(\mathbf{r}')\right|^{2} d\mathbf{r}\, d\mathbf{r}'\,, \tag{3.16}$$

which measures the spatial extension of the orbitals $\varphi_{i\sigma}\left(\mathbf{r}\right)$. In contrast, the Pipek-Mezey criterion [108] used, e.g., in Ref. [99] measures the mean number of atoms over which the molecular orbitals extend. For this purpose, it evaluates the so-called *atomic population operator*, which projects the molecular orbitals onto the atomic basis sets of single atoms in the molecule. Hence, this procedure is intrinsically linked to the description of orbitals via atomic basis sets and can not be used straightforwardly if one solves the KS equations on a uniform grid as done in PARSEC [64]. Finally, the orbitals introduced by Edminston and

Ruedenberg [27] maximize the Hartree self-interaction energy, i.e.,

$$L_{\mathrm{ER}}^{\sigma} = \sum_{i=1}^{N_{\sigma}} E_{\mathrm{Hart}} \left[|\varphi_{i\sigma}|^2 \right] \, . \tag{3.17}$$

As a result of the study presented in Fig. 3.1, the Edminston Ruedenberg criterion is equivalent to the minimization of the total self-interaction energy for the simple case of Gaussian orbital densities. Note however that for more complex orbital densities this may no longer be the case.

Having chosen a criterion for localization, one has to find a way to numerically find its minimum or maximum, respectively. To this end, several approaches exist in the literature. The most often applied optimization algorithm originally suggested by Edminston and Ruedenberg [27] determines the optimum unitary transformation by consecutive two by two rotations among the orbitals, i.e., the so-called *Jacobi-sweeps*, until convergence is reached. The optimum rotation angle for each iterative step can be determined analytically from the respective localization criterion, e.g., L_{ER}^{σ} or L_{FB}^{σ}. Further details of the Jacobi-sweeps approach can be found, e.g., in Refs. [27] and [108]. For the purpose of this thesis, in particular for the *Garza-SIC* calculations presented in publication 2 and as an initial guess for the numerical procedure presented in section 3.3.3, the Jacobi-sweeps algorithm employing both the Foster-Boys and the Edminston-Ruedenberg localization has been implemented in PARSEC [64]. On a side note, there exist a couple of more involved algorithms that employ, e.g., a direct optimization of the localization criterion L^{σ} along its gradient [27, 35] using some conjugate gradient technique, or an accelerated *direct inversion of iterative subspace* (DIIS) algorithm [123]. However, the Jacobi-sweeps algorithm has been chosen for our implementation because of a couple of significant advantages: it is straightforward to implement, it converges reliably and for all systems discussed in this thesis its computational costs are bearable.

An important property of the different localization schemes is how they scale with the size of the system. This is particularly important as one of the usually brought forward arguments that speak for SIC approaches as compared to EXX calculations is their superior scaling behavior: the computation time needed for calculating the SIC energy scales linearly with the number of electrons M, for EXX it scales $\sim M^2$. However, it turns out [108] that traditional algorithms to find the localizing transformation scale $\sim M^3$ for the Foster-Boys localization and even $\sim M^5$ for the Edminston-Ruedenberg localization. Clearly, this turns the advantage of the SIC-approaches into a significant disadvantage. However, it has been demonstrated that by employing highly sophisticated linear scaling techniques and an accelerated DIIS-like algorithm for the orbital localization, the computation of Edminston-Ruedenberg orbitals can actually be done in a time proportional to M [123]. Although, to the best of my knowledge, this procedure has not yet been implemented in any SIC approach so far, it clearly offers an interesting option for future applications within the LOC-OEP methodology. Hence, LOC-OEP remains an interesting alternative for calculations on systems with an increasing number of electrons.

3.3.3. The energy-minimizing unitary transformation

The unitary transformation that is actually needed in the LOC-OEP approach is the one which leads to the absolute minimum of the total SIC energy for a given set of KS orbitals,

i.e., for a given density. A relation that allows to find this unitary transformation was first introduced by Pederson, Heaton, and Lin in 1984 in the context of orbital-specific SIC [96] and since then addressed by several authors [50, 29, 138, 85, 86]. Pederson *et al.* considered an infinitesimal orthogonal transformation U_{ij}^σ (see Eq. (2.19)) with matrix elements $U_{ii}^\sigma = 1$, $U_{ij}^\sigma = \omega_{ij}^\sigma \, \forall \, i < j$, and $U_{ij}^\sigma = -\omega_{ji}^\sigma \, \forall \, i > j$. Following Ref. [96], the minimization of the total SIC energy $E_{\rm t}^{\rm SIC}$, i.e.,

$$0 = \left(\frac{\partial E_{\rm t}^{\rm SIC}}{\partial \omega_{kl}^\sigma} \right)_{\omega_{ij}^\sigma = 0} \tag{3.18}$$

where $l > k, j > i \, \forall \, k, l, i, j$ together with Eqs. (2.17) and (2.19) then yields

$$\left\langle \, \tilde{\psi}_{i\sigma} \, \middle| \, \tilde{v}_{i\sigma}^{\rm SIC} - \tilde{v}_{j\sigma}^{\rm SIC} \, \middle| \, \tilde{\psi}_{j\sigma} \, \right\rangle = 0 \,. \tag{3.19}$$

Eq. (3.19) is called the *symmetry condition*, as it is straightforward to show that it is equivalent to the requirement of hermiticity of the Lagrange-multipliers matrix of Eq. (2.14), i.e., $\lambda_{ij}^\sigma = \lambda_{ji}^\sigma \, {}^*$. The orbitals $\tilde{\psi}_{i\sigma}$ which fulfill Eq. (3.19) minimize the total energy.

Eq. (3.19) can be used in order to find the energy-minimizing unitary transformation for LOC-OEP. Employing a unitary transformation which takes the set of KS orbitals $\{\varphi_{i\sigma}\}$ to the set of energy-minimizing orbitals $\{\tilde{\varphi}_{i\sigma}\}$ via Eq. (2.20), Eq. (3.19) can be rewritten to

$$\sum_{k,l=1}^{N_\sigma} U_{ik}^\sigma U_{jl}^\sigma \left\langle \, \varphi_{k\sigma} \, \middle| \, \tilde{v}_{i\sigma}^{\rm SIC} - \tilde{v}_{j\sigma}^{\rm SIC} \, \middle| \, \varphi_{l\sigma} \, \right\rangle = 0 \,, \tag{3.20}$$

where with the localized orbital densities $\tilde{n}_{i\sigma} = |\tilde{\varphi}_{i\sigma}|^2$

$$\tilde{v}_{i\sigma}^{\rm SIC} = -v_{\rm Hart} \left[\tilde{n}_{i\sigma} \right] (\mathbf{r}) - v_{\rm xc,\sigma}^{\rm LDA} \left[\tilde{n}_{i\sigma}, 0 \right] (\mathbf{r}) \,. \tag{3.21}$$

Solving Eq. (3.20) for U_{ij}^σ yields the energy-minimizing unitary transformation needed for LOC-OEP.

Pederson *et al.* [97] proposed a double iteration procedure using the Jacobi-sweeps technique for solving the symmetry condition. In our implementation we follow a different approach which is based on an idea introduced by Fois *et al.* [29]. By evaluating $U_{ij}^\sigma = \delta_{ij} + \tau_{ij}^\sigma$ in the symmetry condition (3.20), Fois *et al.* found an iterative equation for τ_{ij}^σ (see Ref. [29] and appendix A.3 for details). As the resulting U_{ij}^σ does not guarantee unitarity, the authors proposed to apply a Gram-Schmidt procedure to the U's after having solved the iterative equation for the τ's. However, we found that one can significantly speed up the convergence of the τ-iteration by including a symmetric Löwdin-orthogonalization [77, 83] directly in the iterative equation for the τ's. A detailed derivation of this improved algorithm for solving the symmetry condition for U_{ij}^σ can be found in appendix A.3.

As shown in Ref. [97], the symmetry condition can be straightforwardly carried over to the case of fractional occupation numbers by replacing the orbitals $\varphi_{i\sigma}$ by $\sqrt{f_{i\sigma}}\varphi_{i\sigma}$ and the localized orbitals $\tilde{\varphi}_{i\sigma}$ by $\sqrt{\tilde{f}_{i\sigma}}\tilde{\varphi}_{i\sigma}$, respectively. This allows to find a unitary transformation K_{ij}^σ as defined in Eq. (3.6) that preserves the density and the number of particles for fractional occupation numbers (see discussion in section 3.2). The solution of the symmetry condition for K_{ij}^σ follows the same lines as for integer occupation numbers (see appendix A.3.).

The symmetry condition (3.20) allows to find the energy-minimizing orbitals to be used in LOC-OEP. As the convergence of the iterative equation for the τ's is significantly improved by a good initial guess for the orbitals, we found that it is recommendable to start the τ-iteration from roughly converged Foster-Boys or Edminston-Ruedenberg orbitals.

The spatial localization of the energy-minimizing orbitals depends crucially on the system of interest. However, it is consistently found that the energy-minimizing orbitals are significantly more localized in space than the KS orbitals. Examples of the spatial distribution of the energy-minimizing orbitals can be found, e.g., in publication 2.

3.3.4. Localized orbitals and exact exchange

The fact that the orbitals which minimize the SIC energy are typically well localized in space gives rise to an interesting analogy of the LOC-OEP approach to EXX. As can be derived from Eq. (1.13), the exact exchange energy $E_{\mathrm{x}}\left[\{\varphi_{i\tau}\}\right]$ is invariant under unitary transformation of the orbitals. Such a unitary transformation may be useful from a computational point of view in order to facilitate the calculation of the exchange energy $E_{\mathrm{x}}\left[\{\varphi_{i\tau}\}\right]$. In particular spatially localized orbitals yield very small non-diagonal contributions, i.e., terms in Eq. (1.13) with $j \neq k$, which may therefore be neglected. Interestingly, the sum over the remaining diagonal contributions equals the Hartree correction part of Eq. (2.10) as evaluated with localized orbitals. Therefore, SIC approaches working with localized orbitals take into account the dominant contribution to the exact exchange energy although only evaluating its diagonal elements. If the localizing transformation can be computed efficiently (see discussion in previous sections), they therefore provide for a competitive alternative to exact exchange calculations for large molecules due to their superior scaling behavior ($\sim M$ instead of $\sim M^2$) and the consistent inclusion of correlation.

Note that an illustrative example of the close analogy of EXX and LOC-OEP is provided in Fig. 3 of publication 2. There, the ground-state energy of He_2^+ is plotted as a function of the internuclear distance. LOC-OEP and EXX-KLI yield the same asymptotic behavior and a similar equilibrium bond length. However, the total energy curves are shifted relative to each other by a constant due to the neglect of the correlation energy in EXX. This leads to a significantly improved dissociation limit of LOC-OEP as compared to EXX-KLI. On a side note, a similar behavior is found for the relative eigenvalue spectra of the organic semiconductors discussed in publication 3. Typically, the eigenvalue spectra of LOC-KLI and EXX-KLI differ mainly by a constant which is introduced by the neglect of correlation in the EXX approach.

Chapter 4.

Introduction to the publications

This chapter introduces the four publications collected in Part III of this thesis. Publication 1 deals with the calculation of linear polarizabilities of molecular chains using the KS-OEP methodology. Section 4.1 sketches the problems that arise in polarizability calculations for extended molecular systems within KS-DFT and elaborates the motivation for using SIC approaches to improve upon the performance of commonly used functionals. In addition, it discusses the relationship of the results obtained in publication 1 with more recent SIC calculations and explains how the findings of this comparison motivate the development of the GOEP approach.

The derivation and discussion of the GOEP methodology is the central aspect of publication 2. As the GOEP approach has already been introduced in sections 2.2.2 to 2.2.5 of this thesis, section 4.2 focuses on a different major result obtained in publication 2, i.e., the performance of the GOEP approach in calculating dissociation curves for diatomic molecules. It is explained why this problem poses a severe challenge to common density functionals, why this is related to the self-interaction problem, and how GOEP performs for the intricate dissociation of He_2^+.

Publication 3 shows that self-interaction also plays a major role in the prediction of reliable KS eigenvalue spectra for organic semiconductor molecules. Section 4.3 introduces the technique of combining DFT calculations with photoelectron spectroscopy measurements in order to gain important information on the electronic structure of organic semiconductors. It is discussed how self-interaction can destroy the physical reliability of the KS eigenvalues and thus lead to the misinterpretation of eigenvalue spectra obtained from commonly used functionals. Publication 3 shows that an easy criterion for the reliability of the KS eigenvalue spectrum can be based on the OSIE introduced in section 2.2.6 and that the GOEP approach yields reliable eigenvalues also in those cases for which semilocal functionals typically fail.

Finally, publication 4 discusses the reasons for a fluorescence quenching that has been observed experimentally [117] in a recently synthesized system [6] composed of two organic semiconductor molecules that are linked by a saturated, flexible hydrocarbon bridge. Section 4.4 introduces and discusses the most important experimental results of Ref. [117] and explains how a theoretical study based on DFT, TDDFT, and molecular dynamics (MD) calculations can help to clarify the origin of the fluorescence quenching. It is shown that the fluorescence is quenched by charge transfer between the two organic semiconductors. Charge-transfer excitations are identified using the NTO approach introduced in section 1.6.4. The problems that arise within the TDDFT approach for these excitations are discussed in the spirit of section 1.6.3. MD simulations allow for an analysis of the system's dynamics in solution. Combining the results obtained from DFT, TDDFT, and MD calculations, our study thus facilitates a consistent explanation of the experimentally obtained results.

4.1. Polarizabilities of molecular chains

Molecular chains, in particular conjugated polymers, have a large linear and nonlinear electrical response. Together with their cheap production and easy processibility, this feature makes them highly interesting candidates for nonlinear optical devices [52]. Hence, there is a need for a large-scale but computationally feasible electronic structure theory which gives a good description of the properties of these systems. Regarding the typical size of conjugated polymers, DFT appears to be the natural choice for this purpose. However, over the last years several studies have shown that the accurate prediction of electronic response properties of extended molecular systems is one of the most severe challenges for density functionals, with Refs. [18, 34, 39, 90, 15, 120, 53] just being a few examples from a vast body of literature. Generally speaking, almost all semilocal functionals overestimate the linear and nonlinear response of molecular chains dramatically. For example, the polarizabilities and hyperpolarizabilities as calculated from LDA or GGAs can be off by more than 100% as compared to high-quality quantum-chemical calculations, even for rather short conjugated chains with less than 10 monomeric units [18].

In order to establish a benchmark test for the performance of density functionals in predicting accurate response properties of extended molecular systems, one typically resorts to a model system which allows to reduce the numerical costs while retaining the typical bond-alternating structure, i.e, the hydrogen chain. This system of single hydrogen atoms arranged in a chain with alternating intermolecular distances of 2 and 3 bohrs, respectively, has been introduced by Champagne *et al.* [17] and frequently referred to since then in the literature [4, 18, 34, 66, 68, 87, 90, 99, 113, 112, 120, 135]. All of these studies highlight the important role played by the field-counteracting response originating from the step-like structure of the exact exchange-correlation potential. As discussed in section 1.5.3, a charge transfer induced by an external electric field leads to a field-counteracting step-structure in the exact v_{xc}. As a consequence, functionals which show a derivative discontinuity in E_{xc} typically yield significantly improved response properties for the hydrogen chain as compared to LDA or GGAs [34, 90, 68, 4, 99]. This observation is further strengthened by the findings of Refs. [4, 53]. The authors of these publications demonstrate that the inclusion of a derivative discontinuity term in a semilocal functional can significantly improve the functionals performance for polarizability calculations of molecular chains. However, in Ref. [4] it is also shown that the mere presence of a step-like structure in the exchange-correlation potential is often not enough, in particular if the potential is not a functional derivative of a corresponding energy functional. Clearly, these findings underline the importance of working with potentials that are at least approximate functional derivatives.

The crucial impact of the step-like structure of the response term in v_{xc} in combination with the considerations discussed in section 1.5.4 suggests that self-interaction plays a major role for the failure of semilocal functionals to predict accurate response properties. This consideration is the basic driving force behind the work presented in publication 1, in which the linear electrical response of hydrogen chains is calculated within the KS-KLI and the KS-OEP approach. The relevance of this investigation is underlined by the fact that, almost simultaneously to our work, a couple of other groups have worked on very similar problems. In Refs. [113, 112] Ruzsinszky *et al.* present calculations of polarizabilities and hyperpolarizabilities of hydrogens chains with the orbital-specific SIC-approach of Eq. (2.18). In the work of Pemmaraju *et al.* [99], linear polarizabilities of hydrogen chains are calculated using an approximate self-interaction corrected KS potential. Although the authors call their ap-

proach "KLI-SIC", it actually involves a modified version of the Garza-SIC approach [33], in which the KS orbitals in the KS-KLI potential, i.e., Eq. (2.25) with the orbital-specific potentials of Eq. (2.27), are replaced by localized orbitals. In contrast to Garza *et al.* however, the authors of Ref. [99] used Pipek-Mezey orbitals instead of Foster-Boys orbitals. As discussed in more detail in section 2.2.4 and in publication 2, the resulting potential-functional can be viewed as an approximation to LOC-KLI. However, there is no straightforward way of improving this approach to a full OEP level.

From a fundamental point of view, our work is characterized by the fact that it is the only approach in which a self-interaction correction of LDA is done within KS theory but without employing any approximation. Hence, it allows to distinguish clearly between effects of the SIC and those that are introduced by using the KLI approximation in the potential. Note that the importance of doing a full OEP calculation instead of using the KLI approximation in calculating the polarizabilities of hydrogen chains has been stressed before, even for the usually noncritical case of EXX [68]. Publication 1 demonstrates that the difference between KLI and full OEP calculations is even more pronounced for the case of the SIC. It is shown that KS-OEP yields polarizabilities that are in excellent agreement with high-quality benchmark calculations [17, 16], whereas the KS-KLI results can be off by more than 50%. Although the dramatic failure of KS-KLI for extended molecular systems has been known in the literature for a couple of years [33, 95], publication 1 is the first to show that this failure is due to the KLI approximation and not due to the SIC functional itself. The reasons for the failure of KS-KLI are buried in the unitary invariance problem. Whereas KS-OEP leads to strongly localized KS orbitals, the self-consistent KS-KLI orbitals remain delocalized over the whole system. The unitary invariance problem thus leads to significantly different self-interaction corrections and, as a direct consequence, to dramatically different results for most observables.

Importantly, the dramatic failure of the KLI approximation to KS-OEP does not challenge the validity of the KLI approximation in general. As discussed in section 1.4.2, it has been known that the KLI approximation yields reliably good results only as long as the approximation does not substantially affect the self-consistent iteration. As demonstrated in publication 1, the latter assumption can no longer be uphold in the case of KS-OEP, at least not for extended molecular systems. For a more detailed analysis of the failure of KS-KLI the reader is referred to publication 1 and appendix A.2.

Fig. 4.1 shows the linear polarizability of hydrogen chains calculated with the different SIC approaches discussed above as a function of the chain length. Here, all KS methods working without an additional unitary transformation are plotted together with the non-KS PZ-SIC results from Ref. [113] in part a). Part b) shows the results obtained from SIC-approaches working with an additional unitary transformation in the potential. The SIC approaches are compared to the polarizabilities obtained from LDA calculations and to those recently obtained from high-quality benchmark calculations using a coupled cluster singles and doubles calculation with perturbative estimate of triples (CCSD(T)) [16]. Except for the PZ-SIC and the CCSD(T) calculations, all polarizabilities shown in Fig. 4.1 were calculated in a customized version of PARSEC [64], thus allowing for a fair comparison of the different approaches. In addition, we employed the same energy-minimizing unitary transformation for all SIC approaches shown in part b). Despite our slightly different approach (real-space grid, energy-minimizing unitary transformation), our calculations show reasonable agreement with the polarizabilities obtained in Refs. [87] and [99], respectively. This suggests that using a numerically less costly localization criterion than the symmetry condition may
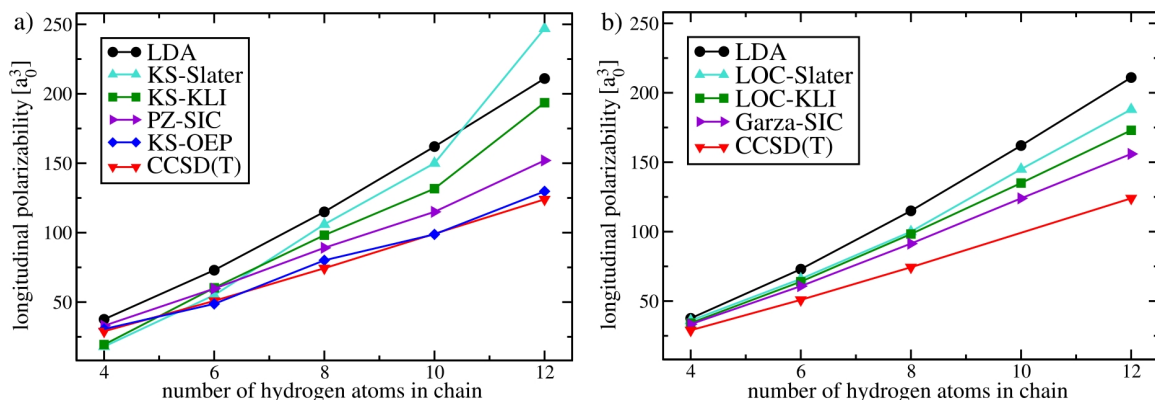
Figure 4.1: Longitudinal polarizability of model hydrogen chains in atomic units as a function of the chain length. Polarizabilities have been calculated in PARSEC [64] using different SIC approaches with (b) and without (a) an additional unitary transformation among the orbitals (see discussion in text) and compared to the LDA results. Recent high-quality coupled cluster calculations (CCSD(T)) from Ref. [16] are taken as a benchmark. PZ-SIC results were taken from Ref. [113]. For an overview of the abbreviations of functionals see also appendix A.4.

be a possible alternative for future applications of LOC-OEP.

The comparison shown in Fig. 4.1 allows for several conclusions:

i) Among all discussed SIC-methods, KS-OEP yields those hydrogen-chain polarizabilities that are closest to the benchmark CCSD(T) results. The good performance of KS-OEP is one of the basic findings of publication 1.

ii) The localization of the orbitals used in the SIC is essential. KS-OEP and PZ-SIC yield self-consistent orbitals that are localized in space. However, in case one can not use exact OEP or PZ-SIC calculations, e.g., because of the high numerical costs for larger molecules, it is clearly necessary to include an additional unitary transformation of the orbitals.

iii) The failure of KS-KLI for extended molecular systems is firmly underlined by Fig. 4.1 a). The polarizability is underestimated for short chains and significantly overestimated for longer ones, thus indicating a clear trend to a growing overestimation for increasing chain lengths. The same reasoning holds for KS-Slater, which performs even worse than KS-KLI due to the absence of the response part of the potential.

iv) The response part of the GOEP potential is essential for both GOEP approaches. The performance improves when going from G-Slater over G-KLI to G-OEP. This is in line with previous findings, e.g., for EXX-OEP [90, 68].

v) The deviation of KS-OEP from the benchmark CCSD(T) results alternates with the number of H_2 pairs in the chain. The same behavior can be found for PZ-SIC. Obviously, this is a consequence of the localization of the self-consistent orbitals. In contrast, neither the LDA or CCSD(T) results nor the polarizabilities obtained from the approaches working with a unitary transformation of the orbitals show this symmetry dependent behavior.

In addition, the good performance of the Garza-SIC approach is quite surprising. In publication 2, it is argued that Garza-SIC and LOC-KLI, if employed with the same unitary transformation, deviate in the response part of the potential. At least this explains the difference between LOC-KLI and Garza-SIC in calculating polarizabilities. However, it remains unclear why Garza-SIC yields better results than all other SIC approaches shown in

Fig. 4.1 b). However, despite its good performance for the hydrogen chains Garza-SIC suffers from a different inherent problem. It is a potential functional which, due to its inherent approximations, most likely does not correspond to any energy functional. Hence, there is no straightforward way of improving this approximative approach, e.g., to a full OEP level. Even worse, serious problems arise, e.g., in the time-dependent case due to the violation of the *zero-force theorem* [93, 92] and in those cases in which the energy functional or its derivatives need to be evaluated directly (see, e.g., Refs. [66] and [4]). These are serious drawbacks which clearly limit the practical usefulness of this approximation. Still, the good performance of Garza-SIC for the hydrogen chains as first demonstrated in Ref. [99] clearly underlines the importance of a unitary transformation of the KS-orbitals in those cases in which one cannot do a full KS-OEP calculation. The solution to this puzzle is to employ the unitary transformation directly in the SIC-energy and derive the corresponding OEP potential. The result of this derivation is the GOEP approach introduced in publication 2 and further discussed in section 2.2.2. Publication 2 further discusses the performance of the newly developed GOEP approach in calculating ionization potentials, HOMO-LUMO gaps and total energies for a set of small molecules. The following section however focuses on the performance of GOEP in calculating dissociation curves of small molecules.

4.2. Dissociation of diatomic molecules

The accurate description of dissociation processes is a challenge for common density functionals. This is mainly because of two reasons. First, commonly used functionals tend to dissociate a neutral molecule AB to fractionally charged fragments A^{+q} and B^{-q}. This empirical finding can be rationalized by the fact that these functionals do not fulfill the principle of integer preference due to the lack of a derivative discontinuity (see discussion in sections 1.5.3 and 1.5.4). As can also be depicted from Fig. 1.3, the NaCl molecule for example will dissociate to $Na^{+0.4}$ and $Cl^{-0.4}$, with an energy lowering of about 1 eV in an LDA calculation [100, 114]. An analogous effect has also been observed for LiF, LiCl and NaF using GGAs and hybrid functionals [94, 26]. Due to the close relation between the principle of integer preference and the many-electron self-interaction problem (see the discussion in sections 1.5.4 and 2.1.2), the authors of Refs. [114] argue that this failure of common density functionals can be traced back to the presence of many-electron self-interaction.

The second reason for the failure of commonly used functionals for dissociation processes is closely related but somewhat better known [102, 5, 40]. Symmetric charged radicals such as H_2^+ and He_2^+ show very unrealistic binding energy curves, although both fragments are identical and thus carry the same fractional charge during the dissociation process. For H_2^+ for example, the dissociation process typically ends up with half an electron sitting on each dissociated proton. However, the total energy of the dissociated system is dramatically too low as an unambiguous consequence of the spurious one-electron self-interaction.

In publication 2, we tested the performance of the GOEP methodology for the dissociation of He_2^+. Being a two-center three-electron system, He_2^+ belongs to the typically used set of benchmark tests used in the literature [5, 40]. Fig. 4.2 shows the basic result, i.e., the ground state energy of He_2^+ as a function of the internuclear distance for different functionals. The red lines denote the exact nonrelativistic dissociation limit [115] and the experimental equilibrium bond length [141], respectively. LDA predicts a too large equilibrium bond length as well as a spurious energy barrier in the dissociation curve at around 2 angstroms. Note
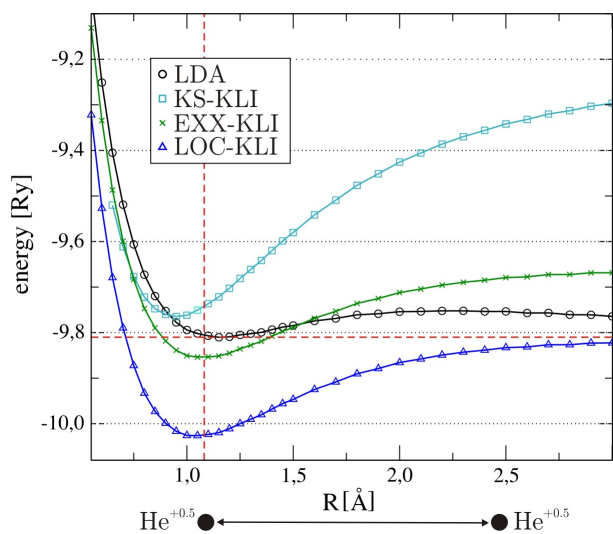
Figure 4.2: He_2^+ dissociation: ground state energy as a function of the internuclear distance R. Dashed red lines mark the energy of the exact nonrelativistic dissociation limit at -9.81 Ry [115] and the experimental equilibrium bond length at 1.081 angstroms [141], respectively.

that, due to one-electron self-interaction, the LDA energy falls off to even lower energies for larger distances, thus yielding a dramatically wrong dissociation energy [115]. In contrast, the self-interaction free EXX-KLI approach yields a correct asymptotic behavior. However, due to the neglect of correlation, the dissociation energy obtained from EXX-KLI is significantly too low.

As a consequence of the consistent inclusion of correlation and the correction of self-interaction, the LOC-KLI approach yields an accurate dissociation energy and a reasonable though somewhat too low equilibrium bond length. Note that the LOC-OEP results depicted in Fig. 3 of publication 2 are very close to the LOC-KLI results plotted in Fig. 4.2. This is in line with the overall finding of publication 2 that LOC-KLI is a very good approximation to LOC-OEP, even for extended molecular systems. In contrast, the dissociation curve obtained from KS-KLI supports the finding of publication 1: KS-KLI yields unphysical results for extended molecular systems as a consequence of the unitary invariance problem. Note that, although both KS-KLI and LOC-KLI are free from one-electron self-interaction, only the LOC-KLI approach yields a reliable description of the He_2^+ dissociation. This underlines the importance of the unitary invariance problem, even in a system with only three electrons. Another interesting conclusion that can be drawn from Fig. 4.2 is the close analogy of the LOC-KLI curve with the one from EXX-KLI. As derived in publication 2, the constant by which the EXX-KLI and the LOC-KLI curve in Fig. 4.2 differ solely arises from the neglect of correlation in the EXX approach. A discussion of this interesting property of LOC-KLI is given in section 3.3.4.

4.3. Photoelectron spectra of organic semiconductors

Photoelectron spectroscopy has emerged as one of the most important techniques for clarifying the electronic structure of molecules and solids. The combination of such measurements with DFT-based electronic structure calculations allows to gain far reaching physical insight, especially in those cases where other methods of determining a material's electronic structure are hard to apply. Formally, this approach is justified by Görling-Levy perturbation theory. Following the discussion in section 1.5.5, KS eigenvalues can be interpreted as
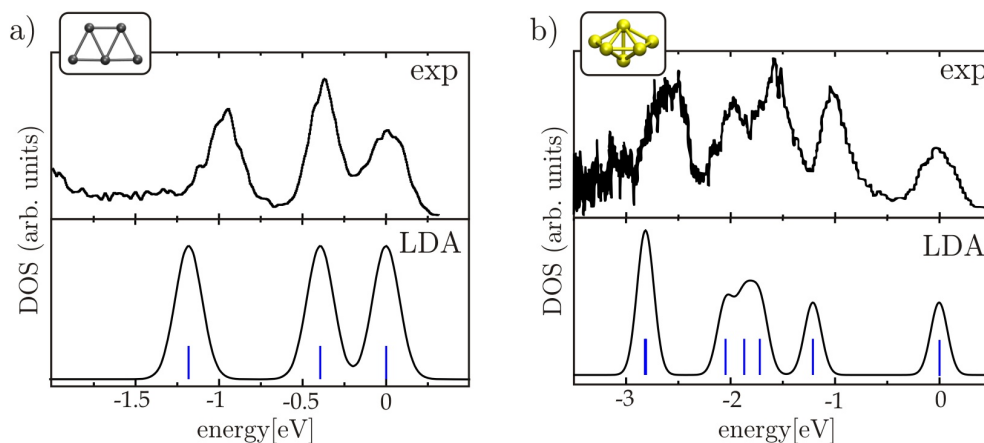
Figure 4.3: Comparison of experimental photoelectron spectra of a) Na_5^- [91] and b) Si_6^- [62] with KS density of states (DOS). LDA KS eigenvalues (blue lines) were calculated with PARSEC [64] and superimposed with Gaussians (black line) of $\sigma = 0.08$ eV to make visual comparison easier. The HOMO-peaks of both the experimental and the KS spectrum were shifted to 0.

approximations to electron removal energies as long as they are derived from a high-quality functional [20]. In practice however, it is often unclear under which circumstances a functional is *accurate enough* to predict a reliable eigenvalue spectrum for a particular system of interest. Whereas for some systems LDA or GGAs yield spectra that compare surprisingly well to the experimental spectrum, they may fail dramatically for others. Quite frequently, the only way out is to do the calculation with different functionals and choose the one which yields the best agreement with experiment. Clearly, this considerably limits the practical usefulness of this method and triggers the need for an easy criterion which can serve as a warning against possible misinterpretation of the KS eigenvalue spectrum. Publication 3 shows that such a criterion can be based on the OSIE introduced in section 2.2.6.

The physical interpretation of KS eigenvalue spectra obtained from LDA or GGA calculations has been used very successfully in the past [11, 2, 56, 20, 62, 63, 132, 92]. In particular, this concept has been proven to be of importance in the field of small cluster physics. Whereas the ionic structure of small inorganic clusters is often neither accessible by any experimental nor theoretical technique alone, the combination of theory and experiment frequently allows to determine the geometrical structures rather accurately. On the theoretical side, the main problem is that the high-dimensional energy-landscape of small clusters typically has a large number of local minima with rather similar total energies. However, the comparison of the corresponding KS eigenvalue spectra with the experimental photoelectron spectrum frequently allows to determine the present ionic configuration reliably. This interplay between theory and experiment has been used very successfully in the past [57, 2, 56, 62, 92]. An example is provided in Fig. 4.3. Here, the KS eigenvalues of the small clusters Na_5^- and Si_6^- obtained from LDA-calculations and superimposed with a Gaussian broadening of $\sigma = 0.08$ eV are compared to the corresponding experimental photoelectron spectra [62, 91]. Although there are a number of small deviations, the agreement of theory and experiment is surprisingly good, in particular in view of the various approximations that go into this comparison.

Due to the great success of this concept for inorganic clusters, a number of approaches exist

to apply it to other systems as well. Important examples that are of great fundamental and practical interest are organic semiconductor materials. In recent years, considerable progress has been made in raising the technological usability of organic molecules in a new class of (opto)-electronic devices, e.g., organic light-emitting diodes, transistors and solar cells. The advantages of these materials are obvious: light weight, mechanical flexibility, tunability of electronic properties, low costs, and easy processability. The ever growing interest in organic molecular semiconductors triggers the need for a detailed understanding of the electronic properties of these materials. Their electronic structure can be investigated by ultraviolet photoemission spectroscopy (UPS) either in thin solid films or with single molecules in the gas phase. The comparison of the experimental spectra with DFT-based electronic structure calculations then allows to gain far reaching insight into intermolecular bondings and polarization [136, 47, 23, 55, 110, 79, 116]. For quite a number of organic semiconductors, the spectra obtained from LDA or GGA calculations compare quite well with experimental UPS spectra. The usually observed small differences between the measured and calculated spectra are commonly ascribed to the various approximations that go into this comparison. However, from time to time systems are found for which semilocal functionals fail dramatically in predicting the measured spectra. One example is the PTCDA molecule, a paradigm system in the field of organic semiconductors [23].

Fig. 4.4 compares the KS eigenvalue spectra of PTCDA for different functionals to the experimental gas phase photoelectron spectrum reported in Ref. [23]. To make visual comparison easier, the KS eigenvalues are convoluted with Gaussians and all spectra are aligned so that the HOMO-peaks match. Note that the experimental spectrum shows a pronounced gap marked by the shaded area between the HOMO and the HOMO-1 peak. The semilocal functionals LDA and PBE predict several eigenvalues to be right in the middle of the experimental gap, thus failing completely to predict an accurate density of states. The authors of Ref. [23] solve this problem by going over to a hybrid functional. As can be depicted from the green curve in Fig. 4.4, B3LYP predicts a correct gap and an overall reliable eigenvalue spectrum.

The findings of Ref. [23] trigger a number of obvious questions: How can it be that semilocal functionals fail completely for PTCDA but work reliably for rather similar systems such as pentacene [47, 129]? Why do semilocal functionals fail for PTCDA and why does B3LYP work? Can we predict under which circumstances and for which systems semilocal functionals fail?

The fact that going over to a functional which includes parts of HF-exchange opens the gap in PTCDA triggers the assumption that the failure of semilocal functionals might be related to the self-interaction problem. Ref. [23] provides further indications for this assumption by looking at the spatial distribution of the highest occupied LDA orbitals (see Fig. 4.5). The orbitals corresponding to those LDA eigenvalues that lie inside the shaded area of Fig. 4.4, i.e., inside the gap of the experimental spectrum, are enclosed in red boxes. It is evident that the structure of the orbitals inside the gap is fundamentally different from the structure of the other orbitals. However, following the discussion in section 3.3.1, the structure of orbital densities has a significant influence on the corresponding SIE due to the unitary invariance problem. Further, as discussed in section 2.2.6, the presence of self-interaction in the used functional can influence the KS eigenvalue spectrum significantly if different orbitals suffer from a different amount of OSIE. Looking at the orbital structures of PTCDA in Fig. 4.5, it is to be expected that, e.g., HOMO-5 and HOMO-7 suffer from roughly the same amount of self-interaction whereas the self-interaction energies of, e.g., HOMO-5 and HOMO-4 can
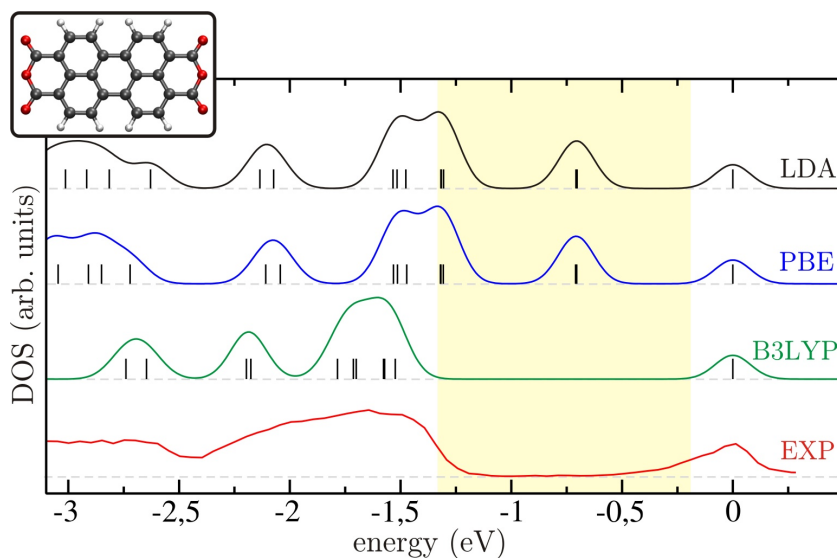
Figure 4.4: Experimental photoelectron spectrum of PTCDA (red line) from Ref. [23] compared to KS eigenvalue spectra obtained from LDA (black), PBE (blue), and B3LYP (green) calculations in TURBOMOLE [32, 1, 133]. KS eigenvalues are superimposed with Gaussians (colored lines) of width $\sigma = 0.08$ eV and all HOMO-peaks are set to 0 to make visual comparison easier. The shaded area marks the pronounced gap in the experimental spectrum. This gap is absent in the KS-DOS obtained from semilocal functionals.

be expected to be rather different.

In publication 3, we establish that it is indeed the combination of self-interaction in the used functional and varying spatial structure in the highest occupied orbitals of the studied system that causes the failure of semilocal functionals. We show this by plotting the OSIE for a set of test systems. It is consistently found that in those systems for which semilocal functionals yield reliable eigenvalue spectra, the OSIE is roughly the same for all of the highest occupied orbitals. In these cases, the OSIE simply shifts the whole eigenvalue spectrum by a constant. However, as the experimental and theoretical spectra are typically shifted so that the HOMO-peaks match, this constant does not have any consequences for the comparison of theory and experiment. If however the highest occupied orbitals suffer from significantly different amounts of OSIE, using a functional which is not free from self-interaction will distort the eigenvalue spectrum significantly. Publication 3 shows that this is indeed the case for PTCDA and thus explains the findings of Ref. [23].

In summary, publication 3 has four important messages:
i) The spatial structure of the highest occupied orbitals enters the reliability of the occupied KS eigenvalue spectrum as a decisive factor. If the highest occupied orbitals have significantly different spatial structures, it is to be expected that semilocal functionals will not yield reliable eigenvalue spectra.
ii) The OSIE introduced in section 2.2.6 can serve as a warning against the misinterpretation of KS eigenvalue spectra. If the highest occupied orbitals suffer from significantly different amounts of OSIEs, the KS eigenvalue spectrum obtained from semilocal functionals is not reliable. The OSIE criterion is computationally cheap, easy to implement and can be computed solely from quantities obtained in an LDA or GGA calculation.
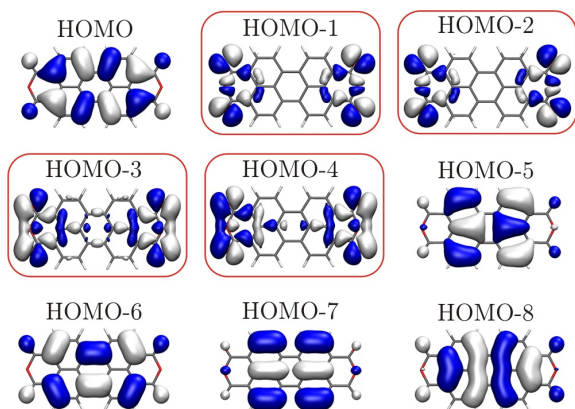
Figure 4.5: Highest occupied orbitals of PTCDA as obtained from an LDA calculation in PARSEC [64]. Red boxes mark the orbitals for which the corresponding eigenvalues lie inside the HOMO/HOMO-1 gap of the experimental spectrum, i.e., in the shaded area of Fig. 4.4. The different spatial structures of the orbitals in red boxes give a hint that self-interaction may play a prominent role in the failure of semilocal functionals.

iii) A self-interaction correction using the LOC-KLI approach yields reliable eigenvalue spectra of organic semiconductors also in such cases where semilocal functionals fail. This demonstrates that self-interaction is the major reason for the failure of semilocal functionals. In this context, it is interesting to note that the self-interaction correction cures the failures of LDA without introducing any empirical parameters. Note that B3LYP also yields a reliable spectrum for PTCDA, however, on the basis of 8 empirically fitted parameters.
iv) The OSIE methodology suggests an easy shortcut that leads to a correct eigenvalue spectrum: if the OSIE $e_{i\sigma}$ is a good approximation to the total shift of the eigenvalues, i.e., to $\Delta\epsilon_{i\sigma}$ defined in Eq. (2.30), an unphysical LDA spectrum could be corrected simply by subtracting $e_{i\sigma}$ from the LDA eigenvalues on an orbital-by-orbital basis. However, as will be discussed in appendix A.1, in those cases in which self-interaction has a significant influence on the eigenvalue spectrum, self-consistency effects of the SIC are typically rather large. As a consequence, $e_{i\sigma}$ as calculated from LDA quantities typically overestimates the actual shift $\Delta\epsilon_{i\sigma}$ significantly in such cases. This and other arguments discussed in more detail in appendix A.1 limit the practical usefulness of this *a posteriori* correction. However, we found that one can estimate the self-interaction corrected eigenvalues for PTCDA and NTCDA rather accurately from LDA quantities by using an expression introduced by Perdew and Zunger in the context of atomic SIC calculations [106]. More details on this approximation can be found in publication 3 and appendix A.1.

In addition to PTCDA, publication 3 also studies the eigenvalue spectrum of the similar but smaller organic semiconductor NTCDA. It is found that the spectrum of NTCDA calculated from LDA or GGAs is significantly distorted due to a varying OSIE in the highest occupied orbitals. In particular, it is shown that the order of the highest occupied orbitals changes dramatically when going from LDA to LOC-OEP. Note that, only shortly after our work, a gas phase spectrum of NTCDA was published in Ref. [116]. The B3LYP eigenvalue spectrum for NTCDA agrees well with experiment, as does the LOC-OEP spectrum. In particular, the authors of Ref. [116] found by a detailed experimental study of the vibrational broadening of the HOMO-peak, that the HOMO of NTCDA is a "non-bonding molecular orbital" [116]. This finding confirms that the HOMO found from the LDA-calculation is indeed wrong and that LOC-OEP correctly predicts a change in the ordering of the highest occupied orbitals.

Publications 1-3 highlight the important role played by the self-interaction problem in predicting accurate KS eigenvalues, KS gaps, dissociation and charge transfer properties of organic polymers and molecular semiconductors by virtue of DFT calculations. A sound understanding of the problems and prospects of different density functionals is clearly needed

in order to be able to use DFT calculations as a tool for understanding and improving organic electronic devices. An example for such an application of DFT for organic semiconductors is provided in publication 4.

4.4. Fluorescence quenching in an organic donor-acceptor dyad

In the past decades, considerable progress has been made in improving the performance and efficiency of organic semiconductor devices. From the basic research side, this progress is fueled by a rich variety of experimental and theoretical studies of the properties and structure of organic molecular semiconductors. In this context, especially tailored model systems based on small π-conjugated molecules play a particularly important role as they allow to improve our understanding of energy- and charge-transfer processes in organic materials.

The organic dyes perylene bisimide (PTCDI) and triphenyl diamine (TPD) are among the most prominent compounds used in these model systems (see Fig. 4.6 for details on the chemical structures). Both PTCDI and TPD show strong fluorescence in the visible range and the emission spectrum of TPD overlaps with the absorption spectrum of PTCDI. Hence, TPD and PTCDI are an ideal pair to study resonant excitation energy transfer. Following this line of thought, a donor-bridge-acceptor (DBA) system consisting of TPD as an energy donor (D), PTCDI as an energy acceptor (A) linked by a saturated and flexible organic bridge (B) has recently been synthesized [6] and studied [117] by time-resolved fluorescence spectroscopy measurements.

Traditionally, the transfer of excitation energy between two molecules with spectral overlap is treated within the Förster-resonant-energy-transfer (FRET) methodology [30]. FRET approximates the donor and acceptor molecules as point dipoles. Higher order multipoles as well as all kinds of electronic and vibrational couplings between D, A, a possible bridge, and the surrounding medium are neglected. With these approximations, *Fermi's golden rule* allows to find a rate expression for the energy transfer which employs only quantities that can be measured in the experiment and the distance r between D and A. The transfer rate itself can also be determined experimentally by comparison of the D lifetime in the presence of A to the lifetime of the free D. Due to the typical distance dependence of the dipole-dipole interaction $\sim r^{-6}$, FRET has been used very successfully as a ruler on the nanoscale, e.g., for monitoring conformational changes in proteins. However, over the years many studies showed that the approximations used in FRET can break down rather easily, especially if the distance between D and A is reduced. Refs. [65, 9, 10, 49, 45, 44] are just a few examples from a vast body of literature that deals with the breakdown of the Förster-formula.

The authors of Ref. [117] used FRET to determine the mean distance between PTCDI and TPD in the DBA system presented in Fig. 4.6. By measuring the change in the D fluorescence decay rate, the authors derived a D-A distance that corresponds to a fully stretched conformation of the bridge. However, they also found evidence on other electronic processes in the system: the decay rate of A in DBA is substantially increased as compared to free A, thus indicating an efficient quenching process of the A fluorescence in the bridged system. This quenching can also be observed if one excites DBA directly at the A absorption energy, i.e., it occurs independently from the excitation energy transfer. A possible and
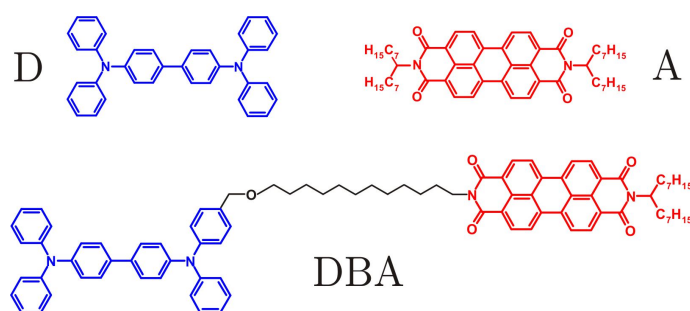
Figure 4.6: The organic molecular semiconductors discussed in publication 4: TPD (D), PTCDI (A), and donor-bridge-acceptor molecule (DBA).

frequently invoked explanation for fluorescence quenching in this type of DBA systems is charge transfer between D and A, which can be caused either by a superexchange coupling through the saturated bridge [51] or by orbital overlap between D and A as a consequence of a collapse of the bridge in solution. As for the former, a superexchange coupling as strong as the one observed here would be quite unusual considering the length of the saturated bridge. As for the latter, a collapse of the bridge seems to contradict the findings of the FRET experiment. However, if D and A are strongly coupled electronically, the FRET methodology used to derive the D-A distance in Ref. [117] might no longer be applicable. Still, if the bridge is not stretched in solution, one would expect this coupling to have a significant influence on the fluorescence spectrum itself and not only on the lifetimes.

In summary, the experimental findings of Ref. [117] alone are not conclusive. In publication 4 it is shown that a theoretical analysis employing DFT and TDDFT as a tool to study the electronic properties of the DBA system can shed new light on the processes observed in DBA. The importance of the self-interaction problem for the alignment of KS eigenvalues (see publication 3), for the calculation of ionization potentials (see publication 2), and for the evaluation of charge transfer problems (see publication 1), in particular for charge transfer excitations (see discussion in section 1.6.3), demands high standards on the used functionals and underlines the importance of a careful and thorough interpretation of the obtained results. In publication 4, we compare the results obtained from DFT and TDDFT calculations both with other theoretical studies of PTCDI [107] and TPD [78] as well as with the experimental results from Refs. [6] and [117]. We discuss the problems concerning the calculation of ionization potentials, KS gaps, and charge-transfer excitations. As for the latter, we employ and compare a set of functionals using different fractions of HF-exchange and analyse the obtained excitation spectrum with the help of the natural transition orbitals introduced in section 1.6.4 in order to distinguish between charge-transfer and pure valence excitations. Our calculations take into account an empirical dispersion correction of the used functionals [38] as well as a continuum model for the solvent [58]. The dynamics of the DBA system in solution are analyzed by means of classical MD [109, 3] (note that further details on the MD calculations are given in publication 4).

By comparing the calculations for a mixture of free donors and acceptors to those for the bridged DBA molecule in stretched conformation, publication 4 finds that the large HOMO-LUMO-gap of the saturated bridge keeps the electronic spectra of D and A completely separate. Hence, the direct influence of the bridge on the ground- and excited-state spectra of D and A is negligible and a superexchange coupling through the bridge can be ruled out.

However, by employing MD simulations of DBA in different solvents, publication 4 reveals that it is the mechanical influence of the bridge that causes the A-fluorescence quenching. The bridge folds in solution so that donor and acceptor stack at a distance of ~ 5 angstroms, which is typical for π-π stacks. DFT calculations of DBA in this configuration show that the orbitals of donor and acceptor overlap, thus yielding an energy gain of approximately 0.55 eV as compared to the stretched DBA. As a consequence, the stacked configuration is thermally stable. The strong electronic coupling between D and A opens up a non-radiative de-excitation pathway of the A excitation, which includes charge transfer and recombination. As a consequence, the A-fluorescence is quenched efficiently. In addition, the FRET-methodology is no longer applicable.

Finally, TDDFT calculations on the folded DBA explain why the strong electronic coupling between D and A can not be observed directly in the fluorescence spectrum. The DBA-exciplex shows major excitations at the original excitation energies of D and A. However, an analysis with the help of NTOs shows that the nature of the DBA excitations has changed significantly as compared to free D and A. In addition, in DBA three excitation energies can be found in the energetic vicinity of the original D excitation. Due to the large vibrational broadening of the fluorescence spectrum, these three excitations can not be distinguished directly in the measured spectrum. However, the coupling leads to a multi-exponential decay of the DBA-fluorescence at the donor-emission energy. This is in agreement with recent experimental studies and thus supports the findings of publication 4.

Bibliography

[1] R. Ahlrichs, M. Bär, M. Häser, H. Horn, and C. Kölmel, Chem. Phys. Lett. **162**, 165 (1989).

[2] J. Akola, M. Manninen, H. Häkkinen, U. Landman, X. Li, and L.-S. Wang, Phys. Rev. B **62**, 13216 (2000).

[3] N. L. Allinger, Y. H. Yuh, and J. H. Lii, J. Am. Chem. Soc. **111**, 8551 (1989).

[4] R. Armiento, S. Kümmel, and T. Körzdörfer, Phys. Rev. B **77**, 165106 (2008).

[5] T. Bally and G. N. Sastry, J. Phys. Chem. A **101**, 7923 (1997).

[6] P. Bauer, H. Wietasch, S. M. Lindner, and M. Thelakkat, Chem. Mater. **19**, 88 (2007).

[7] A. D. Becke, Phys. Rev. A **38**, 3098 (1988).

[8] A. D. Becke, J. Chem. Phys. **104**, 1040 (1996).

[9] D. Beljonne, J. Cornil, R. Silbey, P. Millié, and J.-L. Brédas, J. Chem. Phys. **112**, 4749 (2000).

[10] D. Beljonne *et al.*, Proc. Nat. Acad. Sci. U.S.A. **99**, 10982 (2002).

[11] N. Binggeli and J. R. Chelikowsky, Phys. Rev. Lett. **75**, 493 (1995).

[12] S. F. Boys, Rev. Mod. Phys. **32**, 296 (1960).

[13] M. E. Casida, in *Recent Developments and Applications in Density-Functional Theory*, edited by J. M. Seminario, pp. 391–439 (Elsevier Science, Amsterdam, 1996).

[14] D. M. Ceperley and B. J. Alder, Phys. Rev. Lett. **45**, 566 (1980).

[15] B. Champagne, F. A. Bulat, W. Yang, S. Bonness, and B. Kirtman, J. Chem. Phys. **125**, 194114 (2006).

[16] B. Champagne and B. Kirtman, Int. J. Quant. Chem. **109**, 3103 (2009).

[17] B. Champagne, D. H. Mosley, M. Vračko, and J.-M. André, Phys. Rev. A **52**, 178 (1995).

[18] B. Champagne *et al.*, J. Chem. Phys. **109**, 10489 (1998).

[19] J. Chen, J. B. Krieger, Y. Li, and G. J. Iafrate, Phys. Rev. A **54**, 3939 (1996).

[20] D. P. Chong, O. V. Gritsenko, and E. J. Baerends, J. Chem. Phys. **116**, 1760 (2002).

[21] E. R. Davidson, Rev. Mod. Phys. **44**, 451 (1972).

[22] P. A. M. Dirac, Proc. Camb. Phil. Soc. **26**, 376 (1930).

[23] N. Dori, M. Menon, L. Kilian, M. Sokolowski, L. Kronik, and E. Umbach, Phys. Rev. B **73**, 195208 (2006).

[24] R. M. Dreizler and E. K. U. Gross, *Density Functional Theory*, pp. 10–19 (Springer, Berlin, 1990).

[25] A. Dreuw and M. Head-Gordon, Chem. Rev. **105**, 4009 (2005).

[26] A. D. Dutoi and M. Head-Gordon, Chem. Phys. Lett. **422**, 230 (2006).

[27] C. Edminston and K. Ruedenberg, Rev. Mod. Phys. **35**, 457 (1963).

[28] P. Elliott, K. Burke, and F. Furche, in *Reviews in Computational Chemistry*, edited by K. B. Lipkowitz and T. R. Cundari, pp. 91–165 (Wiley, Hoboken, NJ, 2009), also arXiv:cond-mat/0703590.

[29] E. S. Fois, J. I. Penman, and P. A. Madden, J. Chem. Phys. **98**, 6352 (1993).

[30] T. Förster, Ann. Phys. **437**, 55 (1948).

[31] J. M. Foster and S. F. Boys, Rev. Mod. Phys. **32**, 300 (1960).

[32] F. Furche and D. Rappoport, in *Computational and Theoretical Chemistry*, vol. 16, edited by M. Olivucci, pp. 93–128 (Elsevier, Amsterdam, 2005), chapter III of Computational Photochemistry.

[33] J. Garza, J. A. Nichols, and D. A. Dixon, J. Chem. Phys. **112**, 7880 (2000).

[34] S. J. A. van Gisbergen *et al.*, Phys. Rev. Lett. **83**, 694 (1999).

[35] S. Goedecker and C. J. Umrigar, Phys. Rev. A **55**, 1765 (1997).

[36] A. Görling, Phys. Rev. A **54**, 3912 (1996).

[37] T. Grabo, T. Kreibich, S. Kurth, and E. K. U. Gross, in *Strong Coulomb Correlation in Electronic Structure: Beyond the Local Density Approximation*, edited by V. Anisimov (Gordon & Breach, Tokyo, 2000).

[38] S. Grimme, J. Comput. Chem. **25**, 1463 (2004).

[39] M. Grüning, O. V. Gritsenko, and E. J. Baerends, J. Chem. Phys. **116**, 6435 (2002).

[40] M. Grüning, O. V. Gritsenko, S. J. A. van Gisbergen, and E. J. Baerends, J. Phys. Chem. A **105**, 9211 (2001).

[41] O. Gunnarsson and B. I. Lundqvist, Phys. Rev. B **13**, 4274 (1976).

[42] J. Harris and R. O. Jones, J. Phys. F **4**, 1170 (1974).

[43] J. G. Harrison, R. A. Heaton, and C. C. Lin, J. Phys. B **16**, 2079 (1983).

[44] E. Hennebicq, D. Beljonne, C. Curutchet, G. D. Scholes, and R. J. Silbey, J. Chem. Phys. **130**, 214505 (2009).

[45] D. Hofmann, *Anregung und Energietransfer in molekularen Systemen*, Diploma thesis, University of Bayreuth (2008).

[46] P. Hohenberg and W. Kohn, Phys. Rev. **136**, B864 (1964).

[47] K. Hummer and C. Ambrosch-Draxl, Phys. Rev. B **72**, 205205 (2005).

[48] J. F. Janak, Phys. Rev. B **18**, 7165 (1978).

[49] S. Jang, M. D. Newton, and R. J. Silbey, Phys. Rev. Lett. **92**, 218301 (2004).

[50] R. O. Jones and O. Gunnarsson, Rev. Mod. Phys. **61**, 689 (1989).

[51] K. D. Jordan and M. N. Paddon-Row, Chem. Rev. **92**, 395 (1992).

[52] D. R. Kanis, M. A. Ratner, and T. J. Marks, Chem. Rev. **94**, 195 (1994).

[53] A. Karolewski, R. Armiento, and S. Kümmel, J. Chem. Theory Comput. **5**, 712 (2009).

[54] D. Kasinathan *et al.*, Phys. Rev. B **74**, 195110 (2006).

[55] S. Kera, H. Yamane, H. Fukagawa, T. Hanatani, K. K. Okudaira, K. Seki, and N. Ueno, J. Electron Spectrosc. Relat. Phenom. **156-158**, 135 (2007).

[56] S. N. Khanna, M. Beltran, and P. Jena, Phys. Rev. B **64**, 235419 (2001).

[57] H. Kietzmann *et al.*, Phys. Rev. Lett. **77**, 4528 (1996).

[58] A. Klamt and G. Schüürmann, J. Chem. Soc. Perkin Trans. **2**, 799 (1993).

[59] W. Kohn and L. J. Sham, Phys. Rev. **140**, A1133 (1965).

[60] J. B. Krieger, Y. Li, and G. J. Iafrate, Phys. Rev. A **46**, 5453 (1992).

[61] J. B. Krieger, Y. Li, and G. J. Iafrate, Phys. Rev. A **45**, 101 (1992).

[62] L. Kronik, R. Fromherz, E. Ko, G. Ganteför, and J. R. Chelikowsky, Nat. Mater. **1**, 49 (2002).

[63] L. Kronik, R. Fromherz, E. Ko, G. Ganteför, and J. R. Chelikowsky, Eur. Phys. J. D **24**, 33 (2003).

[64] L. Kronik *et al.*, Phys. Status Solidi B **243**, 1063 (2006).

[65] B. P. Krueger, G. D. Scholes, and G. R. Fleming, J. Phys. Chem. B **102**, 5378 (1998).

[66] S. Kümmel and L. Kronik, Comput. Mater. Sci. **35**, 321 (2006).

[67] S. Kümmel and L. Kronik, Rev. Mod. Phys. **80**, 3 (2008).

[68] S. Kümmel, L. Kronik, and J. P. Perdew, Phys. Rev. Lett. **93**, 213002 (2004).

[69] S. Kümmel and J. P. Perdew, Phys. Rev. B **68**, 035103 (2003).

[70] S. Kümmel and J. P. Perdew, Phys. Rev. Lett. **90**, 43004 (2003).

[71] D. C. Langreth and J. P. Perdew, Solid State Commun. **17**, 1425 (1975).

[72] C. Lee, W. Yang, and R. G. Parr, Phys. Rev. B **37**, 785 (1988).

[73] R. van Leeuwen, Phys. Rev. Lett. **82**, 3863 (1999).

[74] M. Levy, Proc. Natl. Acad. Sci. USA **76**, 6062 (1979).

[75] M. Levy, Phys. Rev. A **26**, 1200 (1982).

[76] M. Levy, Phys. Rev. A **52**, R4313 (1995).

[77] P.-O. Löwdin, J. Chem. Phys. **18**, 365 (1950).

[78] M. Malagoli and J.-L. Brédas, Chem. Phys. Lett. **327**, 13 (2000).

[79] N. Marom, O. Hod, G. E. Scuseria, and L. Kronik, J. Chem. Phys. **128**, 164107 (2008).

[80] M. A. L. Marques and E. K. U. Gross, Annu. Rev. Phys. Chem. **55**, 427 (2004).

[81] R. L. Martin, J. Chem. Phys. **118**, 4775 (2003).

[82] N. Marzari and D. Vanderbilt, Phys. Rev. B **56**, 12847 (1997).

[83] I. Mayer, Int. J. Quant. Chem. **90**, 63 (2002).

[84] N. D. Mermin, Phys. Rev. **137**, A1441 (1965).

[85] J. Messud, P. M. Dinh, P.-G. Reinhard, and E. Suraud, Chem. Phys. Lett. **461**, 316 (2008).

[86] J. Messud, P. M. Dinh, P.-G. Reinhard, and E. Suraud, Phys. Rev. Lett. **101**, 096404 (2008).

[87] J. Messud, Z. Wang, P. M. Dinh, P.-G. Reinhard, and E. Suraud, Chem. Phys. Lett. **479**, 300 (2009).

[88] P. Mori-Sánchez, A. J. Cohen, and W. Yang, J. Chem. Phys. **125**, 201102 (2006).

[89] P. Mori-Sánchez, A. J. Cohen, and W. Yang, Phys. Rev. Lett. **100**, 146401 (2008).

[90] P. Mori-Sánchez, Q. Wu, and W. Yang, J. Chem. Phys. **119**, 11001 (2003).

[91] M. Moseler, B. Huber, H. Häkkinen, U. Landman, G. Wrigge, M. A. Hoffmann, and B. v. Issendorff, Phys. Rev. B **68**, 165413 (2003).

[92] M. Mundt, *Orbital functionals in Time-Dependent Density-Functional Theory*, Ph.D. thesis, University of Bayreuth (2007).

[93] M. Mundt, S. Kümmel, R. van Leeuwen, and P.-G. Reinhard, Phys. Rev. A **75**, 050501(R) (2007).

[94] M. M. Ossowski, L. L. Boyer, M. J. Mehl, and M. R. Pederson, Phys. Rev. B **68**, 245107 (2003).

[95] S. Patchkovskii, J. Autschbach, and T. Ziegler, J. Chem. Phys. **115**, 26 (2001).

[96] M. R. Pederson, R. A. Heaton, and C. C. Lin, J. Chem. Phys. **80**, 1972 (1984).

[97] M. R. Pederson, R. A. Heaton, and C. C. Lin, J. Chem. Phys. **82**, 2688 (1985).

[98] M. R. Pederson and C. C. Lin, J. Chem. Phys. **88**, 1807 (1988).

[99] C. D. Pemmaraju, S. Sanvito, and K. Burke, Phys. Rev. B **77**, 121204(R) (2008).

[100] J. P. Perdew, Adv. Quant. Chem. **21**, 113 (1990).

[101] J. P. Perdew, K. Burke, and M. Ernzerhof, Phys. Rev. Lett. **77**, 3865 (1996).

[102] J. P. Perdew and M. Ernzerhof, in *Electronic Density Functional Theory: Recent Progess and New Directions*, edited by J. F. Dobson, G. Vignale, and M. P. Das (Plenum, New York, 1998).

[103] J. P. Perdew, M. Ernzerhof, and K. Burke, J. Chem. Phys. **105**, 9982 (1996).

[104] J. P. Perdew, R. G. Parr, M. Levy, and J. L. Balduz Jr., Phys. Rev. Lett. **49**, 1691 (1982).

[105] J. P. Perdew and Y. Wang, Phys. Rev. B **45**, 13244 (1992).

[106] J. P. Perdew and A. Zunger, Phys. Rev. B **23**, 5048 (1981).

[107] F. Pichierri, J. Mol. Struct. **686**, 57 (2004).

[108] J. Pipek and P. G. Mezey, J. Chem. Phys. **90**, 4916 (1989).

[109] P. Ren and J. W. Ponder, J. Phys. Chem. B **107**, 5933 (2003).

[110] C. Risko *et al.*, J. Phys. Chem. C **112**, 13215 (2008).

[111] E. Runge and E. K. U. Gross, Phys. Rev. Lett. **52**, 997 (1984).

[112] A. Ruzsinszky, J. P. Perdew, and G. I. Csonka, Phys. Rev. A **78**, 022513 (2008).

[113] A. Ruzsinszky, J. P. Perdew, G. I. Csonka, G. E. Scuseria, and O. A. Vydrov, Phys. Rev. A **77**, 060502(R) (2008).

[114] A. Ruzsinszky, J. P. Perdew, G. I. Csonka, O. A. Vydrov, and G. E. Scuseria, J. Chem. Phys. **125**, 194112 (2006).

[115] A. Ruzsinszky, J. P. Perdew, G. I. Csonka, O. A. Vydrov, and G. E. Scuseria, Phys. Rev. A **126**, 104102 (2007).

[116] J. Sauther, J. Wüsten, S. Lach, and C. Ziegler, J. Chem. Phys. **131**, 034711 (2009).

[117] C. Scharf, K. Peter, P. Bauer, C. Jung, M. Thelakkat, and J. Köhler, Chem. Phys. **328**, 403 (2006).

[118] N. Schuch and F. Verstraete, Nature Physics **5**, 732 (2009).

[119] A. Seidl, A. Görling, P. Vogl, J. A. Majewski, and M. Levy, Phys. Rev. B **53**, 3764 (1996).

[120] H. Sekino, Y. Maeda, M. Kamiya, and K. Hirao, J. Chem. Phys. **126**, 014107 (2007).

[121] R. T. Sharp and G. K. Horton, Phys. Rev. **90**, 317 (1953).

[122] P. J. Stephens, F. J. Devlin, C. F. Chabalowski, and M. J. Frisch, J. Phys. Chem. **98**, 11623 (1994).

[123] J. E. Subotnik, Y. Shao, W. Liang, and M. Head-Gordon, J. Chem. Phys. **121**, 9220 (2004).

[124] J. D. Talman and W. F. Shadwick, Phys. Rev. A **14**, 36 (1976).

[125] W. M. Temmerman, A. Svane, Z. Szotek, and H. Winter, in *Electronic Density Functional Theory: Recent Progess and New Directions*, edited by J. F. Dobson, G. Vignale, and M. P. Das (Plenum, New York, 1998).

[126] W. M. Temmerman, Z. Szotek, and H. Winter, Phys. Rev. B **47**, 11533 (1993).

[127] M. Thiele, *Correlated electron dynamics and memory in time-dependent density functional theory*, Ph.D. thesis, University of Bayreuth (2009).

[128] K. S. Thygesen, L. B. Hansen, and K. W. Jacobsen, Phys. Rev. Lett. **94**, 026405 (2005).

[129] M. L. Tiago, J. E. Northrup, and S. G. Louie, Phys. Rev. B **67**, 115212 (2003).

[130] S. Tretiak and S. Mukamel, Chem. Rev. **102**, 3171 (2002).

[131] N. Troullier and J. L. Martins, Phys. Rev. B **43**, 1993 (1991).

[132] G. Tu, V. Carravetta, O. Vahtras, and H. Agren, J. Chem. Phys. **127**, 174110 (2007).

[133] TURBOMOLE V5.10 2008, a development of University of Karlsruhe and Forschungszentrum Karlsruhe GmbH, 1989-2007, TURBOMOLE GmbH, since 2007; available from http://www.turbomole.com.

[134] C. A. Ullrich, P.-G. Reinhard, and E. Suraud, Phys. Rev. A **62**, 053202 (2000).

[135] P. Umari and N. Marzari, J. Chem. Phys. **131**, 094104 (2009).

[136] E. Umbach and R. Fink, in *Proceedings of the International School of Physics Enrico Fermi, Course CXLIX*, edited by V. M. Agranovich and G. C. La Rocca (IOS Press, Amsterdam, 2002).

[137] S. H. Vosko, L. Wilk, and M. Nusair, Can. J. Phys. **58**, 1200 (1980).

[138] O. A. Vydrov and G. E. Scuseria, J. Chem. Phys. **122**, 184107 (2005).

[139] O. A. Vydrov, G. E. Scuseria, and J. P. Perdew, J. Chem. Phys. **126**, 154109 (2007).

[140] G. H. Wannier, Phys. Rev. **52**, 191 (1937).

[141] J. Xie, B. Poirier, and G. I. Gellene, J. Chem. Phys. **122**, 184310 (2005).

[142] K. Yabana and G. F. Bertsch, Phys. Rev. B **54**, 4484 (1996).

Appendix

A.1. The orbital self-interaction error in KS-KLI and LOC-KLI

The orbital self-interaction error (OSIE) derived in section 2.2.6 is an approximation to the shift of an eigenvalue subject to a self-interaction correction following the GOEP methodology. As demonstrated in publication 3, the OSIE can serve as a warning against misinterpretation of eigenvalue spectra obtained from semilocal functionals. In general, the OSIE is defined via the semilocal exchange-correlation potential $v_{\mathrm{xc},\sigma}^{\mathrm{sl}}$ and the orbital-specific potentials $u_{\mathrm{xc},i\sigma}^{\mathrm{G}}$ of the SIC (see Eq. (2.23)). Then, the OSIE is the approximate shift in the eigenvalue spectrum when changing the potential from $v_{\mathrm{xc},\sigma}^{\mathrm{sl}}$ to the GOEP belonging to the chosen orbital-specific potentials $u_{\mathrm{xc},i\sigma}^{\mathrm{G}}$. Assuming the semilocal potential to be the LDA-potential in the following, the OSIE thus depends on the unitary transformation used in SIC-GOEP. As a consequence, the OSIE corresponding to KS-OEP is expected to be different to the OSIE corresponding to LOC-OEP. In this appendix, the OSIEs corresponding to KS-OEP and LOC-OEP are discussed and compared in detail using the example of the organic molecular semiconductor PTCDA (see also publication 3).

With the KS orbitals φ_i and orbital densities $n_i(\mathbf{r}) = |\varphi_i(\mathbf{r})|^2$ (spin indices are omitted for clarity) obtained from a self-consistent LDA calculation and with the corresponding energy-minimizing orbitals $\tilde{\varphi}_j$ with densities $\tilde{n}_j(\mathbf{r}) = |\tilde{\varphi}_j(\mathbf{r})|^2$ one can plot and compare a number of quantities.

$$e_i^{\mathrm{KS}} \overset{(2.36)}{=} \left\langle \varphi_i \left| v_{\mathrm{xc}}^{\mathrm{LDA}}[n] - u_{\mathrm{xc},i}^{\mathrm{KS}} \right| \varphi_i \right\rangle \overset{(2.27)}{=} \left\langle \varphi_i \left| v_{\mathrm{Hart}}[n_i] + v_{\mathrm{xc}}^{\mathrm{LDA}}[n_i] \right| \varphi_i \right\rangle, \quad \text{(A.1)}$$

$$\Delta\epsilon_i^{\mathrm{KS}} \overset{(2.30)}{=} \epsilon_i^{\mathrm{LDA}} - \epsilon_i^{\mathrm{KSKLI}} \quad \text{(A.2)}$$

are the OSIEs and self-consistent eigenvalue shifts corresponding to KS-KLI,

$$e_i^{\mathrm{LOC}} \overset{(2.36)}{=} \left\langle \varphi_i \left| v_{\mathrm{xc}}^{\mathrm{LDA}}[n] - u_{\mathrm{xc},i}^{\mathrm{LOC}} \right| \varphi_i \right\rangle \overset{(2.29)}{=} \sum_{j=1}^{N} U_{ji} \left\langle \varphi_j \left| v_{\mathrm{Hart}}[\tilde{n}_j] + v_{\mathrm{xc}}^{\mathrm{LDA}}[\tilde{n}_j] \right| \varphi_i \right\rangle, \quad \text{(A.3)}$$

$$\Delta\epsilon_i^{\mathrm{LOC}} \overset{(2.30)}{=} \epsilon_i^{\mathrm{LDA}} - \epsilon_i^{\mathrm{LOCKLI}} \quad \text{(A.4)}$$

are the OSIEs and self-consistent eigenvalue shifts corresponding to LOC-OEP,

$$L_i^{\mathrm{FB}} := \iint |\varphi_i(\mathbf{r})|^2 (\mathbf{r} - \mathbf{r}')^2 |\varphi_i(\mathbf{r}')|^2 \, d\mathbf{r} \, d\mathbf{r}' \quad \text{(A.5)}$$

is the Foster-Boys localization of the KS orbital φ_i according to Eq. (3.16), and

$$\delta_i^{\mathrm{KS}} \overset{(2.4)}{=} E_{\mathrm{Hart}}[n_i] + E_{\mathrm{xc}}^{\mathrm{LDA}}[n_i] \quad \text{(A.6)}$$

is the self-interaction energy of the KS orbital-density n_i. Self-consistency effects can be

tested by evaluating Eq. (2.33). Hence, we compare the self-consistent eigenvalue shifts $\Delta\epsilon_i^{\mathrm{KS}}$ and $\Delta\epsilon_i^{\mathrm{LOC}}$ to the *one-shot* eigenvalue shifts

$$\eta_i^{\mathrm{KS}} := \left\langle \varphi_i \left| v_{\mathrm{xc}}^{\mathrm{LDA}}[n] - v_{\mathrm{xc}}^{\mathrm{KSKLI}}[n] \right| \varphi_i \right\rangle \overset{(2.34)}{=} e_i^{\mathrm{KS}} - \left(\bar{v}_{\mathrm{xc},i}^{\mathrm{KSKLI}} - \bar{u}_{\mathrm{xc},i}^{\mathrm{KS}} \right) \qquad (\mathrm{A.7})$$

and

$$\eta_i^{\mathrm{LOC}} := \left\langle \varphi_i \left| v_{\mathrm{xc}}^{\mathrm{LDA}}[n] - v_{\mathrm{xc}}^{\mathrm{LOCKLI}}[n] \right| \varphi_i \right\rangle \overset{(2.34)}{=} e_i^{\mathrm{LOC}} - \left(\bar{v}_{\mathrm{xc},i}^{\mathrm{LOCKLI}} - \bar{u}_{\mathrm{xc},i}^{\mathrm{LOC}} \right), \qquad (\mathrm{A.8})$$

respectively. The validity of the first-order perturbation-theory argument of Eq. (2.35) can then be tested by comparing η_i^{KS} and η_i^{LOC} to e_i^{KS} and e_i^{LOC}, respectively.

Fig. A.1 plots these quantities as calculated with PARSEC [64] for the PTCDA molecule introduced in publication 3. Part a) denotes the self-interaction energies δ_i^{KS} of the KS orbital densities $|\varphi_i|^2$ for the highest occupied LDA orbitals according to Eq. (A.6). Part b)
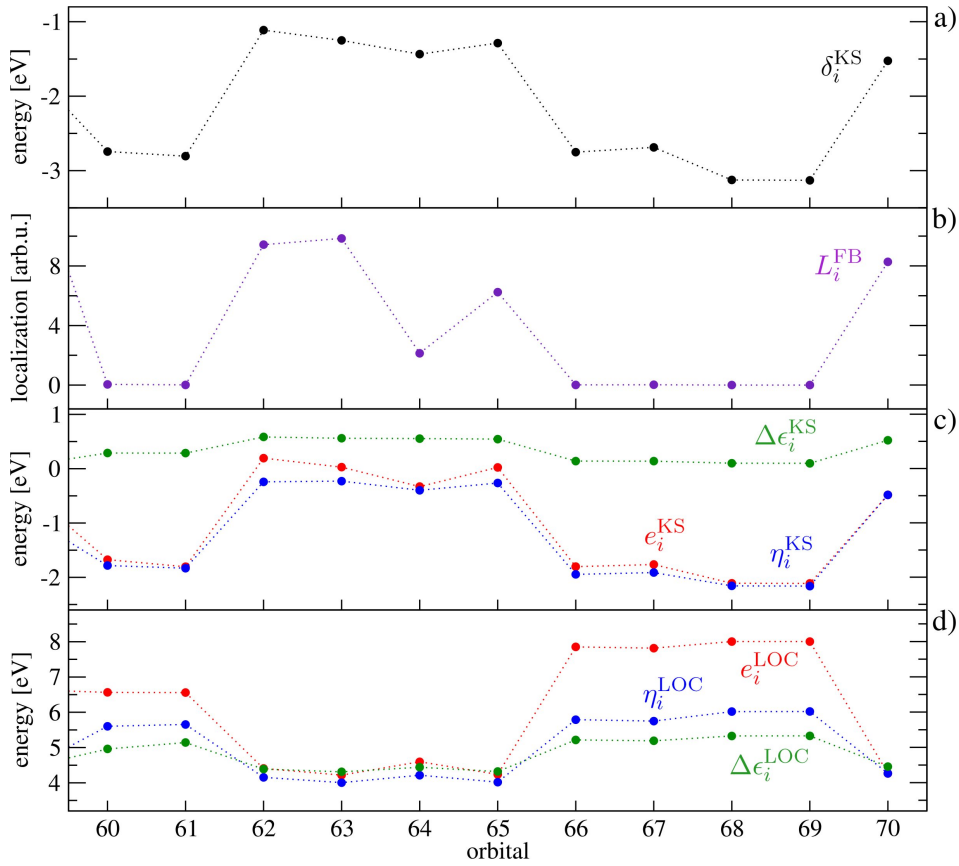
Figure A.1: Self-interaction error and orbital-localization in PTCDA: a) Self-interaction energy according to Eq. (A.6); b) Foster-Boys orbital-localization according to Eq. (A.5); c) OSIE e_i^{KS} (red), self-consistent eigenvalue shift $\Delta\epsilon_i^{\mathrm{KS}}$ (green), and *one-shot* eigenvalue shift η_i^{KS} (blue) for the KS-KLI approach according to Eqs. (A.1), (A.2), and (A.7), respectively; d) OSIE e_i^{LOC} (red), self-consistent eigenvalue shift $\Delta\epsilon_i^{\mathrm{LOC}}$ (green), and *one-shot* eigenvalue shift η_i^{LOC} (blue) for the LOC-KLI approach according to Eqs. (A.3), (A.4), and (A.8), respectively. The HOMO is orbital number 70. Dashed lines are just a guide to the eye. For comparison with the corresponding orbital structures please see Fig. 4.5.

shows the corresponding Foster-Boys localization L_i^{FB}. These two plots quantify what has already been derived in section 4.3 and publication 3 qualitatively from just looking at the orbital structures of PTCDA in Fig. 4.5. The orbitals HOMO-1 to HOMO-4 are significantly less localized than the other highest occupied orbitals. The different orbital structures yield different self-interaction energies. In section 4.3, this has been identified as the reason for the failure of semilocal functionals in predicting a correct eigenvalue spectrum for PTCDA. Note that δ_i^{KS} is negative for all KS orbitals, i.e., the LDA self-interaction energy exceeds the Hartree self-interaction energy. This is an important difference to smaller systems such as atoms or small molecules, for which the KS orbitals are usually more localized so that δ_i^{KS} is positive. Note further that there is a clear correlation between L_i^{FB} and δ_i^{KS}. This finding is in line with the discussion in section 3.3.1 and it is a consequence of the unitary invariance problem.

Part c) of Fig. A.1 shows the OSIE e_i^{KS} (red), the self-consistent eigenvalue shift $\Delta\epsilon_i^{\mathrm{KS}}$ (green), and the *one-shot* eigenvalue shift η_i^{KS} (blue) for the KS-KLI approach according to Eqs. (A.1), (A.2), and (A.7), respectively. The OSIE e_i^{KS} follows the same trend as δ_i^{KS}. Self-consistency effects have a large influence on the eigenvalue shifts, as can be derived from a comparison of $\Delta\epsilon_i^{\mathrm{KS}}$ and η_i^{KS}. However, the relative eigenvalue shift is basically scaled by a factor and the general trends are preserved. Comparison with e_i^{KS} further shows that the first-order perturbation theory argument holds. Hence, the approximations used in section 2.2.6 are reasonable and the relative OSIE can be seen as a reliable indicator for actual shifts in the eigenvalue spectrum due to self-interaction.
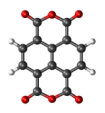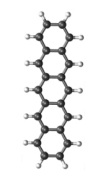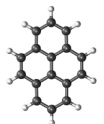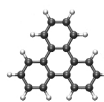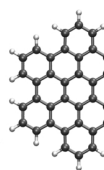
Part d) shows the OSIE e_i^{LOC} (red), the self-consistent eigenvalue shift $\Delta\epsilon_i^{\mathrm{LOC}}$ (green), and the *one-shot* eigenvalue shift η_i^{LOC} (blue) for the LOC-KLI approach according to Eqs. (A.3), (A.4), and (A.8), respectively. As a consequence of the localization of the energy-minimizing orbitals, all OSIEs e_i^{LOC} are manifestly positive. As in the case of KS-KLI, self-consistency effects and the perturbation theory argument of Eq. (2.35) basically scale the relative eigenvalue shift by a factor. The most striking finding of part d) however is that, at least on a relative scale, all three plotted quantities follow the opposite trend as for KS-KLI. For example, HOMO-1 to HOMO-4 are shifted downwards relative to the HOMO in LOC-KLI and upwards in KS-KLI. Comparison of c) and d) clearly reveals a negative correlation between e_i^{LOC} and e_i^{KS} and between $\Delta\epsilon_i^{\mathrm{LOC}}$ and $\Delta\epsilon_i^{\mathrm{KS}}$, respectively. In search for a more quantitative measure of this correlation, we evaluate the *partial correlation function*

$$\kappa\left(\alpha,\beta\right) = \frac{1/N\sum_{i=1}^{N}\left(\alpha_i - \bar{\alpha}\right)\left(\beta_i - \bar{\beta}\right)}{\sqrt{1/N\sum_{i=1}^{N}\left(\alpha_i - \bar{\alpha}\right)^2}\sqrt{1/N\sum_{i=1}^{N}\left(\beta_i - \bar{\beta}\right)^2}} \quad \in [-1,1]\,, \qquad (A.9)$$

$$\bar{\alpha} = 1/N\sum_{i=1}^{N}\alpha_i\,, \quad \bar{\beta} = 1/N\sum_{i=1}^{N}\beta_i \qquad (A.10)$$

of the eigenvalue shifts in KS-KLI and LOC-KLI for a number of organic semiconductors in the following. If these two quantities are indeed negatively correlated, one expects the κ-value to be close to -1; if there is no correlation, κ vanishes. Table A.1 shows $\kappa\left(\Delta\epsilon^{\mathrm{KS}}, \Delta\epsilon^{\mathrm{LOC}}\right)$ for the organic molecular semiconductors PTCDA, NTCDA, Pentacene, Pyrene, Triphenylene (TPL), and Hexabenzocoronene (HBC). A clear negative correlation between the self-consistent eigenvalue shifts in KS-KLI and LOC-KLI can be found for all molecules.

As an important consequence of the above discussion, the OSIE evaluated with the orbital-

	PTCDA	NTCDA	Pentacene	Pyrene	TPL	HBC
$\kappa\left(\Delta\epsilon^{\mathrm{KS}}, \Delta\epsilon^{\mathrm{LOC}}\right)$	-0.96	-0.95	-0.93	-0.86	-0.88	-0.92

Table A.1: Partial correlation function κ of the self-consistent eigenvalue shifts of KS-KLI and LOC-KLI as compared to LDA following Eq. (A.9) for a set of organic molecular semiconductors.

specific potential of KS-KLI can indeed serve as a measure for the reliability of eigenvalue spectra obtained from semilocal functionals. However, due to self-consistency effects and as a consequence of the perturbation theory argument of Eq. (2.35), the relative OSIE is typically scaled by a factor as compared to the relative eigenvalue shift in a self-consistent calculation. Although the eigenvalue shifts in LOC-KLI and KS-KLI take completely different values, they are strongly negatively correlated. Hence, both the OSIE evaluated with the orbital-specific potential of KS-KLI and the self-interaction energy δ_i^{KS} of the KS orbital densities reliably indicate possible eigenvalue shifts in a LOC-KLI calculation. This is the basic finding of publication 3.

In this context, it is interesting to note that the approximative correction of the LDA eigenvalue $\epsilon_i^{\mathrm{LDA}}$ used in Eq. (2) of publication 3, i.e.,

$$\epsilon_i^{\mathrm{est}} = \epsilon_i^{\mathrm{LDA}} - 0.94 \int \left(|\varphi_i|^2\right)^{\frac{4}{3}} d\mathbf{r} - \langle\, \varphi_i \,|\, v_{\mathrm{c}}^{\mathrm{LDA}}[|\varphi_i|^2, 0] \,|\, \varphi_i \,\rangle. \qquad (A.11)$$

corrects the LDA eigenvalues in the same direction as the GKLI approach (see publication 3 for examples). At first sight, this finding is quite surprising, as Eq. (A.11) is evaluated with the KS orbitals and not with localized orbitals. However, it can be rationalized by the fact that Eq. (A.11) is based on an approximative correction scheme which has originally been introduced by Perdew and Zunger [106] for the special case of atoms, i.e., it is assumed that the orbitals used in the self-interaction correction are localized in space. Hence, the localization of orbitals is already incorporated in the approximation used to derive Eq. (A.11).

Note that the results discussed above provide a new perspective on the failure of the KS-KLI approach. The latter will be discussed in appendix A.2.

A.2. The failure of KS-KLI

It has been known for quite a long time in the literature that the KS-KLI approach, although being rather successful for small atoms [19, 134], yields unrealistic results for molecules [33, 95]. The idea to employ localized orbitals instead of KS orbitals in the KS-KLI potential [19, 134] was inspired by the empirical finding that a direct variation of the total energy with respect to the orbitals typically leads to orbitals that are rather localized in space [106]. The results presented in this work further strengthen the importance of the
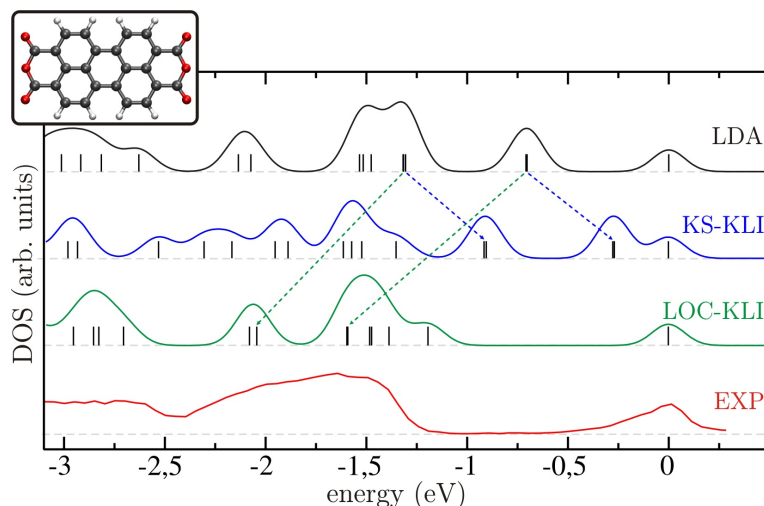
Figure A.2: KS eigenvalue spectra obtained from LDA (black), KS-KLI (blue), and LOC-KLI (green) compared to the experimental photoelectron spectrum (red). The blue and green arrows denote the shifts of the LDA eigenvalues corresponding to HOMO-1 to HOMO-4 in KS-KLI and LOC-KLI, respectively. KS eigenvalues are superimposed with Gaussians of width $\sigma = 0.08$ eV and all HOMO-peaks are set to 0 to make visual comparison easier.

localizing transformation. In particular, the performance of the different SIC-approaches for the linear response of hydrogen chains (see Fig. 4.1 and discussion in text) demonstrates that using localized orbitals is essential. Publication 1 shows that the self-consistent KS orbitals themselves can be localized in space due to a symmetry-break in the self-consistent iteration. As a consequence, KS-OEP yields very accurate results for the response of model hydrogen chains. However, it is an empirical finding that KS-KLI, in contrast to KS-OEP, never leads to a symmetry-break. Hence, KS-KLI orbitals are typically delocalized over the whole system. Importantly, the orbitals found from a self-consistent KS-KLI calculation are not those KS orbitals that minimize the total energy corresponding to the SIC-functional. The inability of the KS-KLI approach to yield the energy-minimizing KS orbitals has to be ascribed to the nature of the KLI-approximation. The latter is based on the assumption that the used approximation in the potential does not spoil the self-consistent iteration. Publication 1 clearly demonstrates that this assumption can not be uphold for the SIC-functional.

The findings of appendix A.1 provide a new perspective on the failure of the KS-KLI approach for extended molecular systems. Table A.1 shows that the relative eigenvalue shift of KS-KLI is negatively correlated to the relative eigenvalue shift of LOC-KLI for a set of organic molecular semiconductors. From publication 3 it is further known that LOC-KLI yields a reliable eigenvalue spectrum for PTCDA. Fig. A.2 compares the KS eigenvalue spectra of LDA, KS-KLI, and LOC-KLI to the experimental photoelectron spectrum. The eigenvalue shifts of KS-KLI and LOC-KLI for the crucial orbitals HOMO-1 to HOMO-4 are indicated by the blue and green arrows, respectively. As a consequence of the results provided in Table A.1, the LDA eigenvalues are shifted in opposite directions in KS-KLI and LOC-KLI, thus yielding two completely different eigenvalue spectra. In contrast to LOC-KLI, KS-KLI does not at all improve upon the LDA spectrum. Actually, the KS-KLI spectrum is even worse. With the analysis of appendix A.1, the reason for this failure is

obvious. KS-KLI corrects the eigenvalues *in the wrong direction.* The reason behind this failure is the unitary invariance problem. In contrast to the energy-minimizing orbitals, delocalized KS-KLI orbitals are obviously not suitable for calculating the self-interaction error in many-particle systems. Still, the strong correlation between the KS-KLI and the LOC-KLI shift shows that the delocalized KS-KLI or LDA orbitals carry important information on the self-interaction in many-particle systems. The art of doing a self-interaction correction in many-particle systems is thus to extract this information from the delocalized KS orbitals in a correct manner. This is the basic idea behind the unitary transformation employed in the GOEP approach.

A.3. How to solve the symmetry condition

According to the discussion in section 3.3.3, the energy minimizing unitary transformation needed in the LOC-OEP and LOC-KLI approach can be found by solving the symmetry condition (3.20). Following an idea of Fois *et al.* [29], one can replace the U_{ij}^σ in Eq. (3.20) by the transformation $T_{ij}^\sigma = \delta_{ij} + \tau_{ij}^\sigma$, with $\tau_{ij}^\sigma = -\tau_{ji}^\sigma$ (note that all orbitals and thus the unitary transformations between them are chosen to be real in this appendix). However, the thus obtained T_{ij}^σ is not strictly unitary:

$$\sum_{k=1}^{N_\sigma} T_{ik}^\sigma T_{jk}^\sigma = \delta_{ij} + \underbrace{\tau_{ij}^\sigma + \tau_{ji}^\sigma}_{=0} + \sum_{k=1}^{N_\sigma} \tau_{ik}^\sigma \tau_{jk}^\sigma \neq \delta_{ij} \,. \tag{A.12}$$

By employing Löwdin's method of symmetric orthogonalization [77, 83], the nonorthogonal orbitals

$$\tilde{\varphi}_{i\sigma}^{\mathrm{no}}(\mathbf{r}) = \sum_{j=1}^{N_\sigma} T_{ij}^\sigma \varphi_{j\sigma}(\mathbf{r}) \tag{A.13}$$

can be orthonormalized by multiplication with the *Löwdin matrix*

$$C_{ij}^\sigma := \left(S_{ij}^\sigma\right)^{-1/2} := \left\langle \tilde{\varphi}_{i\sigma}^{\mathrm{no}} | \tilde{\varphi}_{j\sigma}^{\mathrm{no}} \right\rangle^{-1/2} \,. \tag{A.14}$$

By construction, the Löwdin-orthogonalized orbitals

$$\tilde{\varphi}_{j\sigma}(\mathbf{r}) = \sum_{m=1}^{N_\sigma} C_{jm}^\sigma \tilde{\varphi}_{m\sigma}^{\mathrm{no}}(\mathbf{r}) = \sum_{k,m=1}^{N_\sigma} C_{jm}^\sigma T_{mk}^\sigma \varphi_{k\sigma}(\mathbf{r}) \tag{A.15}$$

are those orthonormal orbitals that are closest in the least-squares sense to the original non-orthogonal orbitals $\tilde{\varphi}_{m\sigma}^{\mathrm{no}}(\mathbf{r})$. With this, the symmetry condition (3.20) reads

$$\sum_{k,m=1}^{N_\sigma} C_{jm}^\sigma T_{mk}^\sigma \sum_{l,n=1}^{N_\sigma} C_{in}^\sigma T_{nl}^\sigma \underbrace{\left\langle \varphi_{k\sigma} \mid \tilde{v}_{j\sigma}^{\mathrm{SIC}} - \tilde{v}_{i\sigma}^{\mathrm{SIC}} \mid \varphi_{l\sigma} \right\rangle}_{=:\langle k \mid j - i \mid l \rangle} = 0 \,. \tag{A.16}$$

Regarding the Löwdin matrix one derives

$$S_{ij}^{\sigma} := \left\langle \tilde{\varphi}_{i\sigma}^{\text{no}} | \tilde{\varphi}_{j\sigma}^{\text{no}} \right\rangle = \sum_{p,q=1}^{N_{\sigma}} T_{ip}^{\sigma} T_{jq}^{\sigma} \underbrace{\left\langle \varphi_{p\sigma} | \varphi_{q\sigma} \right\rangle}_{= \delta_{pq}} = \sum_{q=1}^{N_{\sigma}} T_{iq}^{\sigma} T_{jq}^{\sigma}. \tag{A.17}$$

During the self-consistent iteration of the τ's (see below), the non-orthogonality of T_{ij}^{σ} is small for every iteration step. Hence, one can approximate [77]

$$C_{ij}^{\sigma} = \left(S_{ij}^{\sigma} \right)^{-1/2} \approx \delta_{ij} - \frac{1}{2} \left(S_{ij}^{\sigma} - \delta_{ij} \right) \overset{(A.17)}{=} \frac{3}{2} \delta_{ij} - \frac{1}{2} \sum_{q=1}^{N_{\sigma}} T_{iq}^{\sigma} T_{jq}^{\sigma}. \tag{A.18}$$

By inserting Eq. (A.12) and $\tau_{jq}^{\sigma} = -\tau_{qj}^{\sigma}$ one thus obtains

$$C_{ij}^{\sigma} \approx \frac{3}{2} \delta_{ij} - \frac{1}{2} \left(\delta_{ij} - \underbrace{\sum_{q=1}^{N_{\sigma}} \tau_{iq}^{\sigma} \tau_{qj}^{\sigma}}_{=: \left(\tau_{ij}^{\sigma} \right)^2} \right) = \delta_{ij} + \frac{1}{2} \left(\tau_{ij}^{\sigma} \right)^2. \tag{A.19}$$

For the unitary transformation U_{ij}^{σ} this yields

$$U_{ij}^{\sigma} = \sum_{k=1}^{N_{\sigma}} C_{ik}^{\sigma} T_{kj}^{\sigma} \approx \sum_{k=1}^{N_{\sigma}} \left(\delta_{ik} + \frac{1}{2} \left(\tau_{ik}^{\sigma} \right)^2 \right) \left(\delta_{kj} + \tau_{kj}^{\sigma} \right) = \delta_{ij} + \underbrace{\tau_{ij}^{\sigma} + \frac{1}{2} \left(\tau_{ij}^{\sigma} \right)^2 + \frac{1}{2} \left(\tau_{ij}^{\sigma} \right)^3}_{=: \omega_{ij}^{\sigma}}. \tag{A.20}$$

Note that, similar to T_{ij}^{σ}, also U_{ij}^{σ} is not strictly unitary due to the approximation in the Löwdin matrix provided in Eq. (A.18). However, we find that by taking into account an additional order in τ_{ij}^{σ}, the unitarity of U_{ij}^{σ} is significantly improved as compared to T_{ij}^{σ}. Note that, if necessary, this approach can be improved straightforwardly by taking into account further orders in the expansion of the Löwdin matrix (see Ref. [77]).

By inserting Eq. (A.20) into the symmetry condition (A.16) one obtains after some algebra

$$\left\langle j \left| j - i \right| i \right\rangle + \sum_{l=1}^{N_{\sigma}} \omega_{il}^{\sigma} \left\langle j \left| j - i \right| l \right\rangle + \sum_{k=1}^{N_{\sigma}} \omega_{jk}^{\sigma} \left\langle k \left| j - i \right| i \right\rangle + \sum_{k,l=1}^{N_{\sigma}} \omega_{il}^{\sigma} \omega_{jk}^{\sigma} \left\langle k \left| j - i \right| l \right\rangle = 0. \tag{A.21}$$

Adding the auxiliary zeros

$$\sum_{l=1}^{N_{\sigma}} \delta_{jl} \tau_{il}^{\sigma} - \tau_{ij}^{\sigma} = 0, \tag{A.22}$$

$$-\sum_{k=1}^{N_{\sigma}} \delta_{ik} \tau_{jk}^{\sigma} + \tau_{ji}^{\sigma} = 0, \tag{A.23}$$

and again using $\tau_{ij}^{\sigma} = -\tau_{ji}^{\sigma}$ one derives

$$2\tau_{ij}^{\sigma} = \tau_{ij}^{\sigma} - \tau_{ji}^{\sigma} = \langle j \,|j-i|\, i\rangle \quad + \sum_{l=1}^{N_{\sigma}} \omega_{il}^{\sigma} \langle j \,|j-i|\, l\rangle + \delta_{jl}\tau_{il}^{\sigma} \qquad (A.24)$$

$$+ \sum_{k=1}^{N_{\sigma}} \omega_{jk}^{\sigma} \langle k \,|j-i|\, i\rangle - \delta_{ik}\tau_{jk}^{\sigma}$$

$$+ \sum_{k,l=1}^{N_{\sigma}} \omega_{il}^{\sigma} \omega_{jk}^{\sigma} \langle k \,|j-i|\, l\rangle \; .$$

With $\omega_{ij}^{\sigma} = \tau_{ij}^{\sigma} + \frac{1}{2}\left(\tau_{ij}^{\sigma}\right)^2 + \frac{1}{2}\left(\tau_{ij}^{\sigma}\right)^3$ one finally obtains an iterative equation for the τ's:

$$\tau_{ij}^{\sigma} = \tau_{ij}^{0} \; + \; \frac{1}{2}\Bigg\{ \sum_{l=1}^{N_{\sigma}} \left[\left(\tau_{il}^{\sigma} + \frac{1}{2}(\tau_{il}^{\sigma})^2 + \frac{1}{2}(\tau_{il}^{\sigma})^3\right) \langle j \,|j-i|\, l\rangle + \delta_{jl}\tau_{il}^{\sigma} \right] \qquad (A.25)$$

$$+ \sum_{k=1}^{N_{\sigma}} \left[\left(\tau_{jk}^{\sigma} + \frac{1}{2}\left(\tau_{jk}^{\sigma}\right)^2 + \frac{1}{2}\left(\tau_{jk}^{\sigma}\right)^3\right) \langle k \,|j-i|\, i\rangle - \delta_{ik}\tau_{jk}^{\sigma} \right]$$

$$+ \sum_{k,l=1}^{N_{\sigma}} \left(\tau_{il}^{\sigma} + \frac{1}{2}(\tau_{il}^{\sigma})^2 + \frac{1}{2}(\tau_{il}^{\sigma})^3\right) \left(\tau_{jk}^{\sigma} + \frac{1}{2}\left(\tau_{jk}^{\sigma}\right)^2 + \frac{1}{2}\left(\tau_{jk}^{\sigma}\right)^3\right) \langle k \,|j-i|\, l\rangle \Bigg\} ,$$

where $\tau_{ij}^{0} = \frac{1}{2} \langle i \,|i-j|\, j\rangle$ can be interpreted as the 0th order solution. Note that one immediately obtains the iterative equation proposed by Fois *et al.* [29] if one replaces the ω_{ij}^{σ} by τ_{ij}^{σ} on the right hand side of Eq. (A.24) or Eq. (A.25), respectively.

The solution of Eq. (A.25) now follows an iterative procedure:

(i) Start with some set of orbitals $\varphi_{k\sigma}$. This could be the KS orbitals. However, a faster convergence can be achieved by using localized orbitals such as Foster-Boys or Edminston-Ruedenberg orbitals as initial guess.

(ii) Calculate the corresponding τ_{ij}^{0}, $\langle k \,|j-i|\, l\rangle$ and the orbital-specific SIC-potentials $\tilde{v}_{i\sigma}^{\mathrm{SIC}}$ according to Eq. (3.21).

(iii) Insert $\tau_{ij}^{\sigma} = \tau_{ij}^{0}$ on the right hand side of Eq. (A.25) and derive the new τ_{ij}^{σ}.

(iv) Use the new τ_{ij}^{σ} in order to calculate the unitary transformation U_{ij}^{σ} and a new set of orbitals. Note that U_{ij}^{σ} can be calculated approximately via Eq. (A.21). However, we derive U_{ij}^{σ} by applying an explicit Löwdin orthogonalization on $T_{ij}^{\sigma} = \delta_{ij} + \tau_{ij}^{\sigma}$.

(v) Calculate the corresponding $\langle k \,|j-i|\, l\rangle$ and the orbital-specific SIC-potentials $\tilde{v}_{i\sigma}^{\mathrm{SIC}}$ according to Eq. (3.21), insert on the right hand side of Eq. (A.25), calculate a new τ_{ij}^{σ} and repeat until the symmetry condition (3.20) is satisfied.

We find that by employing the Löwdin orthogonalization of T_{ij}^{σ} in Eq. (A.25), the τ-iteration converges significantly faster and more reliably as compared to the procedure proposed by Fois *et al.* for many systems. However, an essential step for improving the convergence of Fois' iterative procedure is to replace the proposed Gram-Schmidt orthogonalization of U_{ij}^{σ} by a symmetric Löwdin orthogonalization.

Fractional occupation numbers can be introduced into the iterative solution of the symmetry condition just be replacing the orbitals $\varphi_{i\sigma}$ by $\sqrt{f_{i\sigma}}\varphi_{i\sigma}$ and the localized orbitals $\tilde{\varphi}_{i\sigma}$ by $\sqrt{\tilde{f}_{i\sigma}}\tilde{\varphi}_{i\sigma}$, respectively. One thus obtains the energy-minimizing unitary transformation K_{ij}^{σ}

to be used in Eq. (3.6). Basically, the iterative solution of the symmetry condition for fractional occupation numbers follows exactly the same lines as for integer occupation. However, one has to take into account that, although K_{ij}^σ is unitary, the localized orbitals obtained from Eq. (3.6) are no longer orthogonal (see Eq. (3.10)). As a consequence, the Löwdin orthogonalization employed in the τ-iteration does not orthogonalize the localized orbitals themselves but only the transformation matrix.

In some cases, it might be useful to split the iterative procedure in an inner and an outer iterative loop. In the inner loop, Eq. (A.25) would be solved iteratively for τ_{ij}^σ for fixed $\langle k\,|j-i|\,l\rangle$ and $\tilde{v}_{i\sigma}^{\mathrm{SIC}}$. Only in the outer loop, the U_{ij}^σ, $\langle k\,|j-i|\,l\rangle$ and $\tilde{v}_{i\sigma}^{\mathrm{SIC}}$ are updated using the converged τ_{ij}^σ. Note however that the inner loop usually only converges reliably if one includes the orthogonalization of τ_{ij}^σ directly in the iterative equation as done in Eq. (A.25). In our implementation, we usually start the iterative procedure with roughly converged Foster-Boys or Edminston Ruedenberg orbitals. With this initial guess, the algorithm usually converges within some tens of (outer) iterative steps.

A.4. List of used functionals and their abbreviations

This appendix provides a short overview of all functionals used or referred to in this work and their abbreviations.

LDA:
Local density approximation with correlation contributions in the parametrization of Ref. [105].

PBE:
Non-empirical generalized gradient approximation (GGA) provided by Perdew, Burke and Ernzerhof [101].

BLYP:
Semiempirical GGA, which combines Becke88 exchange [7] with the correlation functional given by Lee, Yang, and Parr [72].

B3LYP:
Hybrid functional according to Eq. (1.25), which employs the Becke88 GGA for exchange $E_{\mathrm{x}}^{\mathrm{B88}}$ [7], the GGA for correlation given by Lee, Yang, and Parr $E_{\mathrm{c}}^{\mathrm{LYP}}$ [72], and the $E_{\mathrm{xc}}^{\mathrm{LDA}}$ in the parametrization of Vosko, Wilk and Nusair [137]. The empirical parameters were determined to $a_0^{\mathrm{HF}} = 0.20$, $a_x = 0.72$, and $a_c = 0.81$ [122], respectively.

EXX-OEP:
Exact exchange orbital functional according to Eq. (1.13) evaluated with the OEP-methodology introduced in Eqs. (1.15)-(1.17).

EXX-KLI:
KLI-approximation to EXX-OEP as provided in Eq. (1.21).

Self-interaction corrections play a particular important role in this thesis. Due to the problems discussed in section 2, the SIC proposed by Perdew and Zunger, i.e., Eq. (2.10), leaves the foundations of KS DFT by introducing orbital-specific potentials. Further, the unitary invariance problem allows to define many different SICs on the basis of Eq. (2.10) by using different orbitals in the SIC energy. This leads to a large variety of different

approximative or exact approaches to define an exchange-correlation potential corresponding to Eq. (2.10). The abbreviations used in this thesis for the different approaches are provided below. Note that all presented SICs refer to a SIC of LDA.

PZ-SIC:
Derivation of Eq. (2.10) directly with respect to the orbitals leads to the orbital-specific potentials of Eq. (2.13). Frequently, an orthogonality constraint is applied in the minimization of the energy functional. One thus obtains the system of self-consistent equations (2.18). By introducing orbital specific potentials, PZ-SIC is outside the foundations of KS theory.

GOEP:
Orbital functionals such as Eq. (2.10) that are not invariant under unitary transformation can be brought back under the umbrella of KS DFT by virtue of the generalized optimized effective potential approach derived in publication 2 and further explained in section 2.2.2. Solving Eq. (2.22) yields the optimized effective potential to any orbital-functional and unitary transformation of interest. In this thesis, two particular choices for the unitary transformation U_{ij}^σ are used for the SIC functional of Eq. (2.10):

KS-OEP:
Abbreviation for Kohn-Sham SIC-GOEP. The energy functional is provided in Eq. (2.26). It employs the KS orbital densities in the SIC of LDA following Eq. (2.10). Hence, the unitary transformation in the GOEP methodology is chosen to be the identity matrix, the set of localized orbitals $\tilde{\varphi}_{i\sigma}$ (see Eq. (2.20)) equals the set of KS orbitals and the GOEP equation (2.22) reduces to the standard OEP-equation (1.15). $v_{\mathrm{xc},\sigma}^{\mathrm{KSOEP}}$ can be derived following the methodology discussed in section 3.1.

LOC-OEP:
Abbreviation for localized SIC-GOEP. The energy functional is provided in Eq. (2.28). It employs the energy-minimizing orbital densities in the SIC of LDA following Eq. (2.10). The unitary transformation can be derived from solving the symmetry condition (3.20). With this, one obtains $v_{\mathrm{xc},\sigma}^{\mathrm{LOCOEP}}$ by virtue of the GOEP equation (2.22) following the methodology discussed in section 3.1.

GKLI:
KLI-approximation to GOEP as provided in Eq. (2.25). Note that this is an approximation in the potential and not in the energy functional. Similar to GOEP, GKLI is generalized in the sense that it works for any orbital-functional and unitary transformation. Again, two cases are of particular interest in this thesis:

KS-KLI:
KLI-approximation to KS-OEP, i.e., use the orbital-specific potentials $u_{\mathrm{xc},i\sigma}^{\mathrm{KS}}$ from Eq. (2.27) in the GKLI expression (2.25).

LOC-KLI:
KLI-approximation to KS-OEP, i.e., use the orbital-specific potentials $u_{\mathrm{xc},j\sigma}^{\mathrm{LOC}}$ from Eq. (2.29) in the GKLI expression (2.25).

G-Slater:
Crude approximation to GOEP. The Slater-approximation is derived by setting $\bar{v}_{\mathrm{xc},i\sigma}^{\mathrm{GKLI}} - \bar{u}_{\mathrm{xc},i\sigma}^{\mathrm{G}} = 0$ in the GKLI potential of Eq. (2.25). Hence, the response part of the GOEP potential is completely neglected. As a consequence, the Slater-approximation misses one of the key-features of self-interaction free orbital-functionals, i.e., the good response properties (see discussion in section 4.1 and publication 1).

KS-Slater:
Slater-approximation to KS-OEP.

LOC-Slater:
Slater-approximation to LOC-OEP.

Garza-SIC:
Approximative exchange-correlation potential for the SIC first proposed by Garza *et al.* [33] and later referred to by other authors [95, 99]. In this approximation, the KS orbitals in the expression for the KS-KLI potential are replaced by localized Foster-Boys or Pipek-Mezey orbitals, respectively. As discussed in publication 2, the thus newly defined potential functional can be seen as an approximation to the LOC-KLI potential. However, in contrast to the LOC-KLI case the used orbitals are not the energy-minimizing orbitals, and there is no straightforward way of improving the Garza-SIC approach to a full-OEP level.

Acknowledgment

I am grateful to **all people who have supported and accompanied me on my way** and thereby made this thesis possible. In particular I would like to thank . . .

the supervisor of this thesis **Dr. Stephan Kümmel** for this extraordinary support, his advice, his commitment to science, for sharing his deep knowledge and physical understanding with me and for playing a brilliant devil's advocate. I have greatly benefitted both personally and scientifically from working with him.

all senior researchers that shared their rich knowledge on density functional theory and organic semiconductors with me, in particular **Dr. Jürgen Köhler**, **Dr. Mukundan Thelakkat**, **Dr. Leeor Kronik**, and **Dr. Sergei Tretiak**. This work would not have been possible without their scientific input.

the **Studienstiftung des dt. Volkes**, which supported me during my studies and while writing this thesis. In addition, the Studienstiftung financed my participation in a language course, supported several stays abroad and enabled me to meet a lot of inspiring people. It is a remarkable organization with great staff, lecturers, and scholars and it was an honor for me to be part of it.

all organizers, lecturers, and students of the **Elite Study Program Macromolecular Science** and the **Elite Network of Bavaria**. In particular, I would like to thank the mentor of the Studienstiftung and chair of the Elite Study Program Macromolecular Science **Dr. Hans-Werner Schmidt**. His dedication and commitment were always inspiring to me.

my former office mate **Dr. Michael Mundt** for the great time in the office, for sharing his deep physical understanding with me, for many serious and many funny discussions about physics and other things, for proofreading the manuscript, and for being a friend.

all **scientific members of the physics department** of the University of Bayreuth, in particular all members and alumni of the **electronic structure and dynamics group** for great talks and group seminars, for many discussions about science and other things during lunch time and tea break and for contributing to a friendly atmosphere.

the **staff of the physics department**, in particular **Werner Reichstein** and **Michael Heimler** for a great office neighborship, interesting discussions, and the always fresh and tasty coffee as well as **Monika Birkelbach** for her help and support in all administrative matters.

my parents for their support, advice and love, for always backing me up and for bringing me back to earth whenever necessary. I am deeply grateful to them for paving the way which I just had to walk along.

my family, my sister and brother, my grandparents, and my parents-in-law for their continuous support, understanding, and advice.

all friends that supported me while writing this thesis. In particular, I would like to thank **Michael Brand** for fun sports hours in the fitness center and even more fun after-sports hours in the pub, for listening, for his advice and most of all for being a friend.

my beloved wife **Heike**, the love of my life and the best friend I ever had. I am deeply grateful for her support and love, for full weeks and wonderful weekends, for listening when needed and giving advice when necessary. Without her this thesis would not be the same.

Thomas Körzdörfer
Bayreuth, 2. Oktober 2009

List of publications

1. **T. Körzdörfer**, M. Mundt, and S. Kümmel,
   Phys. Rev. Lett. **100**, 133004 (2008):
   Electrical Response of Molecular Systems: The Power of Self-Interaction Corrected Kohn-Sham Theory

2. R. Armiento, S. Kümmel, and **T. Körzdörfer**,
   Phys. Rev. B **77**, 165106 (2008):
   Electrical response of molecular chains in density functional theory: Ultranonlocal response from a semilocal functional

3. **T. Körzdörfer**, S. Kümmel, and M. Mundt,
   J. Chem. Phys. **129**, 014110 (2008):
   Self-interaction correction and the optimized effective potential

4. **T. Körzdörfer**, S. Kümmel, N. Marom, and Leeor Kronik,
   Phys. Rev. B **79**, 201205(R) (2009):
   When to trust photoelectron spectra from Kohn-Sham eigenvalues: The case of organic semiconductors

5. **T. Körzdörfer**, S. Tretiak, and S. Kümmel,
   J. Chem. Phys. **131**, 034310 (2009):
   Fluorescence quenching in an organic donor-acceptor dyad: a first principles study

Erklärung

Hiermit erkläre ich, dass ich die vorliegende Arbeit selbstständig und nur unter Zuhilfenahme der angegeben Quellen und keiner weiteren Hilfsmittel angefertigt habe. Die Arbeit wurde in gleicher oder ähnlicher Form keiner anderen Prüfungsbehörde zur Erlangung eines akademischen Grades vorgelegt.

Desweiteren erkläre ich hiermit, dass ich bisher keinen anderweitigen Promotionsversuch unternommen habe.

Bayreuth, den 2. Oktober 2009

Thomas Körzdörfer

Part III.

Publications

Publication 1

Electrical Response of Molecular Systems: The Power of Self-Interaction Corrected Kohn-Sham Theory

T. Körzdörfer, M. Mundt, and S. Kümmel

Physics Institute, University of Bayreuth, D-95440 Bayreuth, Germany

ABSTRACT

The accurate prediction of electronic response properties of extended molecular systems has been a challenge for conventional, explicit density functionals. We demonstrate that a self-interaction correction implemented rigorously within Kohn-Sham theory via the optimized effective potential (OEP) yields polarizabilities close to the ones from highly accurate wave-function-based calculations and exceeding the quality of exact-exchange OEP. The orbital structure obtained with the OEP-SIC functional and approximations to it are discussed.

Electrical Response of Molecular Systems: The Power of Self-Interaction Corrected Kohn-Sham Theory

T. Körzdörfer, M. Mundt, and S. Kümmel

Physics Institute, University of Bayreuth, D-95440 Bayreuth, Germany
(Received 31 July 2007; published 3 April 2008)

The accurate prediction of electronic response properties of extended molecular systems has been a challenge for conventional, explicit density functionals. We demonstrate that a self-interaction correction (SIC) implemented rigorously within Kohn-Sham theory via the optimized effective potential (OEP) yields polarizabilities close to the ones from highly accurate wave-function-based calculations and exceeding the quality of exact-change OEP. The orbital structure obtained with the OEP-SIC functional and approximations to it are discussed.

Gaining microscopic insight into the quantum-mechanical electronic effects that govern energy transfer and charge transfer in processes like light-harvesting, charge separation in organic solar cells, or the response of molecular optoelectronic devices would be extremely beneficial to the understanding of these phenomena. But the computational complexity of solving the many-electron Schrödinger equation leaves little hope that wave-function-based approaches can address these problems any time soon. The formulation of quantum mechanics without a wave function, i.e., density-functional theory (DFT) in the Kohn-Sham framework, is computationally much more efficient and allows us to handle systems with up to several hundreds of electrons. Therefore, it appears as the ideal tool for investigating the above mentioned problems. However, the predictive power of DFT calculations depends crucially on the approximations made in the description of the exchange-correlation effects. Structural, ground-state molecular properties are obtained with reasonable to excellent accuracy using standard, explicit density functionals like the local spin density approximation (LSDA) or generalized gradient approximations (GGAs). But these functionals notoriously fail in the description of charge-transfer processes [1,2] and associated problems like predicting the response [3] or transport [4] properties of extended molecular systems. There is, thus, a serious need for exchange-correlation approximations that allow us to calculate response properties like polarizabilities of extended systems reliably on a quantitative scale and with bearable computational costs.

It has been demonstrated that improvements in the density-functional description of the response of conjugated polymers can be achieved based on current density-functional theory [5] and related ideas [6], or by incorporating full [3,7,8] or partial [9] exact exchange. It has also been argued that correlation effects play a non-negligible role in the proper description of response properties [10]. However, evaluating the Fock integrals in exact-exchange approaches increases numerical costs substantially, and the

computational complexity of approaches using exact exchange with ''compatible'' correlation is significant [11].

In this Letter we demonstrate that these problems can be overcome with a self-interaction correction (SIC) employed rigorously within Kohn-Sham theory. In the SIC-scheme, only direct, i.e., self-exchange integrals, need to be evaluated; thus, computational costs are lowered. OEP-SIC yields highly accurate results for the response of extended molecular systems without involving empirical parameters.

The first ''modern'' SIC was proposed by Perdew and Zunger as a correction to LSDA [12]. They devised the LSDA-SIC functional

$$E_{xc}^{SIC}[n_\uparrow, n_\downarrow] = E_{xc}^{LSDA}[n_\uparrow, n_\downarrow]$$
$$- \left(\sum_{\sigma=\uparrow,\downarrow} \sum_{i=1}^{N_\sigma} E_H[n_{i,\sigma}] + E_{xc}^{LSDA}[n_{i,\sigma}, 0] \right), \quad (1)$$

where E_{xc}^{LSDA} is the LSDA exchange-correlation energy functional, E_H the Hartree (classical Coulomb) energy, $n_\uparrow$ and $n_\downarrow$ the up- and down-spin densities, respectively, $N_\uparrow$ and $N_\downarrow$ the numbers of occupied spin-orbitals, and $n_{i,\sigma}$ the orbital spin densities. Equation (1) is not the only way in which a SIC can be defined [13], but it is plausible and straightforward: The spurious self-interaction effects that are contained in the Hartree energy and the LSDA functional are subtracted on an orbital-by-orbital basis. However, a subtlety is buried in this seemingly simple equation: The functional depends on the orbitals explicitly, i.e., it is not an explicit density functional. The traditional way of approaching this problem has been to minimize the total energy with respect to the orbitals [12,14,15]. This approach is within the realm of the Hohenberg-Kohn theorem, but it is outside the foundations of Kohn-Sham theory: minimizing with respect to the orbitals leads to single-particle equations with orbital-specific potentials instead of a global, local Kohn-Sham potential for all orbitals. But the existence of a common, local potential is one of the features that makes Kohn-Sham DFT attractive: Only with

a local potential is the noninteracting kinetic energy density a well-defined density functional; a local potential considerably simplifies numerical efforts, it facilitates the interpretation of results, and it yields not only corrected occupied eigenvalues, but also corrected unoccupied ones. But on the other hand, Perdew-Zunger SIC [12] has become popular in some areas of solid state physics exactly for the reason that it does not work with one common local potential but with several orbital-specific ones, because orbital-specific potentials straightforwardly allow to take into account orbital localization effects: SIC with orbital-specific potentials can treat, e.g., p and d orbitals of a crystalline solid on a different footing. In this way, Perdew-Zunger SIC can naturally distinguish between localized and delocalized states. In order to benefit from the advantages of working with a local potential without losing the ability to describe localization effects, schemes have been devised which make use of the fact that Eq. (1) is not invariant under transformations of the orbitals that change the individual orbital densities but leave the total density unchanged. Calculating orbitals from a common Hamiltonian and then subjecting these orbitals to localizing transformations has proved to be a successful scheme for solids [16,17] and molecules [18–20].

However, localizing orbital transformations can become computationally involved in large finite systems and in time-dependent calculations. Therefore, yet another variant of the SIC has become popular. It uses the Krieger-Li-Iafrate (KLI) construction [21] to obtain the KLI potential corresponding to Eq. (1) and evaluates Eq. (1) directly with the KLI orbitals [22–25]. This approach has been justified as an approximation to the OEP version of SIC (OEP-SIC), which is defined by evaluating Eq. (1) with the orbitals obtained from the SIC Kohn-Sham potential that follows from the optimized effective potential (OEP) formalism [11]. But to the best of our knowledge, the performance of the OEP-SIC approach itself has remained largely unexplored, and tests of the KLI-SIC approach were restricted to spherical atoms [22]. In this manuscript we demonstrate that OEP-SIC, but not KLI-SIC, allows us to predict electric response coefficients of molecular systems very reli-

ably and may thus become an important tool to investigate charge-transfer questions.

One of the most demanding tests of a functional's ability to adequately describe charge transfer is calculating the polarizability of hydrogen chains. It has been shown that obtaining the response of hydrogen chains correctly is even more difficult than obtaining the response of real polymers like polyacetylene [5]. Therefore, calculating the polarizability of hydrogen chains has become a benchmark test for many-particle approaches from both the density functional [3,5–8] and the wave-function worlds [26,27]. Since a response quantity like the polarizability determines how a system reacts to a field that induces a density shift, calculating the polarizability also probes the ability to correctly describe charge transfer. As a second, positive side effect, investigating hydrogen chains also allows us to address the question of size consistency of the OEP-SIC functional [12,28,29].

Our calculations are based on a real space approach [30], which we employed to calculate the ground-state of hydrogen chains with alternating interatomic distances of 2 and 3 a_0, using KLI-SIC. From the converged KLI-SIC solution we calculated the true OEP following the iterative procedure described in [31], which is more cumbersone for the SIC-LDA functional than for pure exchange, but does converge. The ground-state calculations (no electrical field applied yet) lead to a remarkable result. For the sake of clarity we discuss it using the specific example of the shortest chain, H_4. The KLI solution is spatially symmetric as expected and as depicted in the left part of Fig. 1. It is also manifestly spin unpolarized; i.e., the self-consistent KLI iteration returns to a spin-unpolarized solution from a spin-polarized starting guess. But starting from the spin-unpolarized KLI solution and iterating the OEP to self-consistency without restriction on the spin polarization, we observe a spontaneous change in symmetry. After a few iterations of the OEP self-consistency cycle, the up- and down-spin orbitals separate and each orbital starts to center around one nucleus. For the interatomic distances of 2 and 3 a_0 frequently used in the literature [3,8,26,32], the effect is moderate, but clearly visible, as shown in the middle of
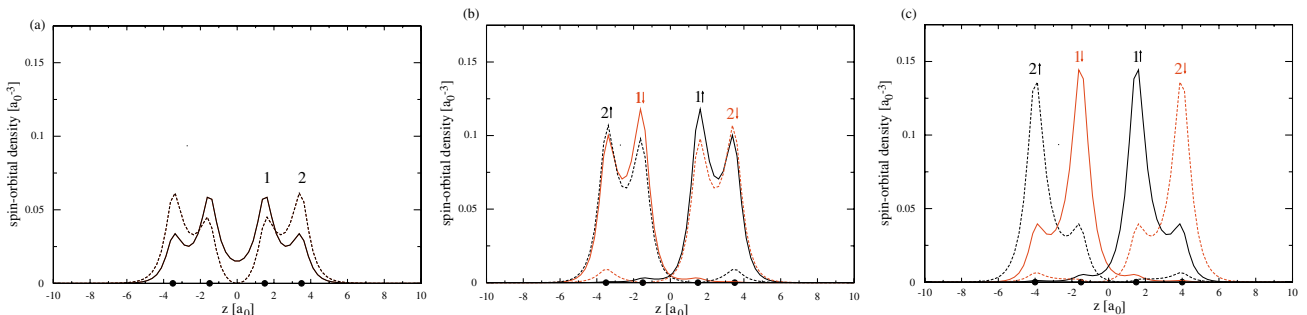

FIG. 1 (color online).   Left: Orbital densities of H_4 with interatomic distances of 2 and 3 bohr (a_0), respectively, obtained from self-consistent KLI-SIC calculation. Up- and down-spin orbitals are identical. Middle: Spin-orbital densities for the same system obtained from self-consistent OEP-SIC calculation. Right: Spin-orbital densities of H_4 with interatomic distances of 2.5 and 3 a_0, respectively, obtained from self-consistent OEP-SIC calculation. The orbital localization increases with increasing interatomic distance.

Fig. 1. If the interatomic distances are increased further, e.g., to 2.5 and 3 a_0 as shown in the right part of Fig. 1, the orbital localization becomes pronounced and one can undoubtedly associate one orbital with one nucleus. This effect is not only observed for H_4, but also for the other hydrogen chains we studied.

A conclusion from this finding is that the KLI-SIC potential is not necessarily a good approximation to the OEP-SIC potential. In order to understand this one should recall that the KLI-potential is justified as a mean-field approximation [11,21,24]: The difference between the true OEP and the KLI-potential is a term of the kind $[1/n(\mathbf{r})]\nabla\mathbf{f}(\mathbf{r})$, where $\mathbf{f}(\mathbf{r})$ is a well-defined function depending on the full spectrum of Kohn-Sham orbitals. Averaged over the density, the term vanishes [21,24]. But implicitly this mean-field argument assumes that the "averaged" term has little influence in the self-consistent iteration so that the density obtained with and without the neglected term are very similar. However, our calculations show that this is not the case for the SIC functional: taking into account the term that is neglected in the KLI potential drives the self-consistent iteration to a very different solution. This is possible because the neglected term contains all orbitals and is thus relevant for unitary (in)variance and greater variational freedom. The breakdown of the KLI-SIC approximation may be a surprise in view of its good performance for atoms [22], but appears less surprising in view of other drawbacks [33].

The hydrogen chain ground-state results also naturally trigger thoughts about the bulk limit that one would reach by adding ever more atoms. We briefly want to ponder this case. Recall that for an infinite lattice of hydrogen atoms with a lattice constant that tends to infinity, the exact Kohn-Sham orbitals are delocalized Bloch orbitals for which the self-interaction correction vanishes on a per atom basis [12]. Using such orbitals in Eq. (1) yields the (wrong) uncorrected LSDA energy. Inherent to the logic of this argument is a certain order of taking the two "infinity limits": first the number of atoms tends to infinity, i.e., an infinite lattice is built, and then the lattice constant is made ever larger.

Our calculations suggest that a different result is obtained if the order of taking these two limits is interchanged. For finite systems of largely separated hydrogen atoms, our OEP-SIC calculations lead to localized orbitals and thus, a self-interaction corrected energy. Now imagine building up an ever larger lattice of hydrogen atoms with ever larger interatomic separation by adding atoms to a finite starting system. At each step of this buildup process, one will be dealing with a large but finite system. Our calculations suggest that at each stage of the buildup process, OEP-SIC will yield localized orbitals and thus a self-interaction corrected energy. This idea is in line with earlier findings that revealed that it makes a great difference whether the surface of an extended system is explicitly taken into account or not [34]. In any case our results show that OEP-SIC can yield localized orbitals that differ

greatly from the KLI orbitals. How strong the OEP-SIC localization is will depend on the specific system. Generally speaking, we expect localization effects to be even more pronounced in SIC schemes using orbital dependent potentials [12] or orbital localizing transformations [16–20].

With the ground-state structure of OEP-SIC discussed we come to the most important aspect of this manuscript, the calculation of the electrical response. As a first test we calculated the response of the two dimers Na_2 and N_2, which can be seen as representing the "extreme ends" of dimer bonding with a soft single and a strong triple bond, respectively. The OEP-SIC polarizability (tensor average in a_0^3) is obtained as 274 for Na_2 (KLI-SIC performs similar) and 10.3 for N_2 (no convergence for KLI-SIC). The value for the sodium dimer compares favorably with the most recent experimental result of 270 [35], the value for the nitrogen dimer is too low but not unreasonable [36]. It is a noteworthy observation that OEP-SIC increases the polarizability (by 12%) for Na_2 (where LDA underestimates) while it decreases it (by 18%) for N_2 (where LDA overestimates); i.e., it works "in the right direction" in both systems. OEP-SIC also yields greatly improved eigenvalues. For CH_4, e.g., OEP-SIC yields $\varepsilon_{HOMO}^{OEP\text{-}SIC} = 14.56$ eV, which compares much better with the experimental ionization energy of 14.42 eV than the LDA value $\varepsilon_{HOMO}^{LDA} = 9.52$ eV.

The true and most important test is how OEP-SIC performs for the response of extended systems where semilocal functionals fail badly. This is tested by calculating the response of the hydrogen chains. The Kohn-Sham SIC longitudinal static electric polarizabilities obtained from an accurate finite field approach [37] are shown in Table I together with LSDA, exact-exchange OEP (OEP-EXX), and fourth-order Møller-Plesset perturbation theory (MP4) results. The MP4 results are close to the exact values and serve as the quasiexact benchmark. The first observation is that the KLI-SIC results vary unsystematically—the polarizability of H_4 is substantially underestimated, whereas the polarizability of all other chains is overestimated. Comparison with OEP-EXX and LSDA shows that KLI-SIC improves over LSDA, but is less accurate than exchange-only theory. The picture changes when SIC is employed with the true, self-consistent OEP instead of with the KLI-approximation: KLI-SIC and OEP-SIC polarizabilities are rather different. Comparing OEP-SIC to the wave-function based results shows that OEP-SIC polarizabilities are within a few percent of the MP4 results in all cases and are noticeably closer to the MP4 values than the exchange-only OEP results, which up to now represented the best density-functional results for such systems.

One may wonder why the SIC functional, in which localization of the orbitals plays an important role, and exact exchange, which is unitarily invariant and thus independent of orbital localization, can both lead to a reasonable description of the chain response. The solution lies in

TABLE I.   Longitudinal polarizability of hydrogen chains in a_0^3 obtained with different exchange-correlation approximations. Møller-Plesset- (MP4) results taken from [38], exact-exchange OEP (OEP-EXX) from [8]. KLI polarizabilities were calculated from the dipole moment; see discussion in [37].

	H_4	H_6	H_8	H_{10}	H_{12}
LSDA	37.6	73	115	162	211
KLI-SIC	19.4	60.3	98.2	131.7	193.6
OEP-EXX	32.2	56.6	84.2	n/a	138.1
OEP-SIC	30.6	48.7	80.1	98.8	129.8
MP4	29.5	51.6	75.9	n/a	126.9

the interpretation of the exchange part of the SIC functional: The Hartree self-interaction correction corresponds to the self-exchange part of the EXX functional, and it is well known that the diagonal (self-)exchange integrals are the dominant part of exchange; i.e., they are noticeably larger than the off-diagonal exchange integrals. The larger the diagonal "classical" parts of the exchange energy are in comparison with its off-diagonal parts, the more accurate becomes the SIC description which neglects the off-diagonal parts. Since the diagonal parts are typically maximal for localized orbitals, it becomes clear why localized orbitals are crucial in the SIC approach. So from this perspective, SIC takes into account the most important part of EXX at the cost of needing to employ localized orbitals, but with the huge benefit of greatly reducing the number of exchange integrals that have to be evaluated. In addition, SIC offers an improvement over bare EXX that can be attributed to the non-EXX parts of the functional. Following [3] one can also show that the improved OEP-SIC polarizabilities stem from a field-counteracting term in the response-part of the exchange-correlation-potential [39]. Thus, SIC is an approach which allows to reliably investigate the electrical response of a broad range of molecular systems [40].

[1] D. J. Tozer, J. Chem. Phys. **119**, 12697 (2003).
[2] N. T. Maitra, J. Chem. Phys. **122**, 234104 (2005).
[3] S. J. A. van Gisbergen *et al.*, Phys. Rev. Lett. **83**, 694 (1999).
[4] C. Toher *et al.*, Phys. Rev. Lett. **95**, 146402 (2005).
[5] M. van Faassen *et al.*, Phys. Rev. Lett. **88**, 186401 (2002).
[6] N. T. Maitra and M. van Faassen, J. Chem. Phys. **126**, 191106 (2007).
[7] P. Mori-Sánchez, Q. Wu, and W. Yang, J. Chem. Phys. **119**, 11 001 (2003).
[8] S. Kümmel, L. Kronik, and J. P. Perdew, Phys. Rev. Lett. **93**, 213002 (2004).
[9] H. Sekino *et al.*, J. Chem. Phys. **126**, 014107 (2007).
[10] F. A. Bulat *et al.*, J. Chem. Phys. **123**, 014319 (2005); B. Champagne *et al.*, J. Chem. Phys. **125**, 194114 (2006).
[11] S. Kümmel and L. Kronik, Rev. Mod. Phys. **80**, 3 (2008).

[12] J. P. Perdew and A. Zunger, Phys. Rev. B **23**, 5048 (1981).
[13] P. Cortona, Phys. Rev. A **34**, 769 (1986); U. Lundin and O. Eriksson, Int. J. Quantum Chem. **81**, 247 (2001); H.-J. Unger, Phys. Lett. A **284**, 124 (2001); P. Novák *et al.*, Phys. Rev. B **67**, 140403(R) (2003); O. A. Vydrov *et al.*, J. Chem. Phys. **124**, 094108 (2006).
[14] S. Goedecker and C. J. Umrigar, Phys. Rev. A **55**, 1765 (1997).
[15] O. A. Vydrov and G. E. Scuseria, J. Chem. Phys. **121**, 8187 (2004).
[16] A. Svane and O. Gunnarsson, Phys. Rev. Lett. **65**, 1148 (1990); Solid State Commun. **76**, 851 (1990).
[17] W. M. Temmerman *et al.*, Phys. Rev. Lett. **86**, 2435 (2001).
[18] M. R. Pederson, R. A. Heaton, and C. C. Lin, J. Chem. Phys. **80**, 1972 (1984); J. Chem. Phys. **82**, 2688 (1985); M. R. Pederson and C. C. Lin, J. Chem. Phys. **88**, 1807 (1988).
[19] J. Garza, J. A. Nichols, and D. A. Dixon, J. Chem. Phys. **112**, 7880 (2000).
[20] S. Patchkovskii, J. Autschbach, and T. Ziegler, J. Chem. Phys. **115**, 26 (2001).
[21] J. B. Krieger, Y. Li, and G. J. Iafrate, Phys. Rev. A **46**, 5453 (1992).
[22] J. Chen *et al.*, Phys. Rev. A **54**, 3939 (1996).
[23] C. A. Ullrich, P.-G. Reinhard, and E. Suraud, Phys. Rev. A **62**, 053202 (2000).
[24] T. Grabo *et al.*, in *Strong Coulomb Correlation in Electronic Structure: Beyond the Local Density Approximation*, edited by V. Anisimov (Gordon & Breach, Tokyo, 2000).
[25] S.-I. Chu, J. Chem. Phys. **123**, 062207 (2005).
[26] B. Champagne *et al.*, J. Chem. Phys. **109**, 10489 (1998).
[27] P. Umari *et al.*, Phys. Rev. Lett. **95**, 207602 (2005).
[28] J. P. Perdew, Adv. Quantum Chem. **21**, 113 (1990).
[29] S. Kümmel and J. P. Perdew, Mol. Phys. **101**, 1363 (2003).
[30] L. Kronik *et al.*, Phys. Status Solidi B **243**, 1063 (2006).
[31] S. Kümmel and J. P. Perdew, Phys. Rev. Lett. **90**, 043004 (2003); Phys. Rev. B **68**, 035103 (2003).
[32] M. Grüning, O. V. Gritsenko, and E. J. Baerends, J. Chem. Phys. **116**, 6435 (2002).
[33] M. Mundt *et al.*, Phys. Rev. A **75**, 050501(R) (2007).
[34] D. Vanderbilt, Phys. Rev. Lett. **79**, 3966 (1997).
[35] D. Rayane *et al.*, Eur. Phys. J. D **9**, 243 (1999); but, comparisons have to be done carefully, see S. Kümmel, J. Akola, and M. Manninen, Phys. Rev. Lett. **84**, 3827 (2000); L. Kronik *et al.*, J. Chem. Phys. **115**, 4322 (2001).
[36] The limited performance of SIC for N_2 [experimental result: 11.7; G. D. Zeiss and W. J. Meath, Mol. Phys. **33**, 1155 (1977)] may have its reason in SIC taking out too much of the local exchange which models nondynamical correlation. N_2 with a triple bond may thus represent the "worst case scenario" for SIC. For a discussion of SIC and nondynamical correlation see, e.g., V. Polo, E. Kraka, and D. Cremer, Mol. Phys. **100**, 1771 (2002).
[37] S. Kümmel and L. Kronik, Comput. Mater. Sci. **35**, 321 (2006).
[38] B. Champagne *et al.*, Phys. Rev. A **52**, 178 (1995); **52**, 1039 (1995).
[39] T. Körzdörfer, Diploma thesis, University of Bayreuth, 2006.
[40] C. D. Pemmaraju, S. Sanvito, and K. Burke, Phys. Rev. B **77**, 121204(R) (2008); A. Ruzsinszky *et al.* (unpublished).

Publication 2

Self-interaction correction and the optimized effective potential

T. Körzdörfer[1], S. Kümmel[1], and M. Mundt[2]

[1]*Physics Institute, University of Bayreuth, D-95440 Bayreuth, Germany*
[2]*Department of Chemical Physics, Weizmann Institute of Science, Rehovot 76100, Israel*

Abstract

Self-interaction is one of the most substantial problems in present-day density functional theory. A widely used approach to overcome this problem is the self-interaction correction (SIC) proposed by Perdew and Zunger. However, the thus given functional does not only depend on the orbitals explicitly, but it is also variant under unitary transformation of the orbitals. In this manuscript, we present a generalized version of the Optimized Effective Potential (OEP) equation which is able to deal with both problems in one go. Calculations for molecules exemplify the approach.

Self-interaction correction and the optimized effective potential

T. Körzdörfer,[1,a)] S. Kümmel,[1] and M. Mundt[2]
[1]*Physics Institute, University of Bayreuth, D-95440 Bayreuth, Germany*
[2]*Department of Chemical Physics, Weizmann Institute of Science, Rehovot 76100, Israel*

Self-interaction is one of the most substantial problems in present-day density functional theory. A widely used approach to overcome this problem is the self-interaction correction proposed by Perdew and Zunger. However, the thus given functional not only depends on the orbitals explicitly but is also variant under unitary transformation of the orbitals. In this manuscript, we present a generalized version of the optimized effective potential equation which is able to deal with both problems in one go. Calculations for molecules exemplify the approach. © *2008 American Institute of Physics.* [DOI: 10.1063/1.2944272]

I. INTRODUCTION

During the past decades, density functional theory (DFT) has become one of the most widely used electronic structure methods because of its ability to provide for an accurate description of numerous properties of many-particle systems such as atoms, molecules, nanostructures, and solids at a bearable computational cost. The breakthrough of DFT was prefaced by the formulation of the Kohn–Sham equations.[1] Kohn and Sham introduced the so-called exchange-correlation potential which, by definition, carries all many-body effects. The corresponding exchange-correlation energy and the classical Coulomb interaction energy

$$E_H[n] = \frac{e^2}{2} \int \int \frac{n(\mathbf{r})n(\mathbf{r}')}{|\mathbf{r} - \mathbf{r}'|} d\mathbf{r}' d\mathbf{r}, \qquad (1)$$

also often called the "Hartree energy", together take into account all of the electron-electron interaction. However, a careful look at Eq. (1) reveals one of the most substantial problems of Kohn–Sham DFT, i.e., self-interaction.[2] This becomes apparent when looking at the hydrogen atom, where the Hartree energy describes the Coulomb interaction energy of one electron with itself. Also in a larger system the interaction of every single electron with itself is accounted for in the Hartree energy, although in this case the self-interaction is less palpable.

At first sight this erroneous treatment of the classical particle-particle interaction is not disturbing, as the exchange-correlation functional (E_{xc}) should, by definition, take care of that. However, while the exact E_{xc} corrects for self-interaction, commonly used approximations such as the local density approximation (LDA) do not entirely correct for self-interaction in many-electron systems.

This shortcoming has been identified as the main reason for notorious failures and serious drawbacks of common density functionals.[3] Typically, self-interaction leads to incorrect dissociation limits,[4,5] underestimation of energy barriers to chemical reactions,[6] and a wrong asymptotic behavior of the exchange-correlation potential[2] (with all its

consequences, such as instability of many experimentally stable anions,[7] absence of a Rydberg series, wrong long range interactions, etc.). Functionals which are not free from self-interaction are not able to describe electron-localization effects in transition metal oxides[8] and widely overestimate charge transfer properties such as the polarizability of molecular chains[9–11] and electronic transport in molecular devices.[12,13]

II. CORRECTING SELF-INTERACTION

As self-interaction is one of the oldest, most substantial, and thus most often discussed problems in DFT, the question arises why it is that hard to find a functional which is completely free from self-interaction. In the following we will discuss this problem in two steps. To begin with, we address the problem of how to define self-interaction in a system with more than one electron. For that purpose we consider an arbitrary many-electron system. Solving the Kohn–Sham equations

$$\left[-\frac{\hbar^2}{2m}\Delta + v_{KS,\sigma}(\mathbf{r}) \right] \varphi_{i\sigma}(\mathbf{r}) = \epsilon_{i\sigma}\varphi_{i\sigma}(\mathbf{r}) \qquad (2)$$

for this system with some approximate exchange-correlation potential $v_{xc,\sigma}^{app}$,

$$v_{KS,\sigma}(\mathbf{r}) = v_{ext}(\mathbf{r}) + e^2 \int \frac{n(\mathbf{r}')}{|\mathbf{r} - \mathbf{r}'|} d\mathbf{r}' + v_{xc,\sigma}^{app}(\mathbf{r}), \qquad (3)$$

yields the corresponding ground-state density

$$n(\mathbf{r}) = \sum_{\sigma=\uparrow,\downarrow} n_\sigma = \sum_{\sigma=\uparrow,\downarrow} \sum_{i=1}^{N_\sigma} n_{i\sigma} = \sum_{\sigma=\uparrow,\downarrow} \sum_{i=1}^{N_\sigma} |\varphi_{i\sigma}(\mathbf{r})|^2, \qquad (4)$$

where N_σ is the number of occupied spin orbitals $\varphi_{i\sigma}$ and $n_{i\sigma}$ are the spin-orbital densities. Given these quantities, how would one know whether the approximate functional is free from self-interaction?

There is an approach that appears quite naturally: By identifying orbital densities with electrons, one can define an interaction energy for every single electron by

$$\delta_{i\sigma} = E_H[n_{i\sigma}] + E_{xc}^{app}[n_{i\sigma},0]. \tag{5}$$

Then, if

$$\sum_{\sigma=\uparrow,\downarrow} \sum_{i=1}^{N_\sigma} \delta_{i\sigma} = 0 \tag{6}$$

holds, declare the functional $E_{xc}^{app}[n_\uparrow,n_\downarrow]$ as being free from self-interaction.

Note that for the exact exchange-correlation functional $E_{xc}^{ex}[n_\uparrow,n_\downarrow]$, Eq. (6) holds for every interacting v representable one-particle density $n_{i\sigma}$. This is due to the fact that $n_{i\sigma}$ can be interpreted as the ground-state density of some one-electron system, and in any one-electron system, the electron-electron interaction vanishes. Consequently, Eq. (6) is a necessary property of $E_{xc}^{ex}[n_\uparrow,n_\downarrow]$. In practice, however, the application of Eqs. (5) and (6) actually reveals *two* drawbacks of commonly used approximations to $E_{xc}^{ex}[n_\uparrow,n_\downarrow]$: First, $\delta_{i\sigma}$ does not vanish in general for one-particle densities. Most of the commonly used density functionals show this failure, i.e., they suffer from "one-electron self-interaction."[14,15] Second, for most of the common density functionals, $\delta_{i\sigma}$ will take different values for different one-particle densities. This is the "unitary invariance problem." In the following we will explain it in detail and demonstrate its great importance for the definition of self-interaction in many-electron systems via Eq. (6). The central aspect is that in a many-electron system, there is no unique way of defining a density for a single electron. Especially, identifying orbital densities with single electrons, as done in Eq. (6), raises the question which orbitals to use. Thus, the definition of self-interaction via Eq. (6) becomes ambiguous.

From a Kohn–Sham DFT perspective, it seems natural to use the Kohn–Sham orbital densities as the one-particle densities needed in Eq. (6). However, orbitals are quantities that are intrinsically linked to the one-particle picture. Strictly speaking, Kohn–Sham orbitals are just auxiliary quantities which yield, when correctly summed up, the ground-state density. Therefore, Kohn–Sham orbital densities can be associated with electrons no less and no more than all other orbital densities which add up to the correct ground-state density. Consequently, a quantification of self-interaction in a many-electron system should be invariant under unitary transformation, i.e., a transformation which changes the individual orbital densities but leaves the total density unchanged. However, for common density functionals, Eq. (6) does not have this property. Clearly, this is a profound drawback of Eq. (6).

The ambiguity in defining self-interaction in a many-electron system via Eq. (6) has led to the search for a more suitable definition of "many-electron self-interaction."[14,15] Recently, progress has been made by studying fractionally charged systems that can arise in charge transfer or dissociation processes.[5,16] These systems are often treated as separated subsystems with noninteger electron number. As Perdew *et al.*[17] argued, in exact Kohn–Sham DFT, the orbital energy of the highest occupied orbital ϵ_{HO} is constant for noninteger particle numbers $M-1<N\leq M$, where M is an

integer, and equal to minus the electron removal energy from the ground state of the M-electron system. Following Janak's theorem,[18] this yields

$$\frac{\partial E}{\partial N} = \epsilon_{HO} = \text{const.} \tag{7}$$

Thus, for the exact E_{xc}, the plot of the ground-state energy E as a function of N is a series of straight line segments with a derivative discontinuity at each integer N. In Ref. 19 the failure of a density functional to fulfill Eq. (7) is traced back to its inherent self-interaction. Following this train of thought, functionals are said to be free from many-electron self-interaction if they show a strictly linear behavior of the ground-state energy for noninteger particle numbers. It has recently been demonstrated that neither the commonly used density or orbital functionals nor the Hartree–Fock approach fulfill this rather stringent requirement.[15,16]

Even though the considerations made above bear a hand in understanding the sophisticated problem of self-interaction in many-electron systems, the construction of functionals which are free from many-electron self-interaction in the sense of Eq. (7) is cumbersome. It has been argued that it requires the mixing of an **r**-dependent fraction of exact exchange (EXX).[20,21] While approaches of this type may offer the highest hopes for overall high accuracy, a lot of improvement and understanding can be gained already by thoroughly investigating how to reach being free from one-electron self-interaction and what the consequences may be. It has also been argued that the correction of one-electron self-interaction in a spirit that we also follow in this paper, although not completely eliminating many-electron self-interaction, does greatly reduce it.[14,22]

Therefore, we will now go back to the question of one-electron self-interaction freeness and the one-electron system. Clearly, in this system, capturing self-interaction is much easier. The reason for this is that, different from the many-electron case, the orbital density now has a clear physical meaning as it equals the ground-state density. Therefore, the self-interaction energy can be unambiguously defined via Eq. (5). This yields a possibility to correct an arbitrary functional $E_{xc}^{app}[n_\uparrow,n_\downarrow]$ by subtracting $\delta_{i\sigma}$ and thus obtaining a self-interaction corrected functional.

The basic idea of the self-interaction correction (SIC) of Perdew and Zunger,[2] which today is by far the most commonly used SIC, is to carry forward this approach to many-electron systems.[23] The obtained functional

$$E_{xc}^{SIC}[n_\uparrow,n_\downarrow] = E_{xc}^{app}[n_\uparrow,n_\downarrow] - \sum_{\sigma=\uparrow,\downarrow} \sum_{i=1}^{N_\sigma} [E_H[n_{i,\sigma}]$$
$$+ E_{xc}^{app}[n_{i,\sigma},0]] \tag{8}$$

is free from one-electron self-interaction. Thus, the SIC of Perdew and Zunger constitutes a plausible and straightforward approximation. However, it carries along the unpleasant features of Eq. (5). The functional depends on the orbitals explicitly, i.e., it is not an explicit density functional. In addition $E_{xc}^{SIC}[n_\uparrow,n_\downarrow]$ is not invariant under unitary transformation of the orbitals. This means that one can define various different and *a priori* equally valid E_{xc}^{SIC} that correspond to a

given charge density. Therefore, the usual way of minimizing the total energy with respect to the density in order to find a system's ground state,

$$\frac{\delta E}{\delta n_\sigma} = 0, \tag{9}$$

cannot be applied in a straightforward manner. As a further consequence, there is no unique way of finding an exchange-correlation potential corresponding to Eq. (8). Thereby, the unitary invariance problem in defining self-interaction in a many-electron system strikes you through the backdoor in the Perdew–Zunger-SIC approach.

The problem of the explicit orbital dependence of Eq. (8) can be overcome by constructing the optimized effective potential (OEP). However, the unitary invariance problem allows the definition of different OEPs depending on which orbital densities are used in Eq. (8). Although all of these potentials correspond to the same orbital-dependent energy expression, they may all show different behaviors and yield different results in practical applications.

The purpose of this manuscript is to discuss and compare different SIC approaches that employ a local, nonorbital-specific potential. Thus, we provide a theoretical framework for SIC-OEP methods working with (or without) explicit unitary transformation of the orbitals. Our presentation is divided into five parts. After a short review of some non-OEP methods that are based on Eq. (8), we derive a generalized OEP equation in Sec. IV. This equation enables us to find the correct OEP for a set of orbitals which differs from the Kohn–Sham orbitals by a unitary transformation. Section V is devoted to the construction of the unitary transformation which yields the minimum of the total energy. Finally, we compare the results of our method to other approaches to construct a local effective potential corresponding to Eq. (8) in Sec. VI and summarize our findings in Sec. VII.

III. REVIEW OF NON-OEP METHODS

Due to its explicit dependence on the orbitals, the self-consistent minimization of the SIC functional of Eq. (8) is more involved than the one for standard density functionals such as LDA. In their original work,[2] Perdew and Zunger directly minimized the functional with respect to the orbitals. By imposing an orthogonality constraint on the orbitals, i.e., by making use of the Lagrange multipliers,

$$\lambda_{ij}^\sigma = \langle \tilde{\psi}_{j\sigma} | \tilde{H}_{i\sigma} \tilde{\psi}_{i\sigma} \rangle, \tag{10}$$

with the effective one-electron Hamiltonian

$$\tilde{H}_{i\sigma} = H_{0\sigma} + \tilde{v}_{i\sigma}^{\text{SIC}}, \tag{11}$$

where

$$H_{0\sigma} = -\frac{\hbar^2}{2m}\Delta + v_{\text{ext}}(\mathbf{r}) + v_H[n](\mathbf{r}) + v_{\text{xc},\sigma}^{\text{app}}[n_\uparrow, n_\downarrow](\mathbf{r}), \tag{12}$$

$$\tilde{v}_{i\sigma}^{\text{SIC}} = -v_H[\tilde{n}_{i,\sigma}](\mathbf{r}) - v_{\text{xc},\sigma}^{\text{app}}[\tilde{n}_{i,\sigma}, 0](\mathbf{r}), \tag{13}$$

one thus derives[24] the system of self-consistent equations

$$\tilde{H}_{i\sigma}\tilde{\psi}_{i\sigma} = (H_{0\sigma} + \tilde{v}_{i\sigma}^{\text{SIC}})\tilde{\psi}_{i\sigma} = \sum_{j=1}^{N_\sigma} \lambda_{ij}^\sigma \tilde{\psi}_{j\sigma}. \tag{14}$$

By introducing orbital-specific potentials, this approach (PZ-SIC) is outside the foundations of Kohn–Sham theory while not leaving the realm of the Hohenberg–Kohn theorem. Due to the unitary invariance problem, the one-electron Hamiltonian $\tilde{H}_{i\sigma}$, and thus the matrix of Lagrange multipliers, is not invariant under unitary transformation of the orbitals. At the minimum of the PZ-SIC energy, the matrix of Lagrange multipliers becomes Hermitian and thus unitarily diagonalizable.[25,26] This has led to the definition of two different types of orbitals: The orthogonal orbitals that minimize the PZ-SIC energy are often referred to as localized orbitals $\tilde{\psi}_{i\sigma}$, as localization of the orbitals naturally increases $E_H[n_{i,\sigma}]$ and thus minimizes $E_{\text{xc}}^{\text{SIC}}[n_\uparrow, n_\downarrow]$ in many systems. In contrast, the so-called canonical orbitals $\psi_{i\sigma}$ are the orbitals that diagonalize the matrix of Lagrange multipliers and typically are delocalized. They are related to the localized orbitals by the unitary transformation U_{ij}^σ,

$$\tilde{\psi}_{i\sigma} = \sum_{j=1}^{N_\sigma} U_{ij}^\sigma \psi_{j\sigma}. \tag{15}$$

As the canonical orbitals diagonalize the Lagrange-multiplier matrix in the minimum of the SIC energy, they can be interpreted as Kohn–Sham-type eigenorbitals of the transformed one-electron Hamiltonians $H_{j\sigma}$ [see Eq. (16)]. The eigenvalues of λ_{ij} are often used as equivalents of Kohn–Sham orbital energies,[26] although recent work suggests a different interpretation.[16]

By applying the unitary transformation U_{ij}^σ, Pederson *et al.*[26] introduced equations similar to Eq. (14) for the canonical orbitals,

$$H_{j\sigma}\psi_{j\sigma} = (H_{0\sigma} + v_{j\sigma}^{\text{SIC}})\psi_{j\sigma} = \sum_{i=1}^{N_\sigma} \epsilon_{ji}^\sigma \psi_{i\sigma}, \tag{16}$$

where

$$v_{j\sigma}^{\text{SIC}} = \sum_{k=1}^{N_\sigma} U_{kj}^\sigma \tilde{v}_{k\sigma}^{\text{SIC}} \frac{\tilde{\psi}_{k\sigma}}{\psi_{j\sigma}}, \tag{17}$$

$$\epsilon_{ji}^\sigma = \sum_{k,l=1}^{N_\sigma} U_{jk}^{\sigma-1} \lambda_{kl}^\sigma U_{li}^\sigma. \tag{18}$$

Here, the SIC potential $v_{j\sigma}^{\text{SIC}}$ associated with the (delocalized) canonical orbital $\psi_{j\sigma}$ can be interpreted as a weighted average of the SIC potentials for the localized orbitals $\tilde{v}_{i\sigma}^{\text{SIC}}$. Thereby the unitary invariance problem provides for the existence of different exchange-correlation potentials for different orbitals that add up to the same density.

PZ-SIC and its successors using localizing transformations have been used successfully for solids[27,28] and molecules.[29–31] It has been shown that these approaches improve dissociation curves,[29] total energies, and energy barriers to chemical reactions.[32] PZ-SIC enhances the agreement of the highest occupied orbital energy of LDA with minus the ionization potential[25,26] (IP) and the localized PZ-SIC

orbitals are able to capture electron-localization effects in crystalline solids.[27,28] However, it was found that it predicts too short bond lengths in molecules[25,31] and it fails badly in the prediction of some basic thermodynamical properties.[30,33] In summary, PZ-SIC often seems to overcorrect in many-electron systems. Therefore, efforts have been made in order to scale down the PZ-SIC in many-electron regions.[34] However, although improving the thermodynamical properties, the scaled down version of the PZ-SIC is inferior to the standard PZ-SIC in terms of many-electron self-interaction freeness.[14]

Having discussed the properties of Eq. (8), the peculiarities of PZ-SIC in regions with many electrons do not come as a surprise. Clearly, they are due to the intrinsic approximation of the PZ-SIC, i.e., to carry forward the concept of one-electron self-interaction to many-electron systems. This approximation becomes manifested in the unitary invariance problem. Therefore, we believe that the unitary invariance problem plays an important role in bridging the concepts of one- and many-electron self-interaction. This assumption is supported by recent work (Ref. 35), in which the many-electron self-interaction problem is directly related to the localization or delocalization of Kohn–Sham orbitals. In the following section, we propose a formalism which allows to approach the unitary invariance problem in the realm of Kohn–Sham DFT by introducing a generalized version of the OEP equation for functionals which are variant under unitary transformation of the orbitals.

IV. A GENERALIZED OPTIMIZED EFFECTIVE POTENTIAL SCHEME

Minimizing Eq. (8) directly with respect to the orbitals leads to single-particle equations with orbital-specific potentials instead of a global Kohn–Sham potential for all orbitals. However, the existence of such a potential is one of the features that makes Kohn–Sham DFT attractive, as it considerably simplifies the numerical efforts and facilitates the interpretation of results. Moreover, the existence of a local potential ensures that the noninteracting kinetic energy is a well-defined density functional. In the literature, various schemes have been proposed to construct a local effective potential from Eq. (8).[26,36–42] However, the most natural definition of a Kohn–Sham potential based on the SIC of Perdew and Zunger has been largely unexplored: the construction of the local effective potential that by virtue of the Kohn–Sham equations leads to orbitals that minimize the total energy, i.e., the OEP.

The OEP method (see Ref. 3 for an overview) is based on the variation in the total energy with respect to a trial potential,[43]

$$\frac{\delta E_{\text{tot}}[\{\varphi_{n\tau}\}]}{\delta v_{\text{KS},\sigma}}\bigg|_{v_{\text{KS},\sigma}=v_{\text{KS},\sigma}^{\text{OEP}}} = 0, \tag{19}$$

or equivalently (by virtue of the Hohenberg–Kohn theorem) with respect to the spin density,[44]

$$\frac{\delta E_{\text{tot}}[\{\varphi_{n\tau}\}]}{\delta n_\sigma} = 0. \tag{20}$$

However, due to the unitary invariance problem discussed above, a problem is buried in Eq. (20). As the SIC functional $E_{\text{tot}}^{\text{SIC}}[\{\varphi_{n\tau}\}]$ is not invariant under unitary transformation of the orbitals, many different total energies can be attached to the same density. Therefore, an OEP based on Eq. (20) is not uniquely defined unless the orbitals with which to construct $E_{\text{tot}}^{\text{SIC}}[\{\varphi_{n\tau}\}]$ are explicitly specified. Based on the experience made with the SIC methods using orbital-specific potentials, at least two options appear reasonable: Either use the Kohn–Sham orbitals, i.e., the eigenorbitals of the Kohn–Sham Hamiltonian, or use the orbitals that minimize $E_{\text{tot}}^{\text{SIC}}[\{\varphi_{n\tau}\}]$ under the constraint of reproducing the density given by the Kohn–Sham orbitals. However, the derivation of the standard OEP equation requires that the orbitals used to construct $E_{\text{tot}}[\{\varphi_{n\tau}\}]$ are eigenorbitals of the Kohn–Sham Hamiltonian. Hence, the usual OEP equation does not allow to use other orbitals than the Kohn–Sham orbitals.

In the following we will investigate how the choice of orbitals that are different from the Kohn–Sham orbitals affects the derivation of the OEP integral equation. These orbitals are related to the Kohn–Sham orbitals $\varphi_{i\sigma}$ by a unitary transformation U_{ij}^σ and will be referred to as localized orbitals $\widetilde{\varphi}_{i\sigma}$, i.e.,

$$\widetilde{\varphi}_{i\sigma} = \sum_{j=1}^{N_\sigma} U_{ij}^\sigma \varphi_{j\sigma}. \tag{21}$$

In the first step, we write the total SIC energy as a functional of the localized orbitals, i.e., $E_{\text{tot}}^{\text{SIC}}[\{\widetilde{\varphi}_{n\tau}\}]$, and derive from Eq. (20) by virtue of the chain rule,

$$v_{\text{xc},\sigma}^{\text{OEP}} = \frac{\delta E_{\text{xc}}^{\text{SIC}}[\{\widetilde{\varphi}_{n\tau}\}]}{\delta n_\sigma(\mathbf{r})}$$

$$= \sum_{\alpha,\beta,\gamma=\uparrow,\downarrow} \sum_{i=1}^{N_\alpha} \sum_{j=1}^{N_\beta} \int\int\int \frac{\delta E_{\text{xc}}^{\text{SIC}}[\{\widetilde{\varphi}_{n\tau}\}]}{\delta \widetilde{\varphi}_{i\alpha}(\mathbf{r}')} \frac{\delta \widetilde{\varphi}_{i\alpha}(\mathbf{r}')}{\delta \varphi_{j,\beta}(\mathbf{r}'')}$$

$$\times \frac{\delta \varphi_{j,\beta}(\mathbf{r}'')}{\delta v_{\text{KS},\gamma}(\mathbf{r}''')} \frac{\delta v_{\text{KS},\gamma}(\mathbf{r}''')}{\delta n_\sigma(\mathbf{r})} d\mathbf{r}' d\mathbf{r}'' d\mathbf{r}''' + \text{c.c.} \tag{22}$$

From Eq. (21) one derives

$$\frac{\delta \widetilde{\varphi}_{i\alpha}(\mathbf{r}')}{\delta \varphi_{j,\beta}(\mathbf{r}'')} = \delta_{\alpha\beta}\delta(\mathbf{r}'-\mathbf{r}'')\left(U_{ij}^\alpha + \sum_{k=1}^{N_\alpha} \frac{\delta U_{ik}^\alpha}{\delta \varphi_{j,\beta}(\mathbf{r}'')} \varphi_{k,\alpha}(\mathbf{r}') \right) \tag{23}$$

and application of first order perturbation theory yields

$$\frac{\delta \varphi_{j,\beta}(\mathbf{r}'')}{\delta v_{\text{KS},\gamma}(\mathbf{r}''')} = \delta_{\beta\gamma} G_{j\gamma}(\mathbf{r}'',\mathbf{r}''') \varphi_{j,\gamma}(\mathbf{r}'''), \tag{24}$$

$$\frac{\delta v_{\text{KS},\gamma}(\mathbf{r}''')}{\delta n_\sigma(\mathbf{r})} = \delta_{\gamma\sigma} \chi_\sigma^{-1}(\mathbf{r}''',\mathbf{r}), \tag{25}$$

with the Green's function

$$G_{j\sigma}(\mathbf{r}',\mathbf{r}) = \sum_{\substack{k=1 \\ k \neq j}}^{\infty} \frac{\varphi_{k\sigma}(\mathbf{r}')\varphi_{k\sigma}^*(\mathbf{r})}{\epsilon_{j\sigma} - \epsilon_{k\sigma}} \qquad (26)$$

and the static Kohn–Sham response function

$$\chi_\sigma(\mathbf{r}',\mathbf{r}) = \sum_{j=1}^{N_\sigma} \sum_{\substack{k=1 \\ k \neq j}}^{\infty} \frac{\varphi_{j\sigma}^*(\mathbf{r}')\varphi_{k\sigma}(\mathbf{r}')\varphi_{k\sigma}^*(\mathbf{r})\varphi_{j\sigma}(\mathbf{r})}{\epsilon_{j\sigma} - \epsilon_{k\sigma}} + \text{c.c.}$$

$$= \sum_{j=1}^{N_\sigma} \varphi_{j\sigma}^*(\mathbf{r}')G_{j\sigma}(\mathbf{r}',\mathbf{r})\varphi_{j\sigma}(\mathbf{r}). \qquad (27)$$

Inserting Eqs. (23)–(27) in Eq. (22) yields the first central result of this manuscript, the generalized OEP equation for unitarily variant orbital functionals:

$$\sum_{j=1}^{N_\sigma} \int \varphi_{j\sigma}^*(\mathbf{r}') \left[v_{\text{xc},\sigma}^{\text{OEP}}(\mathbf{r}') - \frac{1}{\varphi_{j\sigma}^*(\mathbf{r}')} \sum_{i=1}^{N_\sigma} \right.$$

$$\times \left(U_{ij}^\sigma + \frac{\delta U_{ij}^\sigma}{\delta \varphi_{j,\sigma}(\mathbf{r}')} \varphi_{j,\sigma}(\mathbf{r}') \right) \frac{\delta E_{\text{xc}}^{\text{SIC}}[\{\tilde{\varphi}_{n\tau}\}]}{\delta \tilde{\varphi}_{i\alpha}(\mathbf{r}')} \right]$$

$$\times G_{j\sigma}(\mathbf{r}',\mathbf{r})\varphi_{j\sigma}(\mathbf{r}) + \text{c.c.} \, d\mathbf{r}' = 0. \qquad (28)$$

The interpretation of this equation is as follows: Solving Eq. (28) yields the unique local potential $v_{\text{xc},\sigma}^{\text{OEP}}(\mathbf{r})$ that by virtue of the Kohn–Sham equations leads to Kohn–Sham orbitals which, when localized according to Eq. (21), yield the lowest total energy that can possibly be obtained with two sets of orbitals linked by a unitary transformation U_{ij}^σ via Eq. (21). Note that Eq. (28) is general in the sense that it is neither limited to the SIC energy expression (simply replace $E_{\text{xc}}^{\text{SIC}}$) nor to a certain unitary transformation U_{ij}^σ. However, for all functionals which are invariant under unitary transformation of the orbitals, Eq. (28) reduces to the standard OEP equation.

As the generalized OEP equation is nontrivially different from the usual OEP equation, we discuss the relation between the two types of OEP approaches in detail in the following. To this end, first assume that $U_{ij}^\sigma = \delta_{ij}$. With this trivial ansatz for U_{ij}^σ, the difference between the two sets of orbitals vanishes, i.e., $\tilde{\varphi}_{i\sigma} = \varphi_{i\sigma}$, and Eq. (28) reduces to the usual Kohn–Sham OEP equation (KS-OEP). KS-OEP is the most transparent way of calculating an OEP potential corresponding to the SIC functional from Eq. (8) because there is only one Hamiltonian and one set of orbitals, the Kohn–Sham orbitals. Contrary to the elements of the Lagrange-multiplier matrix or its counterparts in other SIC approaches[16] that were mentioned earlier, the Kohn–Sham eigenvalues can be unambiguously associated with the corresponding Kohn–Sham orbitals. This clearly facilitates the interpretation of results. For instance, the Kohn–Sham eigenvalues can directly be used for evaluating Janak's theorem[18] or as input to time dependent linear response methods.[45] Due to the numerical effort of solving the full-OEP equation, the KS-OEP approach so far has remained largely unexplored. Recently, KS-OEP has been tested with great success in calculating the response of extended molecular systems.[46] These results revealed a substantial discrepancy between the full-OEP calculations and the Krieger–Li–Iafrate (KLI) ap-

proximation to the KS-OEP (KS-KLI). Both approaches, i.e., KS-OEP and KS-KLI, will be examined later in this manuscript. Before we do so, we, however, have to return to the drawback which is inherent to the KS-OEP approach when it is used with energy expressions such as the SIC one that are not unitarily invariant: For a given density, KS-OEP does not yield the minimum of the total energy. Therefore, one could argue that KS-OEP does not truly fulfill the variational principle, which is one of the basic theorems of Kohn–Sham DFT.

This drawback can be overcome by finding the unitary transformation matrix U_{ij}^σ which yields those localized orbitals $\tilde{\varphi}_{i\sigma}$ that minimize the total energy under the constraint of reproducing a given density. The problem of finding this localizing transformation will be addressed in Sec. V. Here, we first want to discuss the effect that this transformation has in the OEP equation (28). So in the following we now assume that U_{ij}^σ is the unitary matrix that transforms a set of orbitals in such a way that the transformed orbitals yield the minimum of the total energy under the constraint of reproducing a given density. In this case (LOC-OEP), the solution $v_{\text{xc},\sigma}^{\text{OEP}}(\mathbf{r})$ of Eq. (28) is the unique local potential corresponding to Eq. (8) that leads to Kohn–Sham orbitals which, when localized according to Eq. (21), yield the lowest total energy of the system. Note that this energy will still be higher than the energy obtained from a free variation of the orbitals according to Eq. (14). However, it is the lowest energy that can possibly be obtained by virtue of one local potential corresponding to Eq. (8). In this spirit, the LOC-OEP approach is as close as you can get to the original idea of the OEP.

Equation (28) is formally equivalent to the standard OEP equation if one defines

$$u_{\text{xc},j\sigma}^{\text{loc}}(\mathbf{r}') := \frac{1}{\varphi_{j\sigma}^*(\mathbf{r}')} \sum_{i=1}^{N_\sigma} \left(U_{ij}^\sigma + \frac{\delta U_{ij}^\sigma}{\delta \varphi_{j,\sigma}(\mathbf{r}')} \varphi_{j,\sigma}(\mathbf{r}') \right)$$

$$\times \frac{\delta E_{\text{xc}}^{\text{SIC}}[\{\tilde{\varphi}_{n\tau}\}]}{\delta \tilde{\varphi}_{i\sigma}(\mathbf{r}')}, \qquad (29)$$

as an "orbital-specific potential" similar to the orbital-specific potential

$$u_{\text{xc},i\sigma}^{\text{ui}}(\mathbf{r}') := \frac{1}{\varphi_{i\sigma}^*(\mathbf{r}')} \frac{\delta E_{\text{xc}}^{\text{ui}}[\{\varphi_{n\tau}\}]}{\delta \varphi_{i\sigma}(\mathbf{r}')}, \qquad (30)$$

that appears in the standard OEP equation for a unitarily invariant functional $E_{\text{xc}}^{\text{ui}}[\{\varphi_{n\tau}\}]$ such as EXX [compare, e.g., Eq. (2) in Ref. 47 or p. 12 in Ref. 3]. Despite the obvious formal similarity, the two types of orbital-specific potentials differ nontrivially. By naively employing Eq. (30) one can also define other orbital-specific potentials for localized orbitals,

$$\tilde{u}_{\text{xc},i\sigma}^{\text{loc}}(\mathbf{r}') := \frac{1}{\tilde{\varphi}_{i\sigma}^*(\mathbf{r}')} \frac{\delta E_{\text{xc}}^{\text{SIC}}[\{\tilde{\varphi}_{n\tau}\}]}{\delta \tilde{\varphi}_{i\sigma}(\mathbf{r}')}. \qquad (31)$$

Rewriting Eq. (29) in terms of $\tilde{u}_{\text{xc},i\sigma}^{\text{loc}}(\mathbf{r}')$ while neglecting the variation in the transformation matrix with respect to the orbitals, i.e., setting $\delta U_{ij}^\sigma / \delta \varphi_{j,\sigma} = 0$, yields

$$u_{\text{xc},j\sigma}^{\text{loc}}(\mathbf{r}') = \sum_{i=1}^{N_\sigma} U_{ij}^\sigma \, \tilde{u}_{\text{xc},i\sigma}^{\text{loc}}(\mathbf{r}') \frac{\tilde{\varphi}_{i\sigma}^*(\mathbf{r}')}{\varphi_{j\sigma}^*(\mathbf{r}')}. \tag{32}$$

Thus, a comparison of Eq. (32) with Eq. (17) suggests an interpretation of $u_{\text{xc},j\sigma}^{\text{loc}}(\mathbf{r}')$: the orbital-specific potentials $u_{\text{xc},j\sigma}^{\text{loc}}(\mathbf{r}')$ of Eq. (29) are associated with the Kohn–Sham orbitals and can be regarded as the weighted average of the orbital-specific potentials $\tilde{u}_{\text{xc},i\sigma}^{\text{loc}}(\mathbf{r}')$ of the localized orbitals. The meaning and interpretation of the generalized OEP equation (28) are thus clear. As a final remark we would like to stress that the generalized OEP equation (28) must and will yield different OEPs for different unitary transformation matrices U_{ij}^σ.

The obvious next question is how to solve Eq. (28) in practice. As it differs from the standard OEP equation only in the orbital-specific potentials, all of the standard procedures of solving the OEP equation can be applied. In this manuscript, we use the approach described in Refs. 47 and 48. As solving the OEP equation is a numerically demanding task, a number of approximations to the full-OEP have been proposed.[49–53] A commonly used one is the approximation given by Krieger *et al.*

$$v_{\text{xc},\sigma}^{\text{KLI}}(\mathbf{r}) = \frac{1}{2n_\sigma} \sum_{i=1}^{N_\sigma} \{|\varphi_{i\sigma}(\mathbf{r})|^2 [u_{\text{xc},i\sigma}(\mathbf{r}) + (\bar{v}_{\text{xc},i\sigma}^{\text{KLI}} - \bar{u}_{\text{xc},i\sigma})]\}$$
$$+ \text{c.c.} \tag{33}$$

As the KLI approximation is easy to implement and numerically less demanding than calculating the full OEP, it yields an appealing approach to construct a local effective potential for orbital functionals. Therefore, a number of attempts to use Eq. (33) for the SIC functional can be found in the literature.[36–39] Due to the unitary invariance problem, some approaches[40–42] used localized orbitals in order to evaluate Eq. (33), i.e., they used the potential

$$v_{\text{xc},\sigma}^{\text{Garza}}(\mathbf{r}) = \frac{1}{2n_\sigma} \sum_{i=1}^{N_\sigma} \{|\tilde{\varphi}_{i\sigma}(\mathbf{r})|^2 [\tilde{u}_{\text{xc},i\sigma}^{\text{loc}}(\mathbf{r}) + (\bar{v}_{\text{xc},i\sigma}^{\text{KLI}} - \bar{\tilde{u}}_{\text{xc},i\sigma}^{\text{loc}})]\}$$
$$+ \text{c.c.} \tag{34}$$

Note that this approach (Garza) is different from the KLI approximation to the LOC-OEP (LOC-KLI), which is defined as the potential one obtains from Eq. (33) by replacing $u_{\text{xc},i\sigma}(\mathbf{r})$ with the orbital-specific potentials of Eq. (32): Whereas in Garza's approach all Kohn–Sham orbitals in Eq. (33) are replaced by localized orbitals, LOC-KLI only differs from the KS-KLI approximation in the orbital-specific potentials.

Note, however, that the Slater part of Garza's potential conforms with the Slater part of the LOC-KLI potential, as can be seen by inserting Eq. (32) in Eq. (33). This gives rise to the assumption that both approaches yield similar results in practical application. The examples in Sec. VI show that this is indeed the case. However, although Eq. (34) yields a legitimate way of defining an effective one-particle potential, there is no straightforward way of improving the Garza approach to a full-OEP level. The generalized OEP approach presented here can be interpreted as the unifying concept and the foundation of the earlier developed approaches that use a local potential along with localizing transformations.

V. LOCALIZING TRANSFORMATIONS

The aim of the unitary transformation of the Kohn–Sham orbitals is to find those orbitals $\tilde{\varphi}_{i\sigma}$ which minimize the energy of Eq. (8) while leaving the density unchanged. In order to find the energy-minimizing unitary transformation, we use the method proposed in Ref. 54. The resulting orbitals are typically much more localized in space than the Kohn–Sham orbitals. This observation is by no means surprising, as the PZ-SIC orbitals, i.e., those orbitals that result from a free variation in the total energy with respect to the orbitals, are typically also well localized in space. The reason for this is that the Hartree SIC terms in Eq. (8) increase with increasing localization of the orbitals. This reasoning has led to a variety of different approaches to find localized orbitals that (approximately) minimize the SIC energy, most of them based on localizing transformations which were originally introduced to find orbitals that mimic the chemist's intuition of chemical bonds. Among the most popular localized orbitals are those introduced by Foster and Boys,[55] Edmiston and Ruedenberg,[56] and Pipek and Mezey.[57] The difference between these methods is to be found in the definition of localization (for details, see Ref. 57).

However, this kind of reasoning is based on an oversimplified picture of the impact of the SIC on the structure of the energy-minimizing orbitals. The localization of the orbitals does not only increase the Hartree correction $E_H[n_{i,\sigma}]$ but also the correction of the self-interaction embedded in the local functional, i.e., $E_{\text{xc}}^{\text{LDA}}[n_{i,\sigma}, 0]$. Both contributions have a different sign and are typically of the same order of magnitude. The goal of the energy-minimizing unitary transformation is thus to find the best trade-off between both contributions. Therefore, the degree to which the energy-minimizing orbitals are localized in space does strongly depend on the system. In contrast to the method proposed in Ref. 54, none of the commonly used localizing transformations is able to account for these subtleties. Nevertheless, experience shows that in many systems, the Foster–Boys orbitals provide for an excellent approximation to the energy-minimizing orbitals.

VI. RESULTS AND DISCUSSION

In the following we test different functionals which are all based on the SIC energy expression of Eq. (8). The approximate exchange-correlation functional which is corrected for is in each case the LDA with correlation contributions in the parametrization of Ref. 58 if not stated otherwise. We employ a real space approach using norm conserving pseudopotentials.[59] In all calculations we used LDA pseudopotentials and this, in principle, leads to an inconsistency between the treatment of the exchange-correlation effects in the pseudopotential construction and in the actual molecular calculations. However, we have carefully tested that for the light nuclei which we study here, pseudopotential (in)consistency does hardly influence the results. For example, comparison with all-electron calculations[40] shows
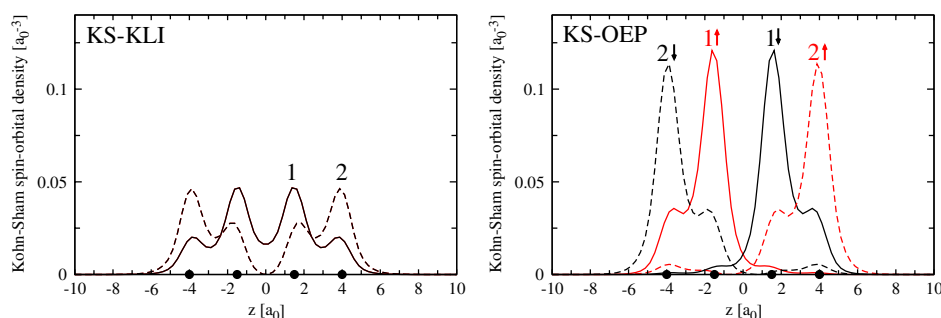
FIG. 1. (Color online) Left: Kohn–Sham orbital densities of H_4 with interatomic distances of 2.5 and 3 bohrs (a_0), respectively, obtained from self-consistent KS-KLI calculation. Up- and down-spin orbitals are identical. Right: Kohn–Sham spin-orbital densities for the same system obtained from self-consistent KS-OEP calculation.

that the largest difference between the highest occupied molecular orbital (HOMO) energies obtained in KS-KLI calculations (without correlation contributions in order to be able to compare to the calculations done in Ref. 40) based on a LDA pseudopotential and the ones obtained in all-electron calculations is observed for H_2O and is of the order of 0.01 Ry. A difference of this smallness may as well be related to basis-set questions and other issues and is at the limit of what is of interest here. The very limited influence of pseudopotential consistency has also been reported in other works.[25] (It should be noted, however, that the picture changes for heavy nuclei, see, e.g., the discussion in Ref. 3.) Experimental geometries are used for all molecules if not stated otherwise.

The systems that we study in the following are chosen such that we span a range of different bonding situations with a few instructive, pertinent molecular systems. Our first test case is a model system of weakly interacting subunits, a chain of four single hydrogen atoms with interatomic distances of 2.5 and 3 bohrs (a_0), respectively. This system provides for a well suited testing ground for the SIC functionals. In the limit of infinite interatomic separation, it goes over into a collection of single, separated hydrogen atoms for which Eq. (8) is exact and unambiguous. Decreasing the interatomic distance will mix the eigenstates of the single atoms and introduce the ambiguousness of Eq. (8) and thus the unitary invariance problem. Therefore, a noticeable difference between the different SIC approaches can be expected. In addition the simplicity of the orbital structure of the H_4 chain facilitates the demonstration of orbital localization effects.

For the sake of completeness, we first briefly address the KS-OEP SIC method, i.e., solving Eq. (28) with $U_{ij}^\sigma = \delta_{ij}$ and thus $\widetilde{\varphi}_{i\sigma} = \varphi_{i\sigma}$ and $u_{\text{xc},j\sigma}^{\text{loc}}(\mathbf{r}') = \widetilde{u}_{\text{xc},j\sigma}^{\text{loc}}(\mathbf{r}')$, so only the Kohn–Sham orbitals are used. We calculate the ground state of H_4 using KS-KLI and from this, the KS-OEP following the iterative procedure of Refs. 47 and 48. The obtained ground-state Kohn–Sham orbitals are presented in Fig. 1. Note that the KS-KLI solution is spatially symmetric as expected, whereas the KS-OEP calculation leads to a spontaneous change in symmetry, ending up in a manifestly spin polarized ground state. The KS-OEP orbitals are clearly localized and can undoubtedly be associated with single nuclei. In contrast, the KS-KLI orbitals are delocalized over all nuclei. This profound difference in the ground-state spin densities does also become apparent in the ground-state energies (see Table I). This is an outstanding result, as all comparable calculations

for other orbital functionals such as EXX show only a minor difference between KLI and OEP ground-state energies and virtually no visible difference in the ground-state densities. This surprising finding has been explained in Ref. 46.

Another surprising aspect of the KS-KLI functional becomes apparent from Table I when comparing the respective SIC ground-state energies to the LDA energy: The KS-KLI ground-state energy of H_4 is not only very different from the KS-OEP, but also significantly higher than the LDA energy. This can be explained by the fact that the SIC correction from Eq. (8) does not only contain the correction of the Hartree self-energy $E_H[n_{i,\sigma}]$ but also the self-interaction energy of the exchange-correlation approximation $E_{\text{xc}}^{\text{LDA}}[n_{i,\sigma},0]$. In contrast to the former, the latter increases the total energy, as it corrects for the overestimation of the (negative) exchange-correlation energy. For the studied hydrogen chain, we find

$$\sum_{\sigma=\uparrow,\downarrow} \sum_{i=1}^{N_\sigma} E_H[n_{i,\sigma}] + E_{\text{xc}}^{\text{app}}[n_{i,\sigma},0] < 0 \qquad (35)$$

if we use spin-orbital densities $n_{i,\sigma}$ from self-consistent LDA or KS-KLI calculations. In contrast, the correction becomes positive when the localized spin-orbital densities from the self-consistent KS-OEP calculation are used.

A careful look at the literature[40,41] reveals that it is well known that KS-KLI can produce unrealistic and curious results when applied to molecules. This was attributed to the unitary invariance problem: orbitals minimizing Eq. (8) are localized orbitals, whereas a local Kohn–Sham potential is supposed to yield orbitals that are delocalized over the whole system. Therefore, localizing transformations were incorporated in KS-KLI in the spirit of Eq. (34). However, our results for the H_4 model system give rise to an alternative interpretation: Fig. 1 shows that a local Kohn–Sham potential (here: KS-OEP) can indeed yield localized Kohn–Sham orbitals. Therefore, the failure of the KS-KLI functional for some molecules might be due the KLI approximation and not due to the absence of a localizing transformation. This assumption is supported by recent calculations of response properties of molecular chains,[46] for which KS-KLI shows unrealistic and unreliable results, whereas the KS-OEP results are close to quantum-chemical accuracy.

In our next step we study the LOC-OEP approach, i.e., solving Eq. (28) with the unitary transformation U_{ij}^σ that minimizes the total energy. Therefore, we calculate U_{ij}^σ via the iterative procedure proposed in Ref. 54 in every step of

TABLE I. Total energy and components of the electronic energy in rydbergs.

		LDA	KS-KLI	KS-OEP	Garza	LOC-KLI	LOC-OEP
H_4	E_{kin}	3.121	2.877	3.312	3.060	3.102	3.139
	E_{hart}	5.622	5.539	5.666	5.651	5.648	5.655
	E_{xc}	−2.157	−1.939	−2.325	−2.225	−2.247	−2.268
	E_{ion}	−14.102	−13.826	−14.184	−14.062	−14.080	−14.104
	E_{tot}	**−4.272**	**−4.105**	**−4.287**	**−4.332**	**−4.332**	**−4.333**
N_2	E_{kin}	26.785	26.393	27.215	26.910	26.849	26.915
	E_{hart}	55.740	55.489	56.121	56.151	56.042	56.127
	E_{xc}	−9.602	−9.369	−9.903	−10.019	−10.003	−10.025
	E_{ion}	−136.832	−136.245	−137.480	−137.239	−137.139	−137.270
	E_{tot}	**−39.724**	**−39.547**	**−39.861**	**−40.066**	**−40.066**	**−40.067**
CO	E_{kin}	29.114	29.060	29.520	29.365	29.325	29.374
	E_{hart}	57.519	57.597	58.024	58.080	58.003	58.060
	E_{xc}	−9.920	−10.030	−10.222	−10.392	−10.382	−10.400
	E_{ion}	−142.463	−142.471	−143.241	−143.174	−143.067	−143.156
	E_{tot}	**−43.216**	**−43.309**	**−43.383**	**−43.586**	**−43.586**	**−43.587**
H_2O	E_{kin}	24.586	24.754	24.792	25.024	24.977	24.986
	E_{hart}	42.624	42.964	42.976	43.307	43.241	43.233
	E_{xc}	−8.230	−8.351	−8.366	−8.742	−8.728	−8.736
	E_{ion}	−107.138	−107.591	−107.632	−108.124	−108.024	−108.018
	E_{tot}	**−34.203**	**−34.268**	**−34.274**	**−34.580**	**−34.580**	**−34.581**
CH_4	E_{kin}	12.846	12.771	12.808	13.046	13.032	13.063
	E_{hart}	30.715	30.759	30.777	31.042	31.012	31.015
	E_{xc}	−6.232	−6.158	−6.180	−6.666	−6.661	−6.674
	E_{ion}	−72.835	−72.814	−72.850	−73.278	−73.238	−73.262
	E_{tot}	**−16.058**	**−15.994**	**−15.998**	**−16.409**	**−16.409**	**−16.410**

the self-consistent iteration. Now two types of orbitals are involved: the Kohn–Sham orbitals, i.e., eigenfunctions of the Kohn–Sham Hamiltonian, and the localized orbitals, i.e., orbitals that minimize the total energy under the constraint of reproducing the density given by the Kohn–Sham orbitals. Figure 2 shows both types of orbitals for a converged LOC-OEP calculation of the H_4 chain. Note that the Kohn–Sham orbitals are delocalized over all nuclei, whereas the energy-minimizing orbitals are much more localized in space. Comparing the LOC-OEP orbitals with the KS-OEP orbitals in Fig. 1, we find that the LOC-OEP Kohn–Sham orbitals are more localized than those from the KS-KLI calculation, whereas the localized LOC-OEP orbitals are more delocalized than the Kohn–Sham orbitals from the KS-OEP calculation. This observation might be surprising at first sight, but

it is a consequence of self-consistency: Localized orbitals lead to a density that is to a large extent localized at the nuclei. As a consequence of localization, the kinetic and the Hartree energy increase whereas the ion-electron and the exchange-correlation energy decrease. Therefore, the balance of these contributions decides to what extent the Kohn–Sham orbitals are localized. However, the additional localizing transformation in the LOC-OEP approach allows to have a delocalized density that provides for reasonably low kinetic and Hartree energies but localized orbitals that gain a lot of exchange-correlation energy. Table I shows the different energy contributions to the ground-state energies. As expected, the LOC-OEP ground-state energy is noticeably deeper than the KS-OEP energy due to the additional variational freedom. This freedom allows for a more delocalized density and
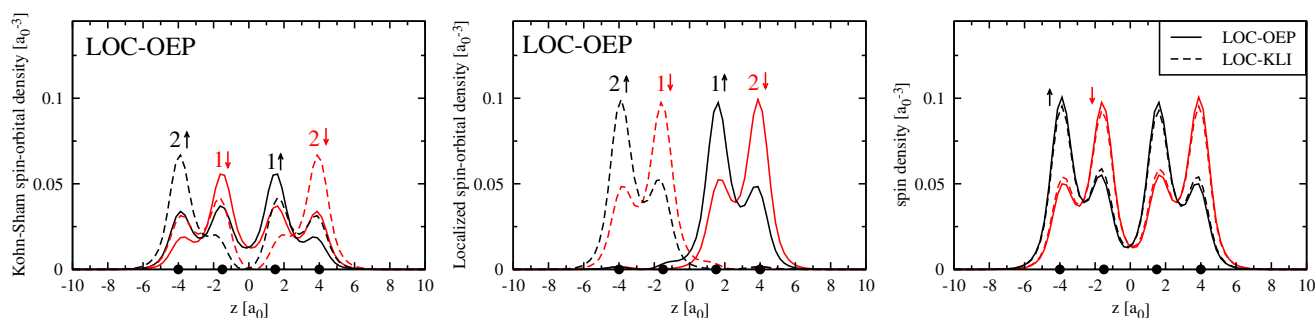
FIG. 2. (Color online) Left: Kohn–Sham spin-orbital densities (i.e., $|\varphi_i|^2$) of H_4 obtained from self-consistent LOC-OEP calculation. Middle: Localized spin-orbital densities (i.e., $|\tilde{\varphi}_i|^2$) for the same calculation. Right: Spin densities from self-consistent LOC-KLI and self-consistent LOC-OEP.

thus a smaller contribution from the kinetic and the Hartree part of the total energy while the exchange-correlation energy is maximized by the unitary transformation of the orbitals. However, in the case of H_4, the unitary transformation [Eq. (21)] does only mix two orbitals per spin direction. Therefore, the additional variational freedom provided by the unitary transformation is limited due to the small number of orbitals. As a consequence, the localized orbitals are less localized than expected.

In summary, the approaches using localizing transformations can be viewed as the search for the "best trade-off" between localized and delocalized orbitals. In contrast, the KS-OEP approach forces the system to decide between extremely localized Kohn–Sham orbitals which yield a large gain in exchange-correlation and external (ionic) energies and completely delocalized Kohn–Sham orbitals that minimize the kinetic and the Hartree energy. The example of the H_4 model system shows that there can be a remarkable shift in ground-state energies by introducing localizing transformations self-consistently, although the variation in the orbitals at a given ground-state density often only has a minor direct effect on the energy.

In this context, it should be mentioned that the KLI approximation to the LOC-OEP, i.e., the LOC-KLI, yields ground-state energies (see Table I) and spin densities (see Fig. 2) close to the ones from the full OEP. This is due to the observation that the localizing transformation acts as an additional driving force for the change in spin symmetry during the self-consistent iteration. Note that both of the approaches working with localizing transformations yield spin-polarized densities that are very similar to the KS-OEP densities from Fig. 1.

In addition we tested Garza's approach,[40] i.e., self-consistently solving Eq. (34) using Foster–Boys orbitals, in order to compare with our method. Table I shows that there is no profound difference in the total energies of Garza's SIC compared to LOC-KLI. Note that all functionals working with localizing transformations yield nearly equal total ground-state energies, but from the fact that the separate contributions to the total energies differ in the different approaches, it is apparent that the ground-state densities in the different approaches are not the same. This behavior might be an indication for a very flat energy landscape, and in our experience this appears to be a typical feature of the SIC.

With the example of the model H_4 chain discussed, we now proceed to real molecules. Table I shows the results of the different SIC schemes for methane, water, carbon monoxide, and the nitrogen molecule. This set of molecules makes for a good testset as it comprises different types of bonding. Obviously, the additional variational freedom of the approaches using localizing transformations consistently leads to a large gain in total energy in the range of 2%–3% when compared to the KS-OEP scheme. In comparison to these energy differences, the deviations in total energy between the different schemes using localizing transformations are negligible. Just like in the example of the hydrogen chain, the large differences in the total energy are caused by the self-consistent inclusion of localization, which leads to noticeable differences in the ground-state densities. Again,

we show the individual contributions to the total energy in order to illustrate this complex behavior. Strikingly, the calculation of the nitrogen molecule shows some of the same features that were observed in the model system H_4. In contrast to the KS-OEP calculation, the KS-KLI energy is substantially higher than the LDA energy. Again, this is due to a change in spin symmetry in the KS-OEP calculation which is not captured by KS-KLI. Interestingly, this break in spin symmetry does not affect all occupied Kohn–Sham orbitals of the nitrogen molecule. Whereas the affected orbitals are spin polarized and distinctly localized, the other orbitals only show minor deviations from standard LDA orbitals. This is an important result as it shows that the H_4 results are not mere artifacts introduced by the simplicity of the model system.

The results for carbon monoxide and water shown in Table I are in line with the expectations: the correction of self-interaction and the additional variational freedom in the approaches using localizing transformations consistently lead to a decrease in the total energy. However, the calculations for methane show a further conspicuity. The total energies of both the KS-KLI and the KS-OEP approach are remarkably higher than the LDA energy. Obviously, methane is another example of a molecule where the self-interaction energy of the LDA exchange-correlation functional is significantly larger than the Hartree self-interaction and thus the correction of Eq. (8) becomes positive. At first sight, this finding seems to contradict the results reported in Ref. 40, where all-electron KS-SIC calculations showed a decrease in the total energy compared to LDA. However, in contrast to our calculations, Garza *et al.* did not include correlation. For comparison with the results of Garza *et al.*, we also did exchange-only LDA calculations on methane and found very good agreement with the all-electron results. The conclusion that follows from this observation is that because of the decrease in the self-interaction energy that is brought about by the LDA correlation, the absolute value of the exchange-correlation energy increases, and it increases to the extent that its self-interaction exceeds the Hartree self-interaction. As a consequence, the SIC correction becomes positive.

The results presented so far underline the importance of the unitary invariance problem for the SIC presented in Eq. (8). The choice of the orbitals with which to construct the OEP significantly influences its properties. Remember that all presented results are for functionals based on LDA that is corrected for self-interaction. However, using different orbital densities in Eq. (8) amounts to defining different functionals. The difference between these functionals lies in the definition of many-electron self-interaction in a density functional treatment. In other words, it is the question of to what extent we can identify orbitals, e.g., the Kohn–Sham orbitals, with electrons. Therefore, the question arises which approach we should buy into. Of course, one might argue that if you feel impelled to identify electrons with some orbitals, the most natural procedure is to choose the Kohn–Sham orbitals. At least they are directly related to the Kohn–Sham eigenvalues whose physical interpretation has been stressed in the literature.[61–63] On the other hand, the presented results make it clear that an approach using the Kohn–Sham orbitals in the

TABLE II. Negative HOMO (ϵ_H) and LUMO (ϵ_L) energies and their difference (gap) in rydbergs compared to experimental IPs and excitation energies (Ref. [66]). Experimental excitation energies refer to final singlet (^{1}) and triplet states (^{3}), respectively.

		LDA	KS-KLI	KS-OEP	Garza	LOC-KLI	LOC-OEP	Expt.
N_2	$-\epsilon_H$	0.77	1.08	1.34	1.33	1.31	1.31	1.14
	$-\epsilon_L$	0.16	0.47	0.66	0.69	0.67	0.64	$\cdots$
	Gap	0.61	0.61	0.68	0.64	0.64	0.67	$0.56^3/0.68^1$
CO	$-\epsilon_H$	0.67	1.09	1.14	1.15	1.15	1.14	1.16
	$-\epsilon_L$	0.16	0.55	0.56	0.62	0.62	0.60	$\cdots$
	Gap	0.51	0.54	0.58	0.53	0.53	0.54	$0.46^3/0.62^1$
H_2O	$-\epsilon_H$	0.54	0.98	0.98	1.10	1.08	1.09	0.92
	$-\epsilon_L$	0.07	0.42	0.44	0.47	0.46	0.45	$\cdots$
	Gap	0.47	0.56	0.54	0.63	0.62	0.64	$0.52^3/0.56^1$
CH_4	$-\epsilon_H$	0.70	1.02	1.07	1.19	1.18	1.18	1.06
	$-\epsilon_L$	0.02	0.32	0.38	0.37	0.36	0.36	$\cdots$
	Gap	0.68	0.70	0.69	0.82	0.82	0.82	$0.80^3/0.82^1$

most rigorous way of defining a single, one-particle potential for Eq. (8), i.e., KS-OEP, does not fully minimize the total energy. In addition, it is well known that the straightforward physical interpretation of Kohn–Sham orbital densities is problematic. Interestingly, this is the original field of application for localizing transformations.[55–57]

Hence, it is to be feared that the only way out is a pragmatic one. Therefore, we compare our calculations to experimental results. Evaluating Janak's theorem [see Eq. (7)],[18] the Kohn–Sham eigenvalue of the HOMO should equal the IP (for the exact functional).[64] Furthermore, the gap energy, i.e., the difference between the HOMO and the lowest unoccupied molecular orbital (LUMO) eigenvalues, should be an approximation to the experimental excitation energy.[60,61] Therefore, we present experimental IPs and excitation energies compared to HOMO and calculated Kohn–Sham gap energies, respectively, in Table II. As expected, the correction of self-interaction improves upon the LDA HOMO energies significantly. However, while the KS-KLI/OEP energies are very close to the experimental IPs for all investigated molecules, the approaches working with localizing transformations seem to overcorrect.

Again, the nitrogen dimer is a case of particular interest. Note the big difference in HOMO energies in the KS-KLI and KS-OEP calculations, which is a direct consequence of the symmetry breaking behavior discussed above. Interestingly, the KS-KLI HOMO is much closer to the IP than the KS-OEP result. However, N_2 is known to be a special case where Hartree–Fock [$-\epsilon_H=1.24$ Ry (Ref. [64])] and exact exchange KLI [$-\epsilon_H=1.28$ Ry (Ref. [64])] yield HOMO energies which are very different from the IP but show an interesting agreement with KS-OEP and the approaches using localizing transformations. The reason for the failure of EXX methods is the importance of static correlation in the triple bonds of the nitrogen molecule. Consequently, semi-local density functionals in which static correlation is mimicked by local exchange[3,65] yield greatly improved results. However, it seems likely that a SIC can destroy this sensitive cancellation of errors. Moreover, it has been argued that there is a close

analogy between EXX and SIC calculations employing localized orbitals.[46,67] Thus, it is plausible that the approaches working with localizing transformations or those leading to substantially localized Kohn–Sham orbitals (such as KS-OEP) are not able to improve upon EXX methods. Therefore, only the fact that the self-consistent KS-KLI calculation does not yield the energy-minimizing density (see Table I and the discussion above) is responsible for the good agreement of its HOMO energy with the experimental IP. In this train of thought, the expected overcorrection of KS-KLI for nitrogen is canceled by its inability to find the true minimum of the total energy. In this light, the good result for the HOMO energy of N_2 that is obtained with KS-KLI looks more like a piece of luck than a piece of systematic physics.

The comparison of the gap energy with experimental excitation energies is less instructive. This is mainly due to the fact that the differences in gap energies between the different SIC approaches are comparable to the differences between experimental singlet and triplet transition energies. Moreover, Kohn–Sham gap energies are not supposed to yield exact excitation energies but only approximations to it. Note that typically, the influence of the unitary transformation on the LUMO is noticeably weaker than its influence on the HOMO. This behavior may have been expected as only the occupied orbitals are accounted for in the unitary transformation.

Summarizing the IP results, it can be said that KS-KLI and KS-OEP show good agreement of the HOMO energies with experimental IPs, whereas the localized SIC approaches seem to overcorrect. However, due to the construction of one local potential for all orbitals, all of the presented SIC approaches do not only correct occupied orbital energies but also unoccupied ones. This is a clear advantage over methods working with orbital-specific potentials.

Finally, we test the generalized OEP approach for a more complex case, i.e., the dissociation of a symmetric two-center three-electron system. This system provides for one of the most striking examples of the failure of common density functionals. Due to their self-interaction error, common func-
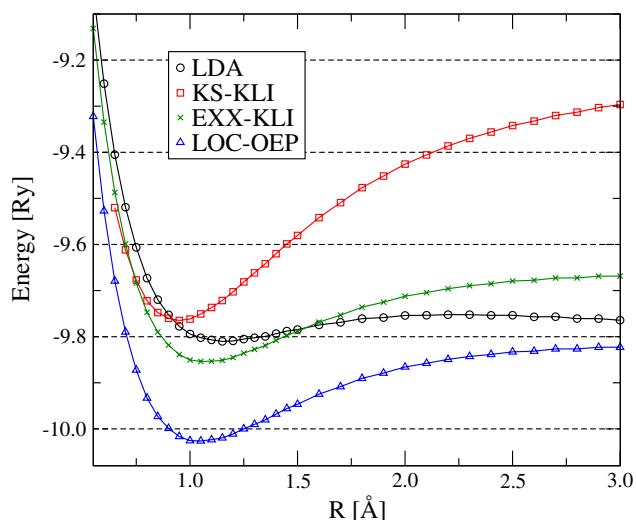
FIG. 3. (Color online) He_2^+ ground-state energy as a function of the internuclear distance R. The energy of the exact nonrelativistic dissociation limit $(R \rightarrow \infty)$ is -9.81 Ry (Ref. 5); the experimental equilibrium bond length is 1.081 Å (Ref. 68).

tionals predict a spurious energy barrier in the dissociation curve at intermediate bond lengths.[69,70] In the course of the discussion of many-electron self-interaction, the ability of functionals to correctly describe the dissociation curves of symmetric charged radicals has recently regained a lot of attention in the literature.[5,16] Figure 3 shows the ground-state energy curve of He_2^+ as computed with LOC-OEP compared to other SIC and non-SIC approaches applying a local potential. As LOC-KLI and Garza's approach both show only minor deviations from LOC-OEP, only the LOC-OEP curve is plotted. LDA shows the well known energy barrier at around 2 Å originating from spurious self-interaction. Not surprisingly, LOC-OEP provides for the lowest total energy of all approaches. Due to the analogy to EXX mentioned above, the LOC-OEP curve deviates from the EXX-KLI curve mainly by a constant shift. This shift originates from the inclusion of local correlation via the LDA functional. This has been tested by calculating a LOC-OEP curve neglecting the local LDA correlation. This curve (not plotted) lies almost on top of EXX-KLI. Note that straightforward KS-KLI provides for a too short bond length and a wrong dissociation limit. This reflects the problems of KS-KLI when applied to molecules, as discussed above. Hence, Fig. 3 impressively demonstrates the importance of consistently including an energy-minimizing unitary transformation in the computation of an OEP for the self-interaction correction of Eq. (8).

VII. CONCLUSION

We have discussed solutions to the problem of finding a single, local Kohn–Sham potential for the SIC proposed by Perdew and Zunger. Two issues have been addressed: the explicit dependence of the Perdew–Zunger energy on the orbitals and its variance under unitary transformation. We developed a generalized OEP scheme that is able to address both problems in one go. We argued that the unitary invariance problem is a direct consequence of the ambiguity in defining self-interaction in a many-electron system. Thus, a

clear and practically applicable definition of many-electron self-interaction on which improved schemes of self-interaction correction can be based is highly desirable. In the presented generalized OEP approach, the just mentioned ambiguity shows up in the pretended arbitrariness of choosing the unitary transformation matrix. In our work, minimizing the energy was used as the criterion to specify the transformation matrix. By presenting full-OEP calculations on a pertinent set of molecules and comparing different SIC schemes, we were able to show that the self-consistent inclusion of a localizing transformation significantly influences the results for the ground-state densities and thus for all electronic properties. Our final conclusion is that although correcting self-interaction in an "orbital-by-orbital" fashion may not lead to the ultimate functional, the OEP based SIC discussed here is an attractive approach incorporating many desirable features into Kohn–Sham DFT.

[1] W. Kohn and L. J. Sham, Phys. Rev. **140**, A1133 (1965).
[2] J. P. Perdew and A. Zunger, Phys. Rev. B **23**, 5048 (1981).
[3] S. Kümmel and L. Kronik, Rev. Mod. Phys. **80**, 3 (2008).
[4] Y. Zhang and W. Yang, J. Chem. Phys. **109**, 2604 (1998).
[5] A. Ruzsinszky, J. P. Perdew, G. I. Csonka, O. A. Vydrov, and G. E. Scuseria, J. Chem. Phys. **126**, 104102 (2007).
[6] K. D. Dobbs and D. A. Dixon, J. Phys. Chem. **98**, 12584 (1994); T. N. Truong and W. Duncan, J. Chem. Phys. **101**, 7408 (1994).
[7] K. Schwarz, Chem. Phys. Lett. **57**, 605 (1978); H. B. Shore, J. H. Rose, and E. Zaremba, Phys. Rev. B **15**, 2858 (1977).
[8] W. M. Temmerman, Z. Szotek, and H. Winter, Phys. Rev. B **47**, 11533 (1993).
[9] S. J. A. van Gisbergen, P. R. T. Schipper, O. V. Gritsenko, E. J. Baerends, J. G. Snijders, B. Champagne, and B. Kirtman, Phys. Rev. Lett. **83**, 694 (1999).
[10] P. Mori-Sánchez, Q. Wu, and W. Yang, J. Chem. Phys. **119**, 11001 (2003).
[11] S. Kümmel, L. Kronik, and J. P. Perdew, Phys. Rev. Lett. **93**, 213002 (2004).
[12] C. Toher, A. Filippetti, S. Sanvito, and K. Burke, Phys. Rev. Lett. **95**, 146402 (2005).
[13] C. Toher and S. Sanvito, Phys. Rev. Lett. **99**, 056801 (2007).
[14] A. Ruzsinszky, J. P. Perdew, G. I. Csonka, O. A. Vydrov, and G. E. Scuseria, J. Chem. Phys. **125**, 194112 (2006).
[15] P. Mori-Sànchez, A. J. Cohen, and W. Yang, J. Chem. Phys. **125**, 201102 (2006).
[16] O. A. Vydrov, E. Scuseria, and J. P. Perdew, J. Chem. Phys. **126**, 154109 (2007).
[17] J. P. Perdew, R. G. Parr, M. Levy, and J. L. Balduz, Phys. Rev. Lett. **49**, 1691 (1982).
[18] J. F. Janak, Phys. Rev. B **18**, 7165 (1978).
[19] J. P. Perdew, Adv. Quantum Chem. **21**, 113 (1990).
[20] A. J. Cohen, P. Mori-Sànchez, and W. Yang, J. Chem. Phys. **126**, 191109 (2007).
[21] J. P. Perdew, A. Ruzsinkszky, G. I. Csonka, O. A. Vydrov, G. E. Scuseria, V. N. Staroverov, and J. Tao, Phys. Rev. A **76**, 040501(R) (2007).

[22] A. Ruzsinszky, J. P. Perdew, G. I. Csonka, G. E. Scuseria, and O. A. Vydrov, Phys. Rev. A **77**, 060502(R) (2008).

[23] It should be mentioned that a vast variety of alternatives to define a self-interaction correction can be found in the literature, e.g., E. Fermi and E. Amaldi, Accad. Ital. Roma **6**, 119 (1934); A. Zunger, Phys. Rev. B **22**, 649 (1980); P. Cortona, Phys. Rev. A **34**, 769 (1986); D. Vogel, P. Krüger, and J. Pollmann, Phys. Rev. B **54**, 5495 (1996); U. Lundin and O. Eriksson, Int. J. Quantum Chem. **81**, 247 (2001); S. Kümmel and J. P. Perdew, Mol. Phys. **101**, 1363 (2002); C. Legrand, E. Suraud, and P.-G. Reinhard, J. Phys. B **35**, 1115 (2002); A. Filippetti and N. A. Spaldin, Phys. Rev. B **67**, 125109 (2003); C. D. Pemmaraju, T. Archer, D. Sánchez-Portal, and V. N. Sanvito, *ibid.* **75**, 045101 (2007). However, a detailed discussion of these approaches is outside the scope of this manuscript.

[24] J. G. Harrison, R. A. Heaton, and C. C. Lin, J. Phys. B **16**, 2079 (1983).

[25] S. Goedecker and C. J. Umrigar, Phys. Rev. A **55**, 1765 (1997).

[26] M. R. Pederson, R. A. Heaton, and C. C. Lin, J. Chem. Phys. **80**, 1972 (1984); **82**, 2688 (1985); M. R. Pederson and C. C. Lin, *ibid.* **88**, 1807 (1988).

[27] A. Svane and O. Gunnarsson, Phys. Rev. Lett. **65**, 1148 (1990).

[28] W. M. Temmerman, H. Winter, Z. Szotek, and A. Svane, Phys. Rev. Lett. **86**, 2435 (2001).

[29] J. Gräfenstein, E. Kraka, and D. Cremer, J. Chem. Phys. **120**, 524 (2004).

[30] O. A. Vydrov and E. Scuseria, J. Chem. Phys. **122**, 184107 (2005).

[31] G. I. Csonka and B. G. Johnson, Theor. Chem. Acc. **99**, 158 (1998).

[32] B. G. Johnson, C. A. Gonzales, P. M. W. Gill, and J. A. Pople, Chem. Phys. Lett. **221**, 100 (1994).

[33] O. A. Vydrov and E. Scuseria, J. Chem. Phys. **121**, 8187 (2004).

[34] O. A. Vydrov, G. E. Scuseria, J. P. Perdew, A. Ruzsinkszky, and G. I. Csonka, J. Chem. Phys. **124**, 094108 (2006).

[35] P. Mori-Sánchez, A. Cohen, and W. Yang, Phys. Rev. Lett. **100**, 146401 (2008).

[36] T. Grabo, T. Kreiblich, S. Kurth, and E. K. U. Gross, in *Strong Coulomb Correlation in Electronic Structure: Beyond the Local Density Approximation*, edited by V. Anisimov (Gordon & Breach, Tokyo, 2000).

[37] J. Chen, J. B. Krieger, Y. Li, G. J. Iafrate, Phys. Rev. A **54**, 3939 (1996).

[38] C. A. Ullrich, P.-G. Reinhard, and E. Suraud, Phys. Rev. A **62**, 053202 (2000).

[39] S.-I. Chu, J. Chem. Phys. **123**, 062207 (2005).

[40] J. Garza, J. A. Nichols, and D. A. Dixon, J. Chem. Phys. **112**, 7880 (2000).

[41] S. Patchkovskii, J. Autschbach, and T. Ziegler, J. Chem. Phys. **115**, 26 (2001).

[42] C. D. Pemmaraju, S. Sanvito, and K. Burke, Phys. Rev. B **77**, 121204(R) (2008).

[43] R. T. Sharp and G. K. Horton, Phys. Rev. **90**, 317 (1953); J. D. Talman and W. F. Shadwick, Phys. Rev. A **14**, 36 (1976).

[44] A. Görling and M. Levy, Phys. Rev. A **50**, 196 (1994).

[45] M. Petersilka, U. J. Gossmann, and E. K. U. Gross, Phys. Rev. Lett. **76**, 1212 (1996); M. E. Casida, in *Recent Developments and Applications in Density Functional Theory*, Theoretical and Computational Chemistry Vol. 4, edited by J. M. Seminario (Elsevier Science, Amsterdam, 1996), p. 391.

[46] T. Körzdörfer, M. Mundt, and S. Kümmel, Phys. Rev. Lett. **100**, 133004 (2008).

[47] S. Kümmel and J. P. Perdew, Phys. Rev. B **68**, 035103 (2003).

[48] S. Kümmel and J. P. Perdew, Phys. Rev. Lett. **90**, 043004 (2003).

[49] J. C. Slater, Phys. Rev. **81**, 385 (1951).

[50] J. B. Krieger, Y. Li, and G. J. Iafrate, Phys. Rev. A **45**, 101 (1992); **46**, 5453 (1992).

[51] O. V. Gritsenko and E. J. Baerends, Phys. Rev. A **64**, 042506 (2001).

[52] F. Della Sala and A. Görling, J. Chem. Phys. **115**, 5718 (2001).

[53] V. N. Staroverov, G. E. Scuseria, and E. R. Davidson, J. Chem. Phys. **125**, 081104 (2006).

[54] E. S. Fois, J. I. Penman, and A. Madden, J. Chem. Phys. **98**, 6352 (1993).

[55] S. F. Boys, Rev. Mod. Phys. **32**, 296 (1960); J. M. Foster and S. F. Boys, *ibid.* **32**, 300 (1960).

[56] C. Edminston and K. Ruedenberg, Rev. Mod. Phys. **35**, 457 (1963).

[57] J. Pipek and P. G. Mezey, J. Chem. Phys. **90**, 4916 (1989).

[58] J. P. Perdew and Y. Wang, Phys. Rev. B **45**, 13244 (1992).

[59] L. Kronik, A. Makmal, M. L. Tiago, M. M. G. Alemany, M. Jain, X. Huang, Y. Saad, and J. R. Chelikowsky, Phys. Status Solidi B **243**, 1063 (2006).

[60] M. Levy, Phys. Rev. A **52**, R4313 (1995).

[61] A. Görling, Phys. Rev. A **54**, 3912 (1996).

[62] D. P. Chong, O. V. Gritsenko, and E. J. Baerends, J. Chem. Phys. **116**, 1760 (2002).

[63] M. Levy, J. P. Perdew, and V. Sahni, Phys. Rev. A **30**, 2745 (1984).

[64] Y.-H. Kim, M. Städele, and R. M. Martin, Phys. Rev. A **60**, 3633 (1999).

[65] M. Ernzerhof, J. P. Perdew, and K. Burke, Int. J. Quantum Chem. **64**, 285 (1997).

[66] A. C. Hurley, *Introduction to the Electronic Theory of Small Molecules* (Academic, London, 1976).

[67] We acknowledge a discussion with R. Car on this subject during the "Safed Summer School on Density functional Theory" in 2007.

[68] J. Xie, B. Poirier, and G. I. Gellene, J. Chem. Phys. **122**, 184310 (2005).

[69] T. Bally and G. N. Sastry, J. Phys. Chem. A **101**, 7923 (1997).

[70] B. Braïda, P. C. Hiberty, and A. Savin, J. Phys. Chem. A **102**, 7872 (1998).

Publication 3

When to trust photoelectron spectra from Kohn-Sham eigenvalues: The case of organic semiconductors

T. Körzdörfer[1], S. Kümmel[1], N. Marom[2], and L. Kronik[2]

[1]*Physics Institute, University of Bayreuth, D-95440 Bayreuth, Germany*
[2]*Department of Materials and Interfaces, Weizmann Institute of Science, Rehovoth 76100, Israel*

Abstract

The combination of photoelectron spectroscopy and density functional theory is an important technique for clarifying a material's electronic structure. So far, however, it has been difficult to predict when the spectrum of occupied Kohn-Sham eigenvalues obtained from commonly used (semi-)local functionals bears physical relevance and when not. We demonstrate that a simple criterion based on evaluating each orbital's self-interaction allows prediction of the physical reliability of the eigenvalue spectrum. We further show that a self-interaction correction significantly improves the interpretability of eigenvalues also in difficult cases such as organic semiconductors where (semi-)local functionals fail.

When to trust photoelectron spectra from Kohn-Sham eigenvalues: The case of organic semiconductors

T. Körzdörfer and S. Kümmel
Physikalisches Institut, Universität Bayreuth, D-95440 Bayreuth, Germany

N. Marom and L. Kronik
Department of Materials and Interfaces, Weizmann Institute of Science, Rehovoth 76100, Israel
(Received 23 April 2009; published 26 May 2009)

The combination of photoelectron spectroscopy and density functional theory is an important technique for clarifying a material's electronic structure. So far, however, it has been difficult to predict when the spectrum of occupied Kohn-Sham eigenvalues obtained from commonly used (semi-)local functionals bears physical relevance and when not. We demonstrate that a simple criterion based on evaluating each orbital's self-interaction allows prediction of the physical reliability of the eigenvalue spectrum. We further show that a self-interaction correction significantly improves the interpretability of eigenvalues also in difficult cases such as organic semiconductors where (semi-)local functionals fail.

PACS number(s): 61.46.−w, 33.60.+q, 31.15.es

Photoelectron spectroscopy has emerged as one of the most important techniques for clarifying the electronic structure of molecules and solids. It plays a particularly important role in nanophysics and interface problems where other methods of determining a material's electronic structure are often hard to apply. Typically, such measurements are complemented by density functional theory (DFT)-based electronic structure calculations. The combination of experiment and theory then frequently allows to gain far-reaching physical insight, and this type of approach has been used very successfully in the past, as exemplified for finite systems by Refs. 1–7.

However, on the theoretical side this concept suffers from the fact that Kohn-Sham eigenvalues are frequently, but not always, good approximations to electron removal energies. Moreover, for some systems the eigenvalue spectrum changes a lot when going from one type of exchange-correlation potential (v_{xc}) to another. Important examples in this respect that are of great fundamental and practical interest are molecules used in organic electronics, e.g., Refs. 8–20. This limits the practical usefulness of interpreting Kohn-Sham eigenvalues because when discrepancies with experiment are observed, one does not know whether they are "real"[21] or just a reflection of the shortcomings of the employed density functional approximation.

Importantly, although Kohn-Sham eigenvalues are not exact quasiparticle excitation energies, the physical interpretation of Kohn-Sham eigenvalues does have a sound theoretical basis and is not coincidental. Interpreting the occupied eigenvalues is not to be confused with the notorious "bandgap problem,"[22] and it is a well-established fact that eigenvalues of energetically high-lying occupied orbitals, to which we restrict our analysis, are good approximations to electron removal energies when computed from a high-quality v_{xc}.[22–27] The pressing question is, then, when a practically used v_{xc} approximation leads to Kohn-Sham eigenvalues that can be trusted.

In this Rapid Communication we demonstrate that orbital self-interaction enters the structure of the occupied Kohn-Sham spectrum as a decisive factor. When different orbitals have significantly different spatial character, e.g., localized vs delocalized, their eigenvalues can carry largely different self-interaction errors (SIEs). In such cases the occupied Kohn-Sham eigenvalue spectrum no longer reflects the physical electron binding. We propose a simple test that does not predict the correct spectrum but can serve as a warning against possible misinterpretation of the occupied Kohn-Sham spectrum. We demonstrate that a parameter-free self-interaction correction (SIC) implemented rigorously within the Kohn-Sham framework[28] yields physically interpretable eigenvalues also in cases where (semi-)local approximations fail. Finally, we suggest a shortcut to approximately incorporate the effects of the SIC without the need to actually go through a SIC calculation.

Figure 1 exemplifies the typical problem that we have in mind. The bottom curve shows the experimental photoelectron spectrum of the 3,4,9,10-perylene tetracarboxylic dianhydride (PTCDA) molecule,[9] which is a paradigm system in the field of organic semiconductors.[8] The top curve shows the occupied eigenvalues obtained from a local density approximation (LDA) calculation in the typically used density-of-states (DOS) interpretation: the eigenvalues are convoluted with a Gaussian and shifted to compensate for the wrong intrinsic asymptotics of the LDA potential.[2,4] For ease of comparison we align all spectra in this Rapid Communication such that the highest-occupied molecular orbital (HOMO) energies match. Although this type of procedure leads to very good agreement with experiment for many systems it fails badly for PTCDA. The second peak of the LDA spectrum is right where the experimental spectrum shows a pronounced gap between the HOMO and the HOMO-1 peak. Using a generalized gradient approximation (GGA) functional hardly changes the picture. This is disconcerting because this part of the spectrum is weakly bound and effects that make the eigenvalue interpretation doubtful for energetically deep lying states[27] are unimportant. It is also puzzling from the perspective that the geometry of PTCDA is well described by (semi-)local functionals, which could lead one to expect an overall correct description.
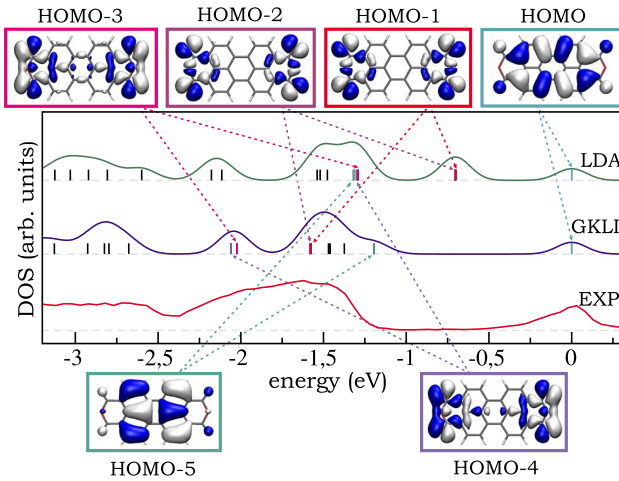
FIG. 1. (Color online) Simulated and measured photoemission spectra of PTCDA. From top to bottom: isosurface plots of Kohn-Sham orbitals (labels HOMO, HOMO-1, etc., refer to the LDA ordering), Kohn-Sham eigenvalues broadened by 0.1 eV for LDA and GKLI, and gas phase experimental data from Ref. 9. Note that the experiment shows a pronounced gap between the HOMO and the HOMO-1 peaks that is reproduced by the GKLI spectrum but not by the LDA one.

By employing the *GW* method or by resorting to hybrid functionals that incorporate empirical parameters, one can obtain a theoretical spectrum that does reproduce the experimental HOMO-HOMO-1 gap[9] but at the price of a tremendously increased computational effort or at the price of an increased computational effort *and* additional parameters that may hinder performance for other systems,[29] respectively. Therefore, from a practical point of view it would be extremely helpful to (i) have a criterion that signals whether the approximative interpretation of the Kohn-Sham eigenvalues is justified for a given system and v_{xc} approximation and (ii) have a method to obtain physically reliable eigenvalues in cases where approximations such as LDA and GGAs fail. Both are presented below.

The desired *a priori* knowledge about the reliability of the Kohn-Sham eigenvalue spectrum, e.g., as obtained with LDA, can be gained simply by evaluating each orbital's SIE,

$$e_i = \langle \varphi_i | v_H[|\varphi_i|^2] | \varphi_i \rangle + \langle \varphi_i | v_{xc}[|\varphi_i|^2, 0] | \varphi_i \rangle. \quad (1)$$

Here, $v_{xc}[|\varphi_i|^2, 0]$ denotes the approximate expression for the (spin-polarized) exchange-correlation potential, in our case LDA, evaluated with the corresponding Kohn-Sham orbital density $|\varphi_i|^2$. v_H is the corresponding Hartree potential. Equation (1) is the change one expects in the ith eigenvalue from first-order perturbation theory when one applies a self-interaction correction.[30]

Self-interaction is one of the most prominent problems in present-day DFT (Ref. 22) and was identified as a fundamental difficulty early on.[30] For the unknown exact exchange-correlation energy functional, the SIE defined in Eq. (1) must vanish when the potentials are evaluated on a one-electron density.[28,30] Since every Kohn-Sham orbital density has the structure of a one-electron density, Eq. (1) should vanish in
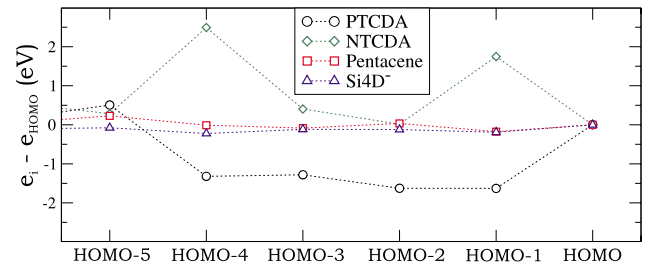
FIG. 2. (Color online) Orbital self-interaction e_i for the least bound LDA orbitals of PTCDA, NTCDA, pentacene, and Si_4D^- relative to the respective e_{HOMO}. Dashed lines are a guide to the eye.

exact DFT. However, it is nonzero when an approximation such as LDA or GGA is employed. Thus, every Kohn-Sham orbital's eigenvalue will be offset to some extent due to orbital self-interaction. In terms of a photoelectron interpretation this need not be a problem if all orbitals suffer from roughly the same amount of SIE because then all occupied eigenvalues will be offset by roughly the same value and the structure of the spectrum will be preserved. However, if a system consists of orbitals, wherein some carry large self-interaction and others little, then the SIE will distort the spectrum and it will no longer reflect the physical nature of the electronic binding.

That orbital self-interaction is indeed a reason for the disagreement seen for PTCDA becomes clear from Fig. 2. It shows $e_i - e_{HOMO}$, i.e., the self-interaction error of each orbital relative to the one of the system's HOMO, evaluated for the highest LDA Kohn-Sham orbitals for four different systems. This relative error is the quantity relevant for the usual comparison to experiment in which the HOMO peaks are aligned. First focusing on the black circles denoting the results for PTCDA, it is evident that the orbitals from HOMO-1 to HOMO-4 carry much larger self-interaction than, e.g., HOMO and HOMO-5. Figure 1 depicts these orbitals and indicates which peak in the DOS interpretation is associated with them. HOMO-1 and HOMO-2 are the orbitals whose eigenvalues lie where the experiment shows a pronounced gap in the spectrum.

In order to check whether this finding is coincidental or systematic we have repeated the analysis for other systems. With Si_4D^- and pentacene we have chosen two very different systems—but for both it is known that the eigenvalues from (semi-)local functionals can quite reasonably be compared to experiment.[4,16,31] Figure 2 reveals that this is in agreement with the e_i analysis: for both systems (and for other clusters that are not shown here and for which LDA also yields a reasonable DOS), all of the high-lying orbitals carry very similar SIE. Thus, we note as a first important result that Eq. (1) can be used to warn against possible misinterpretation of occupied Kohn-Sham eigenvalues.

One may wonder why e_i varies strongly over the orbitals for some systems and hardly varies for others. In a nutshell, the answer is that in systems in which the high-lying occupied orbitals all have a similar spatial structure, they typically also carry similar self-interaction. Returning to the example of PTCDA depicted in Fig. 1 we see that here different
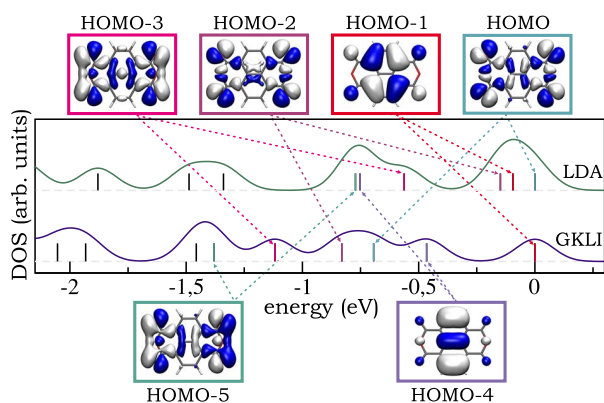
FIG. 3. (Color online) DOS plots for NTCDA from occupied Kohn-Sham eigenvalues as obtained in LDA and GKLI, and isosurface plots of Kohn-Sham orbitals as in Fig. 1. Again, GKLI opens a gap between HOMO and HOMO-1 that is not seen with the LDA.

orbitals have a rather different spatial structure: HOMO and HOMO-5 lead to probability densities that are delocalized over the entire molecule, whereas the other shown orbitals correspond to densities on the anhydride (side) groups. Thus, the observation of largely different e_i can be rationalized by the fact that self-interaction is related to localization.[30,32]

With self-interaction thus identified as a main source of error, the following question arises: what should one do once one has realized through the above analysis that orbital self-interaction is likely to distort the occupied Kohn-Sham spectrum for the system of interest? In view of the above findings it is a natural idea to resort to a density functional which reduces self-interaction. A first-principles parameter-free approach to achieve this is the SIC.[30] It can rigorously be brought under the umbrella of Kohn-Sham theory in the generalized optimized effective potential (GOEP) approach,[28] which includes energy-minimizing orbital transformations in the self-consistent iteration. Therefore, the Krieger-Li-Iafrate (KLI) approximation made to the GOEP (called GKLI) is reliable, whereas the KLI approximation made to the usual optimized effective potential (OEP) equation for the SIC is not.[33] As the SIC approach does include correlation and only requires evaluation of the self-exchange integrals, it is an attractive alternative to pure exact exchange or hybrid functional methods. The middle part of Fig. 1 shows the spectrum of occupied Kohn-Sham eigenvalues obtained using the GKLI approach. As one can see from the relation between the orbitals and their corresponding eigenvalues, the GKLI spectrum corrects the failure of LDA, opening a gap between HOMO and HOMO-1 that corresponds well to the experimentally observed gap.

The data shown in Figs. 2 and 3 for 1,4,5,8-naphthalene tetracarboxylic dianhydride (NTCDA) confirm that the relation between orbital structure and eigenvalue correction is not coincidental. Similar to PTCDA there are orbitals of different spatial structure, and again, switching from LDA to GKLI opens a gap between HOMO and HOMO-1. We also verified that the SIC has practically no effect on the spectrum of pentacene and Si_4D^-. Thus, we have arrived at a second important result: A self-interaction free approach can yield physically interpretable occupied eigenvalues also in cases where (semi-)local functionals fail.
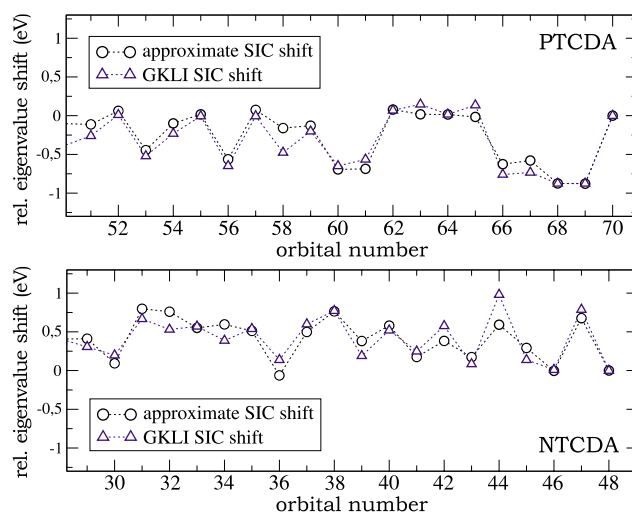

FIG. 4. (Color online) Orbital shift relative to the shift for the HOMO as obtained from the GKLI calculation (blue triangles) and Eq. (2) (black circles) for PTCDA (top) and NTCDA (bottom). The HOMO is orbital number 70 (top) or 48 (bottom), respectively.

Finally, the results so far beg an obvious question: having realized that the problem of physically meaningful eigenvalues is closely related to SIE and orbital structure, can one estimate the effect that the SIC will have on the occupied eigenvalues without actually having to go through a full SIC calculation? The answer is yes. Estimating the Hartree and LDA exchange contributions while neglecting the difference between SI-corrected and uncorrected orbitals as in Refs. 30 and 34, but additionally taking into account LDA correlation, one can estimate (using atomic units) the self-interaction corrected eigenvalue purely from LDA quantities by

$$\varepsilon_i^{\mathrm{est}} = \varepsilon_i^{\mathrm{LDA}} - 0.94 \int (|\varphi_i|^2)^{4/3} d^3r - \langle \varphi_i | v_c^{\mathrm{LDA}}[|\varphi_i|^2, 0] | \varphi_i \rangle.$$

(2)

Figure 4 compares the shift of the GKLI eigenvalues relative to the GKLI shift for the HOMO, i.e., $(\varepsilon_i^{\mathrm{GKLI}} - \varepsilon_i^{\mathrm{GKLI}}) - (\varepsilon_{\mathrm{HOMO}}^{\mathrm{GKLI}} - \varepsilon_{\mathrm{HOMO}}^{\mathrm{GKLI}})$ to the same relative shift evaluated with the estimated eigenvalues, i.e., $(\varepsilon_i^{\mathrm{est}} - \varepsilon_i^{\mathrm{LDA}}) - (\varepsilon_{\mathrm{HOMO}}^{\mathrm{est}} - \varepsilon_{\mathrm{HOMO}}^{\mathrm{LDA}})$. Again, this relative shift is the quantity relevant for the usual comparison to experiment. In view of the simplicity of Eq. (2) which can be evaluated straightforwardly based on the ingredients of a standard LDA code, the approximation works well. Thus, our third result is that via Eq. (2) one can obtain an estimate of the effects that SIC will have on the occupied eigenvalues with very little computational effort.

In summary, we have shown that orbital self-interaction is decisive for the interpretability of the occupied Kohn-Sham spectrum as a DOS as measured in photoelectron spectroscopy. It can serve as a transparent criterion to judge the interpretability of the occupied Kohn-Sham spectrum. A self-

interaction correction implemented within the Kohn-Sham framework can yield reliable spectra also in such cases where (semi-)local density functionals fail, and its effect on the eigenvalues can be estimated with little effort. These findings extend the range of systems for which reliable predictions can be made, as demonstrated here for prototypical organic semiconductor molecules.

[1] N. Binggeli and J. R. Chelikowsky, Phys. Rev. Lett. **75**, 493 (1995); J. Muller, B. Liu, A. A. Shvartsburg, S. Ogut, J. R. Chelikowsky, K. W. Michael Siu, K. M. Ho, and G. Gantefor, *ibid.* **85**, 1666 (2000).

[2] J. Akola, M. Manninen, H. Häkkinen, U. Landman, X. Li, and L.-S. Wang, Phys. Rev. B **62**, 13216 (2000).

[3] S. N. Khanna, M. Beltran, and P. Jena, Phys. Rev. B **64**, 235419 (2001).

[4] L. Kronik *et al.*, Nature Mater. **1**, 49 (2002); Eur. Phys. J. D **24**, 33 (2003).

[5] N. Bertram, Y. D. Kim, G. Ganteför, Q. Sun, P. Jena, J. Tamuliene, and G. Seifert, Chem. Phys. Lett. **396**, 341 (2004).

[6] H. Häkkinen, M. Moseler, O. Kostko, N. Morgner, M. A. Hoffmann, and B. v. Issendorff, Phys. Rev. Lett. **93**, 093401 (2004).

[7] G. Tu, V. Carravetta, O. Vahtras, and H. Agren, J. Chem. Phys. **127**, 174110 (2007).

[8] E. Umbach and R. Fink, in *Proceedings of the International School of Physics "Enrico Fermi,"* edited by V. M. Agrenovich and G. C. La Rocca (IOS Press, Amsterdam, 2002), p. 233.

[9] N. Dori, M. Menon, L. Kilian, M. Sokolowski, L. Kronik, and E. Umbach, Phys. Rev. B **73**, 195208 (2006).

[10] G. Heimel, L. Romaner, J.-L. Brédas, and E. Zojer, Surf. Sci. **600**, 4548 (2006).

[11] N. Marom, O. Hod, G. E. Scuseria, and L. Kronik, J. Chem. Phys. **128**, 164107 (2008); N. Marom, O. Hod, G. E. Scuseria, and L. Kronik, Appl. Phys. A **95**, 159 (2009); **95**, 165 (2009).

[12] C. Risko, C. D. Zangmeister, Y. Yao, T. J. Marks, J. M. Tour, M. A. Ratner, and R. D. van Zee, J. Phys. Chem. C **112**, 13215 (2008).

[13] S. Yanagisawa and Y. Morikawa, Chem. Phys. Lett. **420**, 523 (2006).

[14] M. Rohlfing, R. Temirov, and F. S. Tautz, Phys. Rev. B **76**, 115421 (2007).

[15] M. L. Tiago, J. E. Northrup, and S. G. Louie, Phys. Rev. B **67**, 115212 (2003).

[16] K. Hummer and C. Ambrosch-Draxl, Phys. Rev. B **72**, 205205 (2005).

[17] S. Kera, H. Yamane, H. Fukagawa, T. Hanatani, K. K. Okudaira, K. Seki, and N. Ueno, J. Electron Spectrosc. Relat. Phenom. **156-158**, 135 (2007).

[18] X. Zhan, C. Risko, F. Amy, C. Chan, W. Zhao, S. Barlow, A. Kahn, J.-L. Brédas, and S. R. Marder, J. Am. Chem. Soc. **127**, 9021 (2005).

[19] H. Vázquez, R. Oszwaldowski, P. Pou, J. Ortega, R. Pérez, F. Flores, and A. Kahn, Europhys. Lett. **65**, 802 (2004).

[20] S. Duhm, G. Heimel, I. Salzmann, H. Glowatzki, R. L. Johnson, A. Vollmer, J. P. Rabe, and N. Koch, Nature Mater. **7**, 326 (2008).

[21] "Real" differences may arise from systematic deviations between Kohn-Sham eigenvalues and quasiparticle excitation energies, e.g., for deep lying (Ref. 27) or strongly coupled excitations (Ref. 35), from matrix element effects, or other experimental intricacies.

[22] S. Kümmel and L. Kronik, Rev. Mod. Phys. **80**, 3 (2008).

[23] J. F. Janak, Phys. Rev. B **18**, 7165 (1978).

[24] M. Levy, J. P. Perdew, and V. Sahni, Phys. Rev. A **30**, 2745 (1984); C.-O. Almbladh and U. von Barth, Phys. Rev. B **31**, 3231 (1985).

[25] A. Görling, Phys. Rev. A **54**, 3912 (1996).

[26] C. Filippi, C. J. Umrigar, and X. Gonze, J. Chem. Phys. **107**, 9994 (1997).

[27] D. P. Chong, O. V. Gritsenko, and E. J. Baerends, J. Chem. Phys. **116**, 1760 (2002).

[28] T. Körzdörfer, S. Kümmel, and M. Mundt, J. Chem. Phys. **129**, 014110 (2008). Computational details of our approach can be found in this paper.

[29] J. Paier, M. Marsman, and G. Kresse, J. Chem. Phys. **127**, 024103 (2007).

[30] J. P. Perdew and A. Zunger, Phys. Rev. B **23**, 5048 (1981).

[31] H. Fukagawa, H. Yamane, T. Kataoka, S. Kera, M. Nakamura, K. Kudo, and N. Ueno, Phys. Rev. B **73**, 245310 (2006); O. McDonald *et al.*, Surf. Sci. **600**, 3217 (2006); M. L. M. Rocco *et al.*, J. Chem. Phys. **129**, 074702 (2008).

[32] A study quantifying the amount of localization and its relation to e_i will be presented elsewhere.

[33] T. Körzdörfer, M. Mundt, and S. Kümmel, Phys. Rev. Lett. **100**, 133004 (2008).

[34] R. S. Gadre, L. J. Bartolotti, and N. C. Handy, J. Chem. Phys. **72**, 1034 (1980).

[35] M. Mundt and S. Kümmel, Phys. Rev. B **76**, 035413 (2007); M. Walter and H. Häkkinnen, New J. Phys. **10**, 043018 (2008).

Publication 4

Fluorescence quenching in an organic donor-acceptor dyad: A first principles study

T. Körzdörfer[1], S. Tretiak[2], and S. Kümmel[1]

[1]*Physics Institute, University of Bayreuth, D-95440 Bayreuth, Germany*
[2]*Theoretical Division, Center for Nonlinear Studies (CNLS) and Center for Integrated Nanotechnologies (CINT), Los Alamos National Laboratory, Los Alamos, New Mexico 87545, USA*

ABSTRACT

Perylene bisimide and triphenyl diamine are prototypical organic dyes frequently used in organic solar cells and light emitting devices. Recent Förster-resonant-energy-transfer experiments on a bridged organic dyad consisting of triphenyl diamine as an energy-donor and perylene bisimide as an energy-acceptor revealed a strong fluorescence quenching on the perylene bisimide. This quenching is absent in a solution of free donors and acceptors and thus attributed to the presence of the saturated $CH_2O(CH_2)_{12}$-bridge. We investigate the cause of the fluorescence quenching as well as the special role of the covalently bound bridge by means of time dependent density functional theory and molecular dynamics. The conformational dynamics of the bridged system leads to a charge transfer process between donor and acceptor that causes the acceptor fluorescence quenching.

Fluorescence quenching in an organic donor-acceptor dyad: A first principles study

T. Körzdörfer,[1,a)] S. Tretiak,[2] and S. Kümmel[1]

[1]*Physics Institute, University of Bayreuth, D-95440 Bayreuth, Germany*
[2]*Theoretical Division, Center for Nonlinear Studies (CNLS) and Center for Integrated Nanotechnologies (CINT), Los Alamos National Laboratory, Los Alamos, New Mexico 87545, USA*

Perylene bisimide and triphenyl diamine are prototypical organic dyes frequently used in organic solar cells and light emitting devices. Recent Förster-resonant-energy-transfer experiments on a bridged organic dyad consisting of triphenyl diamine as an energy-donor and perylene bisimide as an energy-acceptor revealed a strong fluorescence quenching on the perylene bisimide. This quenching is absent in a solution of free donors and acceptors and thus attributed to the presence of the saturated $CH_2O(CH_2)_{12}$-bridge. We investigate the cause of the fluorescence quenching as well as the special role of the covalently bound bridge by means of time dependent density functional theory and molecular dynamics. The conformational dynamics of the bridged system leads to a charge transfer process between donor and acceptor that causes the acceptor fluorescence quenching. © *2009 American Institute of Physics.* [DOI: 10.1063/1.3160666]

I. INTRODUCTION

Photoinduced transfer of electronic excitation energy and charges are among the most prominent phenomena both in biology, e.g., in photosynthesis, and in modern material science, e.g., in organic solar cells or light emitting diodes. In the past decades, considerable progress has been made in the understanding of energy and charge transfer processes. Hopes are high that a better understanding will allow one to improve the efficiency of organic photovoltaics (see Refs. 1–4 for an overview). In many investigations, especially tailored model systems based on π-conjugated organic molecules play a prominent role. Examples are molecular switches,[5] light harvesting systems,[6] dendrimers[7] and self-organized polymers[8] based on perylene dyes, J-aggregates,[9] and organic donor-bridge-acceptor (DBA) systems.[10–12]

Among the most prominent organic compounds used in these model systems, as well as in current applications are the π-conjugated dyes perylene bisimide (PTCDI) and triphenyldiamine (TPD) (see Fig. 1). PTCDI is a thermally and photochemically stable organic semiconductor that grows highly ordered thin films on different inorganic substrates and has been incorporated in a variety of electronic devices such as organic field-effect transistors[13] or photovoltaics.[14] TPD is widely used in hole transport layers of photoelectronic devices[15] due to its good hole injection and mobility characteristics. Furthermore, both PTCDI and TPD show strong fluorescence in the visible range[12] and the emission spectrum of TPD overlaps with the absorption spectrum of PTCDI. Thus, TPD and PTCDI are an ideal pair to study resonant excitation energy transfer.

Following this line of thought, a DBA system consisting of TPD (D) as an energy-donor and PTCDI (A) as an energy acceptor linked by a saturated and flexible $CH_2O(CH_2)_{12}$-bridge (B) has recently been synthesized[11] and studied[12] as a model system for excitation energy transfer. Making use of time-resolved and fluorescence emission spectroscopy this study revealed an efficient photoinduced energy transfer from D to A. However, simultaneously a strong quenching of the A-fluorescence was found. As this quenching is absent in a solution of free donors and acceptors, it is obviously attributed to the presence of the saturated bridge. The aim of this manuscript is to clarify the role of the saturated bridge in the quenching process by means of time-dependent density functional theory (TDDFT) and molecular dynamics (MD).

To this end, our manuscript is organized as follows: after a short introduction to the experimental observations, we summarize the used methods in Sec. III. In Sec. IV we present and discuss our results before concluding in Sec. V.

II. THE EXPERIMENT

In the following we introduce the experimental results as far as this is necessary to follow the upcoming discussion. Details can be found in the original publication.[12] The
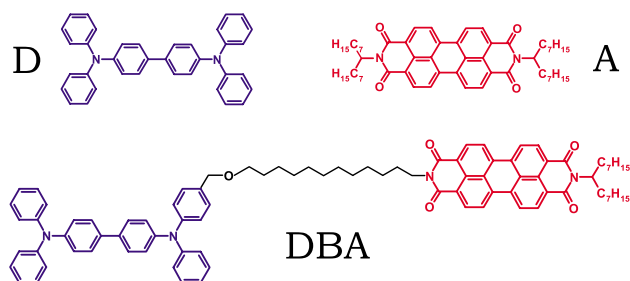

FIG. 1. The investigated materials: TPD (D): N,N'-Bis(3-methylphenyl)-N,N'-bis(phenyl)benzidine, PTCDI (A): 2,9-Bis-(1-heptyl-octyl)-anthra-[2,1,9-def; 6,5,10-$d'e'f'$]-diisochinoline-1,3,8,10-tetraone, DBA molecule: 9-[12-N-(4-benzyloxy)-N,N',N'-triphenyl benzidinedodecyl]-2-(1-hepty-loctyl)-anthra-[2,1,9-def;6,5,10-$d'e'f'$]-diisochinoline-1,3,8,10-tetraone.

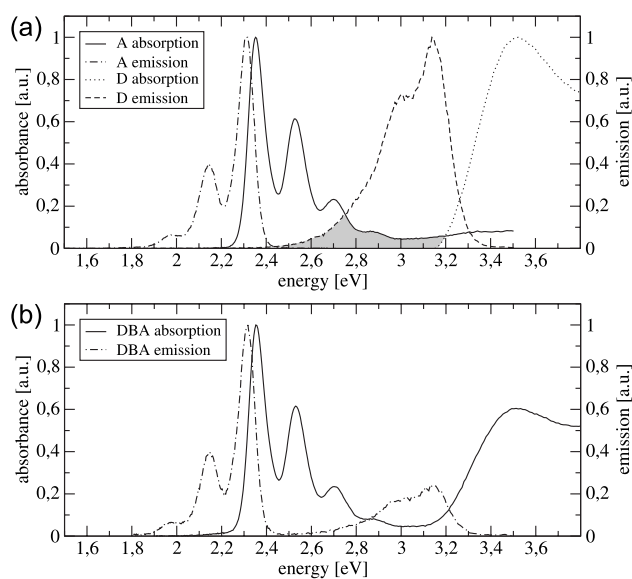a)Electronic mail: thomas.koerzdoerfer@uni-bayreuth.de.

FIG. 2. (a) Absorption and emission spectra of D and A in toluene. (b) Absorption and emission spectra of DBA in toluene. The emission spectrum of DBA has been excited at 3.5 eV (Ref. 17).

system under investigation is the DBA molecule 9-[12-N-(4-benzyloxy)-N,N',N'-triphenyl benzidine-dodecyl]-2-(1-heptyloctyl)-anthra-[2,1,9-def;6,5,10-$d'e'f'$]-diisochinoline-1,3,8,10-tetraone (see Fig. 1), which we will abbreviate as DBA in the following. Initially, D and A were dissolved separately in toluene and investigated via fluorescence spectroscopy. Figure 2(a) shows the absorption and emission spectra of D and A. After chemically linking D and A with the $CH_2O(CH_2)_{12}$-bridge and dissolving the resulting DBA in toluene the absorption spectrum shown in Fig. 2(b) is measured. In addition, Fig. 2(b) provides the emission spectrum of DBA as induced by an excitation at 3.5 eV, i.e., at the absorption energy of D. Obviously, the excitation of D is followed by an efficient excitation energy transfer to A. Thus, the resulting DBA emission spectrum appears as a superposition of the D and A emission spectra. Apart from this, the saturated bridge has only minor effects on the position of the absorption and emission energies.

The decay rates k_D and k_A of D and A, respectively, are provided in Table I. The energy transfer in DBA and in a solution of free donors and acceptors (D+A) leads to an increase in the measured decay rate k_D^{DBA} of D in DBA, i.e.,

$$k_D^{DBA} = k_D + k_{ET}. \qquad (1)$$

Thus, the energy transfer rate k_{ET} can be determined by measuring k_D and k_D^{DBA}. Utilizing k_{ET} in the standard Förster-

TABLE I. Experimental fluorescence energies and decay rates of D, A, D+A (at concentrations c_D=2.3 mM and c_A=6.2 mM) and DBA in toluene as provided in Ref. 12; energies are taken at the maxima of the emission spectra; exp. k_D in DBA is on the edge of the instrument response threshold.

	E_D (eV)	k_D (1/ns)	E_A (eV)	k_A (1/ns)
D	3.1	1.18	$\cdots$	$\cdots$
A	$\cdots$	$\cdots$	2.3	0.25
D+A	3.1	1.75	2.3	0.25
DBA	3.1	>12.5	2.3	0.59

resonant-energy-transfer (FRET)-methodology, the authors of Ref. 12 derive a D-A distance in DBA that corresponds to a fully stretched conformation of the bridge.

Note that Table I reveals evidence on other electronic processes in the system. The substantial increase in the decay rate k_A^{DBA} of A in DBA as compared to free A indicates an efficient quenching process. From

$$k_A^{DBA} = k_A + k_Q, \qquad (2)$$

one finds a quenching rate k_Q of 0.33 1/ns. This finding reveals the presence of an additional nonradiative decay channel in the bridged system. In contrast to the energy transfer process [see. Eq. (1)], this decay channel is absent in a solution of free donors and acceptors. Furthermore, it occurs independently of the energy transfer passage, i.e., the quenching can also be observed if one excites DBA directly at the A absorption.

A possible and frequently invoked explanation for fluorescence quenching in this type of systems is charge transfer. A charge transfer coupling between D and A could be caused either by a superexchange coupling through the saturated bridge (see e.g., Refs. 1, 2, and 16 for an overview of the superexchange formalism) or by a collapse of the bridge in solution that leads to orbital overlap of D and A. As for the former, a superexchange coupling as strong as the one observed here would be quite unusual considering the length of the $CH_2O(CH_2)_{12}$-bridge. Our DFT calculations described below address questions of electronic coupling insofar as they give detailed insight into the electronic properties of the DBA-system. As for the latter, it must be noted that a collapse of the bridge in solution seems to contradict the findings of Ref. 12 concerning the distance between D and A. The derivation of this distance however is based on the FRET-methodology, i.e., D and A are approximated as interacting point dipoles. Higher order multipoles as well as electronic and vibrational couplings of D, B, and A are completely neglected. Depending on the particularities of the investigated system, these approximations can influence the distance-dependence of the energy-transfer rate significantly.[18] Therefore, distances derived by using standard FRET-methodology can either be over- or underestimated. As a consequence, the D-A distance derived in Ref. 12 may not be trustworthy. However, if the hydrocarbon bridge folds so that D and A couple electronically, one would expect this coupling to have a significant influence on the measured DBA-spectra, e.g., similar to the situation found for the PTCDI dimer whose spectrum shows strong deviations from the monomer spectrum due to orbital overlap.[19] Yet Fig. 2 demonstrates that this is not the case.

Summing up these observations one can only conclude that the information from the fluorescence spectroscopy measurements is not conclusive. A theoretical analysis can shed light on these findings. Therefore a detailed study of the role of the bridge in the observed fluorescence quenching by means of DFT, TDDFT, and MD is the aim of this manuscript.

III. METHODOLOGY

Quantum chemical calculations are performed using the linear-response TDDFT formalism as implemented in the TURBOMOLE v5.10 (Ref. 20) and GAUSSIAN03 (Ref. 21) program packages. Ground state molecular geometries of D, A, and DBA are obtained from TURBOMOLE geometry optimization[22] employing an empirical dispersion correction.[23] Unless otherwise noted, all DFT and TDDFT calculations make use of the B3LYP functional[24] and an SVP basis set.[25] No symmetries are enforced. Solution effects are simulated using COSMO.[26,27] The natural transition orbitals (NTO) approach[28] is used to identify and visualize electronic excitations. MD calculations are performed using the TINKER program package[29] and the MM3 force field.[30] Pre- and post-processing operations are performed with the help of VIEW-MOL (Ref. 31) and VMD.[32]

IV. RESULTS AND DISCUSSION

We start our computational analysis by calculating the ground-state geometrical structures and Kohn–Sham (KS) eigenvalue spectra of D and A using DFT. Unless otherwise noted, the C_7H_{15}-sidechains of A are replaced with hydrogens in all quantum chemical calculations presented in this work. Their only purpose in the experiments is to increase the solubility of A. Beyond this, an influence of the sidechains on the ground state and/or the excited state properties of A was observed neither experimentally[12] nor computationally.[33]

The geometrical structures we derived agree with the ones from earlier DFT calculations for D (Ref. 34) and A.[35] For details on bond length and angles we therefore refer the reader to those publications.

According to Janak's theorem,[36] the KS eigenvalue of the highest occupied molecular orbital (HOMO) calculated with the exact density-functional equals the ionization potential (IP).[37] Furthermore the difference between the HOMO and the lowest unoccupied molecular orbital (LUMO) eigenvalues can be interpreted as an approximation to the experimental excitation energy.[38,39] Although strictly speaking the latter approximation is not applicable to hybrid functionals, it is known in the literature that in practice the B3-LYP gap often yields a good approximation to the true optical gap.[40,41] Following this line of thought, one can gain a first insight into the processes involved in the above described experiments by drawing a highly approximative but instructive one-particle picture.

We start by comparing our DFT results with cyclic voltametry experiments.[11] The HOMO energies of -4.90 eV for D and -5.92 eV for A agree well with the experimental IPs of -5.10 and -6.03 eV, respectively. Using the calculated LUMO-energies of -1.16 eV for D and -3.43 eV for A yields approximative excitation energies of 3.74 and 2.49 eV. They compare surprisingly well with the experimentally observed excitation energies of 3.5 and 2.35 eV, respectively.[42] The uppermost box in Fig. 3 sketches the relative position of the HOMO- and LUMO-energies of D and A, drawing an intuitive one-particle picture of the observed processes. As indicated by the left hand sides of the two circles in Fig. 3,
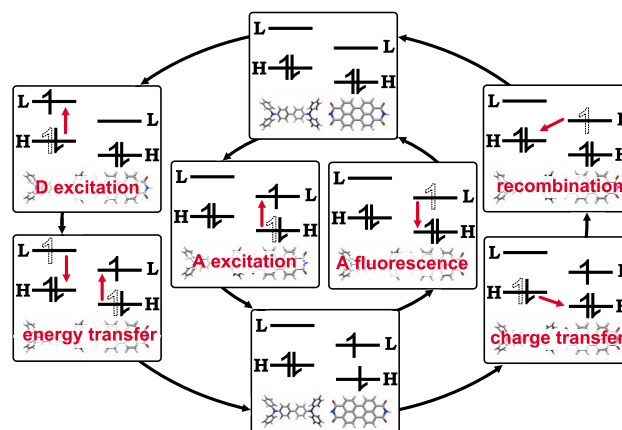

FIG. 3. Approximative one-particle picture of the observed processes in DA following optical excitation. HOMO (H) and LUMO (L) energies are positioned according to DFT results. Energy transfer, charge transfer, and charge recombination are nonradiative processes and therefore cannot be observed directly in fluorescence spectroscopy measurements.

there are two main pathways for going from a mixture of free donors and acceptors in their ground states (DA) to a configuration with an excited acceptor (DA*). While the inner circle indicates the obvious pathway, i.e., the direct excitation of DA at the acceptor absorption energy, the outer circle involves an excitation of DA at the donor absorption energy followed by a nonradiative energy transfer to the acceptor. It is important to recapture that in Ref. 12 these two pathways have been used experimentally to generate DBA* and that for both pathways an efficient quenching of the acceptor fluorescence was found. Therefore, besides the acceptor fluorescence (indicated by the inner circle on the right hand side of Fig. 3) there must exist at least one additional, nonradiative pathway going back from the photoexcited state (DA*) to the ground state (DA).

The approximative one-particle picture suggests such a nonradiative pathway. It is indicated by the outer circle on the right hand side of Fig. 3. Starting from DA*, the system undergoes a charge transfer from the HOMO of D to the HOMO of A. This charge-separated state turns into the neutral state through charge recombination. Obviously, the occurrence of this pathway requires charge transfer coupling between D and A. Contrary to the long-range energy transfer coupling which falls off as $\sim 1/r^3$,[43] charge transfer coupling is a short-range interaction that decays exponentially.[1] As a consequence, there is a wide range of D-A distances in which energy transfer takes place whereas charge transfer does not. Obviously, the D+A mixture investigated in Ref. 12 features such distances. However, the fluorescence quenching in DBA indicates that the inclusion of the saturated bridge introduces charge transfer coupling between D and A and thereby opens the nonradiative de-excitation pathway suggested by the outer circle in Fig. 3.

In order to test the influence of the saturated bridge on the electronic structure of DBA we now calculate the DBA ground state with DFT. We start by analyzing the DBA conformation in which the saturated bridge is completely stretched. Clearly, this constitutes an important limit, not least because the experimental results predict such a

TABLE II. Excitation energies (in eV) and oscillator strengths (in atomic units) of D, A, D+A, and DBA in stretched and folded bridge geometry. The folded bridge geometry is the MD-step 2 geometry (see Fig. 5 and discussion in the text). Corresponding NTOs are provided in Fig. 6.

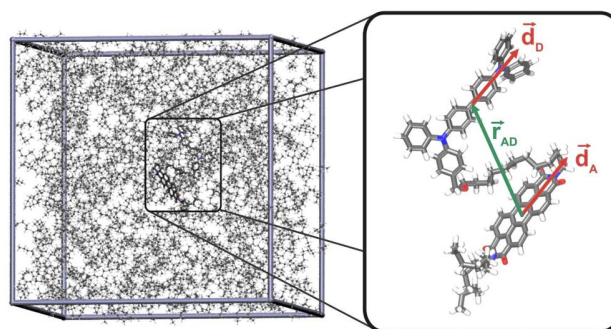| A	D	D+A	DBA stretched	DBA folded
2.41(0.627)	⋯	2.41(0.630)	2.40(0.707)	2.41(0.581)
⋯	⋯	⋯	⋯	3.26(0.107)
⋯	⋯	⋯	⋯	3.28(0.021)
⋯	3.27(1.128)	3.27(1.129)	3.26(1.198)	3.31(0.967)
⋯	⋯	⋯	⋯	3.33(0.010)
3.55(0.056)	⋯	3.55(0.054)	3.53(0.037)	3.58(0.019)
⋯	⋯	⋯	⋯	3.61(0.035)
⋯	3.59(0.015)	3.59(0.014)	3.58(0.016)	3.62(0.017)

FIG. 4. MD-simulation of DBA in pentane. During the calculation, the periodic boundary box including 1170 pentane-molecules and one DBA is kept at a temperature of 298 K and a pressure of 1 atm. The time step used for the MD is 1 fs.

bridge-conformation.[12] The main result of our computational analysis of stretched DBA is that the influence of the saturated bridge on the geometrical and electronical structure of D and A is negligible. The bridge features a large HOMO-LUMO gap of 9.85 eV. As a consequence, it does not affect the electronic spectra of D and A in the energy range close to their HOMO and LUMO eigenvalues. The orbitals of DBA can strictly be separated into A-, B-, and D-orbitals and even for energetically close-lying D- and A-states no splitting of the KS-eigenvalues can be observed within the numerical accuracy. Thus, there is no evidence for a through-bond charge transfer coupling of D and A in the electronic ground-state of stretched DBA. Considering the length and the HOMO-LUMO gap of the saturated hydrocarbon bridge, this finding is in line with earlier works on through-bond couplings (see, e.g., Ref. 16).

Now we go over to excited-state calculations. Table II shows TDDFT excitation energies and oscillator strengths for D, A, D+A, and DBA. For free D and A one obtains strong HOMO-LUMO transitions with large oscillator strengths at 2.41 and 3.27 eV, respectively. This is in good agreement with the experimental absorption spectrum.

For the investigation of D+A, we choose the relative orientation and distance of D and A such that is consistent with the geometry of DBA in a stretched-bridge conformation. Thus, we make sure that possible differences between the stretched DBA and D+A calculations originate only from the inclusion of the bridge. As a large number of excitations with zero or almost zero oscillator strengths is introduced by the simultaneous calculation of D and A in one system, we only provide those excitation energies with oscillator strengths larger than 10^{-2} in one of the geometries. In Table II we compare energies and oscillator strengths of corresponding excitations in different systems. The good agreement of the excitation energies and oscillator strengths of stretched DBA and D+A shows that in this case the influence of the saturated bridge is clearly negligible.

After having investigated the stretched DBA-system, the close lying next step is to investigate other conformations. However, from the computational point of view finding the global minimum of DBA is challenging as the corresponding high-dimensional energy-landscape is very flat. This is a consequence of the large number of energetically inexpensive conformational changes in the bridge. We have performed several steepest descent optimizations starting from different initial geometries. The local minimum in which the steepest descent relaxation ends up is strongly predetermined by the initial guess. Finding the global energy minimum would therefore require extensive simulated annealing, which is computationally costly. Yet more importantly, for further understanding of the experimental data it is not just one minimum that is of interest, but the finite-temperature conformational dynamics of DBA in solution.

Therefore, we now go over to an analysis of the conformational dynamics of DBA in solution (see Fig. 4) using MD. This step is motivated by the fact that up to this point, our results do not give any indication for a charge transfer coupling between D and A in the stretched bridge conformation of DBA. We set up MD-simulations of DBA in different solvents, assuming periodic boundary conditions, room-temperature and pressure. Solvents are taken into account explicitly. Different from the quantum chemical calculations, in the MD we explicitly take into account the C_7H_{15}-sidechains on A as they considerably influence its solubility. For the following analysis, we use the distance ($|\vec{r}_{AD}|$) between D and A, as well as the orientation factor κ^2 defined via the normalized transition dipoles ($\vec{d}_D$ and $\vec{d}_A$) by

$$\kappa^2 = (\cos \Theta_T - 3 \cos \Theta_D \cos \Theta_A)^2, \tag{3}$$

where

$$\cos \Theta_T = \vec{d}_D \vec{d}_A, \tag{4}$$

$$\cos \Theta_D = \vec{d}_D \vec{r}_{AD}, \tag{5}$$

$$\cos \Theta_A = \vec{d}_A \vec{r}_{AD}, \tag{6}$$

(see also Fig. 4). A plot of the the D-A distance and κ^2 as derived from an MD-calculation of DBA in pentane is given in Fig. 5. Starting from a stretched conformation the bridge immediately starts to fold. After 2.5 ns the bridge has collapsed completely. Henceforward, D and A remain stacked at a distance of ~5 Å and go on executing a shear movement in the stacked position (as can be derived from the plot of κ^2). We repeated the MD-simulation using a variety of different polar (ethanole, acetone, and toluene) and unpolar (pentane, decane, dodecane, and hexadecane) solvents. In all
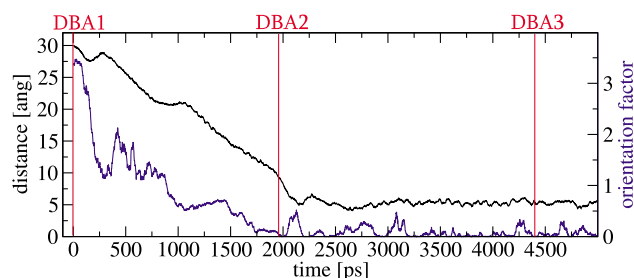
FIG. 5. Distance $|\vec{r}_{AD}|$ between D and A (see Fig. 4) and orientation factor κ^2 [see Eq. (3)] from an MD-calculation of DBA in pentane. Starting from a stretched bridge conformation, the fast folding of the bridge is followed by a shear movement of the stacked D and A.

cases we found qualitatively the same behavior. However, polarity and viscosity of the different solvents influence the average D-A distances and the time scale of the folding process. A detailed analysis of the influence of different solvents on the fluorescence depolarization and on the energy-and charge-transfer rates is thus subject of future experimental and theoretical work.

In this work however, our focus is on the charge transfer coupling between D and A. To this end, we analyze DBA for three different stages of the folding process by means of DFT and TDDFT. These stages are indicated in Fig. 5.

The first step of our MD analysis (DBA1) corresponds to the stretched bridge conformation and has been analyzed in detail above. In step 2 (DBA2) the folding process has evolved to a D-A distance of ~10 Å. Still, we observe no indication for electronic coupling between D and A in the ground-state calculations. In step 3 (DBA3) D and A are stacked at their final distance of ~5 Å. Note that the initial (DBA1) and final (DBA3) geometries of DBA are reoptimized to the next local minimum of the corresponding bridge-conformation. In contrast, the DBA2 geometry is directly taken from the MD.[44] From these calculations we find that the stacked configuration of DBA3 is energetically favored by approximately 0.55 eV as compared to DBA1 due to a π-π-stacking of D and A. The KS-orbitals at the Fermi-

level can no longer be unambiguously associated with D or A and their energies are shifted, e.g., compared to DBA1 the HOMO of A is shifted by +0.2 eV while the HOMO of D is shifted by +0.1 eV. Hence, we can clearly identify electronic coupling between D and A in DBA3 (see also discussion below). As discussed above, the electronic coupling between D and A can explain the fluorescence quenching on A. Importantly, the stacked configuration of DBA3 is thermally stable due to the large π-π-binding energy. Therefore, we expect that the soluted DBA most frequently occurs in the stacked configuration. However, one might wonder why this strong coupling cannot be observed in the experimental spectra. In search for an answer to this question we analyze the excited-state properties of DBA1-3 by means of TDDFT in the following.

A tool that allows us to visualize electronic excitations and thus facilitates the interpretation of the TDDFT results for DBA is the NTOs approach developed in Ref. 28. Given a TDDFT transition density, the NTOs provide its graphical representation in real-space by expanding the electronic excitations in the space of single KS transitions. As a result, TDDFT excitations can be characterized by single particle transitions from a hole-NTO to an electron-NTO. Thus, the NTO approach is frequently used to identify and visualize charge-transfer excitations in TDDFT.[45,46] In our work, we use the NTOs in order to analyze the occurrence of charge-transfer excitations in the folded DBA.

Again, for DBA1 a detailed analysis of the excited state properties is provided above. As a summary of those results, the spectrum of DBA1 is basically a superposition of the excited state spectra of D and A. However, already for DBA2 the picture changes significantly. In Table II, the excitation energies and oscillator strengths of DBA2 (folded DBA) are compared to those of DBA1 (stretched DBA) and D+A. Obviously, a number of "new" excitations with nonvanishing oscillator strengths appear. The analysis of these excitations with the help of NTOs (as provided for one example in Fig. 6) reveals that these new excitations have charge-transfer
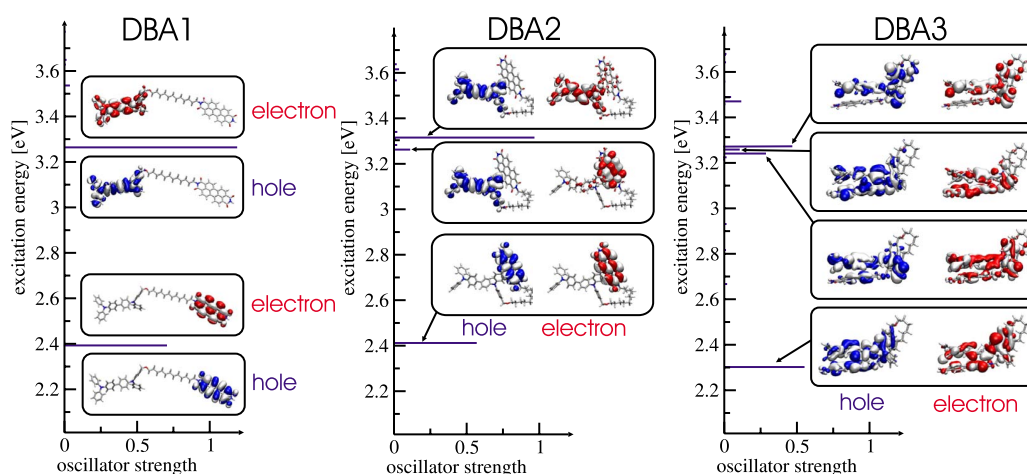

FIG. 6. TDDFT excitation spectra (see also Table II) and NTO of DBA at three stages of the MD (see Fig. 5). While in the stretched bridge conformation only pure D- and A-states occur, the folding introduces charge-transfer states. In the stacked position, a clear separation of D- and A-excitations from charge-transfer excitations is no longer possible.

character, i.e., hole- and electron-NTO are located on different parts of the DBA-molecule with some nonvanishing orbital overlap.

It is well known that local and semilocal functionals typically do not predict charge-transfer excitation correctly.[47] Although B3LYP has been shown to yield reasonable results for some charge-transfer excitations,[45] one cannot expect it to be generally accurate. This expectation is strengthened by the observation that the excitation energies of the new excitations in DBA2 vary by several eV when tuning the fraction of exact exchange in the used functional.[48] However, the purpose of our study is not to predict the energies of the charge-transfer excitations accurately—for our purposes it is enough to establish that charge transfer excitations appear. This is established without doubt by our calculations. For a detailed discussion of the charge-transfer excitation problem in TDDFT and how to deal with it we refer the reader to the pertinent literature.[47,49]

Coming to DBA3, the excitation spectrum still shows major excitations at the original D and A excitation energies. However, the NTO-analysis reveals that the nature of these excitations has changed significantly. Obviously, a clear separation of D and A excitations is no longer possible in DBA3. Moreover, new excitations appear at the excitation energy of D. The corresponding NTOs allow for the interpretation that these are excitations of the newly formed D-A complex.

At this point, one might wonder whether the above mentioned problem of commonly used density functionals in predicting long-range charge-transfer excitations does affect the energy of those new excitations. Note however that it is not possible to distinguish clearly between charge-transfer and noncharge-transfer excitations in DBA3, as one can see from the NTOs shown in Fig. 6. This is due to the strong electronic coupling between D and A that has already been observed in the ground-state calculations. Moreover, in DBA3 the D-A distance and thus the importance of the correct description of long-range charge-transfer excitations of the used density functional is significantly reduced as compared to DBA2. As a consequence, it is reasonable to assume that long-range charge transfer does not play a prominent role in our calculations on DBA3. In order to test the above reasoning we repeated the excited state calculations on DBA3 with a number of functionals that employ different fractions of exact exchange. Different from DBA2 and different from what would be expected for long-range charge-transfer excitations, here the fraction of exact exchange has only a minor effect on the new excitations of the DA complex.[50] Thus our results are not affected significantly by the long-range charge-transfer problem of commonly used functionals.

Note also that although the nature of the excitations shown in Fig. 6 changes drastically when going from DBA1 to DBA3, the shift of the excitation energies is surprisingly small. Considering a vibrational broadening of the experimental spectra of 0.1 eV and a computational accuracy of our approach of approximately the same magnitude, this shift of the excitation energies is negligible. This explains why the

π-π-stacking of D and A cannot be observed directly in the absorption spectra. However, it becomes apparent in the A-fluorescence quenching in DBA.

The results of the above TDDFT analysis of DBA3 allow for an experimental verification of our findings. In case DBA3 *de facto* constitutes the most frequent configuration of DBA in solution, one should be able to find more than one excitation in the immediate energetic vicinity of the D excitation energy. Indeed our calculations indicate that one might not be able to distinguish between these excitations in the absorption spectrum due to vibrational broadening. However, one should be able to find several decay rates at the D-emission energy in the fluorescence spectra. From an experimental point of view this poses a challenge as the efficient energy transfer in DBA strongly shortens the lifetimes (decay rates are increased) of the D fluorescence. For these reasons, k_D^{DBA} could not be determined exactly in Ref. 12 as the corresponding lifetime was shorter than the instrument response function of 80 ps. However, recent studies of DBA employing more involved experimental techniques[51] support the notion of multiple excitation energies in the frequency range of the donor emission.

At this point, it is important to make clear that our verification of the electronic coupling between D and A is a qualitative and not a quantitative one. Therefore, we cannot predict quenching rates or efficiencies. A number of *ab initio* approaches for the calculation of charge transfer rates via Marcus theory[52] can be found in the literature.[53–55] However, these approaches are computationally demanding and yield charge-transfer coupling elements only for one specific distance, configuration and relative orientation of the donor and acceptor molecules. It is also known that the electronic coupling is extremely sensitive to distance, relative orientation and displacement of donor and acceptor.[3,4] In order to use these methods for predicting the experimentally observed quenching rates in our case, we therefore would have to do this type of calculation for every single time step of the MD-simulation. Clearly, this is not an option.

V. CONCLUSION

In this work, we have analyzed the role of the saturated $CH_2O(CH_2)_{12}$-bridge in the fluorescence quenching mechanism in a DBA system that has recently been investigated experimentally. Using TDDFT and comparing calculations for a mixture of free donors and acceptors to those for the bridged DBA molecule in stretched conformation, we were able to show that the large HOMO-LUMO-gap of the saturated bridge keeps the electronic spectra of D and A completely separate. Thus, the direct influence of the bridge on the ground- and excited-state spectra of D and A is negligible. However, MD-simulations of DBA in different solvents revealed that it is the mechanical influence of the bridge that causes the acceptor-fluorescence quenching. The bridge folds in solution so that donor and acceptor stack at a distance of ~5 Å, which is typical for π-π stacks. In this configuration, the orbitals of donor and acceptor overlap and their spectra are electronically coupled. This coupling opens up a nonradiative de-excitation pathway including charge

transfer and recombination. As a consequence, the A-fluorescence is quenched efficiently. TDDFT calculations on the stacked DBA revealed that the electronic coupling of D and A cannot be directly observed in the absorption spectrum due to a surprisingly small shift in the excitation energies. However, the coupling leads to a multiexponential decay of the DBA-fluorescence at the donor-emission energy. This finding is in agreement with recent experimental studies.

ACKNOWLEDGMENTS

[1] M. Newton, Chem. Rev. (Washington, D.C.) **91**, 767 (1991).

[2] S. Speiser, Chem. Rev. (Washington, D.C.) **96**, 1953 (1996).

[3] J.-L. Brédas, D. Beljonne, V. Coropceanu, and J. Cornil, Chem. Rev. (Washington, D.C.) **104**, 4971 (2004).

[4] V. Coropceanu, J. Cornil, D. A. da Silva Filho, Y. Olivier, R. Silbey, and J.-L. Brédas, Chem. Rev. (Washington, D.C.) **107**, 926 (2007).

[5] I. B. Ramsteiner, A. Hartschuh, and H. Port, Chem. Phys. Lett. **343**, 83 (2001); *Molecular Switches*, edited by B. L. Feringa (Wiley-VCH, Weinheim, 2001); M. W. Holman, P. Yan, K.-C. Ching, R. Liu, F. I. Ishak, and D. M. Adams, Chem. Phys. Lett. **413**, 501 (2005).

[6] *Advances in Photosynthesis and Respiration, Light-Harvesting Antennas in Photosynthesis*, edited by B. R. Green and W. W. Parson (Kluwer, Dordrecht, 2003), Vol. 13.

[7] T. Christ, F. Kulzer, T. Weil, K. Müllen, and T. Basché, Chem. Phys. Lett. **372**, 878 (2003); P. Tinnefeld, K. D. Weston, T. Vosch, M. Cotlet, T. Weil, J. Hofkens, K. Müllen, F. C. de Schryver, and M. Sauer, J. Am. Chem. Soc. **124**, 14310 (2002).

[8] U. Anton and K. Müllen, Macromolecules **26**, 1248 (1993); E. E. Neuteboom, S. C. J. Meskers, E. W. Meijer, and R. A. J. Janssen, Macromol. Chem. Phys. **205**, 217 (2004).

[9] H. Fidder, J. Knoester, and D. A. Wiersma, J. Chem. Phys. **95**, 7880 (1991); E. Lang, A. Sorokin, M. Drechsler, Y. V. Malyukin, and J. Köhler, Nano Lett. **5**, 2635 (2005).

[10] W. B. Davis, W. A. Svec, M. A. Ratner, and M. R. Wasielewski, Nature (London) **396**, 60 (1998); C. G. Hübner, V. Ksenofontov, F. Nolde, K. Müllen, and T. Basché, J. Chem. Phys. **120**, 10867 (2004); T. D. M. Bell, A. Stefan, S. Masuo, T. Vosch, M. Lor, M. Cotlet, J. Hofkens, S. Bernhardt, K. Müllen, M. van der Auweraer, J. W. Verhoeven, and F. C. De Schryver, ChemPhysChem **6**, 942 (2005); G. Duvanel, N. Banerji, and E. Vauthey, J. Phys. Chem. A **111**, 5361 (2007); C. Curutchet, B. Mennucci, G. D. Scholes, and D. Beljonne, J. Phys. Chem. B **112**, 3759 (2008).

[11] P. Bauer, H. Wietasch, S. M. Lindner, and M. Thelakkat, Chem. Mater. **19**, 88 (2007).

[12] Ch. Scharf, K. Peter, P. Bauer, Ch. Jung, M. Thelakkat, and J. Köhler, Chem. Phys. **328**, 403 (2006).

[13] G. Horowitz, F. Kouki, P. Spearman, D. Fichou, C. Nogues, X. Pan, and F. Garnier, Adv. Mater. Weinheim, Ger.) **8**, 242 (1996); P. R. L. Malenfant, C. D. Dimitrakopoulos, J. D. Gelorme, L. L. Kosbar, T. O. Graham, A. Curioni, and W. Andreoni, Appl. Phys. Lett. **80**, 2517 (2002).

[14] C. W. Tang, Appl. Phys. Lett. **48**, 183 (1986); L. Schmidt-Mende, A. Fechtenkotter, K. Mullen, E. Moons, R. H. Friend, and J. D. MacKenzie,

Science **293**, 1119 (2001).

[15] V. Bulović, G. Gu, P. E. Burrows, S. R. Forrest, and M. E. Thompson, Nature (London) **380**, 29 (1996); N. Tamoto, C. Adachi, and K. Nagai, Chem. Mater. **9**, 1077 (1997); E. Bellmann, S. E. Shaheen, R. H. Grubbs, S. R. Marder, B. Kippelen, and N. Peyghambarian, *ibid.* **11**, 399 (1999); Y. Shirota, J. Mater. Chem. **15**, 75 (2005).

[16] K. D. Jordan and M. N. Paddon-Row, Chem. Rev. (Washington, D.C.) **92**, 395 (1992).

[17] Experimental spectra supplied by Christiane Hofmann; also see Ref. 12.

[18] B. P. Krueger, G. D. Scholes, and G. R. Fleming, J. Phys. Chem. B **102**, 5378 (1998); D. Beljonne, J. Cornil, R. Silbey, P. Millie, and J.-L. Brédas, J. Chem. Phys. **112**, 4749 (2000); D. Beljonne, G. Pourtois, C. Silva, E. Hennebicq, L. M. Herz, R. H. Friend, G. D. Scholes, S. Setayesh, K. Müllen, and J. L. Brédas, Proc. Natl. Acad. Sci. U.S.A. **99**, 10982 (2002); G. D. Scholes, Annu. Rev. Phys. Chem. **54**, 57 (2003); S. Jang, M. D. Newton, and R. J. Silbey, Phys. Rev. Lett. **92**, 218301 (2004); H. Wiesenhofer, D. Beljonne, G. D. Scholes, E. Hennebicq, J.-L. Brédas, and E. Zojer, Adv. Funct. Mater. **15**, 155 (2005); M. E. Madjet, A. Abdurahman, and T. Renger, J. Phys. Chem. B **110**, 17268 (2006).

[19] A. E. Clark, C. Qin, and A. D. Q. Li, J. Am. Chem. Soc. **129**, 7586 (2007).

[20] R. Ahlrichs, M. Bär, M. Häser, H. Horn, and C. Kölmel, Chem. Phys. Lett. **162**, 165 (1989); F. Furche and D. Rappoport, in *Computational Photochemistry*, edited by M. Olivucci (Elsevier, Amsterdam, 2005), Vol. 16, Chap. III.

[21] M. J. Frisch, G. W. Trucks, H. B. Schlegel *et al.*, Gaussian 03 (Revision D.02), Gaussian, Inc., Wallingford CT (2004).

[22] O. Treutler and R. Ahlrichs, J. Chem. Phys. **102**, 346 (1995).

[23] S. Grimme, J. Comput. Chem. **25**, 1463 (2004); **27**, 1787 (2006).

[24] P. J. Stevens, J. F. Devlin, C. F. Chabalowski, and M. J. Frisch, J. Phys. Chem. **98**, 11623 (1994).

[25] A. Schäfer, H. Horn, and R. Ahlrichs, J. Chem. Phys. **97**, 2571 (1992).

[26] A. Klamt and G. Schüürmann, J. Chem. Soc. Perkin Trans. 2 **1993**, 799.

[27] COSMO is used in all calculations of geometries and excited state energies. Unless otherwise noted we used a permittivity of $\epsilon = 2.0$ for all calculations. This corresponds to the permittivity of dodecane and is close to the permittivity of toluene ($\epsilon = 2.4$) at room temperature, both being solvents primarily used in the experiment of Ref. 12. Note, that in the calculation of the natural transition orbitals (however, not in the energies) solution effects are neglected.

[28] R. L. Martin, J. Chem. Phys. **118**, 4775 (2003).

[29] P. Ren and J. W. Ponder, J. Phys. Chem. B **107**, 5933 (2003).

[30] N. L. Allinger, Y. H. Yuh, and J.-H. Lii, J. Am. Chem. Soc. **111**, 8551 (1989); J.-H. Lii and N. L. Allinger, *ibid.* **111**, 8566 (1989); J.-H. Lii and N. L. Allinger, *ibid.* **111**, 8576 (1989).

[31] J. R. Hill, VIEWMOL Program, Version 2.4, 2003.

[32] W. Humphrey, A. Dalke, and K. Schulten, J. Mol. Graphics **14**, 33 (1996).

[33] For all calculations on PTCDI, we checked the influence of the sidechains on the geometrical structure, the KS-eigenvalues and TDDFT excitation spectra in the relevant energetical range.

[34] M. Malagoli and J.-L. Brédas, Chem. Phys. Lett. **327**, 13 (2000).

[35] F. Pichierri, J. Mol. Struct. **686**, 57 (2004).

[36] J. F. Janak, Phys. Rev. B **18**, 7165 (1978).

[37] M. Levy, J. P. Perdew, and V. Sahni, Phys. Rev. A **30**, 2745 (1984).

[38] M. Levy, Phys. Rev. A **52**, R4313 (1995).

[39] A. Görling, Phys. Rev. A **54**, 3912 (1996).

[40] U. Salzner, J. B. Lagowski, P. G. Pickup, and R. A. Poirier, J. Comput. Chem. **18**, 1943 (1997).

[41] For a detailed discussion of the band-gap problem for hybrids, see, e.g., S. Kümmel and L. Kronik, Rev. Mod. Phys. **80**, 3 (2008).

[42] Experimental excitation energies taken at the maxima of the absorption spectrum.

[43] Th. Förster, Ann. Phys. **437**, 55 (1948).

[44] Reoptimization of the DBA2 geometry using a dispersion correction as provided in Ref. 23 leads to a collapse of the bridge with a final D-A distance of approximately 5 Å. Note that this corresponds to the mean D-A distance found in the MD and thus supports the MD results. Note further that the dispersion correction has only minor effects on the geometry of DBA1 and DBA3.

[45] R. J. Magyar and S. Tretiak, J. Chem. Theory Comput. **3**, 976 (2007).

[46] C. Wu, S. Tretiak, and V. Y. Chernyak, Chem. Phys. Lett. **433**, 305 (2007); E. Badaeva and S. Tretiak, *ibid.* **450**, 322 (2008).

[47] M. E. Casida, F. Gutierrez, J. Guan, F.-X. Gadea, D. Salahub, and J.-P.

Daudey, J. Chem. Phys. **113**, 7062 (2000); D. Tozer, *ibid.* **119**, 12697 (2003); N. T. Maitra, *ibid.* **122**, 234104 (2005); J. Neugebauer, O. Gritsenko, and E. J. Baerends, *ibid.* **124**, 214102 (2006).

[48] We calculated the excitation spectrum of DBA2 using time-dependent Hartree-Fock (TDHF) and functionals using 50% (BHandHLYP), 20% (B3LYP), and no Hartree-Fock exchange (PBE). While the HOMO-LUMO excitations of D and A varied by up to 0.4 eV, the charge-transfer excitations where generally shifted by several eV.

[49] A. Dreuw and M. Head-Gordon, Chem. Rev. (Washington, D.C.) **105**, 4009 (2005).

[50] We calculated the excitation spectrum of DBA3 using TDHF, BHandHLYP, B3LYP, and PBE. The shift of all relevant excitations varied up to 0.4 eV. Thus the long-range charge transfer problem of commonly used functionals does not affect our results on DBA3.

[51] C. Hofmann and J. Köhler, private communication (2009).

[52] R. A. Marcus, J. Chem. Phys. **24**, 966 (1956); Rev. Mod. Phys. **65**, 599 (1993).

[53] G. Pourtois, D. Beljonne, J. Cornil, M. A. Ratner, and J.-L. Brédas, J. Am. Chem. Soc. **124**, 4436 (2002); V. Lemaur, M. Steel, D. Beljonne, J.-L. Brédas, and J. Cornil, *ibid.* **127**, 6077 (2005).

[54] T. Kawatsu, V. Coropceanu, A. Ye, and J.-L. Brédas, J. Phys. Chem. C **112**, 3429 (2008).

[55] Q. Wu and T. van Voorhis, J. Chem. Phys. **125**, 164105 (2006).